EVALUATION OF HYDRAULIC FRACTURE PERFORMANCE IN THE VIKING FORMATION USING A DATA-DRIVEN APPROACH

A Thesis

Submitted to the College of Graduate and Postdoctoral Studies

In Partial Fulfillment of the Requirements

For the

Degree of Master of Science

In the

Department of Civil, Geological and Environmental Engineering

University of Saskatchewan, Saskatoon, SK, Canada

By

Luisa Porras

PERMISSION TO USE

In presenting this thesis in partial fulfillment of the requirements for a Postgraduate degree from the University of Saskatchewan, I agree that the Libraries of this University may make it freely available for inspection. I further agree that permission for copying of this thesis in any manner, in whole or in part, for scholarly purposes may be granted by the professor or professors who supervised my thesis work or, in their absence, by the Head of the Department or the Dean of the College in which my thesis work was done. It is understood that any copying or publication or use of this thesis or parts thereof for financial gain shall not be allowed without my written permission. It is also understood that due recognition shall be given to me and to the University of Saskatchewan in any scholarly use which may be made of any material in my thesis.
Requests for permission to copy or to make other use of material in this thesis in whole or part should be addressed to:

Head of the Department of Civil, Geological and Environmental Engineering
University of Saskatchewan
57 Campus Drive
Saskatoon, SK S7N 5A9, Canada

OR

Dean
College of Graduate and Postdoctoral Studies
University of Saskatchewan
116 Thorvaldson Building, 110 Science Place
Saskatoon, SK S7N 5C9, Canada

ABSTRACT

The exploitation of oil from unconventional reservoirs has increased rapidly due to recent advances in horizontal drilling and multi-stage hydraulic fracturing. One of the main challenges in the exploitation of unconventional resources is the optimization of stimulation designs to maximize well performance. In recent years, data-driven methods have played a vital role in achieving operational, performance, and economic efficiencies in such resources.

In this study, data-driven predictive models were developed to evaluate hydraulic fracture stimulation design parameters and to identify oil production drivers in the Viking Formation. Both Multiple Linear Regression (MLR) and Random Forest (RF) models were used to analyze the data from 845 multi-stage hydraulically fractured horizontal wells in the Viking formation, Saskatchewan, Canada. Reservoir characteristics, such as well geographic location, average gas-oil ratio, net pay, and stimulation design parameters, including completion length, proppant concentration, proppant intensity, were included as inputs in the models. 365-day cumulative oil production (IP365) was used as a metric for well performance.

MLR and RF were successfully used to develop models for predicting IP365. The performance of both models was compared, and RF model was selected for further investigation due to its superior performance. The optimum combination of hyperparameters for RF was found using Random Search and Grid Search methods. Furthermore, the K-Fold Cross Validation approach was employed to validate the predictive and generalization capabilities of the model. The importance of reservoir and stimulation parameters with respect to well performance was determined using the Permutation Feature Importance technique.

Modeling results indicated that completion length has the largest impact on oil production, followed by proppant intensity (proppant volume by completion length) and reservoir characteristics such as net pay. Furthermore, a high gas-oil ratio was found to have a detrimental effect on oil production. Partial dependence plots were used to visualize the relationship between each predictor variable and the model output. Results showed that, on average, wells in the study area with lateral length greater than 750 m tend to have above-average IP365. Proppant intensities

ranging from 0.37 t/m to 0.49 t/m seem to be effective. A diminishing effect on production is observed in wells treated with higher values of proppant intensity. Shapley additive explanations (SHAP) values were estimated to understand well performance on a well-by-well-basis. This method provided insights about the interactions between the predictor variables and the model output.

Results from this study will be helpful for stimulation and production engineers to optimize stimulation designs and maximize well productivity in the Viking Formation. This data-driven approach can be applied to any other plays and seamlessly integrated in workflow processes. Moreover, this methodology allows engineers and geoscientists to make informed decisions in rapidly changing environments.

ACKNOWLEDGEMENTS

First and foremost, I would like to express my gratitude to my supervisor Dr. Christopher Hawkes for his support and supervision during my master's program. His guidance, encouragement and kindness were invaluable. I am very lucky to have such an excellent supervisor. I would also like to thank my committee members Dr. Markus Brinkmann for his knowledge and guidance in data analytics, and Donna Beneteau for her recommendations and revisions.

I would also like to extend my gratitude to Baytex Energy Corp, especially to Arshad Islam for offering his expertise, guidance, and immense support to complete this work successfully. Many thanks to Ryan Semenchuk for his help, data provided, and constructive feedback to make this work better.

Finally, I would like to acknowledge financial support provided by the College of Graduate and Postdoctoral Studies and the College of Engineering, University of Saskatchewan, Baytex Energy Corp. and Mitacs.

This thesis is dedicated to my mother (Carmenza), my sister (Silvia), and my research mentors (Dr. Hawkes and Arshad)

For their endless support and encouragement

TABLE OF CONTENTS

Page

LIST OF TABLES

Page

LIST OF FIGURES

Page

LIST OF SYMBOLS AND ABBREVIATIONS

SYMBOLS:

β_0 — Intercept of the plane

β_n — Regression coefficient

ϵ_i — Error

X_n — Predictor variable

Y — Model output

ABBREVIATIONS:

R^2 — Coefficient of determination

AI — Artificial intelligence

ANN — Artificial neural network

API — American Petroleum Institute

API gravity — 141.5 / specific gravity - 131.5

BOE — Barrel of oil equivalent

CO_2 — Carbon dioxide

CAPEX — Capital expenditures

CV — Cross-validation

DOFFS — Digital oilfields of the future

EDA — Exploratory data analysis

GOR — Gas-oil ratio

ICE — Individual conditional expectation

IP365 — 365-day cumulative oil production

IQR — Interquartile range

MBOE — Million barrels of oil equivalent

ML — Machine learning

MLR — Multiple linear regression

MRMR — Minimum redundancy maximum relevance

NDT — Neural decision tree

NEB — National energy board

OPEX — Operational expenditures

PCA — Principal component analysis

PDP — Partial dependence plot

PLS — Partial least square

RF — Random forest

ROP — Rate of penetration

RPM — Revolutions per minute

RTOC — Real-time operation center

SHAP — Shapley additive explanations

SOM — self-organizing maps

SVM — Support vector machine

SWF — Sand waterfracs

TOC — Total organic carbon

TVD — True vertical depth

WCSB — Western Canadian sedimentary basin

WOB — Weight on bit

XLG — Crosslinked gel

NON-SI UNITS USED IN THIS STUDY

md — millidarcy, a measure of permeability ($\sim 10^{-15} \mathrm{m}^2$)

CHAPTER 1: INTRODUCTION

1.1 Background

Unconventional light oil plays are key hydrocarbon sources that are often challenging to characterize and extract by conventional drilling and pumping techniques due to inherent rock properties, including low porosity and low permeability (Adil Al-Alwani, 2014). The introduction of advanced technologies, such as horizontal drilling and multi-stage hydraulic fracturing, have positively transformed the oil and gas industry over the last few decades (NEB, 2011). The combination of these technologies has unlocked the potential of unconventional resources, allowing for commercial development.

In Canada, the exploitation of oil from unconventional sources has increased rapidly. The Western Canadian Sedimentary Basin (WCSB) is a major oil producing region, with some of the major plays including the Bakken, Viking, Montney, and Duvernay Formations (NEB, 2011). The development schemes of these resources focus on the combination of horizontal drilling and multi-stage hydraulic fracturing to enhance well productivity at an economically feasible rate. According to NEB (2014), Western Canada produced more than 400,000 barrels per day (64,000 m^3 per day) in 2014 due to the successful application of these technologies.

The main difference between conventional and unconventional resources is that unconventional plays are challenging to produce due to low reservoir quality and complicated production mechanisms (Belyadi, Fathi, & Belyadi, 2016). Presently, most “good” resources have been exploited so the industry is focusing on “average” and “poor” resources, as illustrated in Figure 1.1. Advanced technology, research, and time are required to produce plays with a lower reservoir quality. Therefore, the oil and gas industry invests significant planning to develop tight resources. Horizontal lateral length, number of fractured stages, volume of proppant and fluid, and proppant composition are some of the factors to consider when developing a stimulation program.

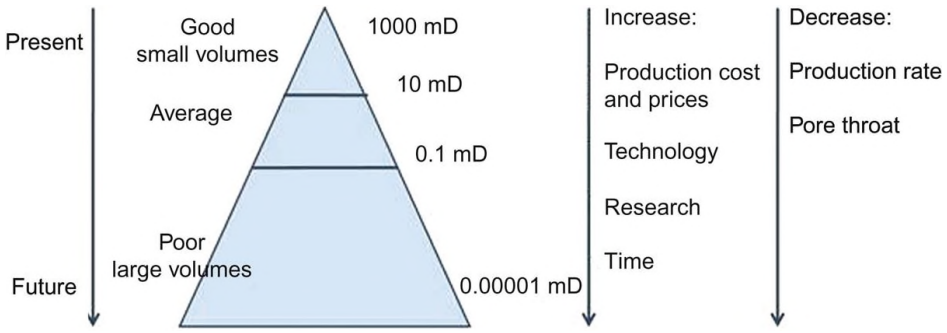

Figure 1.1. Resource pyramid in which resources are divided in three categories based on the formation permeability (Belyadi et al., 2016).

Significant advancements in technology have made characterizing and evaluating well performance more difficult. These difficulties are mainly attributed to the lack of comprehension of the relationships between reservoir properties, hydraulic fracturing procedures and hydrocarbon production rates. Several methods are employed to evaluate the effectiveness of hydraulic fracturing treatments. One of the most popular methods is through simulation tools, in which the fluid flow is modeled inside the reservoir and the hydraulic fracture. However, these models require information about the reservoir and geomechanical characteristics. Since these types of data are generally lacking, some parameters are assumed during reservoir modeling. These assumptions can negatively affect well optimization. Moreover, models need to be calibrated after field data is obtained. Another shortcoming of this method is that the analysis is generally performed at a single well. Therefore, it is difficult to compare a wide range of wells or to produce field recommendations with this approach (Shelley et al., 2014).

An additional challenge for unconventional reservoirs is the fact that development of these resources is relatively costly, and the low oil price environment creates a pressure in the industry to increase the effectiveness and efficiency of operations. Generally, completion costs range from 50% up to 70% of the total capital cost of drilling an unconventional well (Kakar, 2018). Therefore, producers need a better understanding how completion and stimulation designs affect production rates in order to develop successful programs that can maximize well performance.

In light of this, the use of data mining and machine learning techniques have become more attractive due to the possibility of quantitatively determining the relationship between multiple

factors including completion, reservoir, and geological characteristics. The results can then be used to develop field models. Additionally, this approach can handle large datasets, enabling general and high-level analyses (Shelley et al., 2014).

Data mining is defined by The Gartner Group (2013) as “the process of discovering meaningful new correlations, patterns, and trends by sifting through large amounts of data stored in repositories, using pattern recognition technologies as well as statistical and mathematical techniques.” Some of the most popular techniques in data mining include classification, summarization, association rule mining, and clustering (Han et al., 2006).

To extract useful knowledge from the data, every data mining project follows six basic phases, which are presented in Figure 1.2. First, the data from different sources is collected and integrated into a database. Then, the data cleaning is performed by removing noisy data, such as null and untypical values (outliers) (Fawzy et al., 2016). The next phase is data transformation, in which dimension reduction and/or principal component analysis (PCA) is performed (Wang, 2018). Once the data pre-processing steps are completed, pattern recognition starts. Different data mining techniques can be applied to the pre-processed data in order to discover patterns and obtain meaningful results.

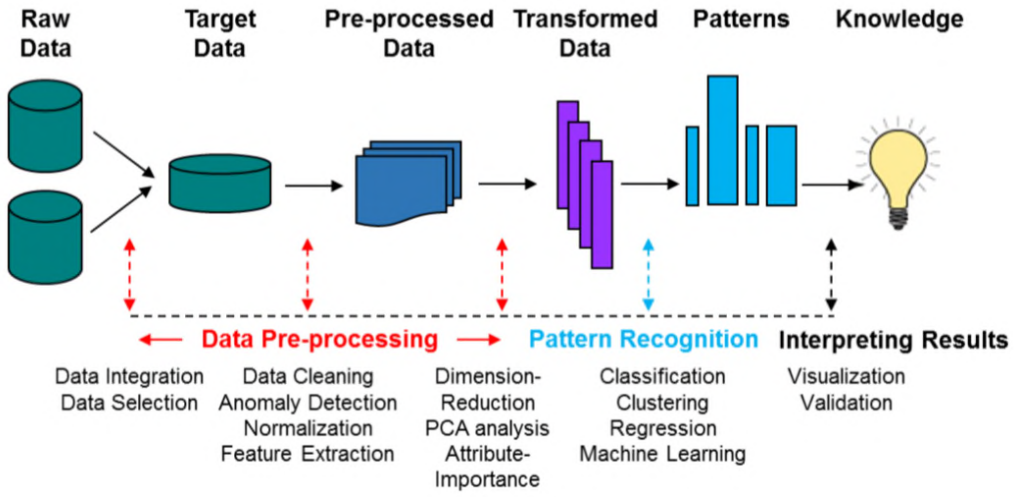

Figure 1.2. Typical phases of a data mining project (Kamath, 1999).

Since the oil and gas industry generates large quantities of data, data driven methods have become an essential part of this industry. Several authors have used data mining techniques in different areas, including drilling and production optimization, reservoir characterization, and well performance evaluation.

Several authors have used data-driven approaches to understand the effect of stimulation programs on well productivity and to forescast production in unconventional reservoirs. Nejad et al. (2015) investigated the effectiveness of the completion strategy and fracture treatment design in the Eagle Ford Shale. A neural network was constructed to predict well productivity and key production drivers were identified. Similarly, Grieser et al. (2008) used a variety of data mining techniques, including a self-organizing map, which is a type of neural network, to analyze Barnett Shale completions. Shuhua & Chen (2016) predicted cumulative oil production in the Bakken Formation using a neural network. Results indicated that proppant per stage is the most influential factor, contributing to 35% of the oil production variance in the study area.

Data-driven methods have demonstrated the potential to evaluate well performance and to forecast production in unconventional and tight reservoirs. However, the application of artificial intelligence and machine learning in the oil and gas industry is still in its infancy (Mohaghegh, 2017). Furthermore, the selection and implementation of the appropiate methods for a particular scenario is a challenging task.
There are many questions to consider when optimizing well performance in a specific area. For example, what are the completion and stimulation parameters that drive production? Based on past experiences, what are the recommended stimulation practices? These questions are frequently asked by engineers, but are difficult to answer due to the complexity of the hydraulic fracture procedures.

This study is intended to address these questions by evaluating the performance of horizontal wells in the Viking Formation. This play is located between East-central Alberta and West-central Saskatchewan. The oil has an API gravity in the range of 30 to 36° (light crude), and is found at shallow depths (around 700 m total vertical depth (TVD)), making the reservoir attractive even in low oil price times (Kohlruss, D., 2015; Mogensen et al., 2012). Horizontal wells in the Viking Formation are routinely stimulated by hydraulic fracturing. However, the

Viking is well known for high decline rates and producing at lower rates than other tight oil play (NEB, 2014). Therefore, it is of practical interest to identify the stimulation parameters that could influence well productivity and identify how to improve well stimulation design.

This study integrates machine learning and statistical methods to better understand and quantify the effects of reservoir and stimulation characteristics on well productivity in the Viking Formation. The goal of this project is to provide an oil production predictive model that will be used to quantify the impact of each predictor variable on oil production. As a result, this project could help operators improve stimulation and completion designs and increase oil production in the Viking Formation. This methodology could also be applied to assess hydraulic fracture performance in other unconventional reservoirs, but the conclusions in this work are field-specific and they should not be generalized.

1.2 Research study area

The research study area is located in West-central Saskatchewan. This area covers townships 32 – 26 and ranges 18 – 26 W3. A total of 875 horizontal multi-stage hydraulically fractured wells are considered. These wells are distributed in 10 fields, including Avon Hill, Kerrobert, Dodsland, Plato North, Whiteside, Prairiedale, Plato, Plenty, Forgan and Eureka, as illustrated in Figure 1.3.

The Viking Formation, containing about 9.2 million m^3 of proved and probable reserves, is considered one of the most important oil reservoirs in Western Canada (NEB, 2011). The Viking overlies the Joli Fou Formation and underlies the Westgate Formation. This formation is made up of marine influenced sandstones and shale, and it is commonly divided in three units: Upper Viking (Viking A), Shale, and Lower Viking (Viking B). The quality and thickness of the reservoir varies according to the location. The Lower Viking is the main reservoir in different pools, including Kerrobert, Plenty, and Prairiedale (Mathison, 2014). The thickness of the reservoir ranges from 175 m in southwestern Alberta to only a few meters in western Saskatchewan (Reinson et al., 1994). The oil pools are found in southwest Saskatchewan and southern and central Alberta. Some of the largest oil fields include Joarcam, Dodsland, Provost, Joffre, and

Crystal. These fields have the highest Initial Established Recoverable Reserves (Reinson et al., 1994).

The exploitation of light crude oil started in the early 1950's and has continued since then. Initially, all wells were drilled vertically in the Viking Formation. Efforts to restore oil production rates have been made, and the introduction of horizontal multi-stage hydraulic fracturing has renewed interest in the Viking Formation (Mathison, 2014; Mogensen et al., 2012). A Detailed description of the Viking Formation can be found in Reinson et al. (1994), Baishev (2017), and Pozzobon (1987). The geological framework of the Viking Formation is described in Chapter 2.

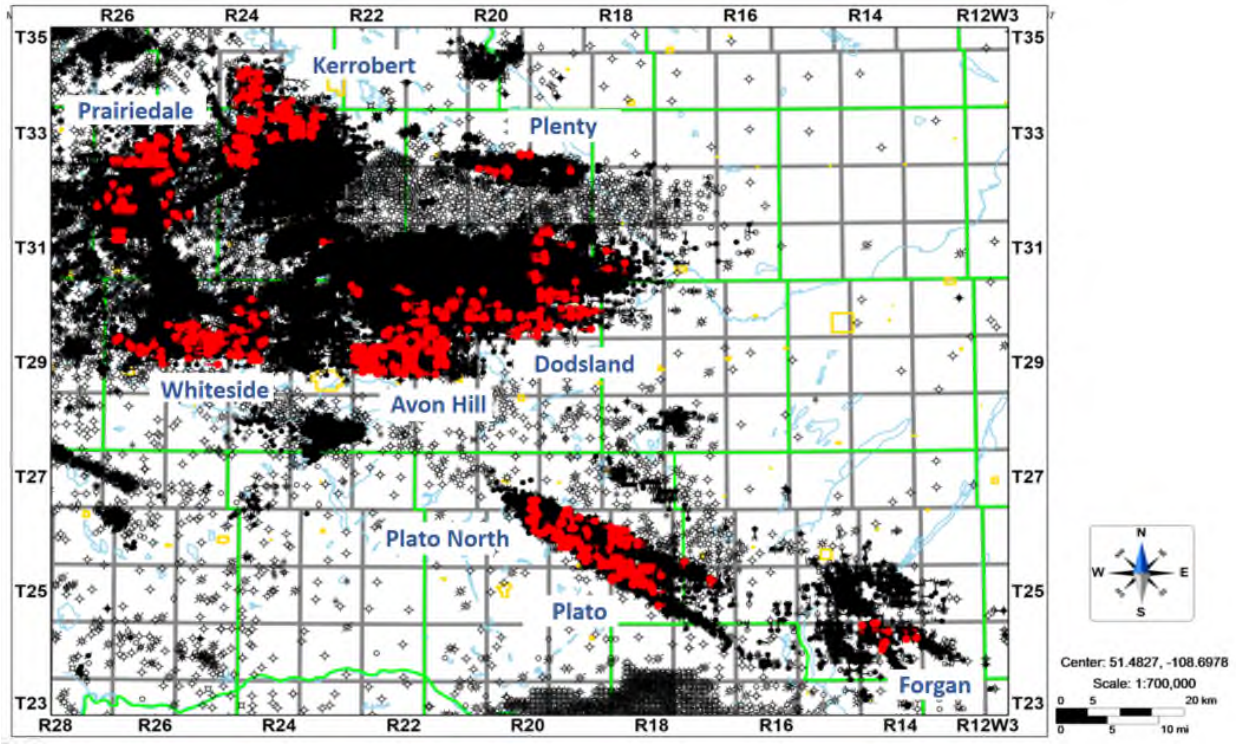

Figure 1.3. Map of southwest Saskatchewan presenting the area of study. Wells studied in this work are denoted with red symbols; all other wells are denoted in black.

1.3 Objectives

The main purpose of this research is to evaluate the performance of hydraulically fractured horizontal wells in the Viking Formation. Specific objectives are as follows:

1. To identify reservoir and stimulation parameters that could have an influence on well productivity in the Viking Formation.

2. To establish well performance drivers on a well-by-well basis.

3. To identify how to improve well stimulation design in the Viking Formation.

1.4 Methodology

In this work, data mining and statistical methods are used to evaluate the effect of multiple predictor variables including well geographic location, reservoir and completion, on hydraulic fracture performance in horizontal wells. Data-driven modeling can incorporate field measurements from different categories and scales to extract complex patterns from large dataset and variables (Mohaghegh, 2019).

These methods provide a high-level understanding of the relationships between hydraulic fracturing procedures and the extraction rates from a heterogeneous formation. A common approach in data mining projects is the cross industry standard process for data mining (CRISP_DM). This structured and systematic method is followed to achieve meaningful results (IBM, n.d.). Figure 1.4 illustrates the six steps of the data mining life cycle.

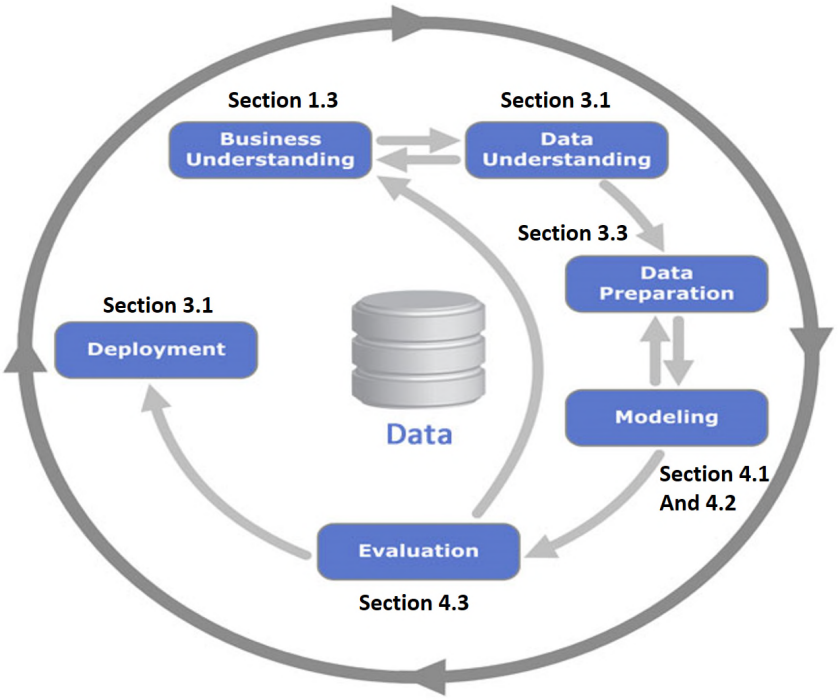

Figure 1.4. CRISP-DM Process diagram (After Jensen, 2012). The section number inserted near each step denotes the section in which this step is described in more detail.

The first step is the definition of the problem and the project objectives, as stated in Section 1.3. The second step is data collection, which is discussed in Section 3.1. The third step refers to data preparation, which involves data cleaning and transformation. Data cleaning is performed to obtain the final dataset for analysis by removing errors and inconsistencies. Additionally, outliers in the dataset are identified.

Data preparation and quality control, as described in Section 3.3, deals with errors and inconsistencies in the dataset. This step is key to obtain the final dataset ready for analysis. The fourth step involves the implementation of a variety of data-driven modeling techniques, including a multiple linear regression and random forest, and the evaluation of the model's performance. Multiple linear regression is a statistical technique which, in this case, serves as a benchmark model to compare the performance of the machine learning technique. The model's performance is evaluated based on how well the model explains the variability of oil production in the first year considering a set of predictor variables; this step is presented in Sections 4.1 and 4.2.

The fifth step includes the analysis and interpretation of the selected model (see Section 4.3). As a part of the model analysis, feature importance is performed to identify the parameters that have the most influence on the variability of well performance in the first year. Moreover, individual conditional expectation (ICE), partial dependence plots (PDP), and feature contributions are some of the techniques used to quantify the effects of the variables on well performance. The final step refers to the deployment phase in which new insights regarding how to improve stimulation designs are formulated. This final step is presented in Section 4.4.

1.5 Research scope

This study focused on the oil producing areas of the Viking Formation (gas reservoirs were not considered). Only publicly available data accessed using commercial software applications, such as GeoVista and Accumap were used to build the database. The study considered horizontal, multi-stage hydraulically-fractured wells. Only wells that came on production at initial reservoir conditions were considered, in order to avoid the effects of secondary recovery processes (e.g., waterflooding) on production. This condition was key to enabling a fair comparison amongst the

wells. As a result, the wells were selected from regions of relatively recent development (2010-2018).

Only wells with complete fracture treatment reports and sufficient production data (at least 365 days of oil production) were included in the analysis. Two different types of data, including discrete and continuous, were considered.

The horizontal wells included in this study were distributed across ten fields. The geological, petro-physical and reservoir characteristics largely vary between fields and within the same field. These characteristics affect hydraulic fracture performance, and ideally, would have been included in the study. However, this type of data was not publicly available. As a result, latitude and longitude, which are indicators of location, are included to account for geological and reservoir quality differences.

The methods used for modeling are purely dependent on the data which in this case, means the data is from field measurements. The main goal of data-driven modeling is to discover patterns between the input and output of the system without considering knowledge of the system physical behavior.

1.6 Thesis Structure

This document contains five chapters. Chapter 2 presents a review of literature relevant to this research project and includes a geological overview of the Viking Formation, the development of data mining methods, the application of data mining techniques in petroleum engineering, and the application of machine learning and artificial intelligence in well performance evaluation.

Chapter 3 describes the data understanding process and modeling workflow. The data collected from this study is presented and the results of the exploratory data analysis are discussed. Additionally, data preparation and final parameters selection for modeling is described. Finally, an overview of the modeling techniques is included.

Chapter 4 discusses the results of each modeling technique. The performance of the models is evaluated and the selected model is interpreted.

Chapter 5 provides conclusions and recommendations.

CHAPTER 2: LITERATURE REVIEW

This literature review focuses on the geological framework of the Viking Formation, the foundations of data mining techniques, and the development of artificial intelligence and machine learning. Furthermore, applications of data mining techniques in petroleum engineering are reviewed and summarized.

2.1 Geological framework

The Viking Formation is considered an important hydrocarbon reservoir in Western Canada. As a result, much research has been conducted in this formation. The term "Viking" was initially applied to the gas-bearing sand located in the Viking-Kinsella field (east-central Alberta) (Slipper, 1918). The formation is Albian age and belongs to the Cretaceous Colorado Group. The Viking is a shallow-marine unit and contains sandstone, siltstones, and shales (Jones, 1961). On average, only about 25% of the formation is clean porous sandstone and conglomerates. The remaining 75% is shaly with low porosity and permeability (Reinson et al.,1994). Generally, it is divided in three units: Upper Viking (Viking A), Shale, and Lower Viking (Viking B). The Upper Viking is a sand dominated unit, containing fine-grained sandstone and mudstone beds while the Lower Viking is made up of shale and silty to sandy mudstones (Borchert, 2018; Reinson et al., 1994).

Figure 2.1 presents the stratigraphic nomenclature for the Viking Formation and equivalents in Alberta, Saskatchewan, Manitoba, Montana and Wyoming. The Viking and its correlative units are extended over the whole Western Canada Sedimentary Basin (Walz et al., 2005). The equivalent units include Bow Island in the southern plains, Paddy Member (Peace River Formation) in the northwest plains, Pelican Formation in the northeast plains and the Newcastle sandstone in Manitoba.

The general stratigraphy of the Viking in southwestern Saskatchewan was first described by Jones (1961), followed by Simpson (1982). Work related to the synthesis of the Viking and equivalent units was presented by Hunt (1954), Stelck (1958), Glaister (1959), and Rudkin, (1964).

In the area of study, the formation lies between two marine shale units, namely the Westgate and Joli Fou Formations, as illustrated in Figure 2.2 (Jones, 1961). The Joli Fou Formation is a marine shale with a small portion of sandstone and is approximately 20 m thick (Walz et al., 2005).

The deposition of the Viking sediments are the result of lateral displacement of the shoreline due to sea-level oscillations (DeWiel, 1956). The deposition of fine-grained marine sediments occurred first, and then the deposition of the Newcastle and Muddy sandstones ocurred. These sands contain plant debris and littoral marine invertebrates in some places (Reinson et al., 1994).

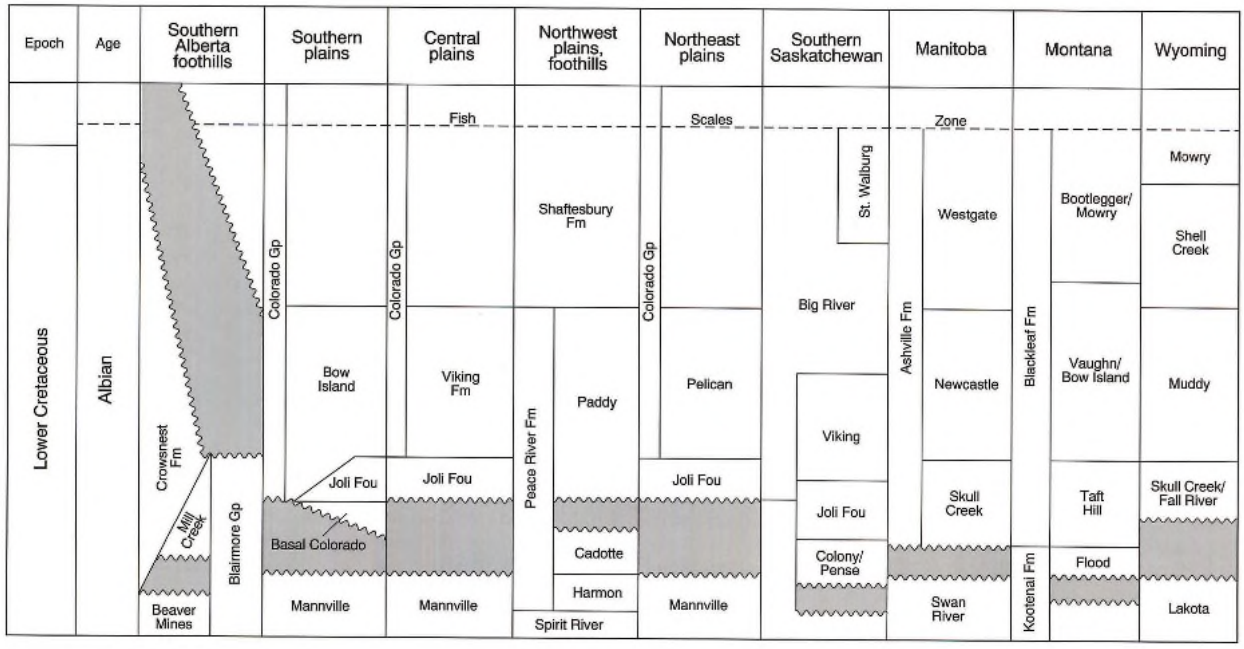

Figure 2.1. Stratigraphic position of the Viking Formation and equivalents units (Reinson et al., 1994).

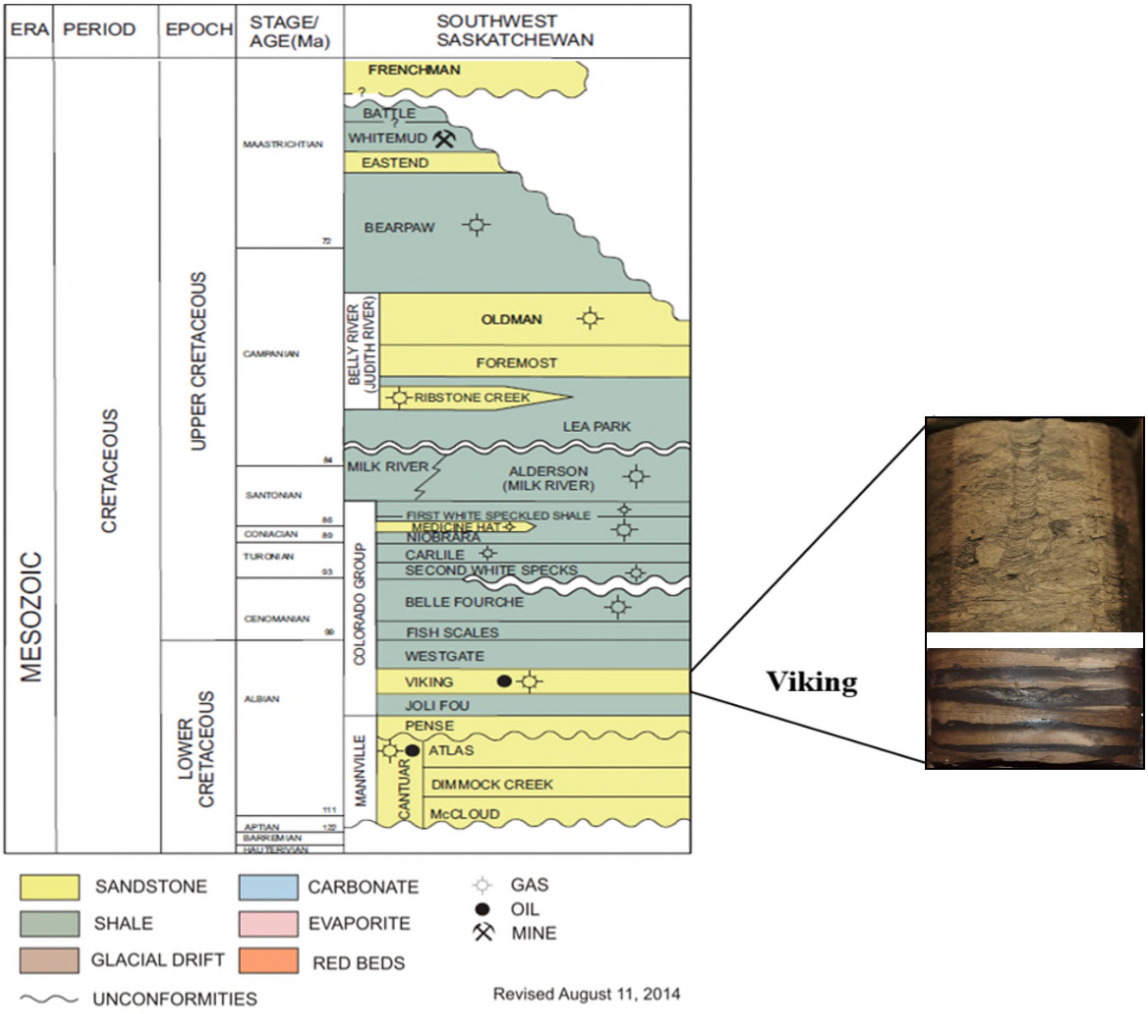

Figure 2.2. Stratigraphic chart of southwest Saskatchewan (Ministry of the Economy, 2014) and core photographs illustrating different reservoir facies in the Viking Formation (after Mathison, 2014).

2.2 Hydrocarbon-bearing reservoir and development

Hydrocarbon production from the Viking has been ongoing since the early 1950's (Mogensen et al., 2012). The most developed areas include Dodsland and Kindersley in Saskatchewan. The reservoir is made up of "centimeter-scaled parallel-laminated and bioturbated oil-bearing sands and interbedded tight shales" (Jans et al., 2014), as illustrated in Figure 2.3.

The Upper Viking has a thickness between two to three meters, while the Lower Viking ranges from three to nine meters (Baishev, 2017). The net-to-gross ratio of the reservoir is hard to establish by using geophysical well logs due to the finely-laminated and interbedded nature of the shales and sandstones (Baishev, 2017; Jans et al., 2014; Mogensen et al., 2012). Based on

core analysis, permeability and porosity ranges from 20 to 80 md, and 15 to 20%, respectively. The Viking is found at a shallow depth of approximately 715 m in the area of study. This results in relatively low drilling and completion costs; however, production is limited due to low reservoir pressure.

Initially, wells were drilled vertically and production was primarily from the upper zone. However, the introduction of horizontal drilling and multi-stage hydraulic fracturing was required due to the low production rates. The combination of these technologies made this play economically more attractive (Baishev, 2017). As of January 2019, 7,937 oil well completions had been placed in the Viking (Saskatchewan). The production from these wells was around 24.5 million m^3 by the end of 2018. On average, production was at a rate of 10,671 m^3/d and the oil gravity was 36° API (Yurkowski, 2019). Main reservoir characteristics for the ten fields considered in this research are summarized in Table 2.1.

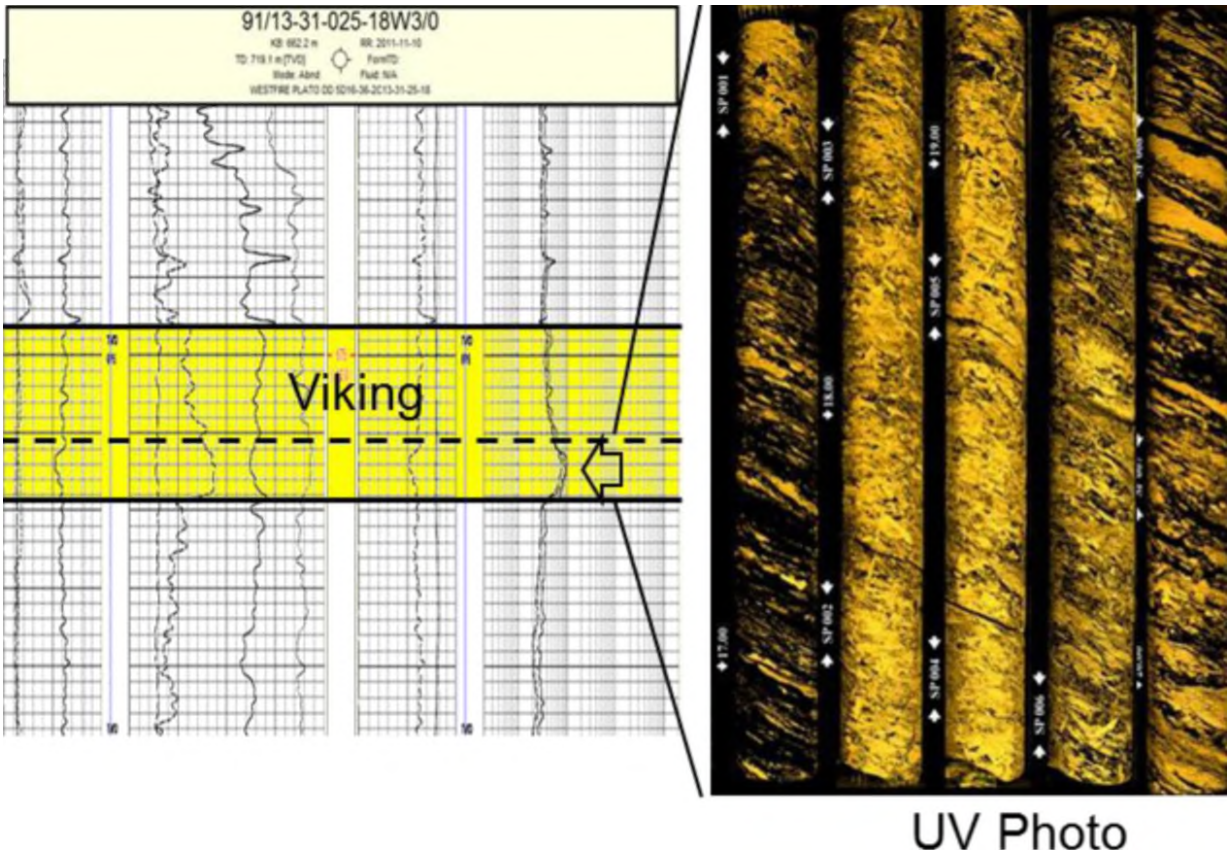

Figure 2.3. Well log and core ultraviolet (UV) photo of the Viking oil-bearing sands (Jans et al., 2014).

Table 2.1. Reservoir characteristics of ten Viking Formation oil fields of interest in Saskatchewan

Field	Discovery year	Area (ha)	Mean Depth (m)	Net pay (m)	Porosity (%)	Water saturation (%)	API (°)	Average GOR (m^3/m^3)	Recovery factor (%)
Avon Hill	1959	11,576	725	3.98	23	45	36.2	73.36	8.6
Kerrobert	1981	27,976	714	2.56	23	45	36.6	99.28	9.80
Dodsland	1956	31,360	671	4.21	22.4	45	36.6	86.69	10.02
Plato North	1978	12,240	705	5.23	23	35	32.1	28.98	9.3
Whiteside	1953	13,049	751	5.65	24	45	31.1	275.89	8.2
Prairiedale	1984	15,704	743	3.88	23	45	31.1	146.60	2.2
Plato	1968	2,218	644	2.7	22	38	33.8	61.75	4.8
Plenty	1985	6,039	640	3.18	23	35	34.4	110.93	5.3
Forgan	1984	567	680	2.6	23	45	36.6	7.47	4.6
Eureka	1954	2,024	724	6.8	23	42	35.2	92.77	4.90

2.2 Foundations of data mining

The concept of data mining has been around since the 1990s and has appeared in different environments including academia, business and medical activities (Gorunescu, 2011). In general, data mining refers to the process of identifying hidden trends in a dataset in order to transform the data into knowledge (Mohaghegh, 2017).

According to Gorunescu (2011), data mining has three main foundations: statistics, artificial intelligence (AI) and machine learning (ML), and database systems (DBS). Statistics provides the foundations for what is known as exploratory data analysis (EDA), which is used to establish patterns between the variables. Some of the techniques employed in EDA are computational methods (i.e., descriptive statistics, correlation matrices, cluster analyses, linear and nonlinear models), and data visualization (i.e., histograms, boxplots, scatterplots and contour plots). AI and ML provide the data processing techniques. AI is based on a human reasoning model, and ML uses techniques to allow computers to learn with training. Database Systems provide a platform

for storing, organizing and accessing data to be analyzed by implementing the techniques described above.

Generally, there are six steps to conduct data mining projects as introduced in Section 1.4. These steps include data collection, cleaning, transformation, mining, pattern recognition and interpretation of the results (Kamath, 2005). A complete description of these steps can be found in Gorunescu (2011). Data mining is a process to construct a data-driven model. Different data mining techniques can be applied to discover patterns and obtain meaningful results. Generally, these techniques are categorized based on their task. The categories include predictive, descriptive, and optimization. Figure 2.4 presents the classification of the different data mining techniques according to their task (Fawzy et al., 2016).

The objective of predictive approaches is to predict future values. This approach typically uses supervised learning algorithms, in which input and output values are required to build the predictive model. Some of the most common methods for prediction include classification, regression, and classifier ensembles. On the other hand, descriptive approaches apply unsupervised learning to better understand past events and discover trends and relationships in the data. In this approach, the input data are used to understand past events. Methods, such as clustering, association, anomaly detection, and dimensionality reduction fall under this approach (Fawzy et al., 2016; Wang, 2018).

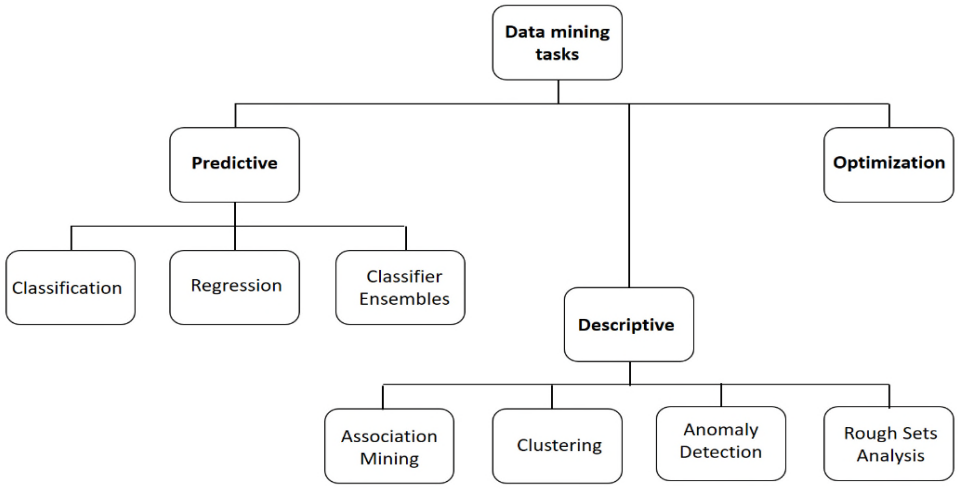

Figure 2.4. Principal data mining tasks (Fawzy et al., 2016).

Data mining techniques have been implemented in several fields to provide solutions to real-life problems. Based on Gorunescu (2011), some of the fields interested in the application of these techniques include:

- Banking and financial services, in which data mining methods are applied to risk assessment, trend analysis, marketing campaigns, forecasting the price of goods and financial disasters, among other applications.
- Health care professionals have implemented data mining methods for predicting costs, computer-aided diagnosis, and visualization techniques.
- The telecommunications industry has used data mining techniques to determine customer profiles, develop strategies for selling products, fraud prediction, and to establish differences in products between companies.

2.3 Development of Artificial Intelligence (AI) and Machine Learning (ML)

The term “artificial intelligence” was initially suggested by John McCarthy in 1956 (Tecuci, 2012). Artificial intelligence creates systems that show characteristics associated with human intelligence like natural language, perception, problem-solving, learning, and adaptation (Tecuci, 2012). The foundations of AI are related to several domains, such as computing, mathematics, linguistics, psychology, neuroscience.

AI systems are implemented to add intelligence to complex applications. Figure 2.5 represents the elements of an intelligent agent. First, the agent observes the environment (i.e., real world, internet, and graphical interface), and based on the environment, the agent executes their required tasks. This agent will continue learning from data, other agents, and its own experience; as a result, their performance will improve continuously. Furthermore, AI systems have the ability to take high-level requests and decide how to complete these with autonomy, and they can collaborate with other agents to increase performance on their tasks (Tecuci, 2012).

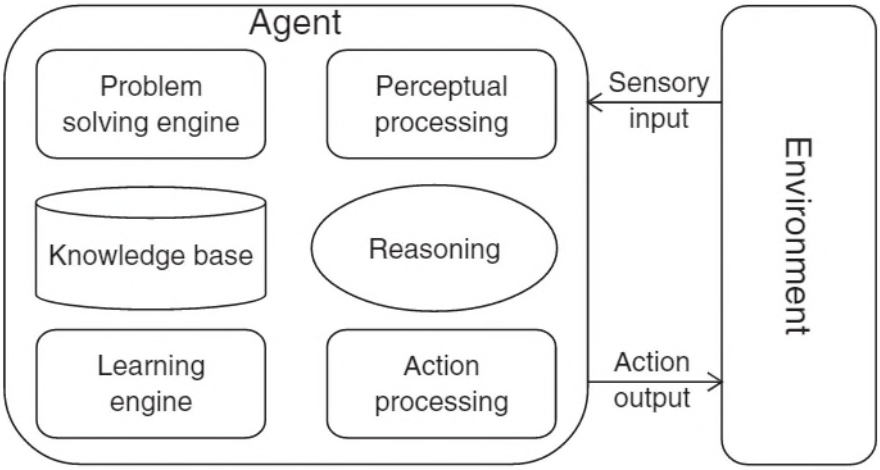

Figure 2.5. Components of a knowledge-based agent (Tecuci, 2012).

AI was split into several areas, such as natural language processing, neural networks, genetic algorithms, and probabilistic reasoning. Additionally, an intelligent system can be developed by using a symbolic or sub-symbolic approach (Tecuci, 2012).

The AI industry started with the creation of expert systems that integrate domain and human problem-solving expertise to improve the businesses (i.e., medical diagnosis, engineering design, intelligence analysis, etc) (Tecuci, 2012). In recent times, AI methods have become more dependent on data than on algorithms due to the increase of computational power and data availability (Tecuci, 2012).

Machine learning is the part of artificial intelligence that allows machines to achieve their tasks by using intelligent software (Mohammed et al., 2016). The foundations of intelligent software are the statistical methods, which are employed to create machine intelligence. The algorithms used in machine learning need data to learn. There are different machine learning methods, such as supervised, unsupervised, semi-supervised and reinforcement learning. In supervised learning, the model learns from labeled data. On the other hand, in unsupervised learning, data presented to the model is unlabeled. Semi-supervised refers to the combination of labeled and unlabeled data. In reinforcement learning, the algorithm learns in an interactive manner by receiving feedback (Mohammed et al., 2016).

In general, the purpose of learning is to build a model that processes the input data and provides the desired output. Sometimes the model can be understood, but at other times it can be a “black box”, which means that the model cannot be interpreted. Since the model is an approximation of a particular process, some errors can be expected. As a result, the performance of the model should be measured (Mohammed et al., 2016).

It is clear that the application of AI and ML has the potential to generate value in different sectors, including advanced technology (“high tech”), health care systems, banking, oil and gas, chemicals and telecommunications, among others. These powerful technologies are at the cutting edge of innovation. Moreover, large volumes of data, computational processing, and affordable data storage have made possible the development of models that analyze complex data and provide high accuracy results at large scales.

2.4 Application of AI and ML in petroleum engineering

Digital oilfields of the future (DOFFS) and intelligent wells using several sensors create large amounts of structured data rapidly. Additionally, these data are complemented with the unstructured data generated by social media and mobile devices used in field operations. Cloud computing allows data management and flexibility. These advances have made data mining methodologies an essential part of the oil and gas industry (Brennan & Schafer, 2014). Several authors have used data mining techniques in different areas, including drilling and production optimization, reservoir characterization, and well performance evaluation.

In the oil and gas industry, three types of models have commonly been used; i.e., mathematical, empirical, and physical. Mathematical models are an approximation of the processes in real life, and are developed according to first principles of science such as conservation of momentum, mass and energy. In this industry, conventional modelling is frequently time consuming because the models must be continually refined until desired results are achieved. Furthermore, several assumptions are made in order to construct these models (Balaji et al., 2018). In contrast, empirical models can be developed more easily and more quickly; however, results cannot be generalized and the accuracy may be low. Physical models can be useful for investigating specific processes and mechanisms at the laboratory scale, but the results are often not readily

applicable at the field-scale; especially for complex, coupled processes (such as hydraulic fracturing) in heterogeneous media.

The implementation of data mining methods in the oil and gas industry offers a wide range of benefits due to the ability to turn complex and large data into knowledge. Data-driven modeling is based on computational intelligence (CI) and machine learning (ML). CI involves artificial neural networks, fuzzy rule-based systems, and evolutionary computing. ML is a subcomponent of AI, and uses the theoretical foundations from CI. These two methods are employed to build the data-driven models in the industry and these provide an alternative to mathematical modeling (Balaji et al., 2018; Brennan & Schafer, 2014).

Some of the main techniques employed in data-driven modeling include artificial neural networks and tree-based methods. Neural networks have shown a great potential for creating predictive models. The main objective for implementing such techniques is to obtain a clear explanation of the problem at hand. This model can be implemented as an alternative when mathematical models are not feasible due to complicated relationships between variables or missing data. The technique can be used for classification and regression tasks (Brennan & Schafer, 2014). In essence, a neural network is an information processing system that is similar to biological neural networks. They can handle nonlinear data and they perform complex functions well.

Tree-based methods are widely used because they are simple and can be easily interpreted. One of the most common methods is “Random Forest (RF)”, which is a collection of decision trees. This supervised learning algorithm can also handle complex data relationships, and the algorithm can be applied to classification and regression problems. RF provides great advantages, such as high predictive capabilities, speed, and their ability to handle multi-attribute data and noise (Aulia et al., 2014; Balaji et al., 2018).

The next subsections present the different application of AI and ML in the oil and gas industry. The application areas are categorized in reservoir characterization, drilling optimization, production optimization, and reservoir management.

2.4.1 Reservoir characterization

Reservoir characterization refers to the calibration and determination of reservoir parameters, such as thickness, net-to-gross ratio, porosity, permeability, and water saturation. Several field measurements including geophysical well logs, production data, core analysis, and mapping of seismic attributes are required to characterize a reservoir (Brennan & Schafer, 2014). Subsurface models explain the fluid flow through the reservoir due to certain natural characteristics. These models are useful to design optimal strategies to exploit the oil and gas that have accumulated in the reservoir.

Traditional reservoir simulation is a bottom-up approach that begins with a geo-cellular model, followed by a dynamic reservoir model. This approach relies on first principles and fluid flow theory. However, it is time-consuming, and a calibration process (history matching) is needed after the model is developed (Brennan & Schafer, 2014). On the other hand, the application of advanced data-driven methods, such as fuzzy logic, pattern recognition, artificial neural networks, and support vector machine, have provided an alternative to traditional reservoir modeling (Kumar, 2012).

Kumar (2012) used neural networks to predict reservoir characteristics, such as porosity and permeability. The model was trained by using several well logs such as gamma-ray, depth, core porosity, and core permeability. Some of the advantages of implementing this method were the high accuracy, reliable prediction, and ability to integrate other attributes (seismic attributes and topography).

Wong et al. (1998) estimated reservoir permeability using the backpropagation neural network model. The predictive model was developed by acquiring data from core and well logs. The neural network was trained using data from two wells and was tested with a third well. Al-Anazi & Gates (2012) used a support vector regression model to predict porosity and permeability in a heterogeneous reservoir using a small sample. Additionally, the performance of support vector regression was compared with a multilayer perceptron neural network model. The results revealed that the support vector regression outperformed the neural network when considering a small sample size.

2.4.2 Drilling optimization

Drilling is one of the most important and complex tasks in the industry. These operations account for almost half of the well costs. Therefore, errors during drilling could be costly and have a negative effect on health, safety and environment. The main goal of drilling optimization is to drill a well in the most efficient way. A few of the skills needed to achieve this goal include, borehole pressure management, drilling fluids engineering, rock mechanics, and drill bit selection (Brennan & Schafer, 2014).

The use of a real-time operation center (RTOC) creates large volumes and a variety of data. Analytical workflows that integrate multidisciplinary data are useful to establish trends and correlation in drilling systems, real-time identification of wellbore issues, well pressure management, and forecasting workflows (Brennan & Schafer, 2014).

Bataee & Mohseni (2011) optimized drilling parameters to achieve the proper rate of penetration (ROP). The parameters considered in the study include bit diameter, depth, weight on bit (WOB), revolutions per minute (RPM), and mud weight. The authors used artificial neural networks to establish correlations between the parameters and genetic algorithms to help with the optimization of drilling parameters. Results indicated that using less mud weight can lead to higher ROP. Additionally, increasing WOB does not necessarily increase ROP.

Pollock et al. (2018) created an artificial intelligence system, in which machine learning algorithms were used to increase the efficiency of directional drilling. The model input was a combination of historical and simulated data related to the information used by directional drillers. These data were utilized to create more efficient decisions based on past experiences. Furthermore, historical data regarding directional drilling was collected to develop a system to control bit orientation. A neural network was trained, and the model was able to minimize deviation and tortuosity in the wellbore trajectory, and maximize ROP.

Abbas et al. (2019) developed two models which included an artificial neural network, and a support vector machine in order to predict a stuck pipe solution for vertical and deviated wells. The models were developed by using data from drilling operations, formation types, and fluid

characteristics. Both models offer great results; however, support vector machine outperformed the neural network. The developed intelligent system was able to offer effective solutions to drilling engineers when they had stuck pipes.

2.4.3 Production optimization

Production optimization is done to reduce unplanned shutdowns, control operational expenditures (OPEX) and capital expenditure (CAPEX) costs, and increase the exploitation of reserves and asset performance. Traditional reservoir simulation and optimization uses numerical models (Brennan & Schafer, 2014). In this bottom-up approach, first the petro-physical and geophysical data are integrated, and then fluid flow is added to obtain a dynamic reservoir model, which in the end is calibrated with historical production data. The final model is used to formulate engineering strategies, such as infill drilling, improve recovery factor, or enhance well performance (Brennan & Schafer, 2014). On the other hand, data-driven methodologies are based on a top-down workflow. Core data, wireline logs, and seismic attributes are some of the data types considered when developing these models. A high-level appreciation of the field and reservoir can be obtained by using these type of methods (Brennan & Schafer, 2014).
Temizel et al. (2017) investigated injection/production practices for waterflooding operations to increase recovery utilizing big data analytics. Past injection and production data were used to establish the optimum injection levels considering multiple factors, such as completion strategies, number and location of producers, vintage of wells, and injection history.

Ebrahimi & Khamehchi (2016) developed a support vector machine (SVM) model to optimize the natural gas lift process, which is traditionally made using numerical simulation software. Results showed that SVM is capable of achieving an optimum solution in a short period of time compared to the simulation software. Additionally, the performance of the model was successfully optimized by using evolutionary algorithms.

Li, Chan, & Nguyen (2013) developed three different predictive models including artificial neural network (ANN), neural decision tree (NDT), and C4.5 (a decision tree learning algorithm), in order to predict oil production and compared the performance of the models. Results indicated that ANN outperformed the other two models in terms of prediction accuracy.

2.4.4 Reservoir management

Reservoir management seeks to maximize the net present value of the hydrocarbon reserves and minimize the expenses, such as CAPEX and OPEX. Lifecycle optimization of the reservoir is crucial to optimize short-term and long-term production. The models must to be updated with production measurements, time-lapse seismic reflection surveys, and other accessible data (Brennan & Schafer, 2014) .

The application of data-driven methods in reservoir management provides a method to construct complex multivariant models. These models can be fed with large amounts of multidisciplinary real-time data generated from sensors in intelligent wells. Therefore, these methods can maximize the integration of knowledge from different areas, increase reliability of reservoir performance, and reduce uncertainty (Brennan & Schafer, 2014). Brown et al. (2017) used artificial intelligence and machine learning to identify oil field rejuvenation opportunities. This data-driven technology integrated geological and well data, such as wireline logs, completion, production/injection by well, and well trajectories. Results showed that opportunities can be rapidly identified and validated. Additionally, this technology can help businesses to make decisions with high confidence and in a timely manner.

Yanfang & Salehi (2014) developed an artificial neural network to predict re-stimulation candidate wells in an oilfield. The model was fed with well geographical and historical production data. The constructed model was able to make prediction with up to 90% accuracy.

Nwachukwu et al. (2018) employed Extreme Gradient Boosting (a decision tree-based ensemble machine learning algorithm) to predict reservoir responses according to injection well locations. Data used in the study was generated using numerical reservoir simulations. Connectivity between wells was introduced in the model input to increase prediction accuracy. Five case studies, including three waterflood and two CO_2 flood scenarios were evaluated. The reservoir responses (model output) were metrics such as profit, cumulative oil/gas produced, and net CO_2 stored. Results from the study demonstrated that this approach can be used as an alternative to numerical simulation and save computational time.

2.5 Application of AI/ML in well performance evaluation and completion design

Hydrocarbon recovery from unconventional reservoirs is a continuous source of economic growth. The integration of various disciplines such as seismic, drilling, completion, geomechanics, production, and data science is vital to the success of commercial and economic development of these highly capital-intensive projects. The advantages of optimizing production and completion design include an increase in well performance, costs reductions, and exploitation of more reserves.

Traditionally, these optimizations are performed using reservoir simulation; however, this strategy is time-consuming and difficult due to the complex processes of hydraulic fracturing in unconventional reservoirs (Wang & Chen, 2016). As a result, data-driven methods provide a promising complement to physics-based techniques for assessing hydraulic fracturing performance and optimizing completion designs. Several authors have demonstrated the potential of these techniques using multi-disciplinary data to construct the models. Such models make it possible to develop a better understanding of the effect of multiple parameters on production performance. This is useful to evaluate the viability of exploration and development of hydrocarbon sources by focusing on parameters that are under operator control. Different artificial intelligence and machine learning methodologies have been applied over the years to facilitate the optimization of horizontal well completion designs in several assets. It is worth mentioning that optimizations can vary from asset to asset.

Shelley et al. (2008) analyzed Barnett Shale completions and their effect on cumulative gas production. A total of 393 wells from 30 fields was considered. Completion and reservoir related parameters were included in the analysis. The authors compared the performance of two fracture stimulation types; namely crosslinked gel (XLG) and sand waterfracs (SWFs). The results from the statistical evaluation indicated that the 12-month cumulative gas production quantities exhibited weak correlation with reservoir and stimulation parameters. Since the results from the statistical and visual analysis were not satisfactory, the authors performed a cluster analysis using self-organizing maps (SOM), which are a type of neural network. Results from the SOM analysis indicated that SWF outperformed XLG treatments. Furthermore, stimulation characteristics, such as volume of proppant, volume of fluid, number of stages, and pump rate can positively or

negatively affect gas production depending on reservoir characteristics and fracture stimulation type.

Mogensen et al. (2012) evaluated and compared the performance of vertical and horizontal multi-stage hydraulically fractured wells in the Viking Formation in Alberta and Saskatchewan. Furthermore, the authors identified the most successful operators in each area and compared field production. The authors proposed the 4^{th} month production rate as an effective production metric to evaluate well performance. Production performance was assessed by using a Purvis plot. The authors found that production from horizontal multi-stage hydraulically fractured wells were 2.8 times higher than vertical wells. Additionally, field performance was evaluated by employing histogram plots. The most productive areas include Redwater and Halkirk.

Nejad et al. (2015) investigated the effectiveness of the completion strategy and fracture treatment design in the Eagle Ford Shale in Gonzales, Karnes and Atascosa counties. The authors recommended the use of statistical and machine learning techniques to select the appropriate variables for the model. An artificial neural network was developed to evaluate hidden correlations between the input and output variables. The model was able to predict production with a coefficient of determination (R^2) greater than 0.80. Additionally, a sensitivity analysis was performed to determine the importance of each parameter. According to this ranking, the depth to the Eagle Ford Shale with respect to sea level was the most important reservoir parameter, followed by the number of stages that employed high-conductivity fracture designs. These two parameters were found to greatly affect hydrocarbon production rates.

Wang & Chen (2016) predicted cumulative oil production in the Bakken Formation in southeastern Saskatchewan using a neural network. Sobol's sensitivity was performed to establish the importance of each variable. The authors used data from 2780 multi-stage hydraulically fractured horizontal wells and 139 vertical wells. Using the vertical wells, the formation thickness was determined by employing the kriging interpolation method. Six-month and eighteen-month cumulative oil production were selected as the dependent variables. Some of the techniques used to develop the neural network model included one-hot encoding, Xavier initialization, a dropout technique, batch normalization, Adelta optimizer, and k-fold cross

validation. The R^2 of the neural network model for six-month and eighteen-month cumulative oil production volumes were 0.58 and 0.56, respectively. According to the Sobol's first and total order indices, the average of proppant placed per stage contributed to the greater variability of the six-month cumulative production. Similar results were found by considering long-term production (eighteen-month oil production).

Shelley et al. (2014) evaluated completion effectiveness and identified production drivers in Marcellus shale in Susquehanna County in Pennsylvania. An artificial neural network (ANN) predictive model was constructed and a sensitivity analysis was performed using the developed model. The authors proposed the use of measurements obtained during drilling as indicators of reservoir and fluid properties due to the absence of reservoir parameters such as total organic carbon (TOC), thickness and porosity, which are generally extracted from geophysical well logs. Average gamma ray, gas counts, mud weights, and rate of penetration were included in the study. Furthermore, 48 hydraulically fractured wells were used to construct the model. Genetic algorithms were employed to identify an appropriate neural network architecture. The ANN model was able to predict the first 30 days cumulative gas production with an R^2 of 0.82. Additionally, results from the sensitivity analysis indicated that reservoir quality and geology have a significant impact on well performance. True vertical depth is the main gas production driver in Marcellus followed by stage count and formation thickness.

Bowie (2018) optimized well designs in Durvernay shale in the Fox Creek area of Alberta by using a multiple linear regression (MLR) and a neural network (ANN). The models were developed using 262 horizontal wells, varying from dry gas to volatile oil producers. The potential effect of each feature on the well performance variance was established by testing one parameter at a time in each model run. It was found that the MLR and ANN explain 63% and 78% of the well performance variance, respectively. Using the ANN model, a sensitivity analysis was performed. Results revealed that there was no benefit obtained in this reservoir by using expensive proppants, such as ceramic or resin coated, or using hybrid fluid systems. Volume of proppant injected was found to be the main driver of well productivity, and fracture pump rate also positively affected production. Furthermore, well performance could be significantly

improved by changing controllable operating parameters, with improvements varying from 19% up to 97% depending on the operator.

Wang & Chen (2016b) developed a data mining workflow to evaluate hydraulic fracture performance in the Montney Formation. The workflow integrated cluster analysis, reduction of dataset dimensionality and an artificial neural network model. A database of 1521 horizontal wells was considered in the study. Stimulation characteristics, such as well geographic location, true vertical depth, completion strategy, proppant and fluid intensity, were included as model inputs. 6-month cumulative production was used as a model output to evaluate well performance. A differential evolution algorithm was employed to optimize the neural network topology. The optimum ANN model predicted production with a determination coefficient of 0.80 using the test data. Results showed that shallower wells (i.e., 1000 m TVD) had average production volumes of only 17.49 million barrels of oil equivalent (MBOE) while deeper wells (i.e., 3000 m TVD) had production volumes as high as 86.33 MBOE. Additionally, high volumes of proppant and fluid pumped positively contributed to oil production.

Clar & Monaco (2019) constructed an artificial neural network model using data from approximately 13,000 horizontal wells landed and completed in the Eagle Ford Shale. Wells were classified as oil or gas producers based on Gas Oil Ratio (GOR). A bootstrap re-sampling technique was employed to evaluate the uncertainty in the model predictions. This novel methodology was validated using a synthetic dataset and then applied to the real dataset from the Eagle Ford. Results indicated that true vertical depth (TVD) was the main oil and gas production driver. The authors suggested that TVD might be related to reservoir pressure and in-situ stresses, which were not included in the study. Furthermore, lateral length was also identified as a key production driver. Fluid intensity could increase gas and oil production by 6% when the volume of fluid was doubled. Proppant intensity enhanced production from 11 % to 16% when the proppant volume was tripled.

Hirschmiller et al. (2019) integrated geoscience and engineering data to identify which geological, reservoir and completion parameters affect well productivity in the Spirit River Formation. The wells were distributed across the entire play. A machine learning model was

developed to predict 12-month cumulative gas production. Recursive feature elimination was used to select the features that provide the highest prediction performance. The developed model was able to predict gas production with an R^2 of 0.53. The importance of features was estimated using the model. Completion length and proppant intensity were the two parameters that mostly affected the variability of gas production in the first year. Additionally, the authors quantified the effect of each feature on well performance by using model-agnostic methods. A spearman coefficient was determined to identify multicollinearity between the variables.

Luo et al. (2019) developed three data-driven models including partial least square (PLS), random forest (RF), and artificial neural network (ANN) in order to establish relationships between subsurface and completion characteristics in the Eagle Ford Formation. The wells included in the study were distributed across the basin. The model's performance was compared by using the coefficient of determination and mean squared error. One-hot encoding method was employed to handle categorical variables. Furthermore, the minimum redundancy maximum relevance (MRMR) method was used to determine the subset of features that are most important to the target parameter. This technique also helped to select features with non-linearity. The models were constructed by using data from 3600 horizontal wells. The output of the model was 6-month cumulative barrels of oil equivalent (BOE). The RF model had the highest performance, with an R^2 of 0.62 in the test set. The authors suggested that the overall accuracy in the models could be improved by adding more data regarding geological and completion parameters, such as reservoir pressure, faults, well spacing and fracture spacing. The parameter ranking indicated that depth is the most influential factor in well productivity in the Eagle Ford.

2.5.1 Summary of reported case studies

Machine learning and artificial intelligence have been widely used to evaluate hydraulic fracture performance and optimize completion designs in several formations. The implementation of these techniques has resulted in a better understanding of well performance, and quantified complex and non-linear relationships between subsurface and completion characteristics. One of the main advantages of data-driven models is that there is no need to make assumptions or introduce any knowledge into the models. However, constraints in the analysis should be considered based on physical principles to ensure that results do not contradict engineering

theories. Additionally, quality data and the integration of multi-disciplinary data are critical to the success of these types of analyses.

Few studies have evaluated hydraulically fractured well performance in the Viking Formation. To the best of the author's knowledge, studies that have applied advanced data mining techniques to assess well performance in the Viking do not exist in the literature. Furthermore, the developed data-driven methodology in this study does identify production drivers at a field and well level by quantifying the effects of each feature based on hydrocarbon production records.

CHAPTER 3: DATA UNDERSTANDING AND PREPARATION

Obtaining an understanding of the data and data preparation are key steps in every data-mining project. Initial insights are gained about the database by using descriptive and graphical techniques to extract useful knowledge. The preparation step refers to the process of cleaning the data and assessing its quality.

This chapter is divided in four major sections. Section 3.1 describes the data collection process, and lists the parameters considered in this study. Section 3.2 presents the exploratory data analysis (EDA) in which descriptive statistics and multiple graphical techniques are used to obtain general information about the dataset. Section 3.3 states the process and methods used to clean and obtain the final dataset for modeling. Finally, section 3.4 presents an overview of the two modeling techniques, including a multiple linear regression and random forest.

3.1 Data Collection

A database of 875 horizontal multi-stage hydraulically fractured wells from the Viking Formation was constructed by collecting data from GeoVista and Accumap. Only wells with complete stimulation reports and at least one year of oil production data were included. The list of parameters, categories, units, source and data type are presented in Table 3.1.

For each horizontal well, 13 parameters were extracted. The features were divided into four categories: well geographic location, reservoir, stimulation, and well performance. Some of these features were collected directly from public databases, others were calculated, and net pay values were provided by Baytex Energy Corp (Baytex). Moreover, two different data types, continuous and discrete, were considered. Details regarding how some of the independent parameters were estimated are given in the next section. The complete database used to perform this study can be found in Appendix A.

Table 3.1. Lists of the dependent and independent variables considered in the study.

No.	Category	Parameter	Units	Source	Data type
Independent Variables					
1	Location (surface coordinates)	Latitude	°	GeoVista	Continuous
2		Longitude	°	GeoVista	Continuous
3	Reservoir	True Vertical Depth	m	GeoVista	Continuous
4		Net pay	m	Baytex	Continuous
5		Average GOR	$\frac{m^3}{m^3}$	Baytex	Continuous
6	Completion and stimulation	Completion length	m	Accumap	Continuous
7		Number of stages		GeoVista	Discrete
8		Average stage spacing	m	Calculated	Continuous
9		Proppant intensity	$\frac{t}{m}$	Calculated	Continuous
10		Fluid intensity	$\frac{m^3}{m}$	Calculated	Continuous
11		Proppant concentration	$\frac{t}{m^3}$	Calculated	Continuous
Dependent Variables					
12	Well performance	365-day cumulative oil production	m^3	GeoVista	Continuous
13		365-day cumulative oil production / completion length	$\frac{m^3}{m}$	Calculated	Continuous

True vertical depth, net pay, and average gas-oil ratio were included as reservoir parameters. Latitude and longitude were incorporated as indicators of well geographical location. These parameters were used to indirectly account for geological differences between wells, in the absence of maps showing regional variations in geological and reservoir properties such as porosity, water saturation, permeability and reservoir pressure.

During hydraulic fracturing treatments, large volumes of fluid and proppant are injected at a high rate and pressure to create tensile fractures in the rocks. This stimulation method is primarily used to increase the permeability of the reservoir (Belyadi et al., 2016). The proppant is pumped

to prevent the closure of the fractures due to in-situ stresses (Belyadi et al., 2016). Completion and stimulation characteristics, including volume of fluid and proppant, completion length, number of stages, average stage spacing and proppant size, play key roles on well performance.

Well performance refers to the production metrics (model output) that will be used to compare and evaluate the different reservoir, stimulation, and proppant selection characteristics. 365-day cumulative oil production, and normalized oil production by completion length were considered as metrics. These metrics allow comparison between well production while accounting for the downtime during operations. It is worth mentioning that the only metric ultimately considered as a model output was 365-day cumulative oil production. Normalized production was only used for comparison purposes during the exploratory data analysis.

3.2 Exploratory Data Analysis

Once the data was collected, exploratory data analysis (EDA) techniques were used as a starting point to gain some insights about the data and identify any errors or inconsistencies. Descriptive statistics, such as mean, standard deviation, minimum, first quartile (25%), median (50%), third quartile (75%), and maximum values provided general information about the dataset. Moreover, EDA graphical techniques were useful to extract knowledge from the database. Histograms were employed to summarize the distribution of the data. Boxplots were created to identify relationships between two variables, identify outliers and refine the dataset. Additionally, cross plots were used to discover trends between a pair of variables. The data visualization for this study was performed by using Matplotlib and Seaborn. These two libraries can be used in Python scripts and provide a high-level interface to create statistical graphics.

3.2.1 Fields in the Viking Formation

The database contained data from 10 fields located in Saskatchewan. Table 3.2 lists the field, the number of wells in each field, and the participation percentage in the whole database (i.e., of the 875 wells in the database, the percentage of wells in a given field).

Figure 3.1 is a graphical representation of the distribution of wells in each field. Avon Hill was the field with the greatest participation in the study, followed by Kerrobert and Dodsland.

Table 3.2. List of the fields located in Saskatchewan considered in this work.

No.	Field	Number of wells	Percentage
1	Avon Hill	212	24.23
2	Kerrobert	139	15.89
3	Dodsland	130	14.86
4	Plato North	120	13.71
5	Whiteside	100	11.43
6	Prairiedale	76	8.69
7	Plato	65	7.43
8	Plenty	17	1.94
9	Forgan	10	11.43
10	Eureka	6	0.68
	Total	875	100

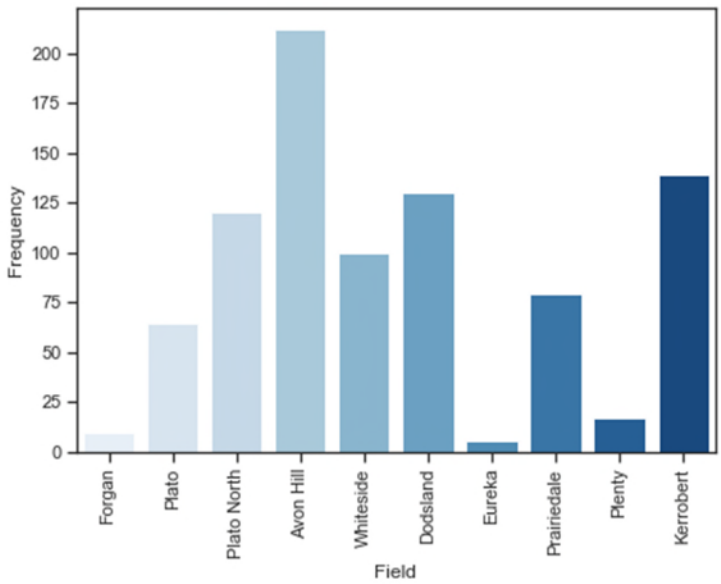

Figure 3.1. Distribution of the horizontal multi-stage hydraulically fractured wells in each field

3.2.2 Major operators in the Viking Formation

A total of seven operators were included in this study. The operators with the highest participation were Baytex, Teine Energy Ltd, and Crescent Point Energy. These three operators accounted for more than 70% of the entire number of wells in the database. Table 3.3 shows a summary of the operators, their well count, and their representative participation percentage in the database. The distribution of the number of wells by operator can be observed in Figure 3.2. The operators serve as a grouping factor to compare well performance due to differences among the parameters that each records in the well log records.

Table 3.3. List of operators in the Viking Formation considered in the study.

No.	Operator	Number of wells	Percentage
1	Baytex	265	30.3
2	Teine Energy Ltd.	230	26.3
3	Crescent Point Energy	177	20.2
4	Whitecap Resources Inc.	94	10.7
5	Ish Energy Ltd.	75	8.5
6	Novus Energy Inc.	29	3.3
7	NAL Resources	5	0.6

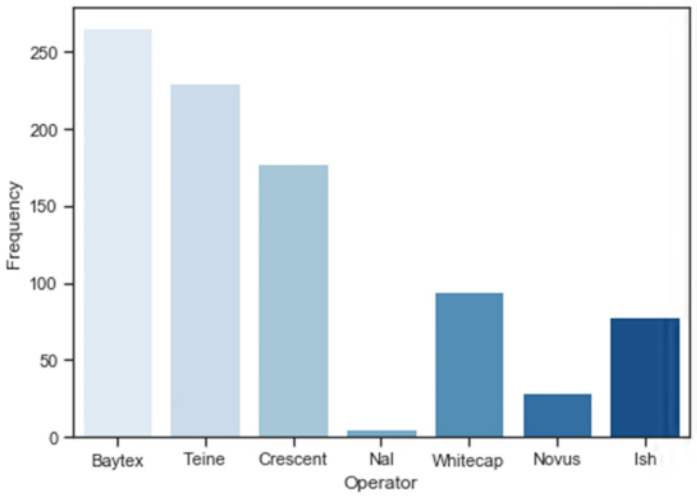

Figure 3.2. Distribution of the horizontal multi-stage hydraulically fractured wells by operator.

3.2.3. Latitude and Longitude

Latitude and Longitude (surface coordinates) were included to account for the fact that geological and reservoir quality may be different at different well locations. Figure 3.3 illustrates the location of each well and the distribution of 365-day cumulative oil production normalized by lateral length. Visualizing the oil production distribution was useful to determine the potential of the different areas. It can be seen that oil production varies across the regions, which suggests that the reservoir quality is highly heterogeneous. Overall, high oil production was observed in the southeast area (Plato North) and low production was observed in the northwest area (Kerrobert and Prairiedale).

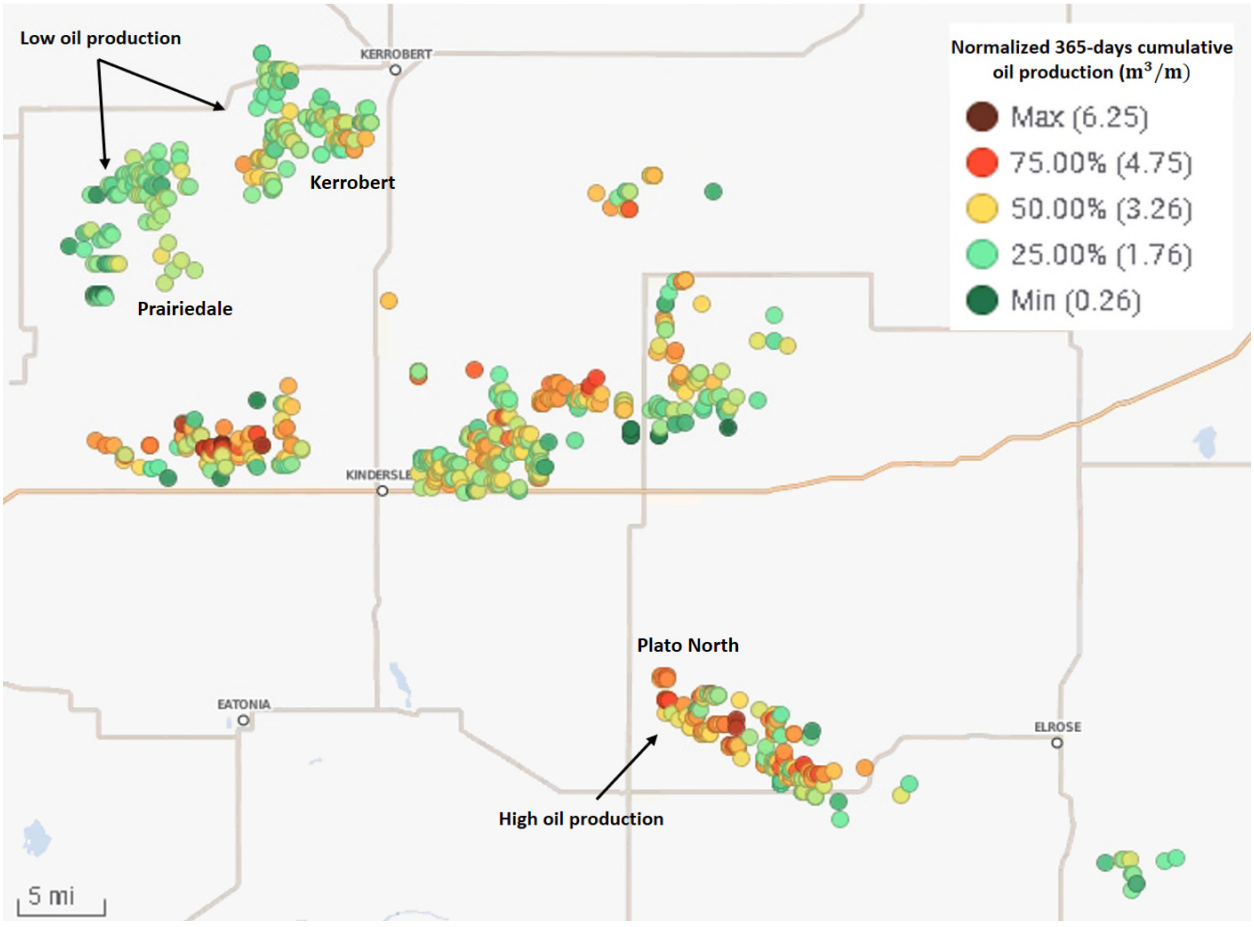

Figure 3.3. Location of each well color coded by normalized 365-day cumulative oil production

3.2.4 Net pay

The net pay refers to the interval of a reservoir that contains recoverable hydrocarbons. The net pay values of the study area were provided by Baytex. The values ranged from 0 m to 7.32 m,

with an average of 3.94 m. Figure 3.4 illustrates a positive weak correlation between net pay and 365-day cumulative oil production, with a correlation coefficient of 0.03.

A net pay map of the Viking Formation, in which the wells were color coded by normalized oil production, was constructed to assess the effect of net pay on initial production (Figure 3.5). It was observed that the net pay of the Viking Formation is highly variable. Furthermore, some of the areas with the highest production, including Whiteside and Plato North, had high net pay values. On the other hand, areas with average low production, such as Forgan and Kerrobert, had low net pay values. These observations indicated that net pay could be one of the main oil production drivers.

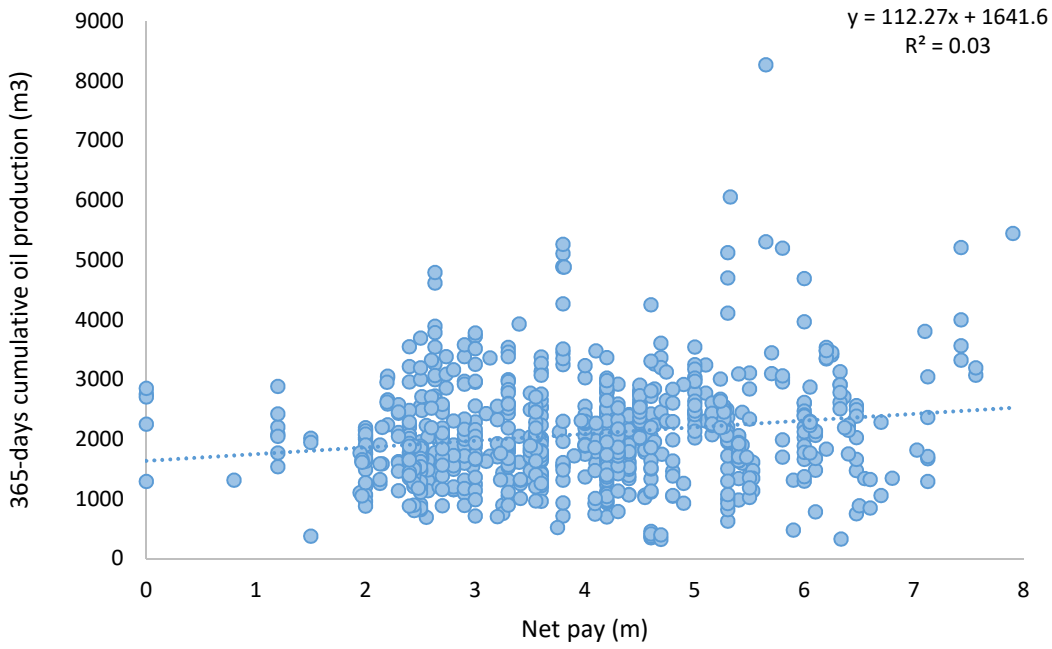

Figure 3.4. Cross plot comparing net pay and 365-day cumulative oil production.

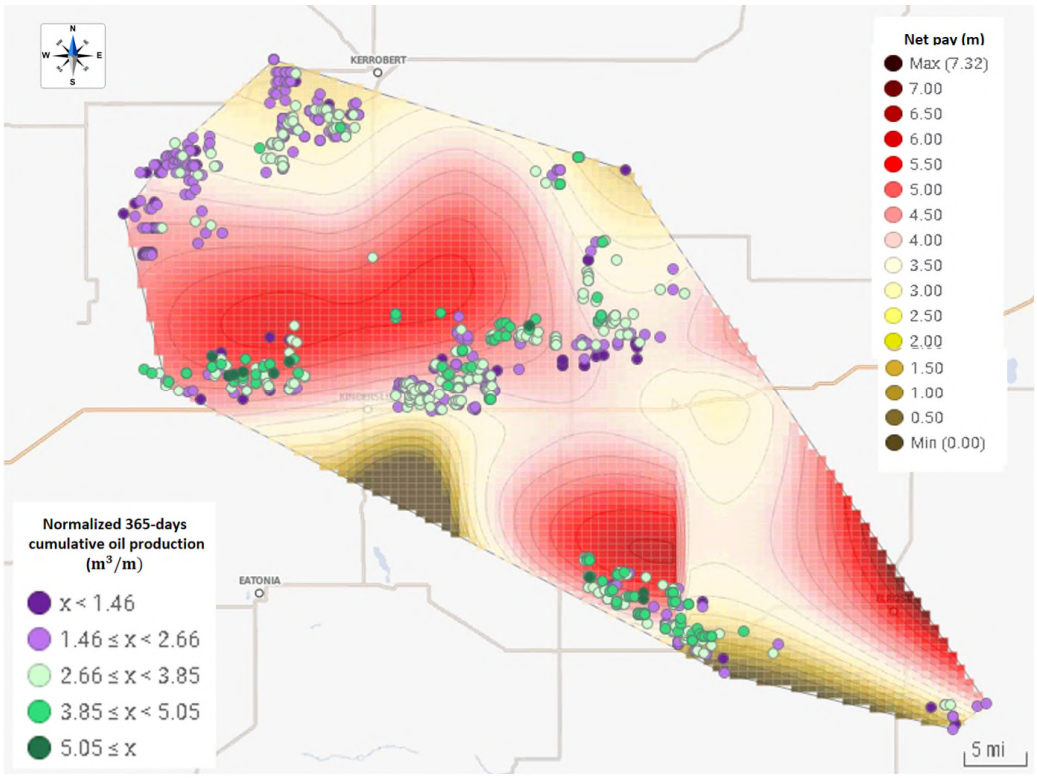

Figure 3.5. A net pay map of the Viking Formation. Net pay values were provided by Baytex Energy Corp.

3.2.5 Average gas-oil ratio (GOR)

The average ratio of produced gas to produced oil (GOR, gas-oil ratio) was introduced in the study to differentiate the potential for oil production in the different areas. It is expected that the higher the GOR (in m^3/m^3), the lower the oil production. This parameter was taken from production data and was calculated by averaging the GOR at 90, 180 and 365 days.

In the study area, the GOR ranged from 0.96 m^3/m^3 up to 1028.9 m^3/m^3, with an average of 102.13 m^3/m^3 (Table 3.4 and Figure 3.6). Most of the wells (≈ 85 %) reported a GOR lower than 200 m^3/m^3. Additionally, Figure 3.7 presents a cross plot between average GOR and 365-day cumulative oil production. As shown in Figure 3.7, no relationship was observed between these two variables (R^2 = 0.0008).

Since the relationship between the variables were nonlinear, it was hard to find a general trend by using a cross plot. Instead, a boxplot, a statistical technique that allows data to be grouped to discover trends, was used. The diagram consists of a box, in which the central mark refers to the

median value, and the bottom and the top of the box corresponds to the first quartile and third quartile of the data, respectively. The whiskers extend from the minimum to the maximum value and exclude outliers.

As seen in Figure 3.8, there was a negative relationship between average GOR and oil production, except for the wells in the range of 0.97 m^3/m^3 to 257.97 m^3/m^3. These later results could suggest a trend because of the high number of wells in this range (784 wells) compared to the others (91 combined). Additionally, a large variability in oil production was observed in the different ranges, which indicates that production was also affected by other factors.

Table 3.4. Descriptive statistics for average gas-oil ratio. The volumes listed (in m^3) represent 365-day cumulative oil production.

Average GOR Range (m^3/m^3)	**Number of wells**	**Mean (m^3)**	**Minimum (m^3)**	**25% (m^3)**	**50% (m^3)**	**75% (m^3)**	**Maximum (m^3)**
0.97-257.97	784	2070.8	326.2	1535.3	1983.3	2491.9	6060.2
257.97-514.97	79	2411.9	353.9	1254.3	2047.7	3125.5	8272.1
514.97-771.97	9	2391.5	376.3	892.8	1705.1	4160.5	5565.6
771.97-1028.97	3	1117.9	452.6	758.7	1064.7	1450.6	1836.6

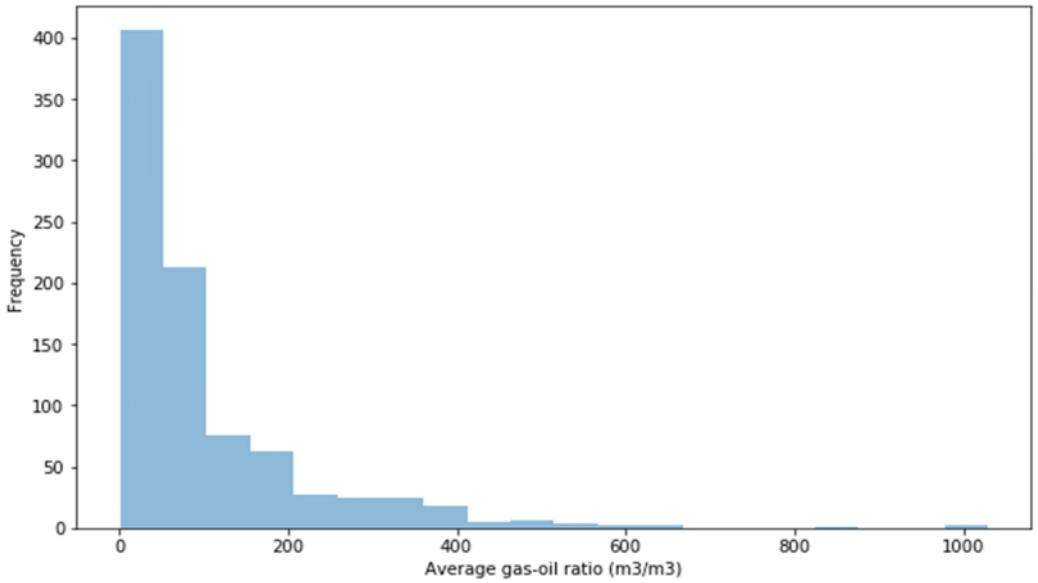

Figure 3.6. Histogram illustrating the distribution of average GOR for wells in the Viking Formation.

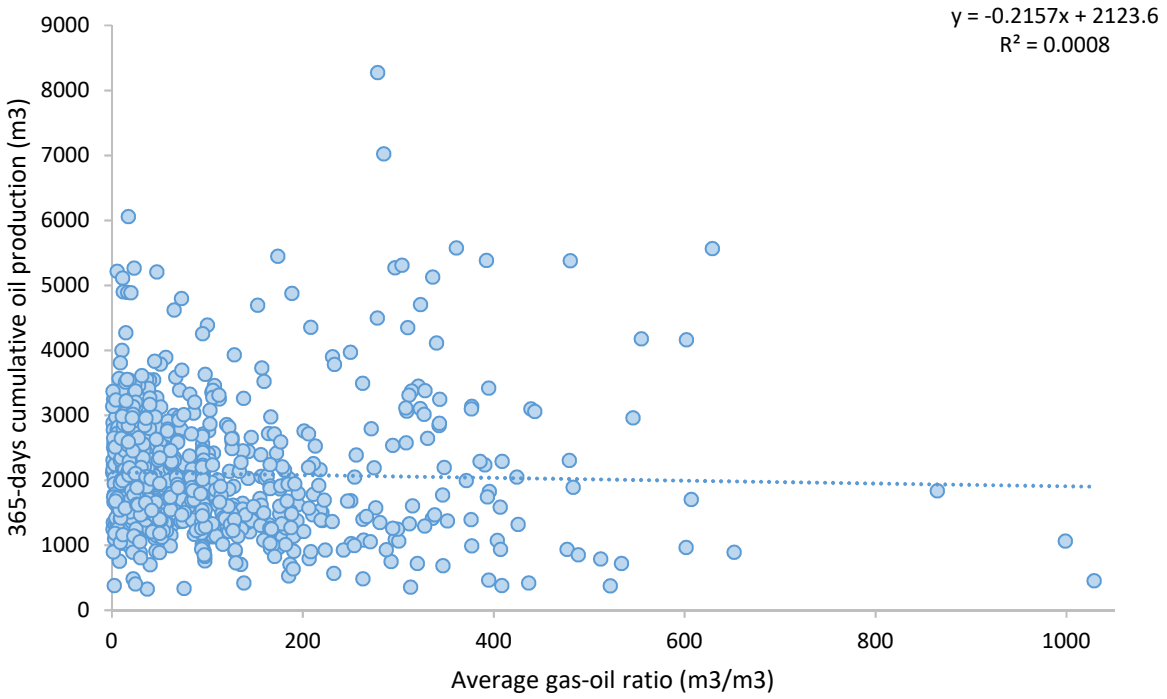

Figure 3.7. Cross plot comparing average GOR and 365-day cumulative oil production.

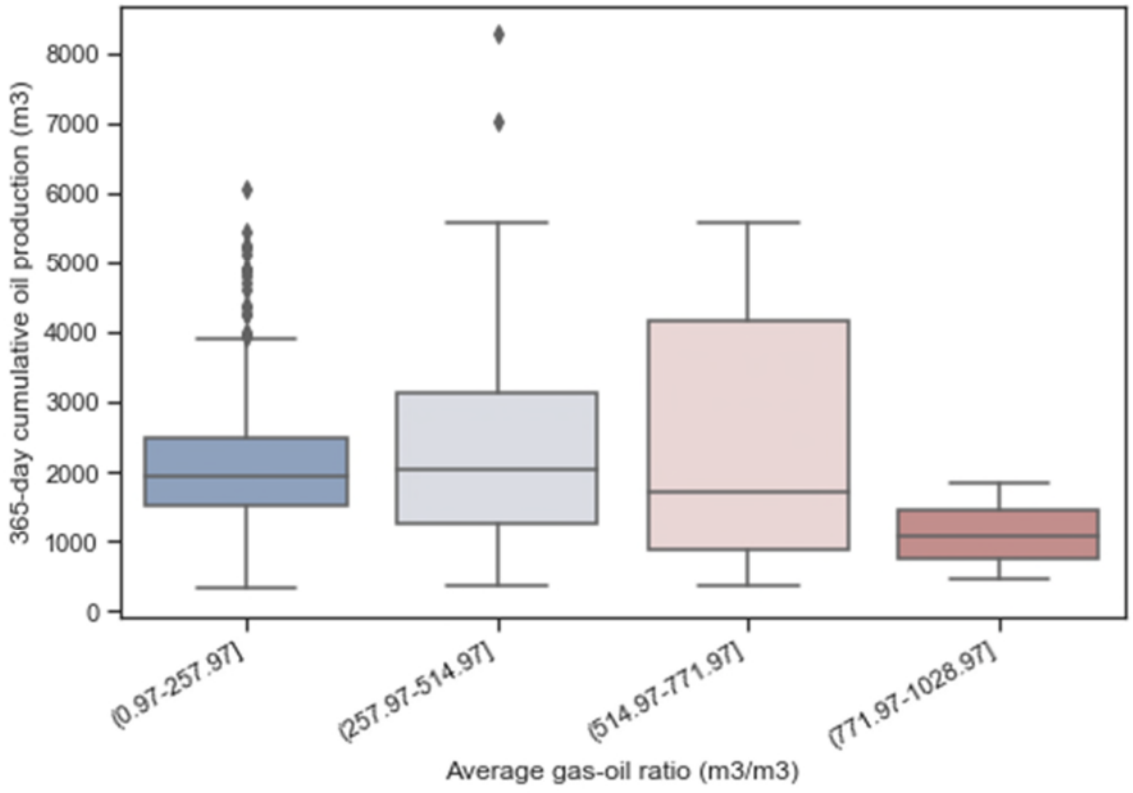

Figure 3.8. Box plot of the effect of average gas-oil ratio on 365-day cumulative oil production.

3.2.6 True Vertical Depth

True vertical depth (TVD) stands for the vertical distance of a well measured from the Kelly Bushing (i.e., drilling rig floor) to the top of the formation. The TVD in the study area ranged from 597.2 m to 806 m. Table 3.5 summarizes the descriptive statistics of this feature.

TVD was included as a proxy for reservoir pressure. This means that deeper wells would have higher production than shallower wells. However, as can be seen in Figure 3.9, there is a weak negative correlation between 365-day cumulative oil production and TVD. Additionally, Figure 3.10 shows that the deeper wells ranging from 753.8 m to 806 m tend to have a lower median oil production than the shallower wells from 597.2 m to 753.8 m. This behavior can be due to the small sample of wells in this range (40 wells) and/or that the deeper areas have lower quality reservoir (e.g., lower porosity and permeability).

Table 3.5. Descriptive statistics for true vertical depth.

TVD Range (m)	Number of wells	Mean (m^3)	Minimum (m^3)	25% (m^3)	50% (m^3)	75% (m^3)	Maximum (m^3)
597.2-649.4	23	2067.1	719.2	1533.3	2120	2684.1	3311.3
649.4-701.6	267	2197	326.2	1595.3	2044.3	2578.4	8272.1
701.6-753.8	545	2094.9	353.9	1495.9	1910.2	2532.2	7023.4
753.8-806	40	1575.5	376.3	999.9	1450.6	2034.5	3387.5

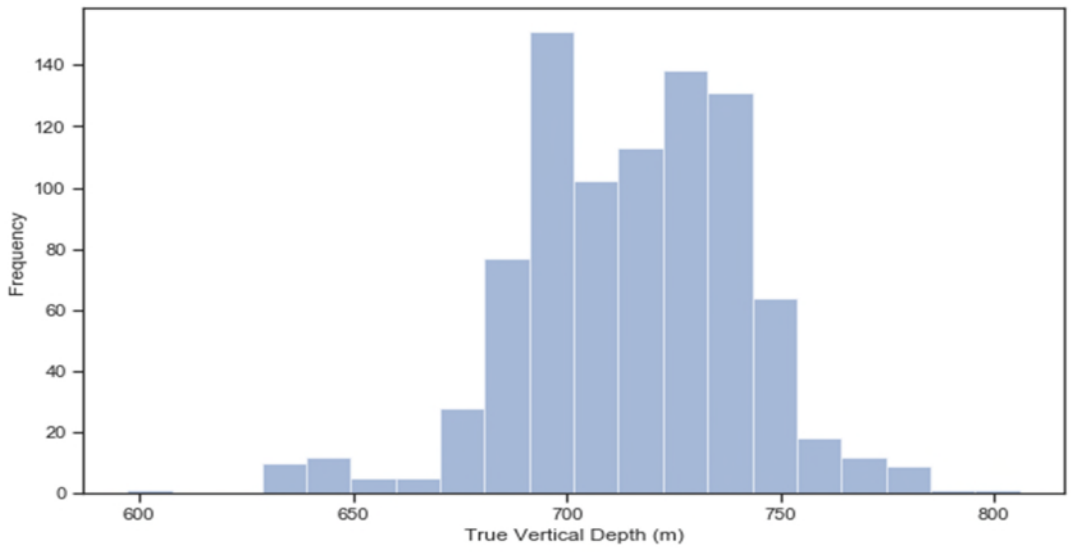

Figure 3.9. Histogram representing the distribution of true vertical depth for wells in the Viking Formation.

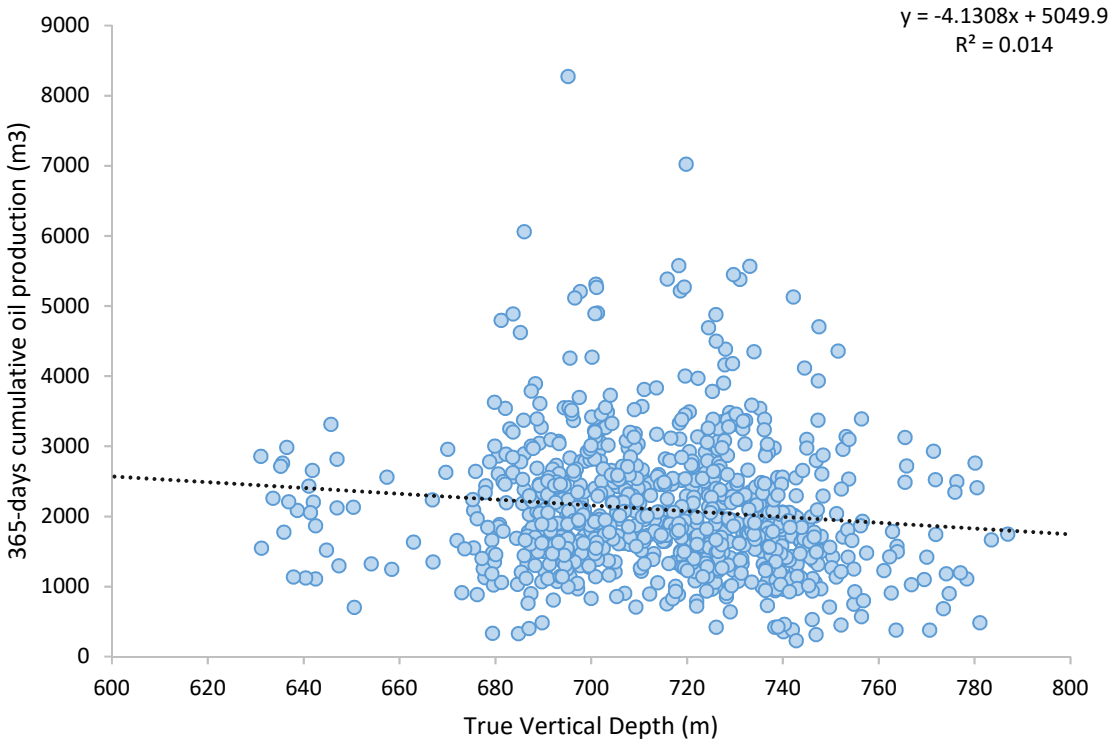

Figure 3.10. Cross plot comparing true vertical depth and 365-days cumulative oil production.

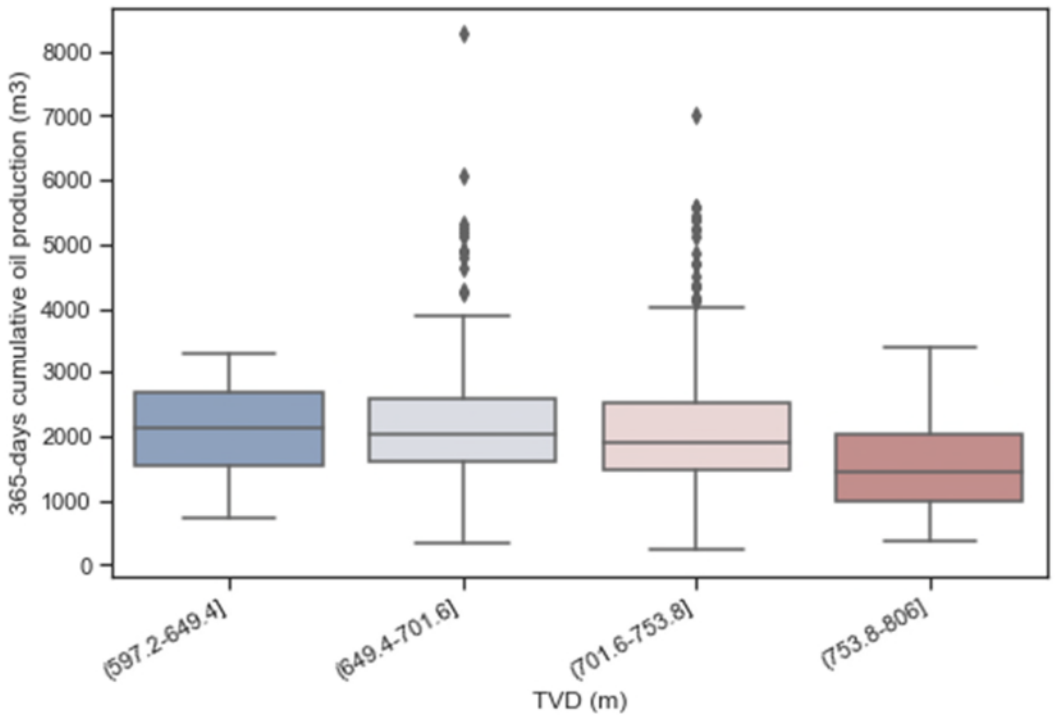

Figure 3.11. Box plot of the effect of true vertical depth on 365-day cumulative oil production.

3.2.7 Completion length

The horizontal well length can range from hundreds to thousands of metres. In the Viking formation, lateral lengths range from 212 m up to 1554.9 m. The majority of the wells had a lateral length ranging from 547.7 m to 883.5 m (Table 3.6 and Figure 3.12), with a mean value of 769.3 m. A small positive linear correlation ($R^2 = 0.274$) between completion length and oil production was seen in Figure 3.13. Figure 3.14 indicated that 365-day cumulative oil production increases with the increase of completion length. Generally, wells with greater lengths have more contact with the hydrocarbon-bearing formation, and this increases the drainage potential (Cho & Shah, 2002).

Table 3.6. Descriptive statistics for completion length.

Length Range (m)	Number of wells	Mean (m^3)	Minimum (m^3)	25% (m^3)	50% (m^3)	75% (m^3)	Maximum (m^3)
212-547.7	4	786.9	326.2	383.2	716.9	1120.6	1387.6
547.7-883.5	700	1897.6	333.5	1447.9	1844.3	2311.9	3549.3
883.5-1219.2	104	2714.5	353.9	1876.4	2573.8	3387.2	7023.4
1219.2-1554.9	67	3360.1	380.1	2486.3	3201.5	4216.9	8272.1

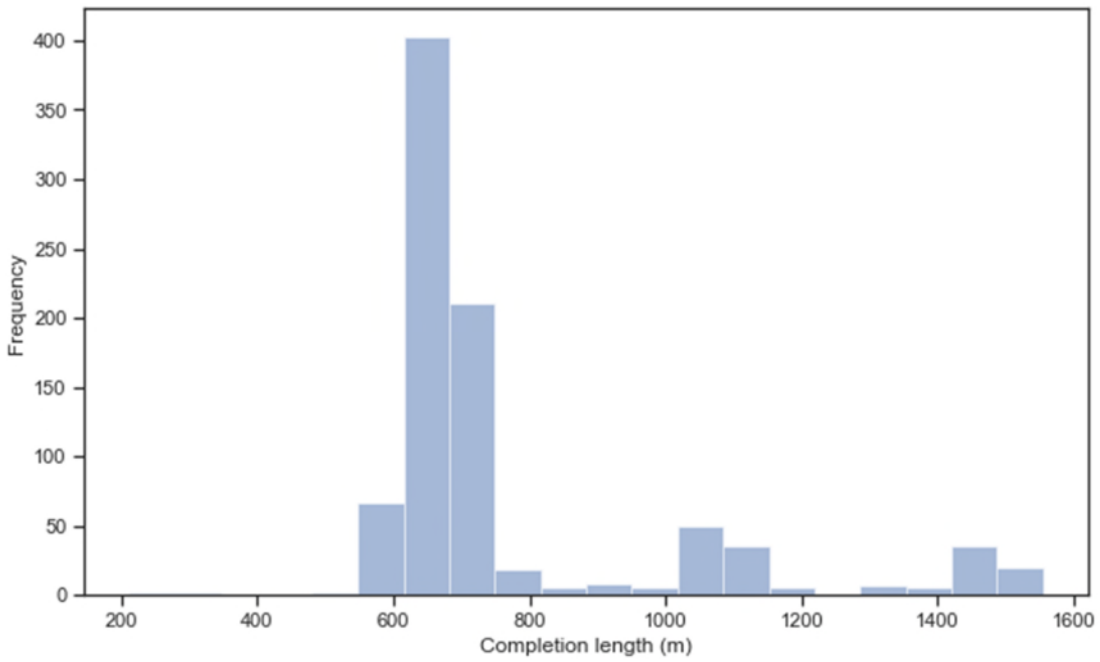

Figure 3.12. Histogram representing the distribution of completion length for wells in the Viking Formation.

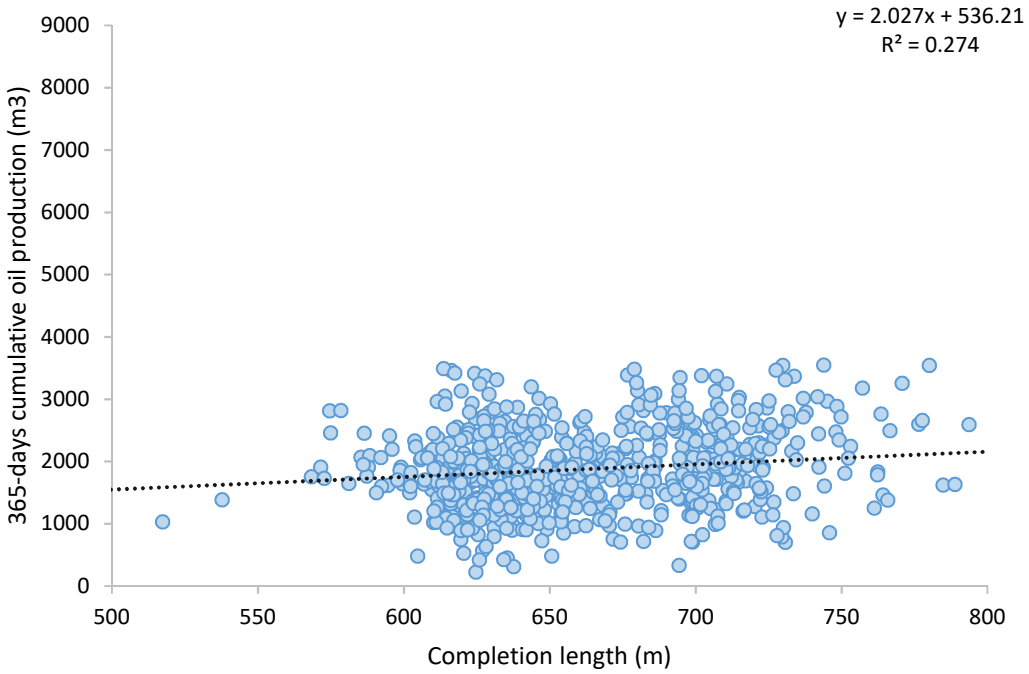

Figure 3.13. Cross plot comparing completion length and 365-day cumulative oil production.

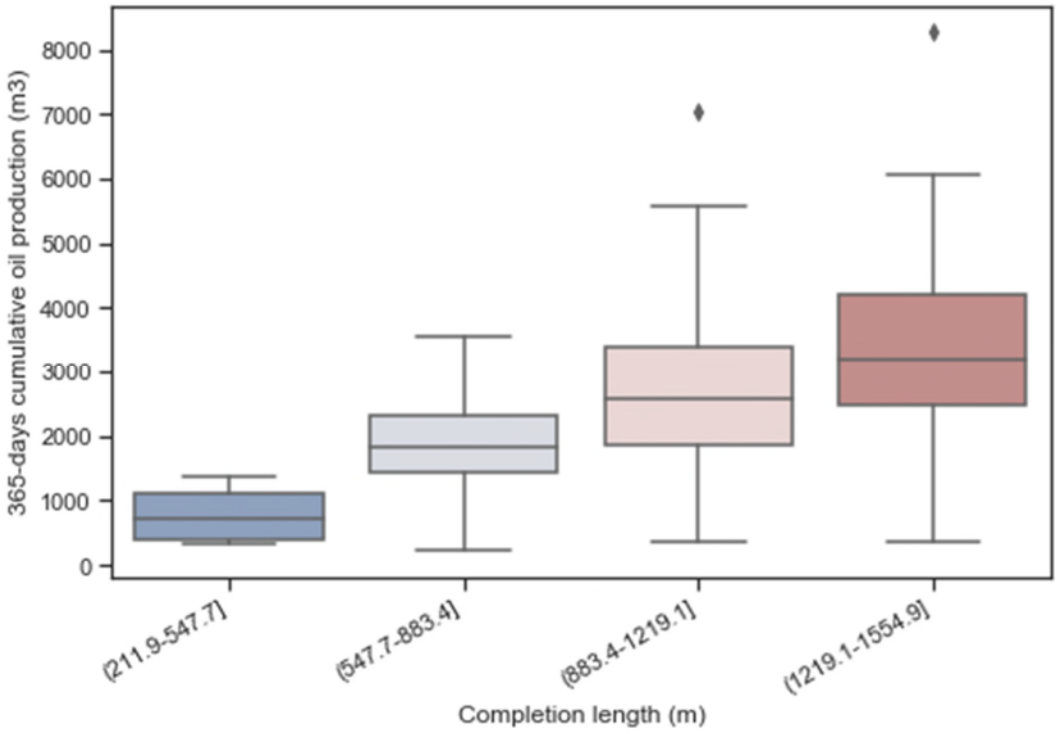

Figure 3.14. Box plot of the effect of completion length on 365-day cumulative oil production

3.2.8 Number of stages

The aim of multi-stage hydraulic fracturing is to increase contact area between the well and the reservoir and thus to enhance productivity. Multiple stages are created to establish an adequate contact with the reservoir (Espinoza, 2019). The number of fractured stages depends on the well lateral length and the spacing between stages. Proppant and fluid are injected at a high pressure in each area of interest to create each stage (Kakar, 2018).

A wide range in the number of stages was observed for the wells in the Viking Formation. The stage numbers ranged from 7 up to 45. Most wells have 18 stages (Table 3.7 and Figure 3.15). The scatterplot between 365-day cumulative oil production and number of stages suggests a modest positive correlation between the variables ($R^2 = 0.288$). Additionally, the boxplot corroborated this positive correlation, indicating that the higher the number of stages, the higher oil production in the first year (Figure 3.16 and Figure 3.17). On average, wells with less than 17 stages exhibited an oil production of $1306.5m^3$, while wells with more than 36 stages had an oil production of $3424.4m^3$.

Table 3.7. Descriptive statistics for number of stages.

Stages Range	Number of wells	Mean (m^3)	Minimum (m^3)	25% (m^3)	50% (m^3)	75% (m^3)	Maximum (m^3)
7-17	25	1306.5	326.2	967.6	1387.6	1700.2	2076.6
17-26	700	1906.4	333.5	1462.4	1863.7	2342.8	3900.1
26-36	88	2946.5	380.1	2046.3	2956.9	3557.3	7023.4
36-45	62	3427.4	884.8	2616.7	3211.3	4235.9	8272.1

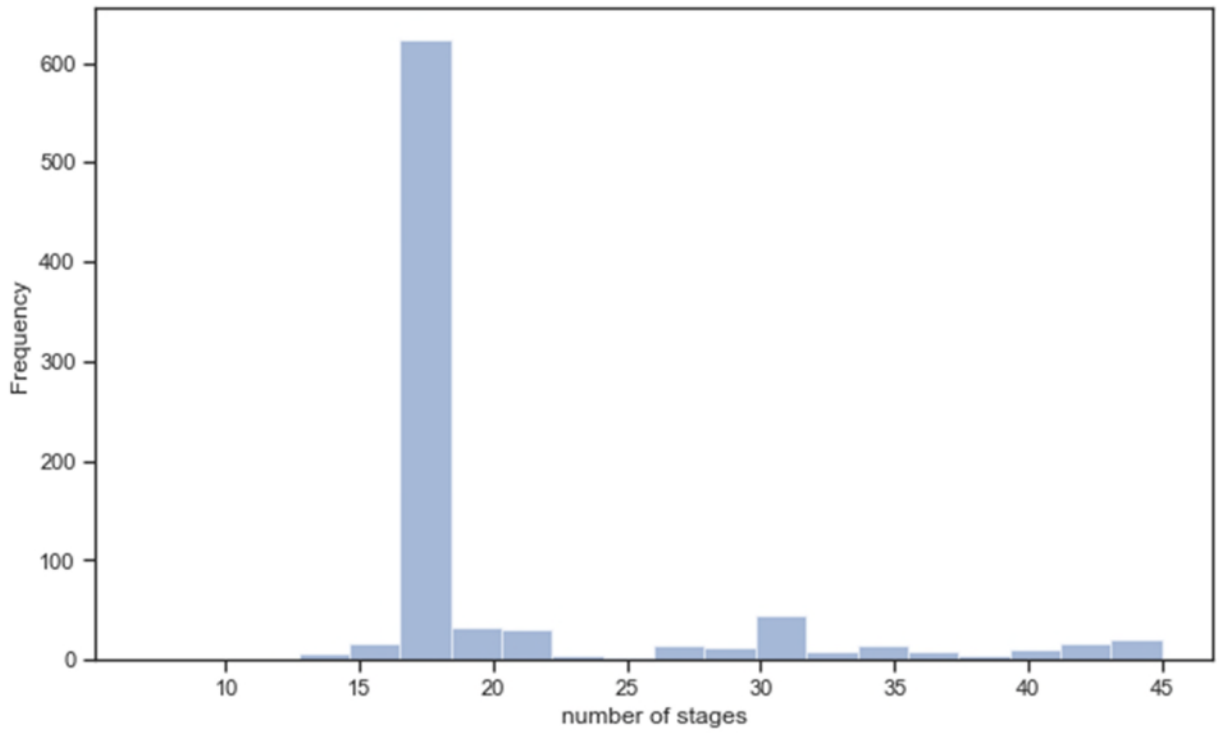

Figure 3.15. Histogram representing the distribution of completion length for wells in the Viking Formation.

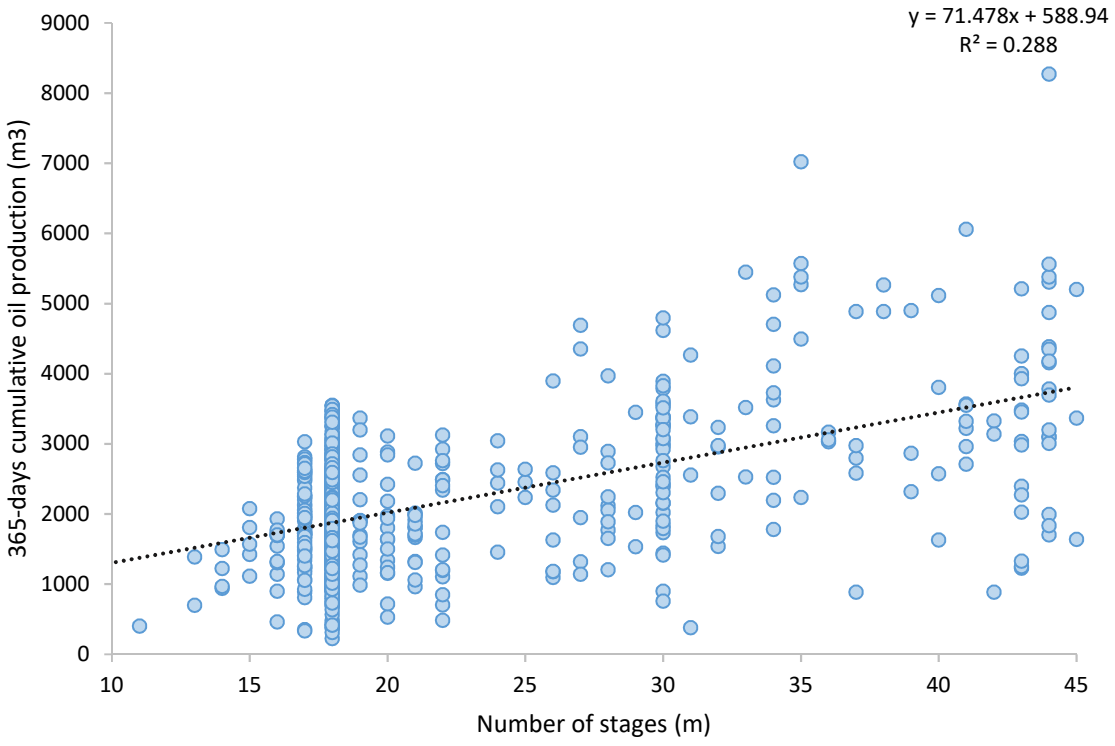

Figure 3.16. Cross plot comparing number of stages and 365-day cumulative oil production.

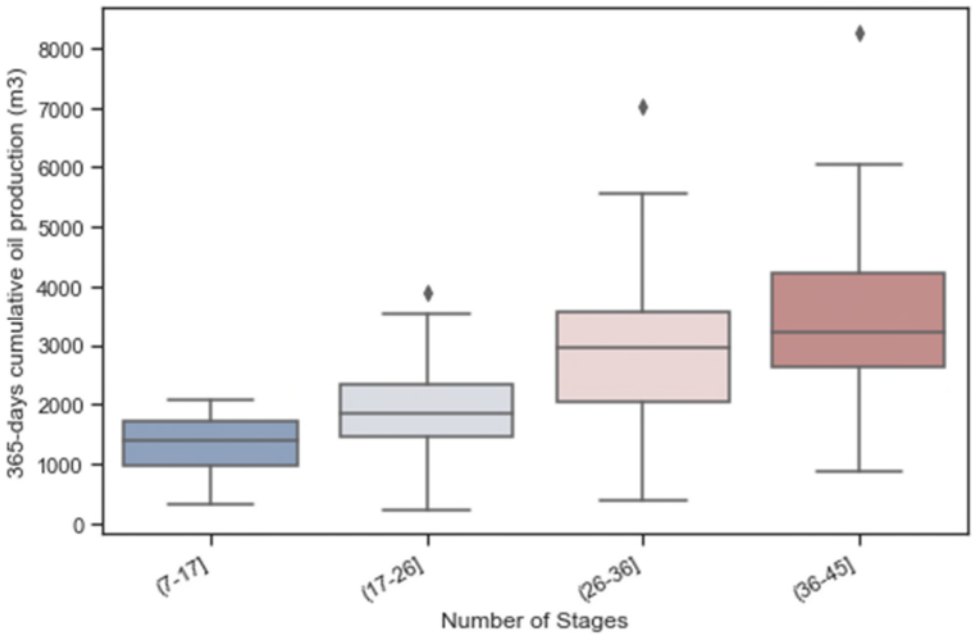

Figure 3.17. Box plot of the effect of number of stages on 365-day cumulative oil production.

3.2.9 Average stage spacing

Average stage spacing refers to the distance between stages completed. This parameter was calculated by dividing the completion length by the number of stages in each well. The stage spacing in the Viking formation ranged from 25.4 m up to 57.4 m. The majority of the wells had stage spacings falling between 33.4 m and 41.2 m, as observed in Table 3.8 and Figure 3.18. The scatterplot comparing 365-day cumulative oil production and stage spacing suggested no association between the variables ($R^2 = 0.006$) (Figure 3.19). On the other hand, the boxplot comparing these two variables indicated that wells with larger stage spacing (more than 49.4 m) tend to have lower oil productions during the first year (Figure 3.20). This can be associated with the fact that wells with larger stage spacings are likely to have a lesser number of stages, which ultimately reduces the contact of the well with the reservoir.

Table 3.8. Descriptive statistics for average stage spacing.

Spacing Range (m)	Number of wells	Mean (m^3)	Minimum (m^3)	25% (m^3)	50% (m^3)	75% (m^3)	Maximum (m^3)
25.4-33.4	113	2488.9	326.2	1647.2	2014.1	3097.7	8272.1
33.4-41.2	691	2056.4	333.5	1489.7	1908.7	2485.8	6060.2
41.2-49.4	61	2073.7	380.1	1493.3	2105.6	2595.5	4269.1
49.4-57.4	10	1020.8	353.9	391.1	573.2	1092.9	3513.1

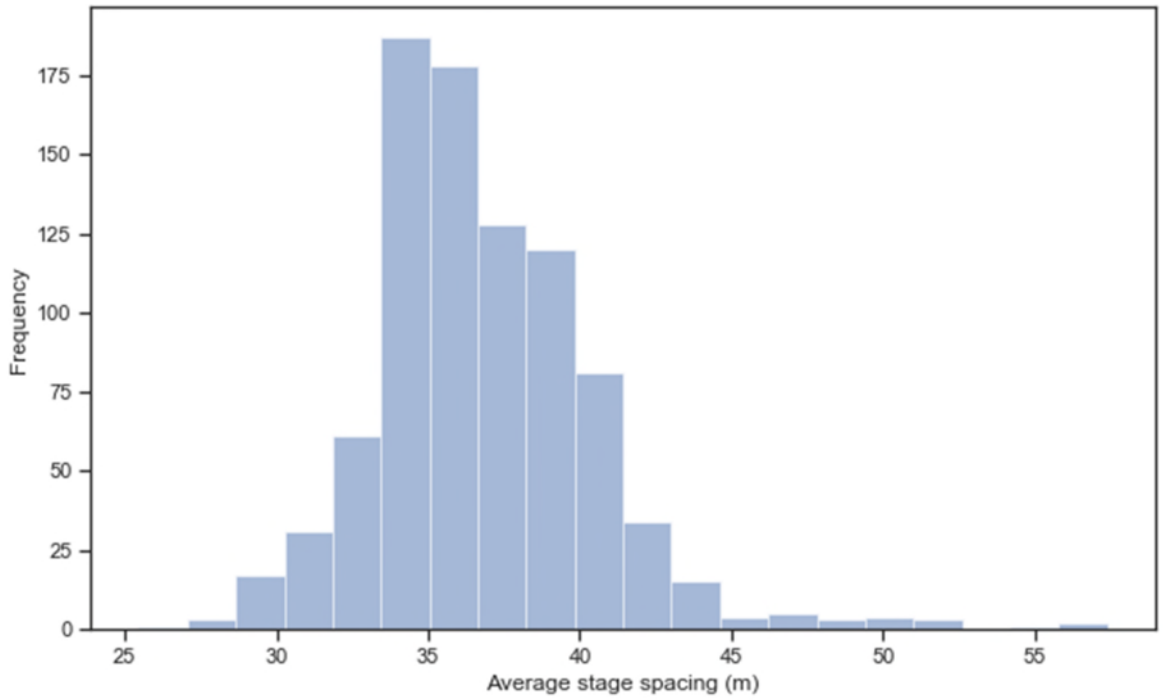

Figure 3.18. Histogram representing the distribution of average stage spacing for wells in the Viking Formation.

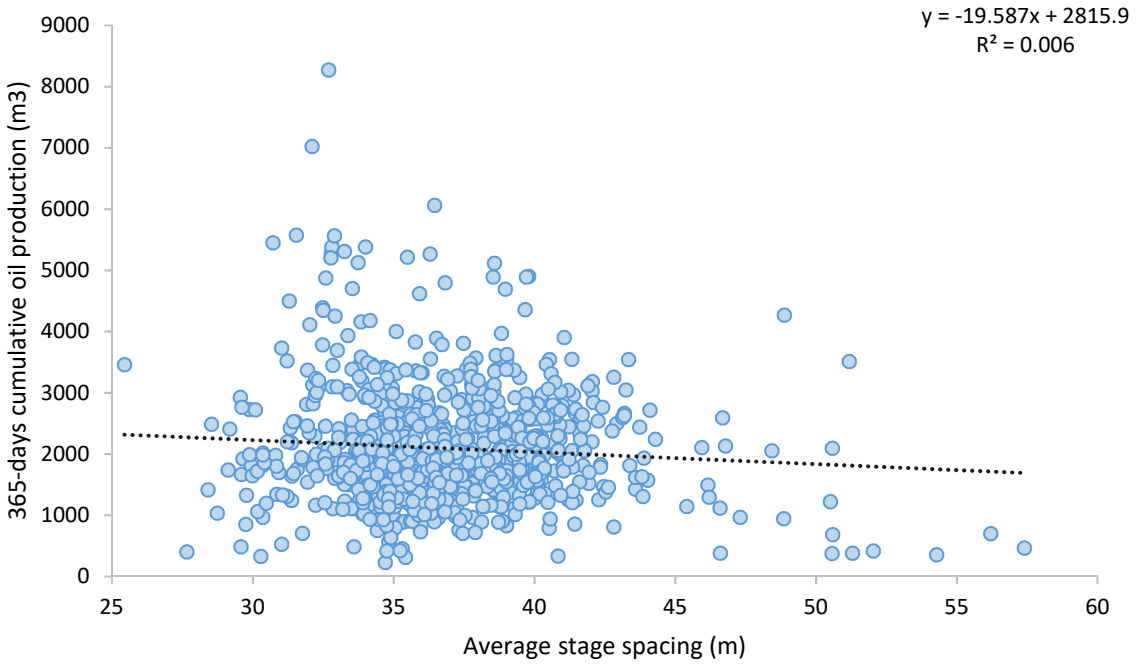

Figure 3.19. Cross plot comparing average stage spacing and 365-day cumulative oil production.

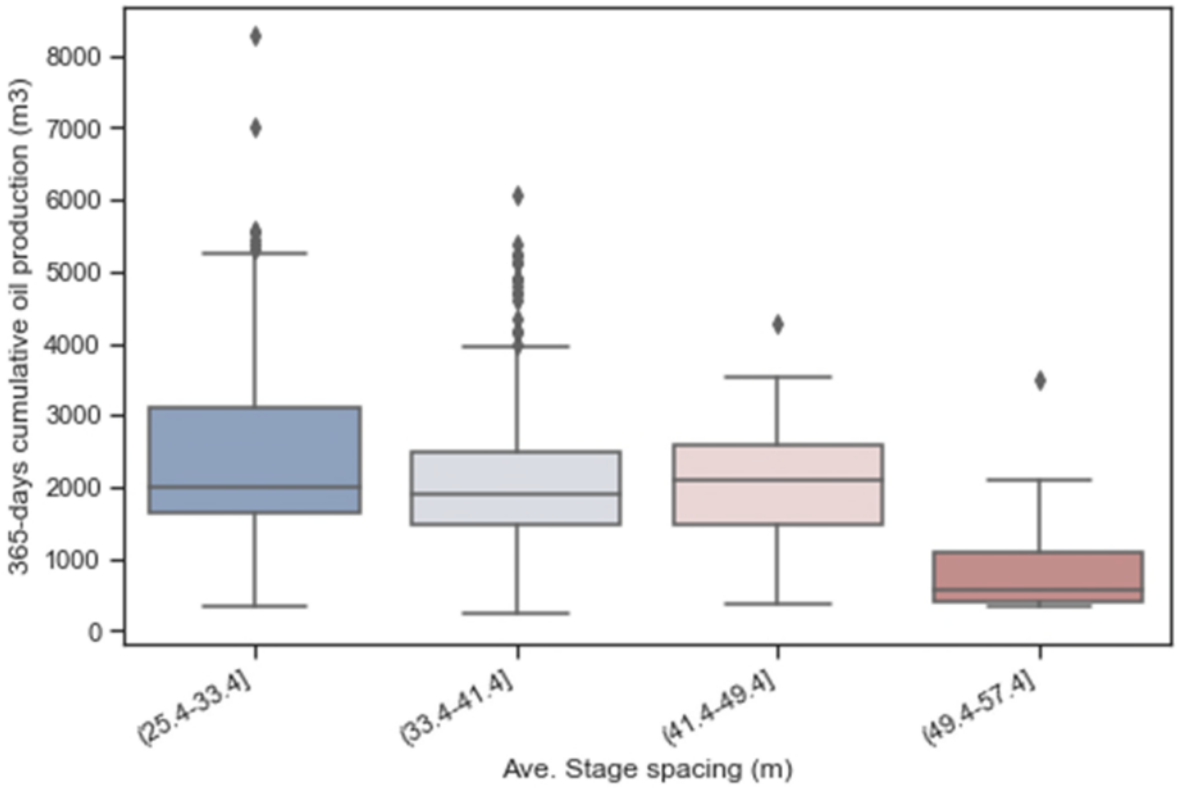

Figure 3.20. Box plot of the effect of average stage spacing on 365-day cumulative oil production.

3.2.10 Proppant intensity

Proppant is employed to maintain fracture aperture or width (i.e., to prop the fractures open). This granular material provides a high conductivity channel for hydrocarbons to flow into the wellbore (Belyadi et al., 2016). Different types of proppant are used during hydraulic fracturing treatments, including sand, precured resin-coated sand, curable resin-coated sand, and ceramic proppant (Belyadi et al., 2016). In this study, the volume of proppant injected was normalized by completion length in each well.

The normalized volume of proppant injected in the Viking Formation ranged from 0.19 t/m to 0.58 t/m (Table 3.9 and Figure 3.21). Most horizontal wells used between 0.35 t/m up to 0.45 t/m, as illustrated in Figure 3.22. A weak positive correlation ($R^2 = 0.06$) was observed between 365-day cumulative oil production and normalized proppant injected. According to Figure 3.23, oil production in the first year tended to increase with the increase of proppant injected. However, the high variability of oil production in the different ranges indicated that production was also influenced by other parameters.

Table 3.9. Descriptive statistics for proppant intensity.

Proppant Range (t/m)	Number of wells	Mean (m^3)	Minimum (m^3)	25% (m^3)	50% (m^3)	75% (m^3)	Maximum (m^3)
0.19-0.29	50	1433.6	333.5	1020.4	1402.1	1866.7	3044.4
0.29-0.39	368	2034.8	326.2	1521.4	1880.7	2352.6	5382.4
0.39-0.48	386	2132.5	417.7	1480.7	1949.3	2526.9	8272.1
0.48-0.58	71	2750.4	528.9	2401.1	2662.8	3113.6	5214.1

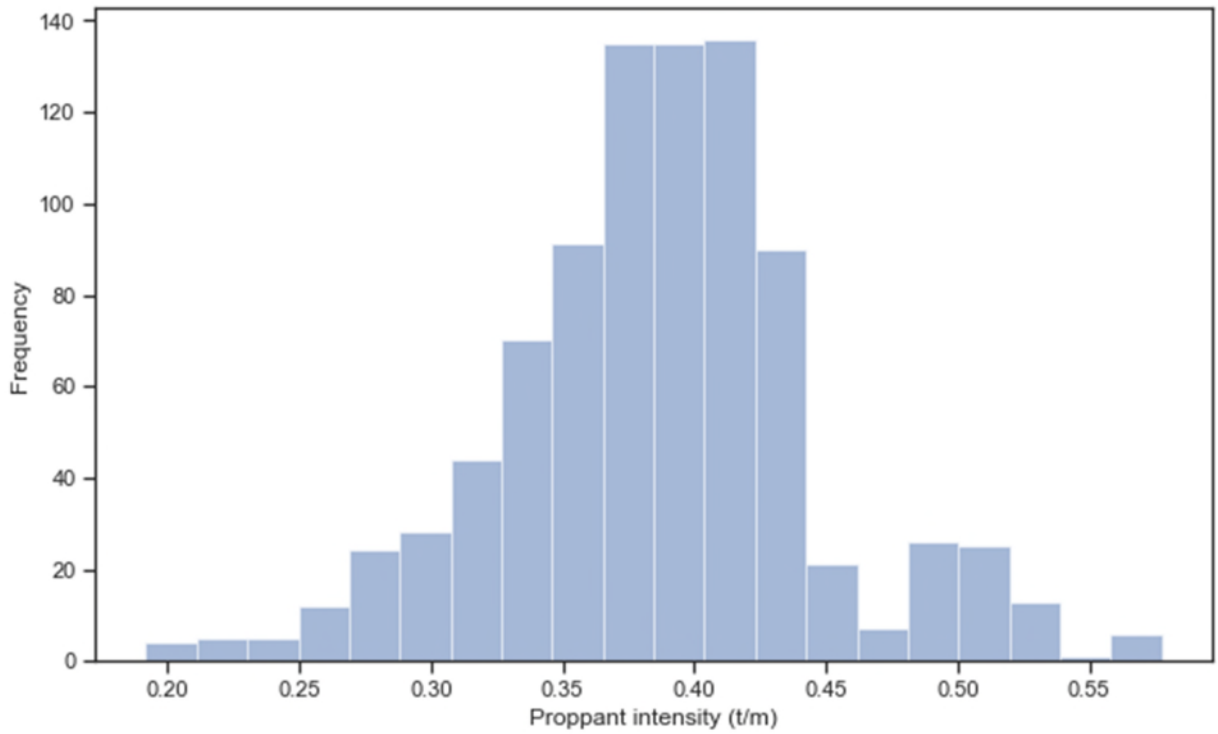

Figure 3.21. Histogram representing the distribution of proppant intensity for wells in the Viking Formation.

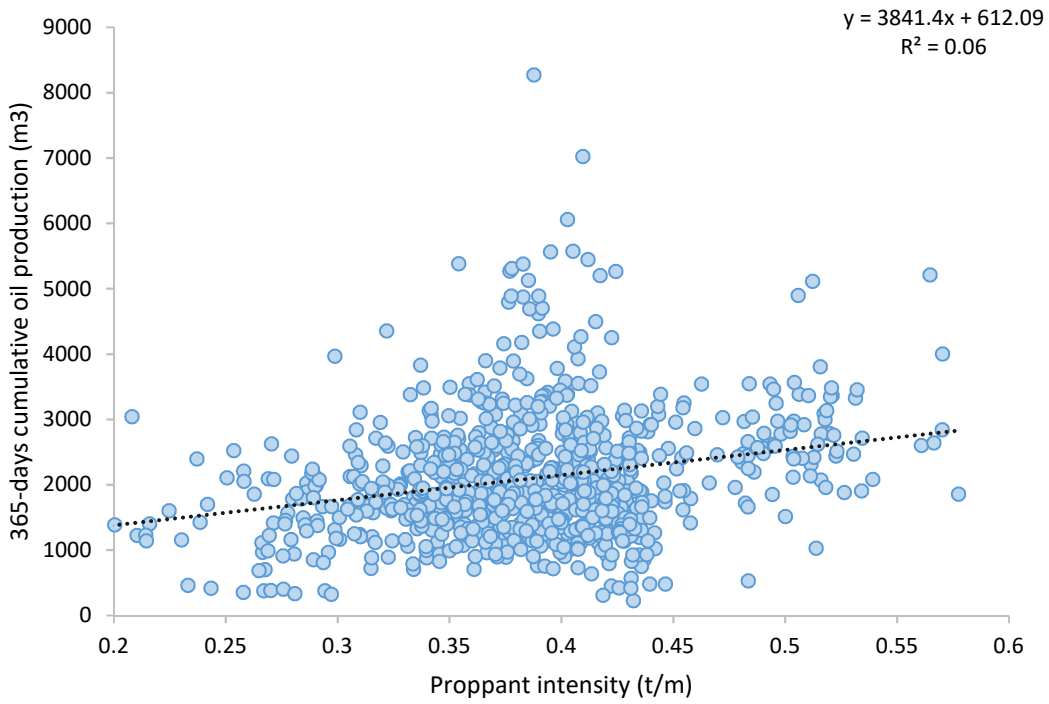

Figure 3.22. Cross plot comparing proppant intensity and 365-day cumulative oil production.

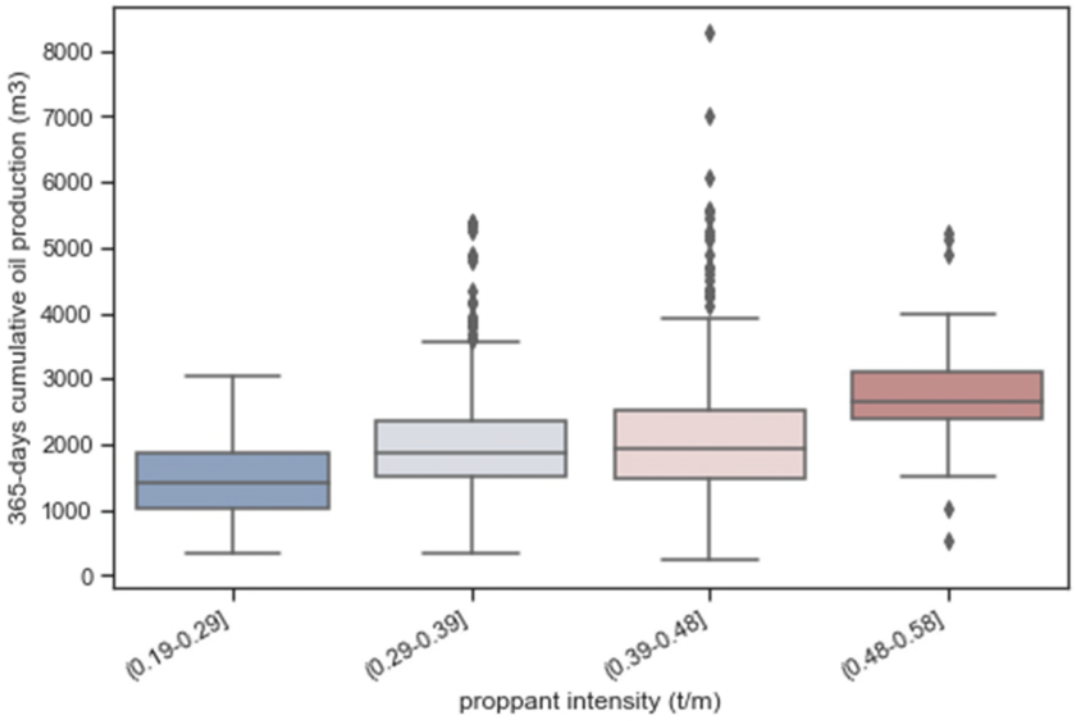

Figure 3.23. Box plot of the effect of proppant intensity on 365-day cumulative oil production.

3.2.11 Fluid intensity

A large volume of fluid is injected downhole to create a fracture system in the reservoir. Generally, the fluid is pumped at a high pressure and rate to yield better surface area (Belyadi et al., 2016). In this work, the volume of fluid injected was normalized by completion length. The normalized volume of fluid pumped ranged from 0.49 m^3/m to 1.58 m^3/m (Table 3.10 and Figure 3.24).

On average, horizontal wells used 0.89 m^3/m Figure 3.25 indicated that normalized volume of fluid has almost no effect on 365-day cumulative oil production ($R^2 = 0.006$). However, the boxplot (Figure 3.26) suggested that a volume of fluid larger than 1.04 m^3/m greatly influenced oil production during the first year. The high variance in oil production in the different ranges revealed that production was highly affected by other factors as well.

Table 3.10. Descriptive statistics for volume of fluid intensity.

Fluid Range (m^3/m)	Number of wells	Mean (m^3)	Minimum (m^3)	25% (m^3)	50% (m^3)	75% (m^3)	Maximum (m^3)
0.49-0.77	135	1878	333.5	1335.4	1886.7	2461.7	4269.1
0.77-1.03	593	2129.9	326.2	1642.1	2008.4	2529.7	6060.2
1.03-1.31	142	2187.6	417.7	1254.6	1660.2	2950.3	8272.1
1.31-1.58	5	2343	1226.6	1902.7	2408.3	2720.9	3456.4

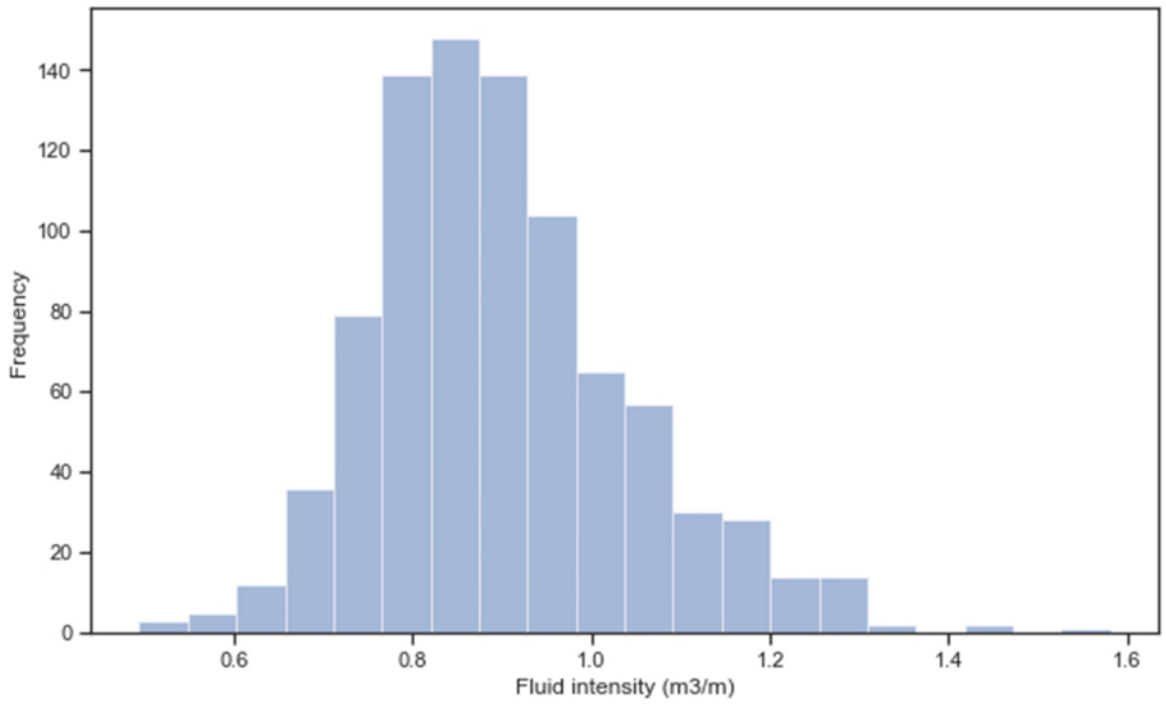

Figure 3.24. Histogram representing the distribution of fluid intensity for wells in the Viking Formation.

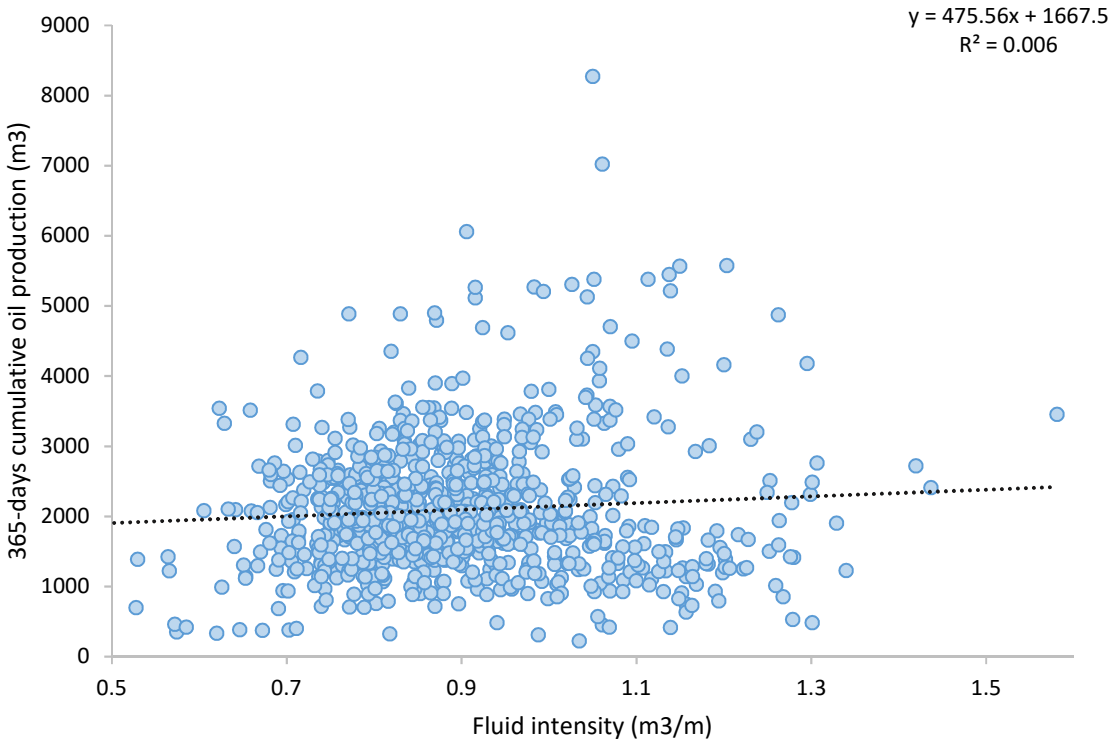

Figure 3.25. Cross plot comparing fluid intensity and 365-day cumulative oil production.

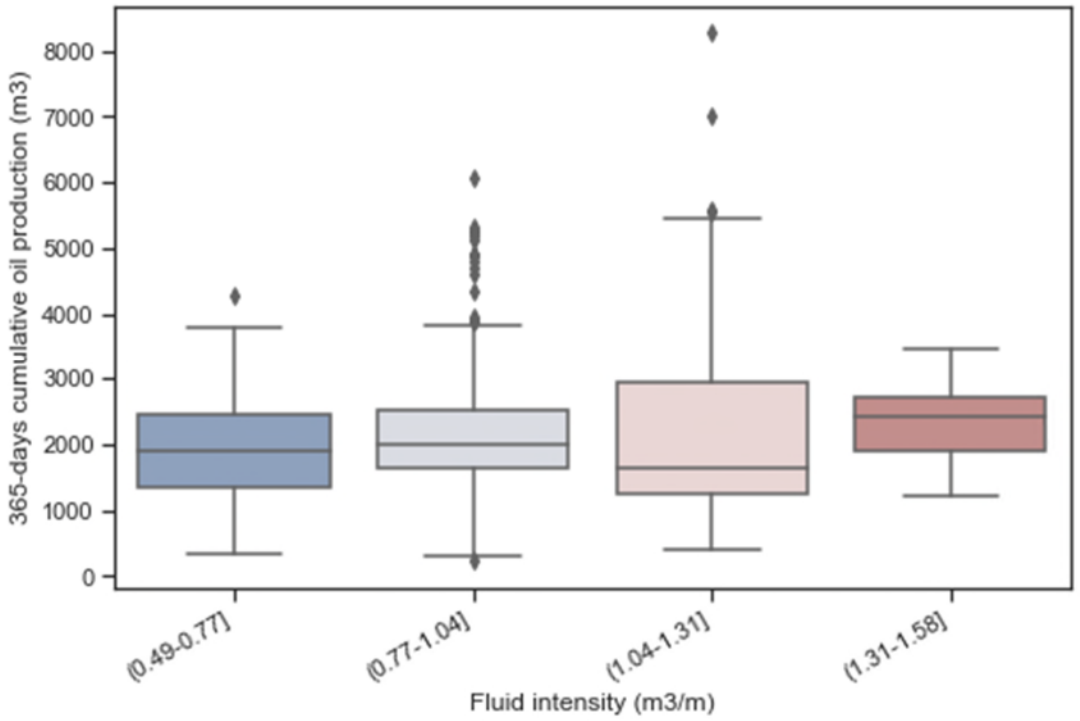

Figure 3.26. Box plot of the effect of fluid intensity on 365-day cumulative oil production.

3.2.12 Proppant concentration

Proppant concentration refers to the total volume of proppant divided by the total volume of fluid pumped. This parameter allows the combination of the effect of proppant and fluid in the horizontal wells. The wells in the Viking Formation were treated with ratios ranging from 0.24 t/m^3 up to 0.74 t/m^3 (Table 3.11 and Figure 3.27). On average, a horizontal well was stimulated with 0.43 t/m^3.

The cross plot between oil production in the first year and proppant concentration suggested a weak positive correlation between these two features (Figure 3.28). Furthermore, a high variability in oil production was observed (Figure 3.27 and Figure 3.29). The boxplot indicated that wells treated with more than 0.49 t/m^3 were likely to have a higher oil production (Figure 3.29).

Table 3.11. Descriptive statistics for proppant concentration.

Concentration Range (t/m^3)	Number of wells	Mean (m^3)	Minimum (m^3)	25% (m^3)	50% (m^3)	75% (m^3)	Maximum (m^3)
0.24-0.37	119	1959	326.2	1246.5	1640.8	2327.3	5574.2
0.37-0.49	582	2038.5	333.5	1499.4	1892.7	2398.8	8272.1
0.49-0.62	170	2397.3	670	1867.4	2442.5	2808.7	5214.1
0.62-0.74	4	2961.9	2137.4	2666.6	3084.3	3379.6	3541.5

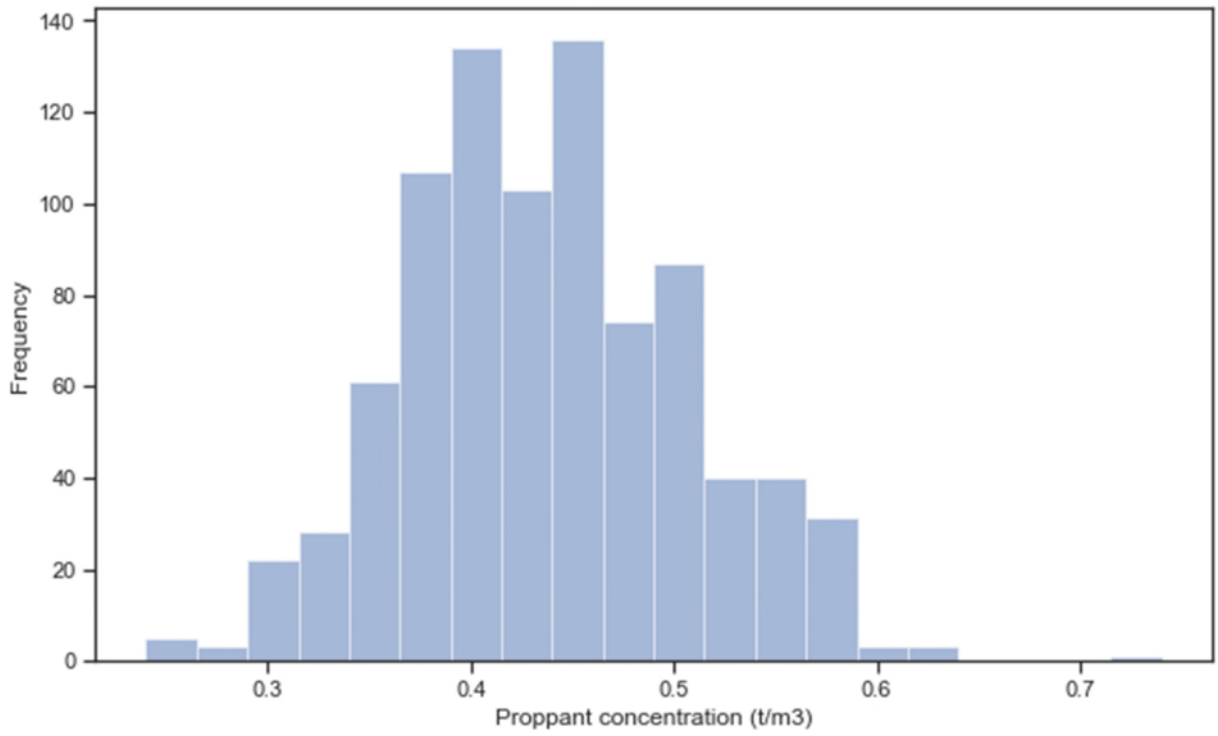

Figure 3.27. Histogram representing the distribution of proppant concentration for wells in the Viking Formation.

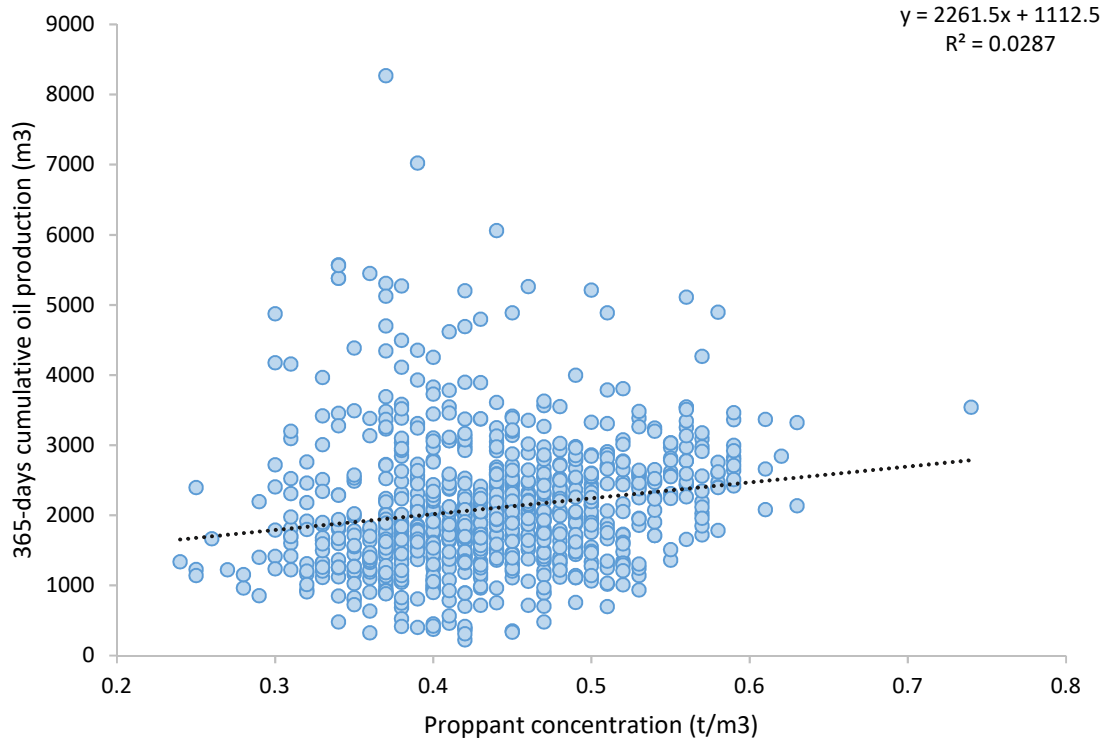

Figure 3.28. Cross plot comparing proppant concentration and 365-day cumulative oil production.

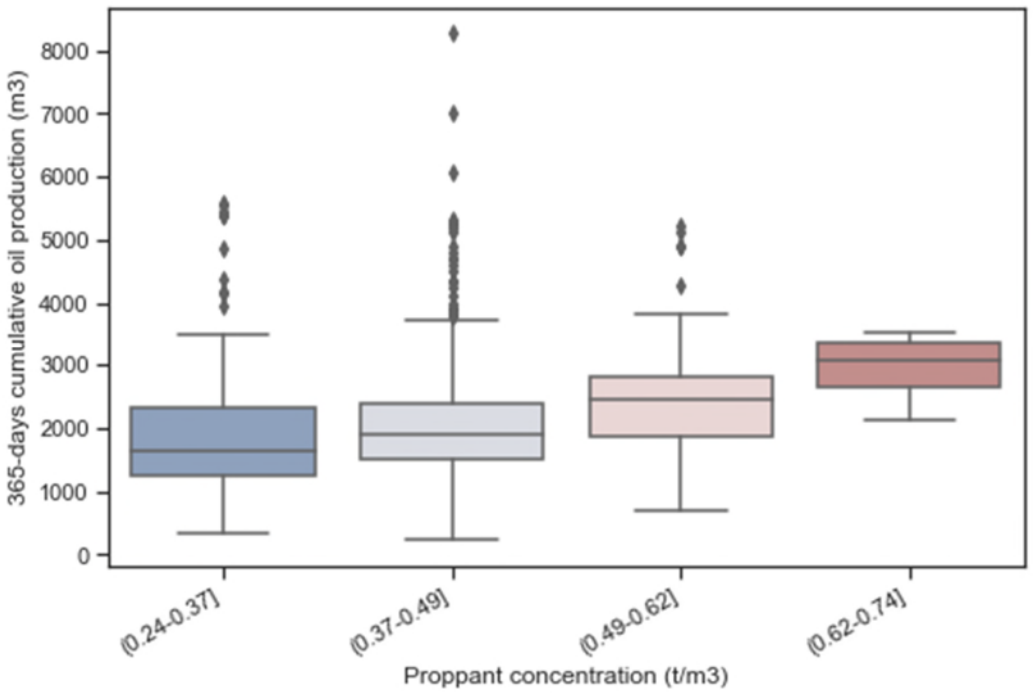

Figure 3.29. Box plot of the effect of proppant concentration on 365-day cumulative oil production.

3.2.13 365-day cumulative oil production

365-day cumulative oil production was selected as a well performance metric. This cumulative oil volume accounted for downtime during operations by deducting days with zero oil production. A production time-period of roughly one year seems to be an appropriate metric because it avoids the impact of well interference that likely occurs in later production time (Wang, 2018). In other words, this parameter is a reflection of how one well performs in its early life, before adjacent wells influence it. Additionally, this well performance metric allows the evaluation of the recent stimulation designs (i.e., wells that were drilled as recently as one year before this study). Figure 3.30 presents the distribution of 365-day oil production. On average, a multi-stage hydraulically fractured well in the Viking produces 2101.6 m^3.

As mentioned before, oil production is highly affected by the lateral length of the well. Therefore, 365-day production was normalized by completion length to compare production performance among operators and fields. A high variability in oil production was observed across the different fields and operators Table 3.12 and Table 3.13).

Regarding the field's performance, Eureka had the highest average oil production (3.55 m^3/m) compared to the all other areas, followed by Plato North (3.42 m^3/m) and Whiteside (3.29 m^3/m) (Table 3.12 and Figure 3.31). On average, Forgan field had the lowest oil production in the first year (1.94 m^3/m).

In terms of production performance by operator, Table 3.13 and Figure 3.32 suggest that on average Whitecap resources had the highest 365-day cumulative oil production (3.24 m^3/m), followed by NAL Resources (3.02 m^3/m), and Teine Energy Ltd (2.99 m^3/m). Ish Energy Ltd achieved the lowest 365-day production.

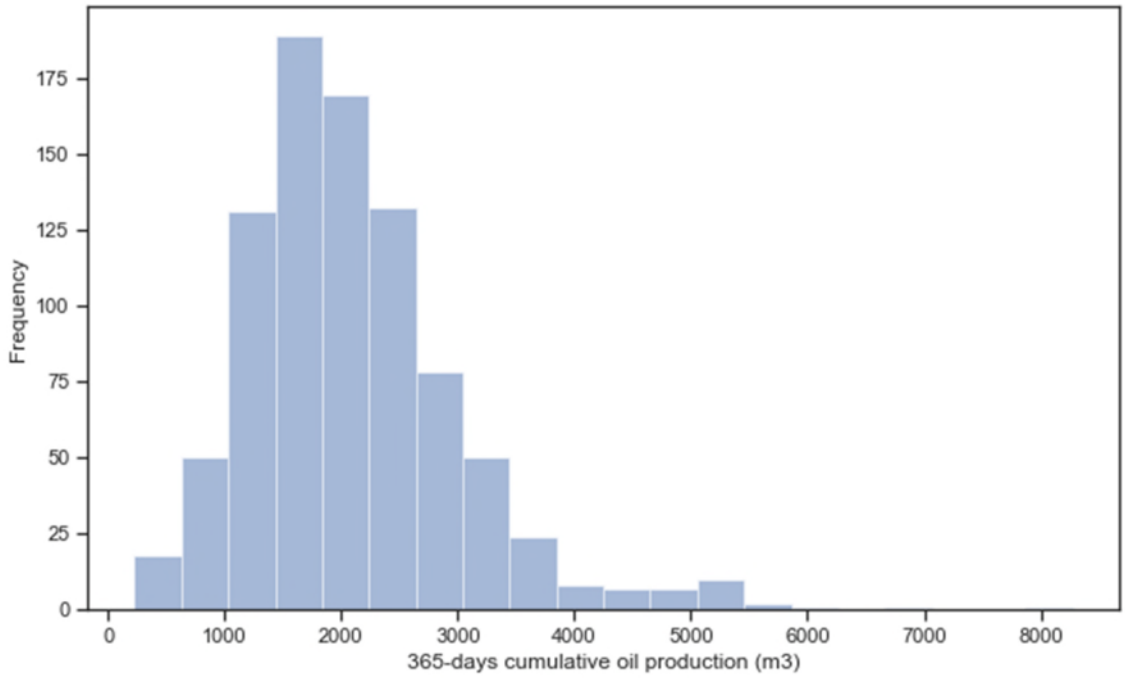

Figure 3.30. Histogram illustrating the distribution of 365-day cumulative oil production for wells in the Viking Formation.

Table 3.12. Descriptive statistics for normalized 365-day cumulative oil production in each field.

Field	Mean (m^3/m)	Standard deviation	Minimum (m^3/m)	25% (m^3/m)	50% (m^3/m)	75% (m^3/m)	Maximum (m^3/m)
Avon Hill	2.65	0.69	0.86	2.16	2.68	3.12	4.81
Kerrobert	2.41	0.69	0.62	1.91	2.36	2.86	3.96
Dodsland	2.74	1.04	0.26	2.09	2.93	3.49	5.05
Plato North	3.42	0.9	0.80	2.8	3.42	4.07	5.61
Whiteside	3.29	1.26	0.48	2.5	3.39	4.11	6.25
Prairiedale	2.03	0.56	0.67	1.65	2.07	2.44	3.06
Plato	2.98	1.02	0.7	2.43	2.88	3.68	5.01
Plenty	2.88	0.98	1.03	2.13	3.06	3.60	4.53
Forgan	1.94	0.61	0.96	1.72	1.88	2.11	2.93
Eureka	3.55	0.88	2.12	3.10	3.82	4.12	4.49

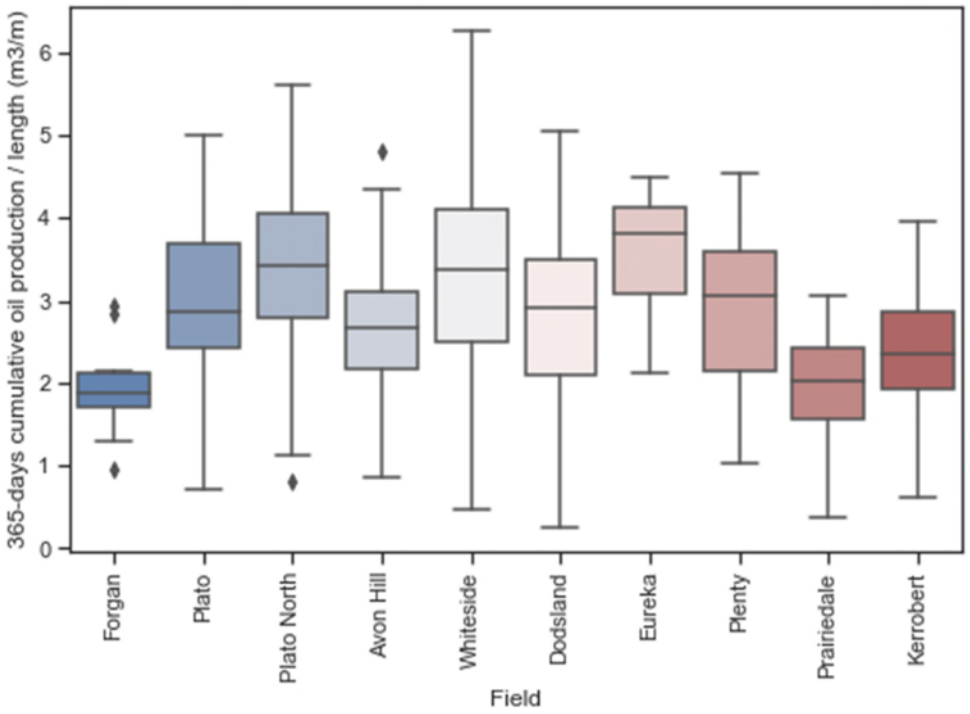

Figure 3.31. Box plots of normalized 365-day cumulative oil production in each field.

Table 3.13. Descriptive statistics for normalized 365-day cumulative oil production normalized by operator.

Operator	Mean (m^3/m)	Standard deviation	Minimum (m^3/m)	25% (m^3/m)	50% (m^3/m)	75% (m^3/m)	Maximum (m^3/m)
Baytex Energy Corp.	2.72	0.87	0.26	2.14	2.74	3.23	5.05
Teine Energy Ltd.	2.99	0.93	0.48	2.30	3.06	3.66	5.13
Crescent Point Energy	2.76	0.86	0.70	2.12	2.75	3.34	5.61
Whitecap Resources Inc.	3.24	1.17	1.04	2.37	3.05	3.84	6.25
Ish Energy Ltd.	2.04	0.56	0.66	1.68	2.07	2.45	3.06
Novus Energy Inc.	2.05	1.35	0.38	0.99	1.69	3.25	4.50
NAL Resources	3.02	0.93	1.56	2.92	2.97	3.59	4.04

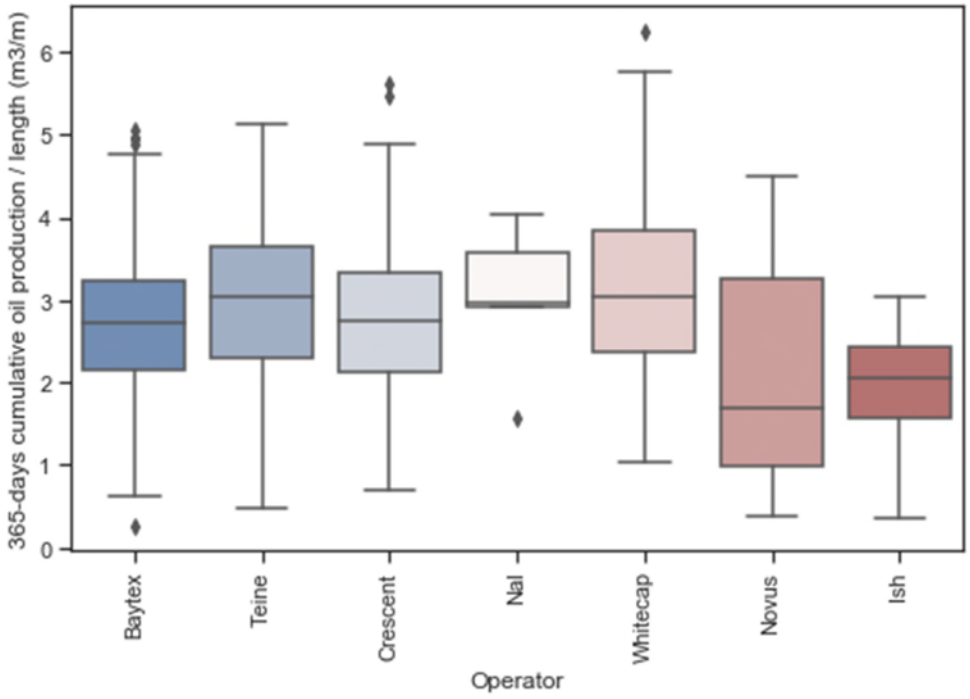

Figure 3.32. Box plots of normalized 365-day cumulative oil production by operator.

3.3 Data preparation and quality control

Data preparation and quality control are key to obtaining a final dataset that is ready for analysis. Quality control is fundamental to obtain reliable data-driven models and good data analyses. Data preparation focuses on the process of removing errors or outliers that the dataset may contain. Different techniques are required to identify and remove such anomalies (Mohaghegh, 2017). The nature of the outliers should be investigated before making any decision. If the outlier is an error, it should be excluded from the analysis. In other cases, the analysis should be performed with the outliers.

To handle missing values in the dataset, two options exist: deletion or imputation (i.e., replacement of missing values with substituted values). In the case of deletion, the data points removed should not introduce a bias in the model. Additionally, these data points can be removed depending on the frequency of their occurrence. For example, remove them if the number of missing points is less than 5% of the sample (Statistics Solutions, n.d.). On the other hand, there are different methods to perform data imputation. The selection of the method depends on the nature of the missing value. It is worth mentioning that imputation does not always provide better results (Swalin, 2018). Additionally, feature engineering is performed to prepare the appropriate input data for the model. It is necessary to eliminate multicollinearity between the predictor variables.

Data for this project was extracted from two databases, including Accumap and GeoVista, and internal data from Baytex. Only horizontal wells within the Viking Formation that had complete stimulation reports, and at least 365-day oil production, were collected. Operators and fields with less than five wells were omitted as it would be hard to make conclusions based on such a small sample.

After collecting the data, the quality was examined by comparing the data in Accumap to that in GeoVista. These two databases contain similar information. Therefore, it was assumed that both programs will have the same values for each well feature. Initially, the top of the Viking Formation was considered in the study, but several inconsistencies were found between the

databases. As a result, formation top was removed and the True Vertical Depth (of each well) was included in the study.

Multicollinearity between the explanatory variables should be avoided to create a more robust model and perform the sensitivity analysis. Moreover, this helps the model train faster and prevent it from establishing invalid correlations between the input and output.
The database contained completion length and number of stages. Since, these two parameters were highly correlated, number of stages was removed and completion length was considered in the study. Additionally, the volume of proppant and fluid injected were correlated to each other. For this reason, the volume of fluid was excluded from the database and the ratio between proppant and fluid injected was preferred. The final parameters considered in the study to build the data-driven models were listed in Table 3.14.

Outliers are observations that are markedly deviated from other observations in the sample (NIST, 2012). It is important to identify the outliers in the database because these can be errors or contain interesting information. In this work, the outliers for all features were estimated by using the interquartile rule. The interquartile rule is as follows (Taylor, 2018):

1. Estimate the interquartile range (IQR) for the data. The IQR is the difference between the third quartile (Q3) and the first quartile (Q1).
2. Multiply the IQR by the number 1.5.
3. Add 1.5 x (IQR) to the third quartile. Any number greater than this is identified as an outlier.
4. Add 1.5 x (IQR) from the first quartile. Any number less than this is identified as an outlier.

Mistyped values were found in the initial dataset by using this method. Furthermore, five wells were identified as outliers due to large 365-day cumulative oil production normalized by completion length. These wells were investigated in detail by checking all other parameters and comparing them to the other wells. Considering the other parameters, no drastic differences were found to explain the reason for such high performance. It is worth mentioning that parameters that directly quantified reservoir quality were not included due to the unavailability of suitable

data (e.g., porosity or permeability maps), and well location was used as a rough proxy for reservoir quality. As such, the wells identified as outliers due to high oil production were retained in this study. Though the high production volumes for these wells may have been due to anomalously good reservoir quality, there was no basis for excluding them based on the parameters included in this study considered. Table 3.15 lists the outliers identified by using the interquartile rule.

Table 3.14. Parameters included in the data-driven predictive models.

Identifier	**Category**	**Parameter**	**Units**	**Source**
Independent Variables				
1	Location (surface coordinates)	Latitude	°	GeoVista
2		Longitude	°	GeoVista
3	Reservoir	True Vertical Depth	m	GeoVista
4		Net pay	m	Baytex
5		Average GOR	$\frac{m^3}{m^3}$	Baytex
6	Completion and stimulation	Completion length	m	Accumap
7		Average stage spacing	m	Calculated
8		Proppant intensity	$\frac{t}{m}$	Calculated
9		Proppant concentration	$\frac{t}{m^3}$	Calculated
Dependent Variables				
10	Well performance	365-day cumulative oil production	m^3	GeoVista

Table 3.15. Lists of outliers based on the interquartile rule. These outliers were retained in this study, as no basis could be found for eliminating them.

UWI	Field	Operator	365-days oil production (m^3)	365-days oil production/ length (m^3/m)
02/08-22-026-19W3/0	Plato North	Crescent Point Energy	3415.7	5.47
01/15-22-026-19W3/0	Plato North	Crescent Point Energy	3459.2	5.61
01/02-31-029-24W3/0	Whiteside	Whitecap Resources Inc.	3491.5	5.69
92/07-33-029-25W3/0	Whiteside	Whitecap Resources Inc.	3417.9	5.54
01/10-35-029-25W3/0	Whiteside	Whitecap Resources Inc.	7023.4	6.25

3.4 Overview of the two modeling techniques used in this study

In this section, summaries of multiple linear regression and random forest modeling techniques are presented. Both methods account for the effect of all predictor variables simultaneously; however, a multiple linear regression assumes a linear relationship among the input and output variables, while random forest is capable of modeling nonlinear and more complex relationships. Additionally, the workflow and tools used to develop each model are discussed.

3.4.1 Multiple linear regression

By definition, multiple linear regression is a method to compare several independent variables to one dependent variable. This approach accounts for the effect of all variables simultaneously and fits a linear relationship to each variable (Cunningham et al., 2012). Equation 3.1 illustrates the model with n predictor variables $X_1, X_2 \dots, X_n$ and a response Y, as follows:

$$Y = \beta_0 + \beta_1 x_{1i} + \beta_2 x_{2i} + \cdots + \beta_n x_{ni} + \epsilon_i \quad \text{Eq. 3.1}$$

ϵ_i corresponds to the error or residual term, and $\beta_0, \beta_1, \beta_2, \dots, \beta_n$ represent the regression coefficients. β_0 is the intercept of the plane Y. β_1 to β_n are the partial regression coefficients. Each regression coefficient value ($\beta_0, \beta_1, \beta_2, \dots, \beta_n$) represents the change in the dependent

variable resulting from one unit change in the independent variable evaluated, holding all other predictor variables constant. The intercept and the regression coefficients are selected to minimize the sum of squared errors (Cunningham et al., 2012).

3.4.1.1 Multiple linear regression workflow

The Python library called StatsModels is used to develop the multiple linear regression model. This powerful module is capable of estimating several statistical models and tests. StatsModels provides different options for linear regression. In this study, the ordinary least squares (OLS) estimator is used. This method chooses the regression coefficients that minimize the sum of the squared errors.

The workflow to develop the multiple linear regression model contains the following steps:

1. Data collection
2. Randomly split the data into training and test sets
3. Create the multiple linear regression model using the training set with 5-fold cross-validation.
4. Evaluate the model using the test set

Once the data is collected, the database is divided into two portions, the training and the test, to assess the performance of the model. The training dataset is the largest one. This set is used to train the model and establish the relationships between the input and output variables. The size of the training set depends on the size of the database. This set can range from 40 to 80% of the entire database (S. D. Mohaghegh, 2017). The test set corroborates the predictive and generalization capabilities of the model. The size of this set is between 10 to 30% of the entire dataset (S. D. Mohaghegh, 2017).

Scikit-learn provides the Model Selection library, in which the class called “train_test_split” is used to divide the data into training and test portions. The original database containing 875 wells was randomly split into training (60%) and test (40%) set. No training was performed on the test dataset.

After dividing the data, the training set was used to develop the multiple linear regression by using the OLS estimator. Finally, the model was fitted on the test data to assess the performance by estimating the coefficient of determination (R^2). This metric is interpreted as the proportion of variance in the dependent variable that may be explained by the independent variable (STHDA, 2018). The value will always range from zero to one.

A value of R^2 close to one means that the input variables explain a great proportion of the variance in the output variable. A disadvantage of R^2 is that this value will always increase when adding more independent variables, even though the variables added have little effect in the model. For this reason, the value of adjusted R^2 will be also considered. This statistic adjusts the R^2 by considering the number of predictor variables (STHDA, 2018). R^2 is estimated as the following:

$$R^2 = 1 - \frac{\sum_{i=1}^{n}(Y_i - \widehat{Y}_i)^2}{\sum_{i=1}^{n}(Y_i - \overline{Y})^2} \qquad \text{Eq.3.2}$$

Y_i corresponds to the actual values of the dependent variable. $\overline{Y}$ is the mean of the actual values, and $\widehat{Y}_i$ is the fitted value.

3.4.2 Random forest

Random forest (RF) is an ensemble learning method mostly used for classification and regression tasks. This machine learning technique was originally proposed by Breiman (2001). Ensemble methods use several base estimators in combination with a learning algorithm to improve the predictive performance of a model (Scikit-learn, n.d.).

Random forest creates many randomized decision trees that split the dataset into smaller groups considering only a subset of the predictors' variables in each group. The subsets follow a hierarchical structure with respect to the model output. The model aggregates the predictions in each individual tree and averages the results (Biau et al., 2008). This process helps to reduce the variance between the trees, and improve the robustness of the model (James et al., 2013). Figure 3.33 illustrates the RF model structure.

According to Genuer et al. (2017), this powerful algorithm provides high performance models with few parameters to tune compared to other algorithms, such as neural networks. Additionally, this technique can handle unbalanced data and missing values, and the runtimes are fast. More details regarding the implementation of RF models can be found in Breiman (2001) and Scikit-learn's random forest documentation.

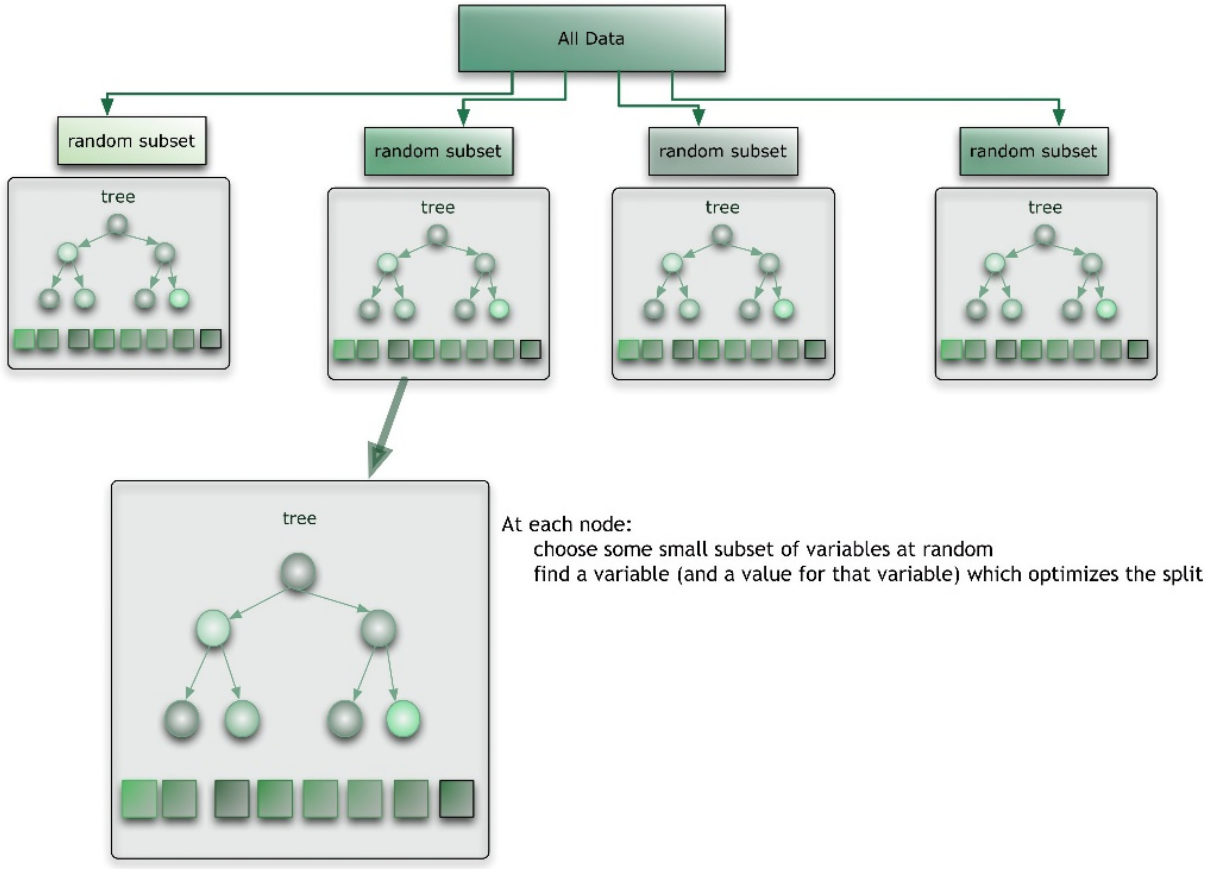

Figure 3.33. Scheme of random forest model (Benyamin, 2012).

3.4.2.1 Random forest workflow:

In this work, a Scikit-learn Python module for machine learning is used to implement the RF algorithm. Two RF models (model A and B) were constructed considering different input features due to multicollinearity problems between the variables (which can affect the model interpretation). The features included in each model are stated in section 4.2 Random forest performance

The workflow used to develop the two RF regression models is summarized in Figure 3.34, and contains the following steps:

1. Data collection,
2. Randomly split the data into training and test set,
3. Create the baseline random forest model,
4. Define the candidates' hyperparameters for the RF model,
5. Evaluate and identify the optimum hyperparameters for the model using grid search and 5-fold cross-validation,
6. Retrain the RF model with the optimized configuration of hyperparameters, and
7. Validate the model using the test set.

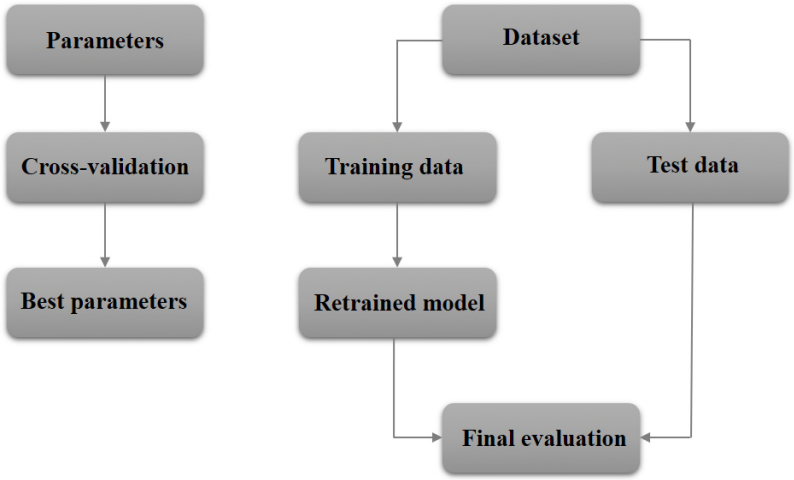

Figure 3.34. Workflow to develop the random forest models. Adapted from "Cross-validation: evaluating estimator performance," Scikit-learn (2019).

The data was split in the same way as in the multiple linear regression model. The training set accounts for 60% of the database and the test set contained the remaining 40%. After splitting the dataset, each RF model was initialized using the hyperparameters default values to obtain a baseline model. Each RF model contains some hyperparameters that define the model architecture. These characteristics can impact the accuracy and efficiency of the model (ODSC, 2019). There are several hyperparameters to tune and the list can be found in the documentation for RF regressor in Scikit-learn (Scikit-learn, 2019). Commonly, four hyperparameters including

n_estimators, max_features, max_depth and min_samples_split are tuned and these are defined as follows:

- N_estimators refers to the number of trees in the forest. Decision trees often increase the model performance because predictions are based on a large variety of trees. It is worth mentioning that a high number of trees is computationally expensive (ODSC, 2019).
- Max_features corresponds to the number of features to consider when finding the optimum split. Typically, a large number of features can increase the model accuracy because trees have more feature options to find the best split. However, this can also induce overfitting of data (ODSC, 2019). According to James et al. (2013), a common number of features that balance between under-fitting and overfitting is equal to the square root of the total number of features in the dataset (3 out of 8 for this work).
- Max_depth is the maximum depth of the tree. Several splits in each tree are made in RFto create more homogeneous groups of data. This allows the model to explain more variance in the data; nonetheless, this can also increase overfitting. For this reason, a wide range of depths should be evaluated to determine the optimum value (ODSC, 2019).
- Min_samples_split refers to the minimum number of data points needed to split each internal node. The selection of this value is based on the number of data points in the training set (ODSC, 2019).

Hyperparameters can be tuned by trial and error. Several models are manually fit with different combination of hyperaparameters and the performance of the models is compared; however, this method can be time consuming (ODSC, 2019). On the other hand, random search and grid search are alternative approaches to find an optimum model architecture. In Python, this can be implemented by using RandomizedSearchCV and GridSearchCV in the Scikit-learn library.

The random search method uses random combinations of hyperparameters to find an optimum combination for the model. The distribution of each hyperparameter and the number of iterations is defined in a grid (Figure 3.35). In this study, 150 models were run, and different hyperparameters values were considered. A disadvantage of this method is that the model results yield high variance because the hyperparameters are randomly sampled from the grid. For this reason, grid search technique was also used in this work.

Grid search creates and evaluates a model for each combination of hyperparameters stated in the grid. Since the possible combinations of hyperparameters are endless, random search is useful to evaluate a wide space and establish a smaller grid for grid search. In this way, it can be guaranteed that grid search is looking into the correct space of hyperparameters.

Figure 3.36 illustrates the candidate hyperparameters that were evaluated in this study using the grid search method. A total of 90 different model structures were trained in order to identify the optimum combination of hyperparameters.

```
# Randomized Search CV

# Number of trees in random forest
n_estimators = [int(x) for x in np.linspace(start = 100, stop = 3000, num = 20)]
# Number of features to consider in each split
max_features = ['auto', 'sqrt']
# Maximum number of levels in the tree
max_depth = [int(x) for x in np.linspace(3, 50, num = 8)]
# Minimum number of samples required to split a node
min_samples_split = [2, 5, 10, 15, 20, 100]

# Create the random grid
random_grid = {'n_estimators': n_estimators,
               'max_features': max_features,
               'max_depth': max_depth,
               'min_samples_split': min_samples_split}

print(random_grid)
```

```
{'n_estimators': [100, 252, 405, 557, 710, 863, 1015, 1168, 1321, 1473, 1626, 1778, 1931, 2084, 2236, 2389, 2542, 2694, 2847, 3
000], 'max_features': ['auto', 'sqrt'], 'max_depth': [3, 9, 16, 23, 29, 36, 43, 50], 'min_samples_split': [2, 5, 10, 15, 20, 10
0]}
```

Figure 3.35. Grid of hyperaparameters evaluated using random search method. This grid was employed for both model A and B

(a)

```
# Potential hyperparameters
param_grid = {
            "n_estimators"      : [1765,1770,1775,1780,1785,1790],
            "max_features"      : ["sqrt"],
            "min_samples_split" : [2,4,6],
            "max_depth": [14,15,16,17,18]
            }
```

(b)

```
# Potential hyperparameters
param_grid = {
             "n_estimators"      : [395,400,405,410,415,420],
             "max_features"      : ["sqrt"],
             "min_samples_split" : [2,4,6],
             "max_depth": [41,42,43,44,45]
             }
```

Figure 3.36. (a) Grid of hyperparameters evaluated in model A using grid search method, and (b) hyperparameters evaluated in model B.

One of the biggest challenges when developing a supervised machine learning model is overfitting the data during the training process. This situation negatively affects the performance of a model using unseen data (test set). Cross-validation is a resampling technique that can help to address this challenge. This method draws samples from the training set and refits the model on each sample to obtain more information about the data (James et al., 2013). In the end, a less biased model is produced because each data point in the training set is used to train and test the model.

The performance of k-fold cross-validation (CV) corresponds to the average in the scores of the evaluated folds. Figure 3.37 presents a scheme of the 5-fold CV method that was implemented in this work by calling the cross_val_score function in Scikit-learn. The training set was split into five cross-validation folds. Each fold contained approximately 12% of the original database. Four folds were added to train the model, and the fifth fold was used to compute the performance.

The random and grid search methods combined with cross validation were implemented to find the optimum hyperparameters for the RF model during the training process. Five iterations were performed for each combination of hyperparameters due to the five-fold cross validation method. Once the hyperameters were optimized, the prediction and generalization capability of the model was assessed by using the test set. The coefficient of determination (R^2) was used to measure the model performance.

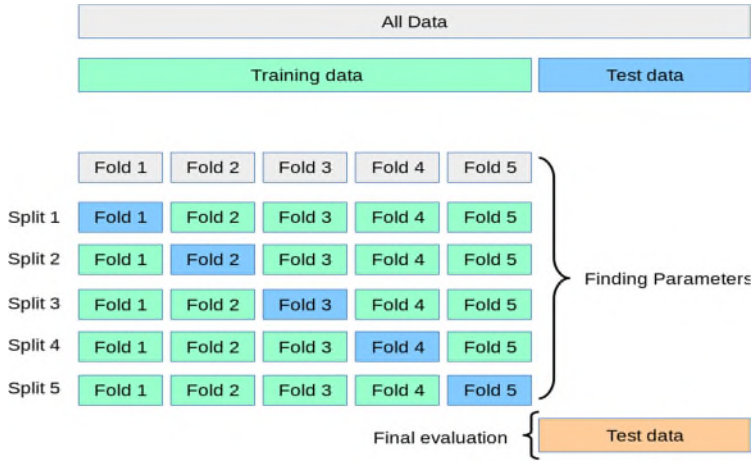

Figure 3.37. Data partitioning scheme using 5-fold cross validation (CV) (Scikit-learn, 2019)

CHAPTER 4: RESULTS

In this chapter, the results from the developed data-driven models are presented. In summary, each section of this chapter will cover the following:

1. The multiple linear regression and random forest models were used to predict 365-day cumulative oil production in the Viking Formation. The performances of both models were compared, then the model with the highest prediction capabilities was selected for further interpretation.
2. The random forest models were used to establish key oil production drivers in the study area. The permutation feature importance technique was employed to identify the features that have the highest impact on the variability of oil production.
3. Using the random forest model B, the effect of each input feature on oil production was interpreted using individual conditional expectation (ICE) and partial dependence plots (PDP). Feature contributions were estimated on a well-by-well level basis to understand what drives production in each well. Case studies between pairs of wells in different areas were made to compare well productivity.

4.1 Multiple linear regression performance

A multiple linear regression model was constructed using nine input features (TVD, net pay, average GOR, latitude, longitude, completion length, average stage spacing, proppant intensity, and proppant concentration) and one output (365-day cumulative oil production). The developed model provided a R^2 values of 0.41 and 0.45 on the training and test sets, respectively. These results indicated that the model was able to explain only 45% of the oil production variance in the study area. The low performance can be mainly attributed to the fact that the model assumes a linear relationship between the variables. The python code utilized to build the regression model is presented in Appendix C.

Figure 4.1 presents a cross plot of the oil production predicted versus the actual values including the training and test sets. The dashed line represents the one-to-one line (45-degree slope). The graph provides evidence that the oil production predictions do not match well with the actual values.

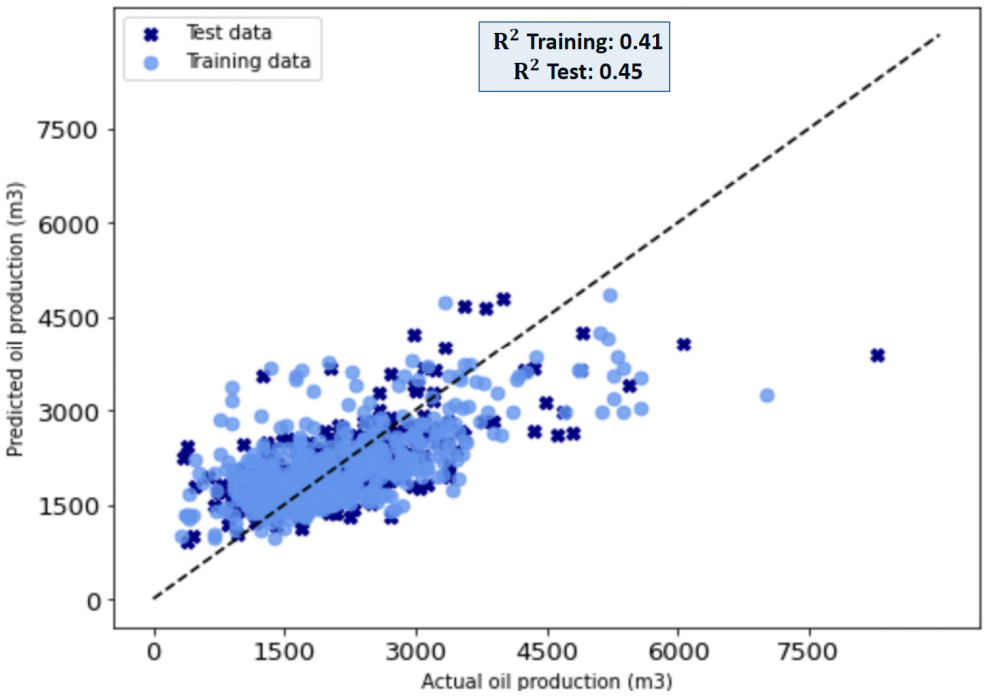

Figure 4.1. Multiple linear regression model results, showing across plot of forecasted versus actual values for 365-day cumulative oil production. The dashed line represents the one-to-one line. R^2 values for the training and test datasets are shown in the box centred near the top of the plot.

4.2 Random forest performance

Two random forest models were trained considering different input features, as follows:

- Model A: TVD, net pay, average GOR, latitude, longitude, completion length, average stage spacing, proppant intensity, and proppant concentration.
- Model B: TVD, net pay, average GOR, latitude, longitude, completion length, and proppant intensity.

Model A was built to assess the importance of proppant intensity, proppant concentration, and average stage spacing on well performance. However, the ICE and PDP plots and SHAP values cannot be estimated using this model because proppant concentration depends on both the variability of proppant and fluid intensity. Therefore, concentration cannot be held constant when developing the ICE and PDP plots for proppant intensity. Additionally, average stage spacing relies on the change of lateral length and the number of stages.

On the other hand, model B was constructed to perform a sensitivity analysis. As a result, proppant concentration and average stage spacing were excluded from this model. Proppant intensity was

retained in the model because this parameter has a higher impact on oil production variability than the other features. The python code used to construct the two RF models is shown in Appendix C.

Table 4.1 summarizes the RF model results. As presented in the table, the coefficients of determination using the test set for model A and B are 0.60 and 0.59, respectively. These results indicate that the models are able to explain over half of the variability in 365-day cumulative oil production. Both models have similar predictive capabilities.

Table 4.1. Random forest modeling results.

	Training R^2	**Test R^2**
Model A	0.94	0.60
Model B	0.95	0.59

Although the coefficients of determination are modest it should be noted that the models have an acceptable range of accuracy considering that they include data from several fields, which increases the variability in reservoir quality. In this case, the low R^2 values can be attributed to the lack of data to fully describe the reservoir quality, inconsistencies in the data that were not identified, and/or operational problems that affect oil production for which no data were available.

The oil prediction results using the training and test data for model A and B are presented in Figure 4.2 and Figure 4.3, accordingly. The data points are grouped along the one-to-one line, which indicates that the predictions have a good match with the actual production values for both the training and test sets.

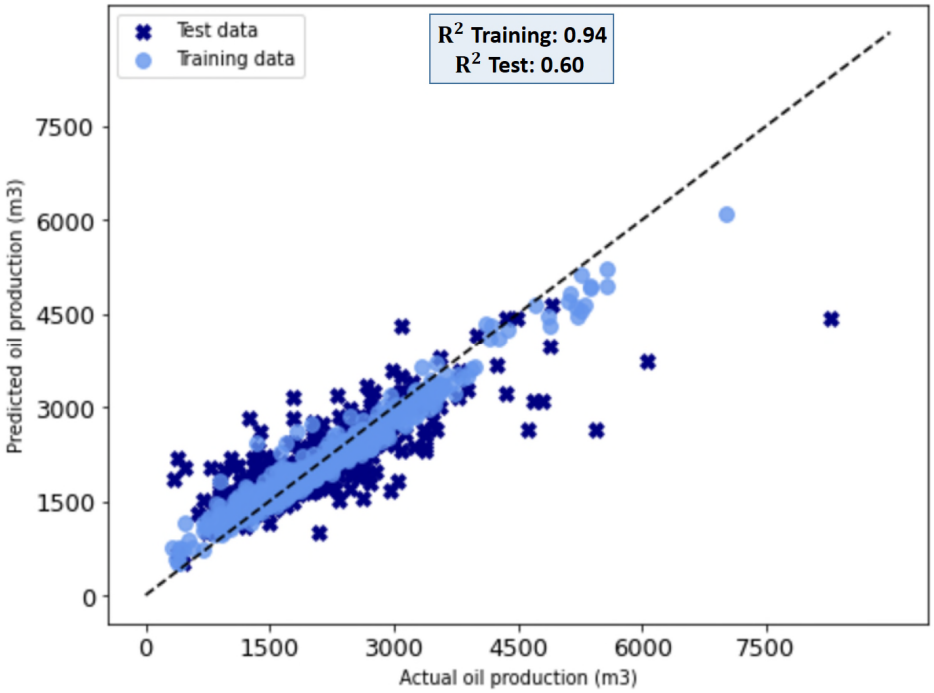

Figure 4.2. RF model A results. Cross plot of the predicted oil production vs the actual values.

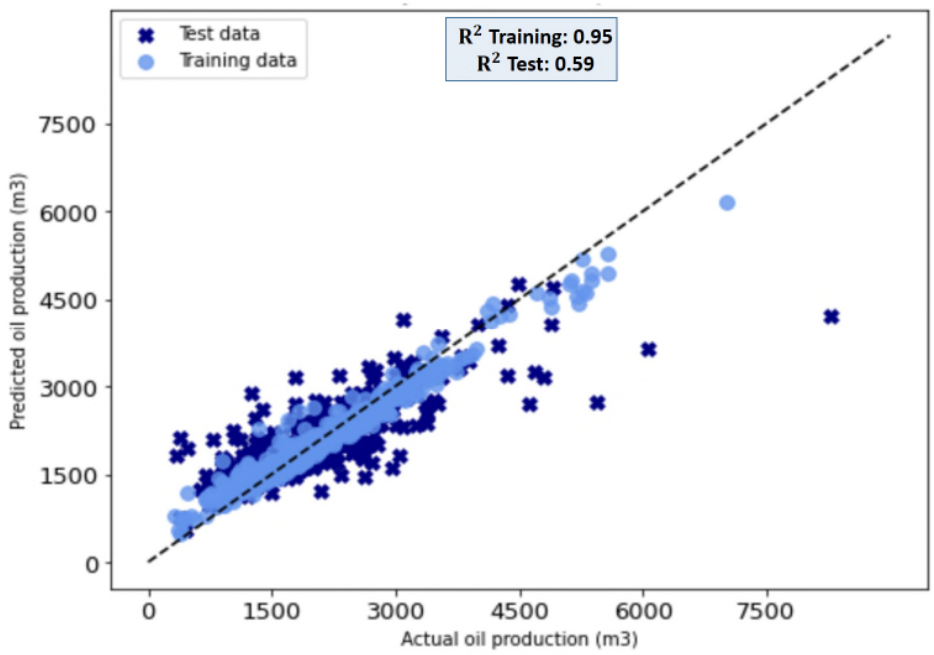

Figure 4.3. RF model B results. Cross plot of the predicted oil production vs the actual values.

4.3 Random forest interpretation

Machine learning models can be easily interpreted by using model-agnostic interpretation methods. In this work, only random forest is analyzed because this model can consider nonlinear and complex relationships between the predictor variables and the outcome. Additionally, the interactions between the features can be examined. The following sections present interpretability methods, such as permutation feature importance, individual conditional expectation (ICE), partial dependence plots (PDP), and shapley additive explanations (SHAP).

4.3.1 Permutation feature importance

The permutation feature importance was introduced by Breiman (2001). This method measures the importance of a feature's value and assigns a prediction error. A feature is considered important if the error of the model is increased by shuffling the feature's values. On the other hand, the feature is not important if, when shuffling the values, the error remains the same because this means that the model avoided the feature during the prediction. The features are sorted by descending error (Molnar, 2019).

In this work, the importance of features was calculated using the test (out-of sample) data to quantify how much each feature contributes to the model performance. The ELI5 python package was employed to estimate each features importance. This package can debug machine learning models and explain the predictions. Moreover, it also implements multiple algorithms for analyzing black-box models, such as random forest. ELI5 estimates the importance of features by determining how much the model score (365-day production) decreases when a feature is not present in the model.

Table 4.2 and Table 4.3 present the feature importance values for models A and B. Furthermore, Figure 4.4 presents a bar chart that compares the results from both models. As observed, the weights of the features in both models are similar. Completion length was the main oil production driver in the study area. Net pay and proppant intensity were the next dominant factors. It is worth noting that completion length and proppant intensity are controlled by the operator when developing the reservoir. Furthermore, well geographic location, which is an indicator of reservoir and geologic characteristics, has a lower effect on well performance than

stimulation parameters (i.e., lateral length and proppant intensity). TVD, proppant concentration, and average stage spacing seemed to have little effect on determining well performance in the Viking Formation.

Table 4.2. Permutation feature importance for the RF model A using the test dataset.

Feature	Feature importance
Completion length	0.48
Net pay	0.10
Proppant intensity	0.08
Average GOR	0.07
Longitude	0.06
Latitude	0.05
Proppant concentration	0.03
TVD	0.02
Average stage spacing	0.01

Table 4.3. Permutation feature importance for the RF model B using the test dataset.

Feature	Feature importance
Completion length	0.47
Proppant intensity	0.11
Net pay	0.10
Average GOR	0.08
Longitude	0.07
Latitude	0.06
TVD	0.03

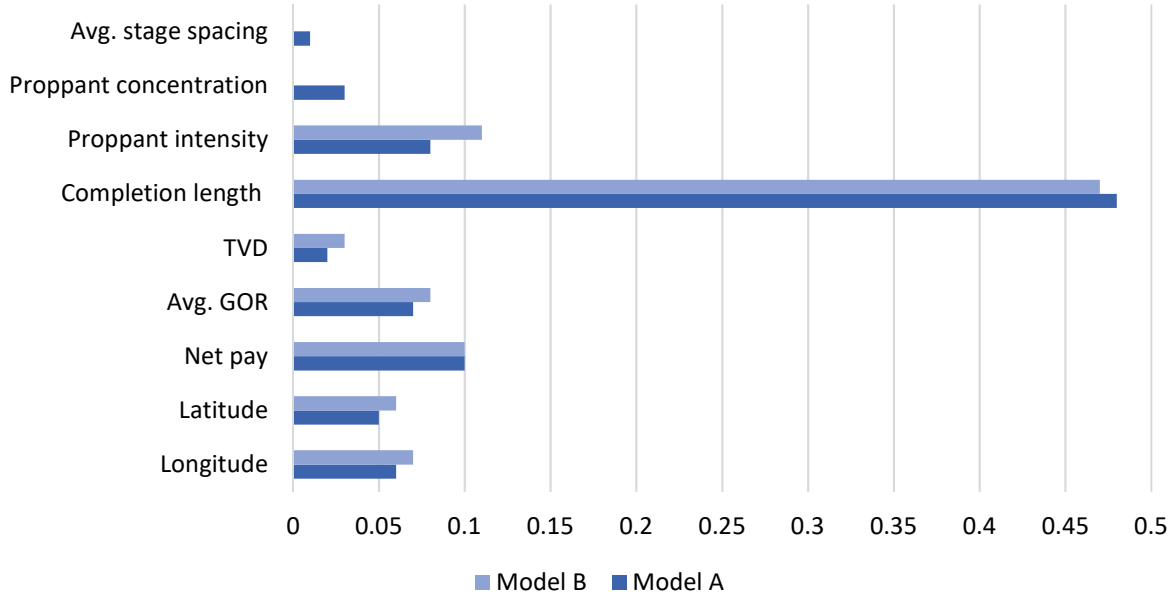

Figure 4.4. Comparison of features importance for model A and B

4.3.2 Partial dependence plots (PDP) and individual conditional expectation (ICE)

The Partial dependence plot (PDP) represents the marginal effect of one feature on a model's predicted outcome. This plot is useful to visualize the relationship between a feature and outcome (Molnar, 2019). The partial dependence function is defined as follows:

$$\hat{f}_{x_s}(x_s) = E_{x_c}[\hat{f}(x_s, x_c)] = \int \hat{f}(x_s, x_c)\, dP(x_C) \qquad \text{Eq. 4.1}$$

Where x_s corresponds to the feature analyzed, x_c represents the other features included in the model $\hat{f}$, and s is the number of features studied which is typically one or two. x_s and x_c compose the total feature space *x*. The PDP marginalizes the model output over the distribution of the features (parameters) in the dataset *c*. In order words, PDP calculates model output based on the change of the features from the minimum up to the maximum value in the dataset *c* (Molnar, 2019).

The partial function $\hat{f}_{x_s}$ shows the average marginal effect on the prediction for a specific value of features S. This function $\hat{f}_{x_s}$ is estimated using the following expression:

$$\hat{f}_{x_s}(x_s) = \frac{1}{n}\sum_{i=1}^{n} \hat{f}\,(x_s, x_C^{(i)}) \qquad \text{Eq. 4.2}$$

In this case, n represents the features count, and $x_C^{(i)}$ corresponds to the actual features values in the dataset (the features that are not considered for analysis). It is worth mentioning that PDP assumes that the features in C are not correlated to the features in S. Otherwise, the PDP could include data points that are unreal (Molnar, 2019).

PDP is considered a global method because it focuses on an overall average effect of a feature. On the other hand, ICE plots illustrate the variability of an individual prediction according to a feature's value change; as a result, this method focuses on indivual instances (Molnar, 2019). ICE and PDP plots were created to better understand the relationships between each predictor variable and the 365-day cumulative oil production.

ICE plots focus on specific wells. One row of data is selected (one well), and the selected feature (i.e., completion length) is changed from the highest to the lowest value in the dataset to estimate the ICE line. The other remaining features are fixed to their actual values. The random forest model is used to predict the 365-day production at each value of the evaluated feature (i.e., completion length). This process is repeated for every well and feature in the database. The PDP is the average of all ICE lines for the evaluated feature. Linear, monotonic or complex relationships between the feature and the target variable can be identified (Molnar, 2019).

Sometimes is difficult to identify trends in the ICE and PDP because the line for each observation starts at different values. To overcome this problem, the lines can be centered at one point in the feature (i.e., starting from zero). In this way, the shape of the lines are accentuated and the relationships between the variables can be easily identified. The ICE and PDP were constructed using the random forest model B and the test dataset. Python's partial dependence plot toolbox was utilized to build the plots. This powerful tool supports all Scikit-learn algorithms.

4.3.2.1 True Vertical Depth ICE and PDP

An uncentered ICE and PDP for true vertical depth is presented in Figure 4.5. The plot illustrates how the oil production varies with respect to the change of TVD. Each blue line illustrates the predictions for a well (ICE lines) and the yellow line (with blue dots) represents the average of all predictions (PDP). The average 365-day cumulative oil production in the test set was 2102.4 m^3, and it was used as a point of reference to evaluate the effect of TVD. As observed, there is not much variability on well performance (i.e., maximum variation of approximately 100 m^3 compared to 365-day cumulative oil volumes of a few thousand m^3), suggesting that TVD has little effect on productivity in the Viking Formation.

Figure 4.6 presents the centered ICE and PDP of TVD. This figure shows that shallower wells between ≈ 631 m and ≈ 680 m negatively affect production. TVD acts as a proxy for reservoir pressure; as a result, it is expected that shallower wells produce less hydrocarbons. Additionally, it is seen that TVD from ≈ 680 m to ≈ 738 m produces an impact on production of 10 m^3 up to 100 m^3. Negative contributions to production are observed in the deeper wells from 738 m to 806 m. The lower performance in the deeper wells can be attributed to the lower reservoir quality or depletion effect. On average, the deeper wells have low net pay (3.6 m), and some of those wells are located in areas with high GOR, such as Prairiedale.

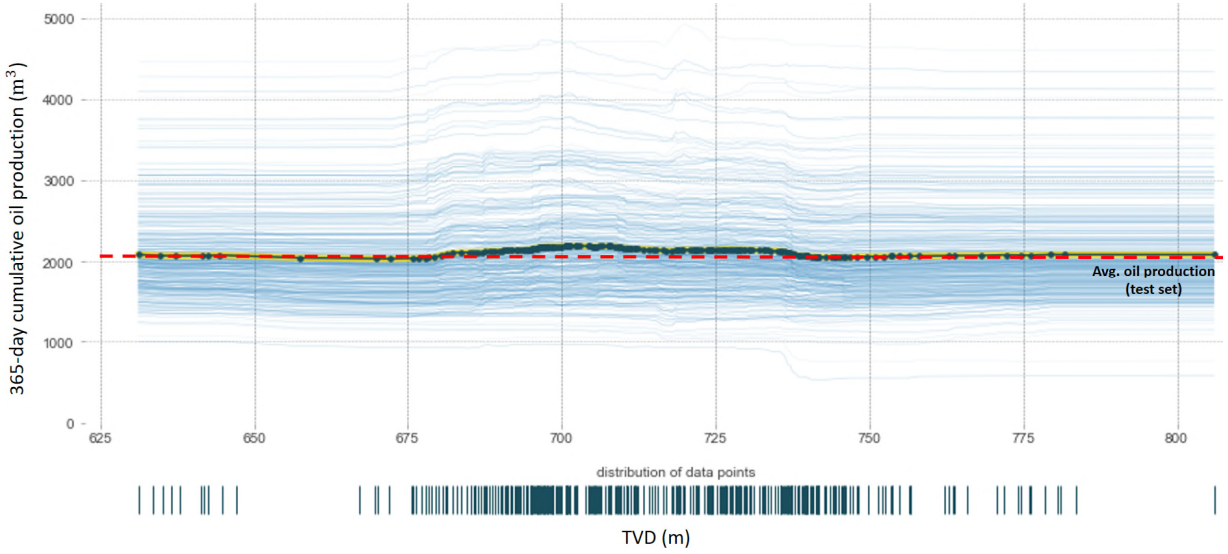

Figure 4.5. Uncentered ICE and PDP for True Vertical Depth, generated using the random forest model B. Each blue line illustrates the predictions for a well (ICE lines) and the yellow line (with blue dots) represents the average of all predictions (PDP). The average 365-day cumulative oil production in the test set was 2102.4 m^3, and it was used as a point of reference to evaluate the effect of TVD.

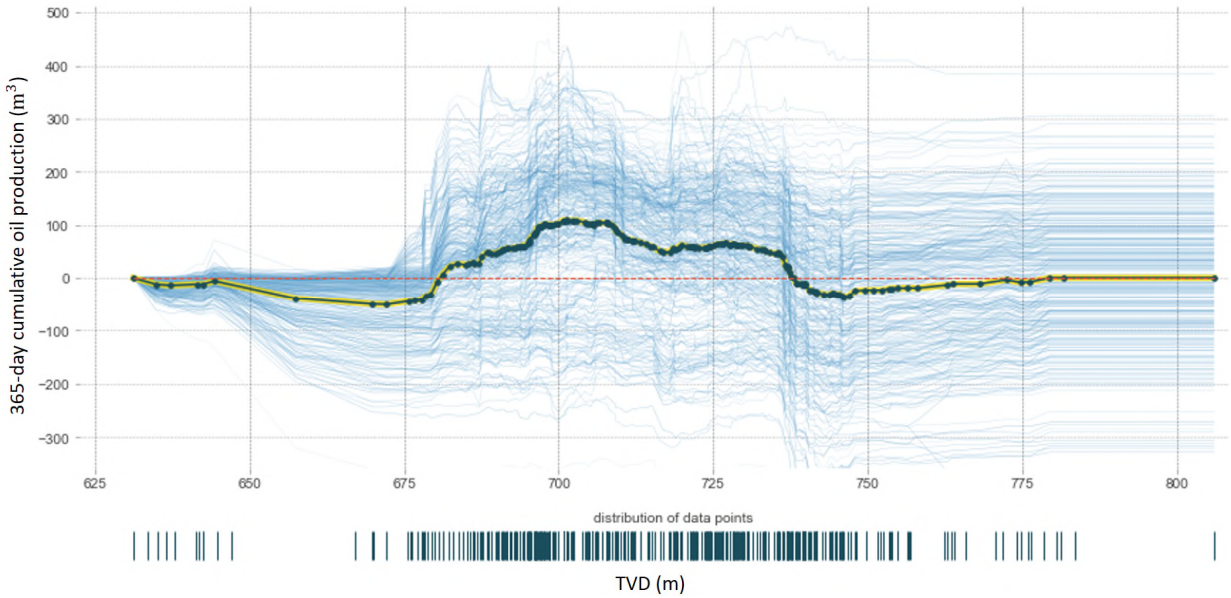

Figure 4.6. Centered ICE and PDP plot for True Vertical Depth, generated using the random forest model B..

4.3.2.2 Net pay ICE and PDP

ICE and PDP for net pay present the oil production response due to the change of net pay while keeping the other variables constant at their true values. As seen in Figure 4.7 and Figure 4.8, net pay values from 0 to ~3.5 m have a minimal impact on well performance. However, there is a positive contribution to production of 5 m^3 up to 440 m^3 from ~3.5 m to ~5.8 m of net pay. It is expected that areas with high net pay produce more hydrocarbon. In this case, it is observed that wells with more than ~6 m of net pay produce less. This response is possibly observed because the areas with high net pay values were already depleted by old vertical wells. Therefore, it is recommended to include the effect of depletion in further studies.

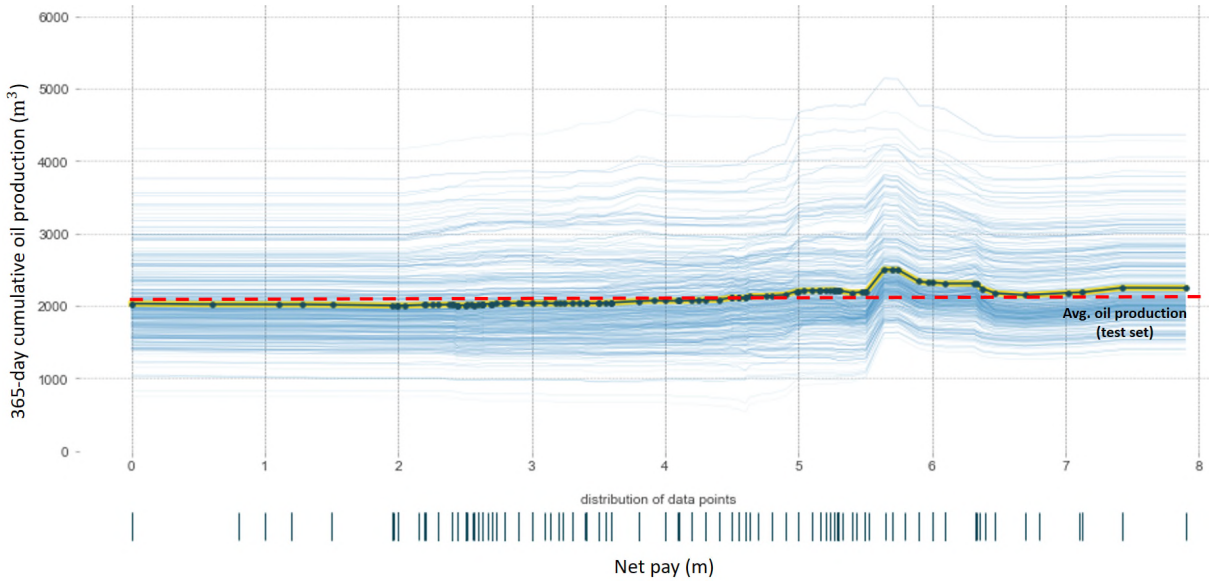

Figure 4.7. Uncentered ICE and PDP for net pay, generated using the random forest model B.

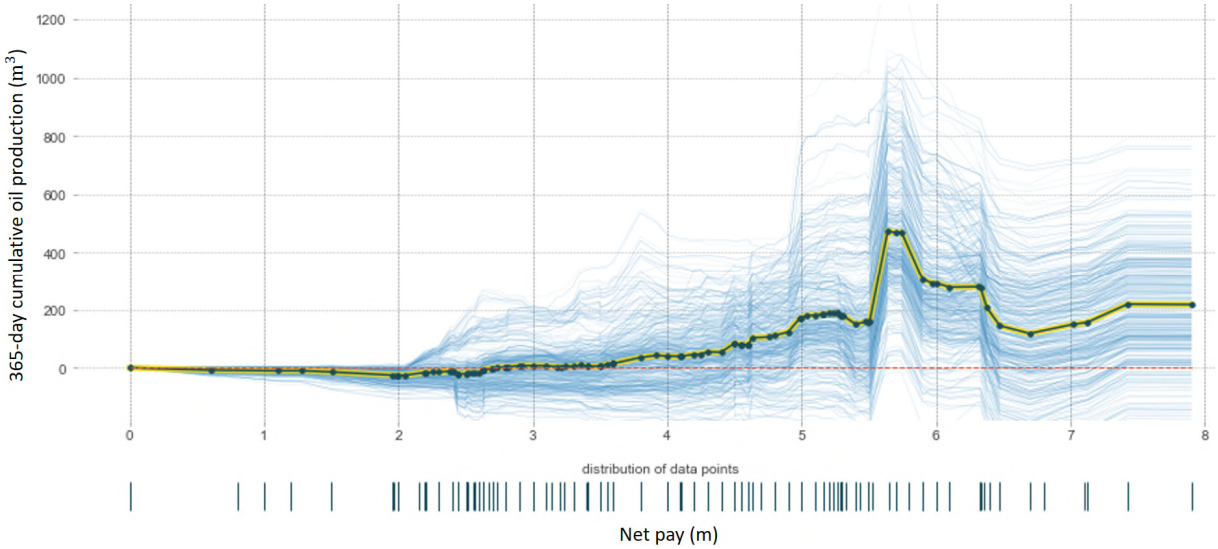

Figure 4.8. Centered ICE and PDP for net pay, generated using the random forest model B.

4.3.2.3 Average gas-oil ratio ICE and PDP

The variation of well performance due to changes on the average GOR is presented in Figure 4.9 and Figure 4.10. A negative relationship between average GOR and oil production is observed. The higher the GOR, the lower the production. Generally, depleted areas tend to have high GOR because of the decrease in reservoir pressure, which allows more gas to come out of solution. Low average GOR from 0.97 to ~40 m^3/m^3 have a minimal effect on production, while high values of GOR (601.6 m^3/m^3) has an impact of - 400 m^3.

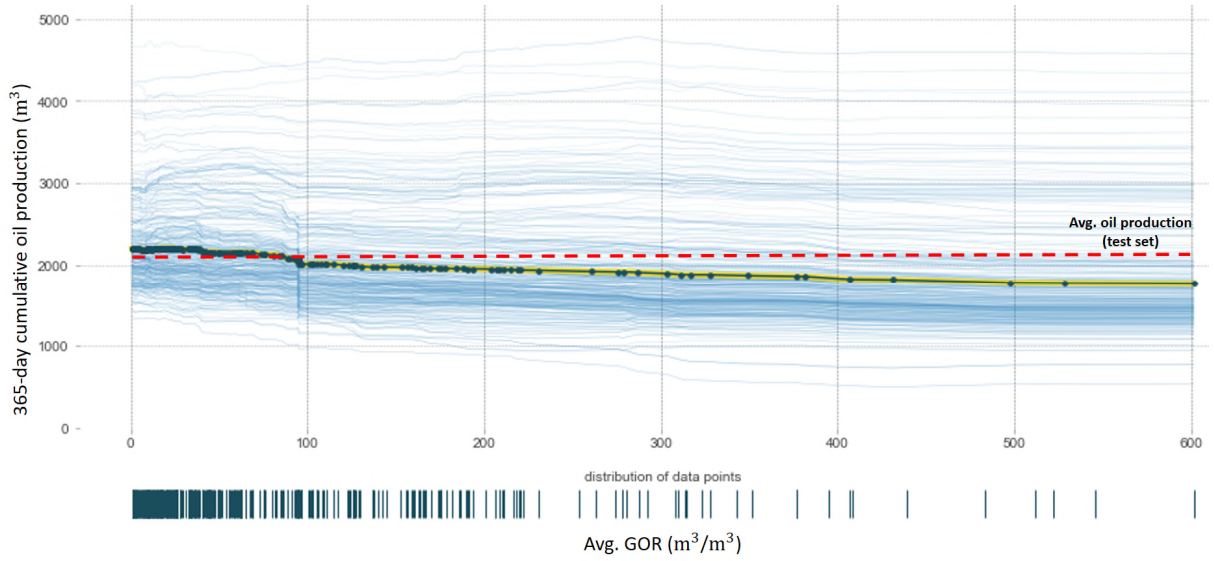

Figure 4.9. Uncentered ICE and PDP for average gas-oil ratio, generated using the random forest model B.

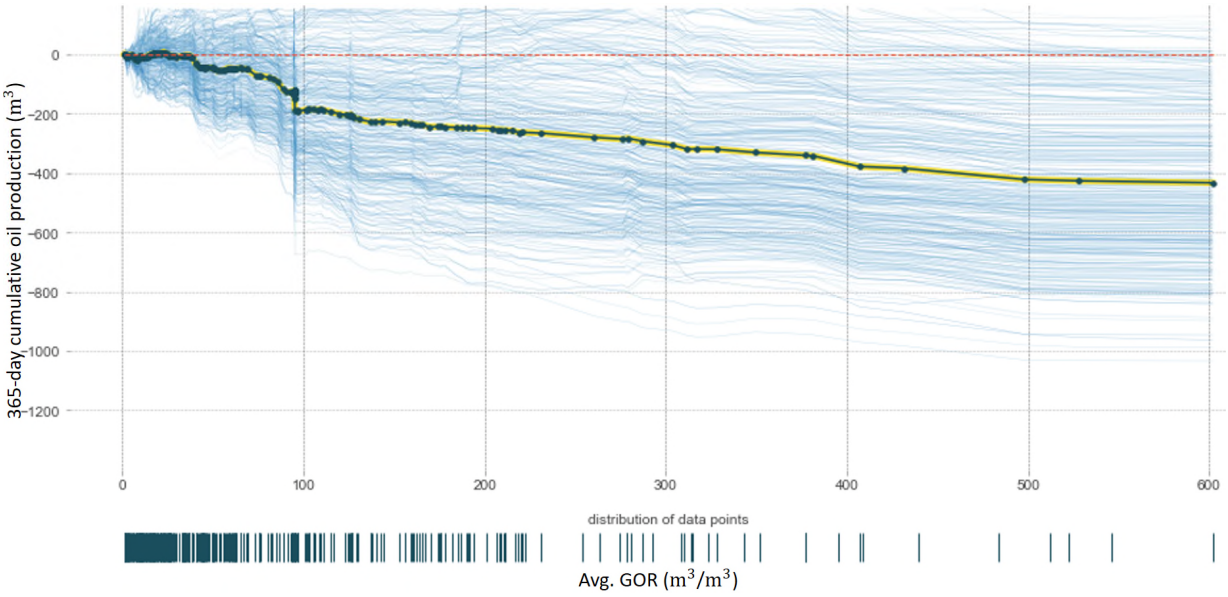

Figure 4.10. Centered ICE and PDP for average gas-oil ratio, generated using the random forest model B.

4.3.2.4 Proppant intensity ICE and PDP

The variation of well productivity because of the change on proppant intensity is illustrated in Figure 4.11 and Figure 4.12. As seen in Figure 4.11, on average a well with a proppant intensity lower than 0.37 t/m tends to produce less oil in the first year than an average well. In contrast, wells treated with proppant intensities higher than 0.37 t/m produce volumes that are above average. Additionally, proppant intensity has an effect ranging from ~1625 m^3at 0.19 t/m to ~2375 m^3 at 0.58 t/m, which is equivalent to an incremental increase of 46% in production.

Figure 4.12 shows the positive relationship between well performance and proppant intensity. The proppant can add up to 750 m^3 using 0.58 t/m in additional oil production in the first year. It is believed that large volumes of proppant are beneficial for well performance because they keep induced hydraulic fractures open. This can lead to larger and higher conductivity factures, which increase production rates. However, a diminishing effect is observed from ~0.49 t/m to 0.58 t/m, which suggests that volumes of proppant within this range have limited impact on production. It is worth noting, however, that this observation is limited by the number of data points in this range (Figure 4.12).

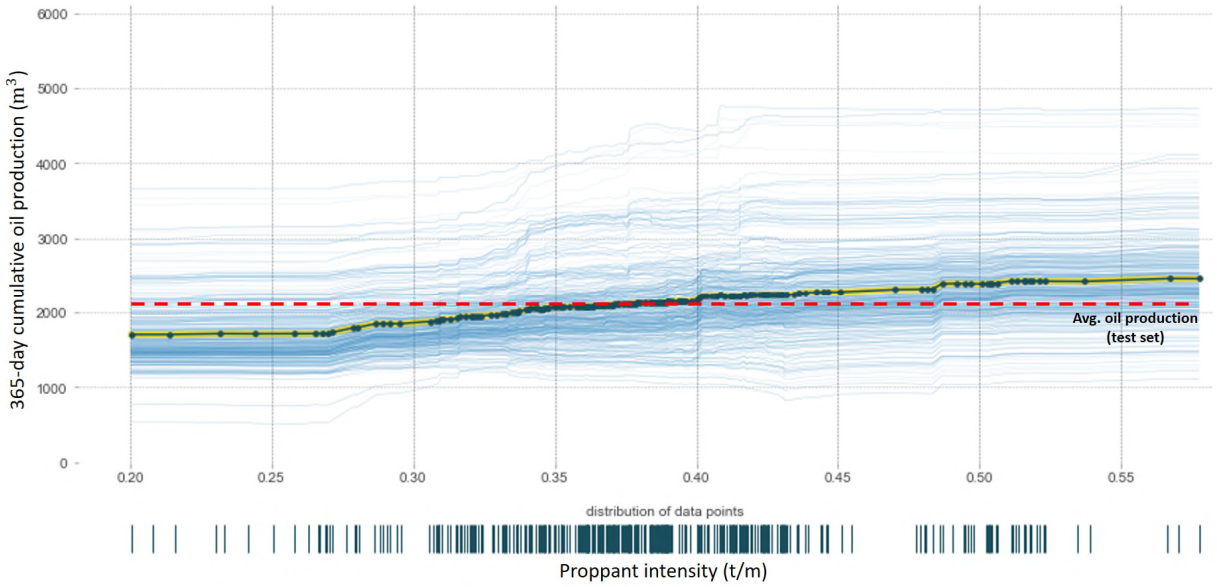

Figure 4.11. Uncentered ICE and PDP for proppant intensity, generated using the random forest model B.

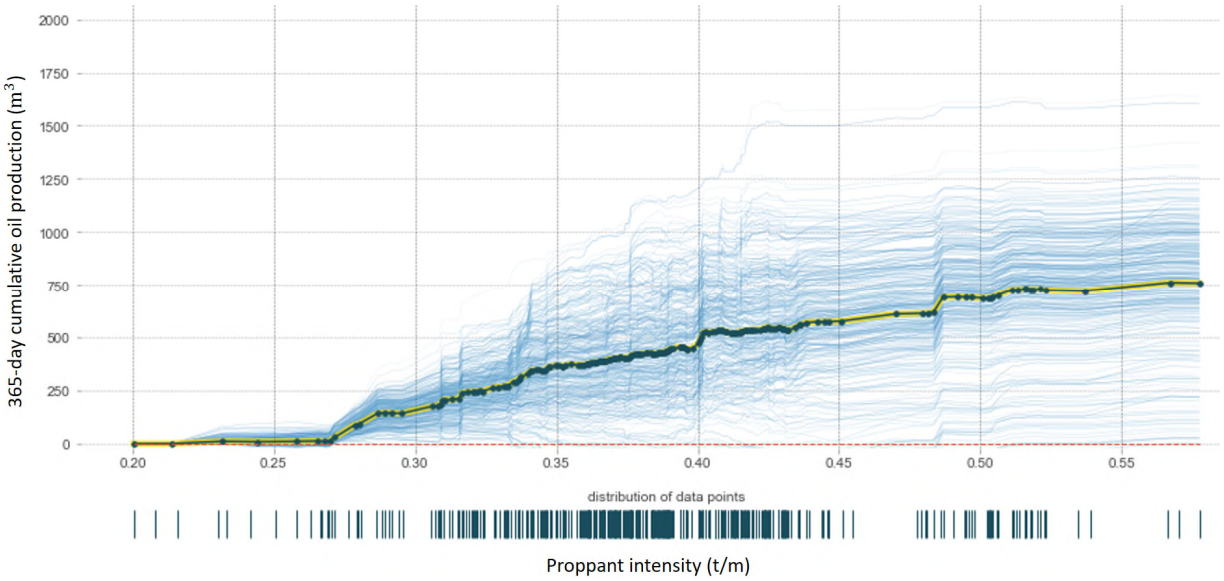

Figure 4.12. Centered ICE and PDP for proppant intensity, generated using the random forest model B.

4.3.2.5 Completion length ICE and PDP

The effect of completion length on well performance is illustrated in Figure 4.13 and Figure 4.14. As seen in Figure 4.13, wells with lateral lengths shorter than ~750 m produce less oil than an average well in the first year while wells with lateral lengths greater than this value produce above the average. Lateral length has an impact ranging from ~1950 m^3 at 212 m to ~3200 m^3 at 1554.9 m, which is equivalent to an incremental increase of 64% in oil production.

Figure 4.14 shows the positive impact that lateral length has on productivity. A large completion length has large contact with the reservoir area, which allows the well to produce more hydrocarbon. Lateral lengths of 1543 m can add production of up to 1250 m^3 of oil per well in the first year in the Viking Formation (Figure 4.14).

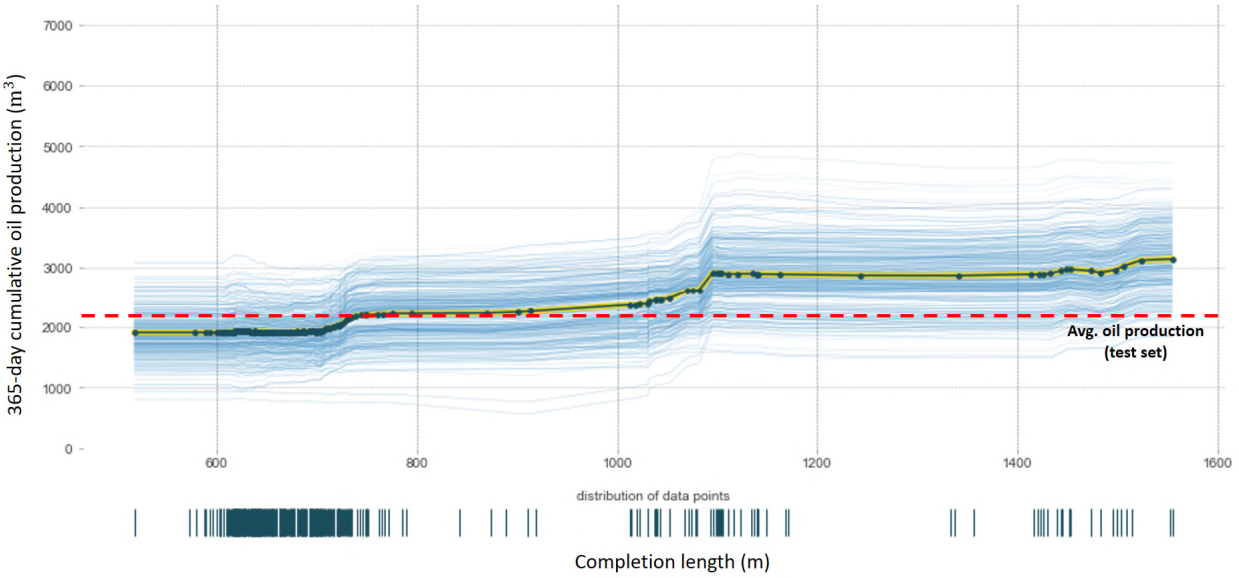

Figure 4.13. Uncentered ICE and PDP for completion length, generated using the random forest model B.

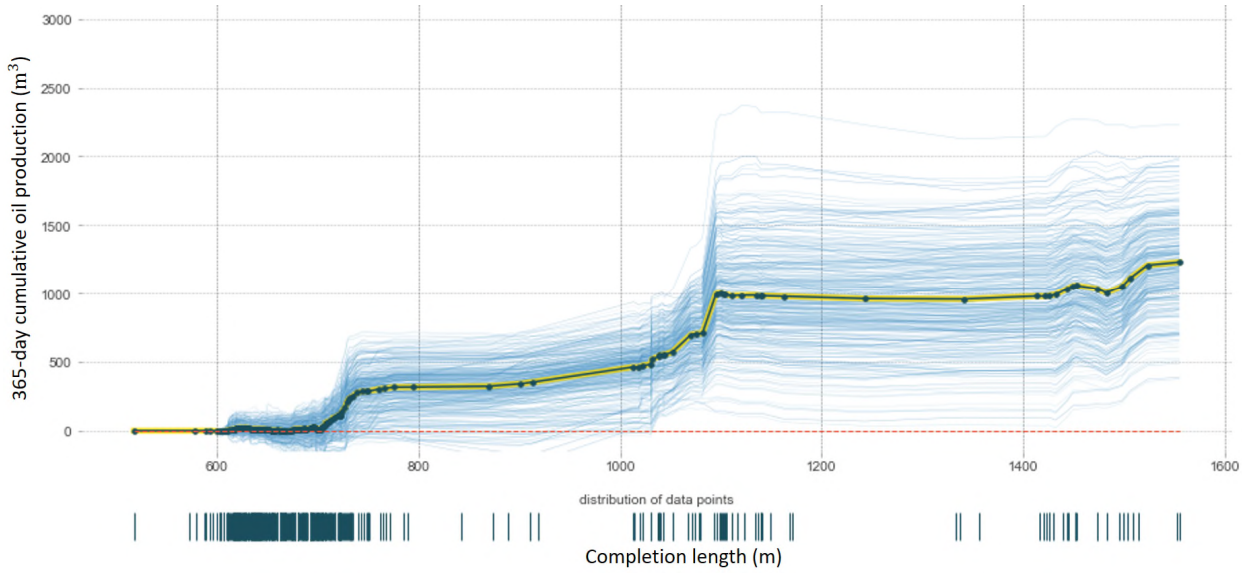

Figure 4.14. Centered ICE and PDP for completion length, generated using the random forest model B.

4.3.3 Shapley additive explanations (SHAP)

Shapley additive explanations (SHAP) was inspired by coalitional game theory, and it was originally introduced by Lundberg and Lee (2016). SHAP aims to provide an explanation for every instance by estimating the contribution of each feature to the prediction. Therefore,

Shapley values are useful to understand how every prediction is calculated and how each feature contributes to the outcome (Molnar, 2019). The Shapley value can be defined as:

$$\emptyset_j(val) = \sum_{S \subseteq \{x_1,\ldots,x_p\} \setminus \{x_j\}} \frac{|S|!\,(p - |S| - 1)!}{p!} (val(S \cup \{x_j\}) - val(S)) \quad \text{Eq. 4.3}$$

The SHAP value of a feature is its contribution to the outcome, which is weighted and summed considering all possible feature combinations. S corresponds to the subset of features included in the model, x represents the vector of feature values in the explained instance, and p refers to the feature's count (Molnar, 2019).

In this work, this technique was used to interpret the oil production predictions on a well-by-well basis. As a result, these values were helpful to understand what drives well productivity in each well. For every well, Shapely values were computed for each feature considered in model B. It is worth noting that the feature contributions (SHAP values) are specific to the combination of features found in each well. Furthermore, these values were measured in the same units of the model outcome (m^3). For instance, a feature's SHAP value of -150 m^3 indicates that the feature reduces oil production by -150 m^3. SHAP values are additive, meaning that the sum of all SHAP values and the average oil production (2101.1 m^3) provides the predicted 365-day cumulative oil production by the machine learning model.

The SHAP values were calculated using shap 0.34.0, which is a Python library for model explainability (Lundberg et al., 2020). This library provides an algorithm specifically for tree ensemble methods, such random forest. Six pairs of wells were selected to understand and compare what drives oil production on a well-by-well basis. Both wells in each pair were located close to each other in order to minimize differences in reservoir quality. Case studies in different areas including Plato North, Kerrobert, Whiteside and Dodsland were analyzed. Additionally, the SHAP values for each feature were plotted and color coded by the operator for comparison purposes and to assist in identifying any trends.

4.3.3.1 Case study: Plato North

Plato North is one of the top producing areas in this study, reporting an average 365-day cumulative oil production of 2390.2 m^3. This area is characterized by having high net pay (average of 5.23 m) and low GOR (average of 29 m^3/m^3).

Table 4.4 presents the actual and SHAP values from the wells 02/12-18-026-18W3/0 and 01/13-18-026-18W3/0. The predicted 365-day cumulative oil production for each well was estimated by adding all feature contributions to the average oil production in the whole set (2101.1 m^3). Both wells have similar input values in all features except in proppant intensity. As seen in Figure 4.15 and Figure 4.16, the main positive contributor for both wells is net pay. Also, since these two wells have short lengths (less than 650 m), this feature has a detrimental effect on performance. Well 02/12-18-026-18W3/0 was treated with 0.16 t/m more proppant than well 01/13-18-026-18W3/0. This difference in proppant had a positive impact on production in the first year, adding 145 m^3 of oil. Well 02/12-18-026-18W3/0 reported an oil production of 2414.7 m^3 (actual value), which is ~15 % greater than the average well, while the other well 01/13-18-026-18W3/0 produced 2130.1 m^3, which is only 1.3% greater than average.

Table 4.4. Feature contributions and actual values for the wells 02/12-18-026-18W3/0 and 01/13-18-026-18W3/0 in Plato North.

UWI	Values	TVD	Net pay	Lati-tude	Longi-tude	Average GOR	Completion length	Proppant intensity	IP365 (m^3)
02/12-18-026-18W3/0	Actual	692.4 m	6 m	51.22 °	-108.50 °	33.73 m^3/m^3	595.1 m	0.45 t/m	2414.7
	Contribu-tion (m^3)	-14.27	188.67	32.19	-0.51	127.52	-253.47	145.71	2326.9
01/13-18-026-18W3/0	Actual	690.8 m	6 m	51.23 °	-108.5 °	51.65 m^3/m^3	620.5 m	0.29 t/m	2130.1
	Contribu-tion (m^3)	-14.93	286.59	53.84	7.22	23.04	-154.52	-232.55	2069.8

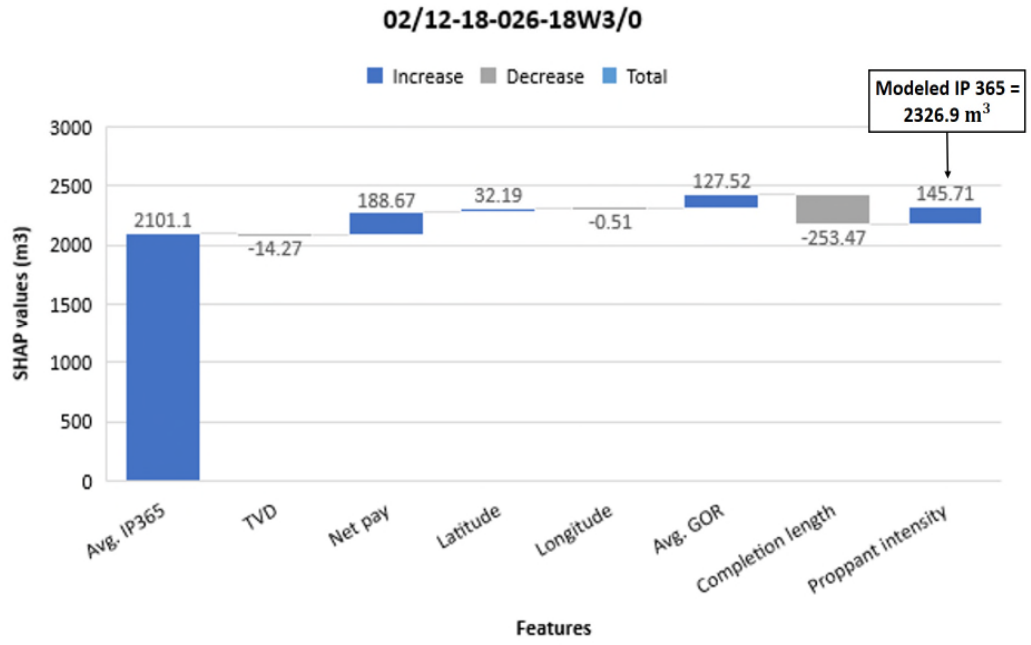

Figure 4.15. Feature contributions (SHAP values) for the well 02/12-18-026-18W3/0 in Plato North. The predicted IP 365 by the RF model was 2326.9 m^3 and the actual was 2414.7 m^3.

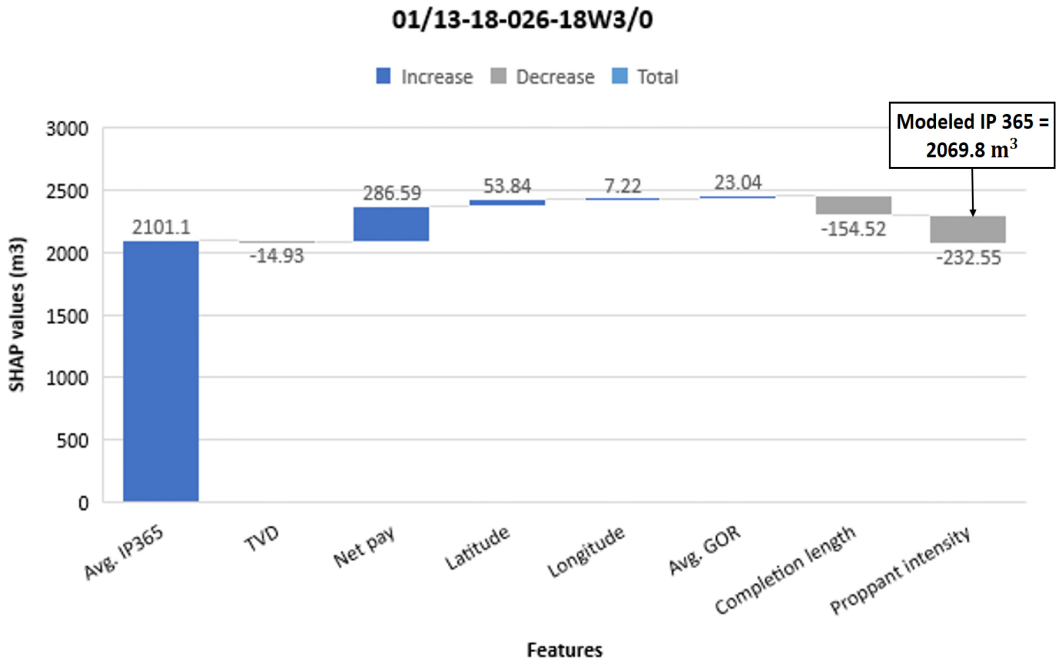

Figure 4.16. Feature contributions (SHAP values) for the well 01/13-18-026-18W3/0 in Plato North. The predicted IP 365 by the RF model was 2069.8 m^3 and the actual was 2130.1 m^3.

The second example from Plato North is presented in Table 4.5. The wells 02/16-17-026-19W3 and 01/14-17-026-19W3 were compared in this case study. As observed in Figure 4.17 and Figure *4.18*, both wells have similar characteristics except for the proppant intensity. The key production drivers in both wells are the low GOR and the high proppant intensity. Well 01/14-17-026-19W3 was treated with 0.03 t/m more proppant than well 02/16-17-026-19W3. As a result, the proppant added 68.48 $m^3$of oil, comparing the proppant contributions of both wells. Furthermore, the oil production of well 01/14-17-026-19W3 was 14% greater than the average, while the other well was only 7% above average.

Table 4.5. Feature contributions and actual values for the wells 02/16-17-026-19W3 and 01/14-17-026-19W3 in Plato North.

UWI	**Values**	**TVD**	**Net pay**	**Lati-tude**	**Longi-tude**	**Average GOR**	**Completion length**	**Proppant intensity**	**IP365 (m^3)**
02/16-17-026-19W3	Actual	715.9 m	4.5 m	51.22 °	-108.61 °	6.14 m^3/m^3	695.4 m	0.48 t/m	2250.4
	Contribu-tion (m^3)	6.41	-3.13	29.61	57.45	99.33	-177.8	202.34	2315.3
01/14-17-026-19W3	Actual	711.1 m	4.5 m	51.22 °	-108.62 °	7.56 m^3/m^3	698.8 m	0.51 t/m	2404.7
	Contribu-tion (m^3)	35	-4.3	35.08	60.19	112.93	-178.2	270.82	2432.6

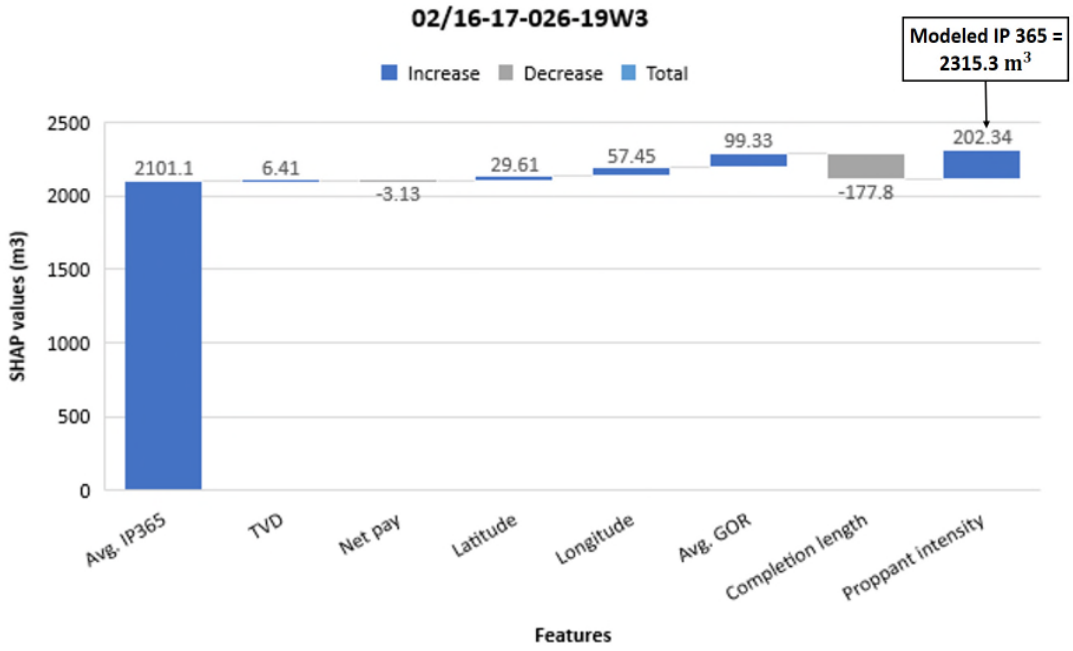

Figure 4.17. Feature contributions (SHAP values) for the well 02/16-17-026-19W3 in Plato North. The predicted IP 365 by the RF model was 2315.3 m^3 and the actual was 2250.4 m^3.

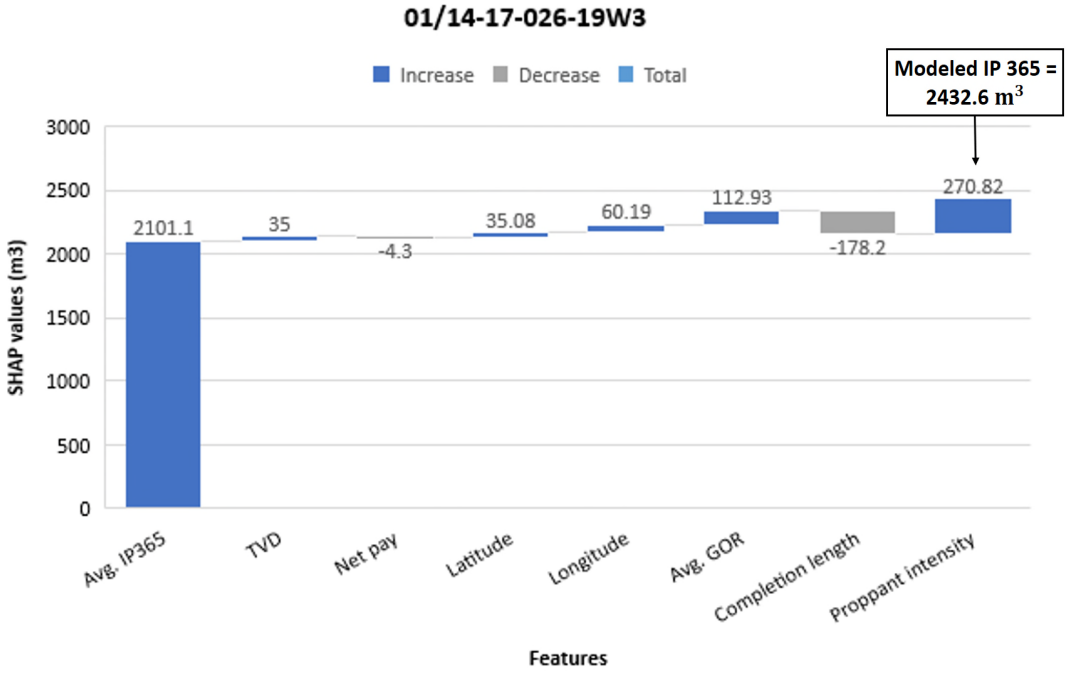

Figure 4.18. Feature contributions (SHAP values) for the well 01/14-17-026-19W3 in Plato North. The predicted IP 365 by the RF model was 2432.6 m^3 and the actual was 2404.7m^3.

4.3.3.2 Case study: Kerrobert

The Kerrobert area has one of the lowest average 365-day cumulative oil production volumes (1928 m^3) in this study. This area is known for being a lower quality reservoir, reporting an average net pay of 2.58 m and average GOR of 100 m^3/m^3.

The first example compares the wells 01/10-07-033-24W3/0 and 01/02-17-033-24W3/0 (Table 4.6). As observed in Figure 4.19 and Figure *4.20*, well 01/10-07-033-24W3/0 has 97.4 m less lateral length and 0.08 t/m more proppant than the other well. Despite the shorter lateral length, the well achieved a slightly higher oil production (283.1 m^3 more than the well 01/02-17-033-24W3/0), which can be attributed to the higher proppant intensity. These results indicate the possibility of short wells achieving good well performance when treated with high proppant intensities.

Table 4.6. Feature contributions and actual values for the wells 01/10-07-033-24W3/0 and 01/02-17-033-24W3/0 in Kerrobert.

UWI	Values	TVD	Net pay	Lati-tude	Longi-tude	Average GOR	Completion length	Proppant intensity	IP365 (m^3)
01/10-07-033-24W3/0	Actual	715.2 m	2.4 m	51.82 °	-109.4 °	125.8 m^3/m^3	628 m	0.43 t/m	2486.2
	Contribu-tion (m^3)	77.51	-39.13	35.64	148.37	9.09	-177.32	113.94	2269.2
01/02-17-033-24W3/0	Actual	706.7 m	2.4 m	51.83 °	-109.36 °	94.91 m^3/m^3	725.4 m	0.35 t/m	2203.1
	Contribu-tion (m^3)	66.32	-46.91	13.38	96.86	9.51	-24.7	-13.38	2202.2

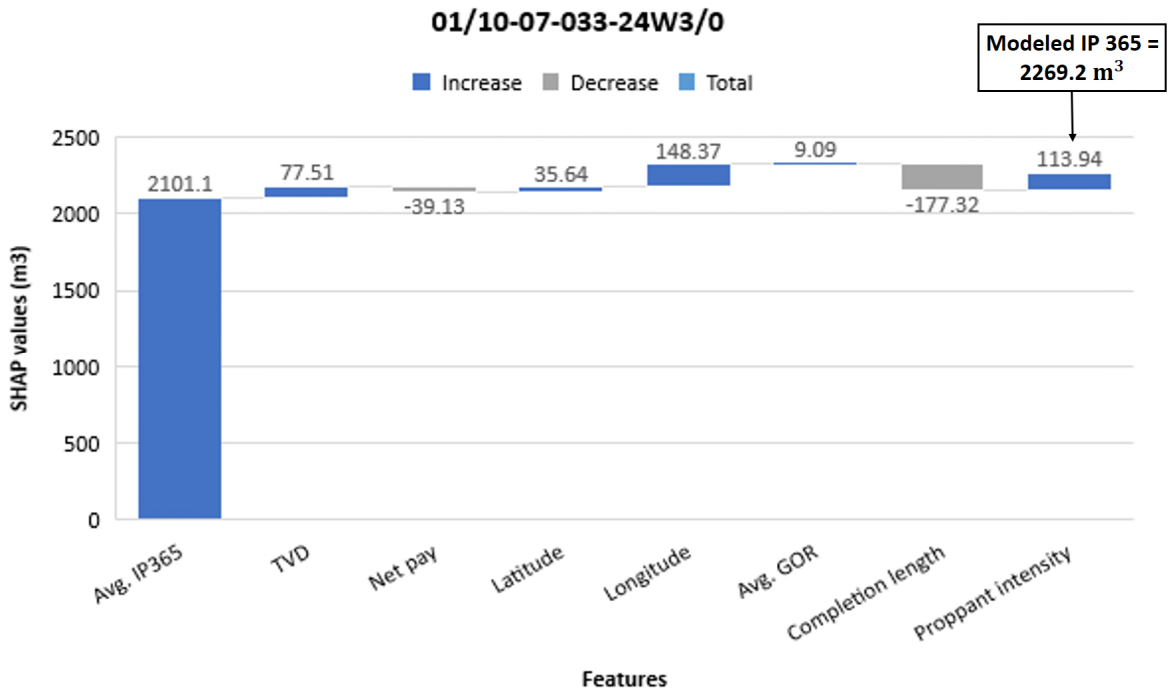

Figure 4.19. Feature contributions (SHAP values) for the well 01/10-07-033-24W3/0 in Kerrobert. The predicted IP 365 by the RF model was 2269.2 m^3 and the actual was 2486.2 m^3.

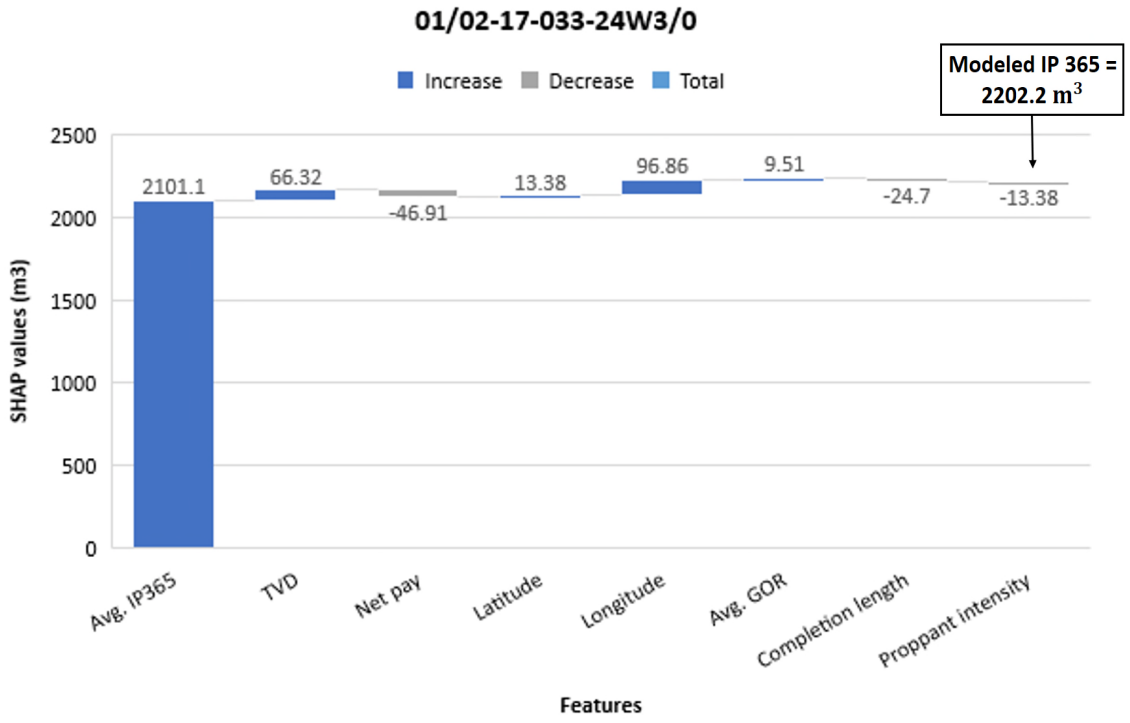

Figure 4.20. Feature contributions (SHAP values) for the well 01/02-17-033-24W3/0 in Kerrobert. The predicted IP 365 by the RF model was 2202.2 m^3 and the actual was 2203.1 m^3.

The second case study compares wells 01/13-28-033-24W3/0 and 01/05-35-033-24W3/0 (Table 4.7). This example demonstrates the effect of completion length on well performance. The two wells have almost the same characteristics, except that well 01/05-35-033-24W3/0 is 2.1 times longer than the other well. SHAP values indicate that the well with a length of 1452.2 m has an impact on well performance of 1099 m^3, while the well with length of 692.9 m has an effect of -230.6 m^3. As seen in the Figure 4.21 and Figure *4.22*, well 01/05-35-033-24W3/0 doubled the oil production of the well 01/13-28-033-24W3/0. Additionally, this well's production was 59% greater than average.

Table 4.7. Feature contributions and actual values for the wells 01/13-28-033-24W3/0 and 01/05-35-033-24W3/0 in Kerrobert.

UWI	**Values**	**TVD**	**Net pay**	**Lati-tude**	**Longi-tude**	**Average GOR**	**Completion length**	**Proppant intensity**	**IP365 (m^3)**
01/13-28-033-24W3/0	Actual	701 m	2.5 m	51.86 °	-109.34 °	97.88 m^3/m^3	692.9 m	0.36 t/m	1545.5
	Contribu-tion (m^3)	10.8	-129.51	-100.3	-38.08	-104.99	-230.6	-48.99	1459.4
01/05-35-033-24W3/0	Actual	697.5 m	2.5 m	51.87 °	-109.29 °	73.33 m^3/m^3	1452.2	0.38 t/m	3695.9
	Contribu-tion (m^3)	102.4	-129.4	-12.12	-9.95	54.15	1099.2	140.6	3345.9

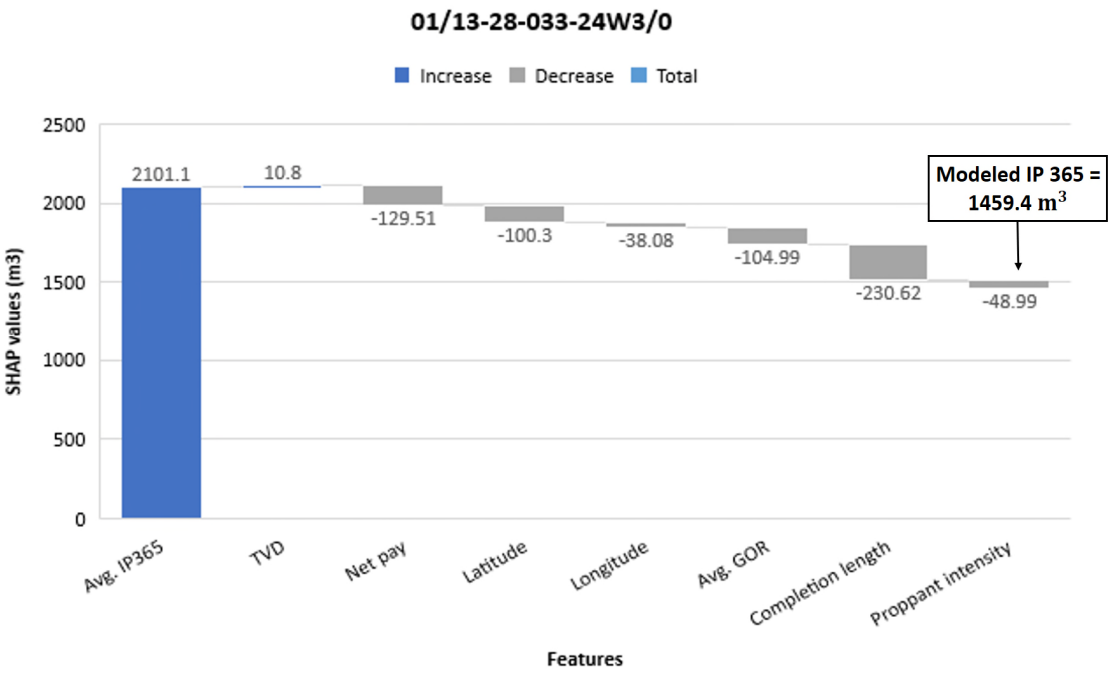

Figure 4.21. Feature contributions (SHAP values) for the well 01/13-28-033-24W3/0 in Kerrobert. The predicted IP 365 by the RF model was 1459.4 m^3 and the actual was 1545.5 m^3.

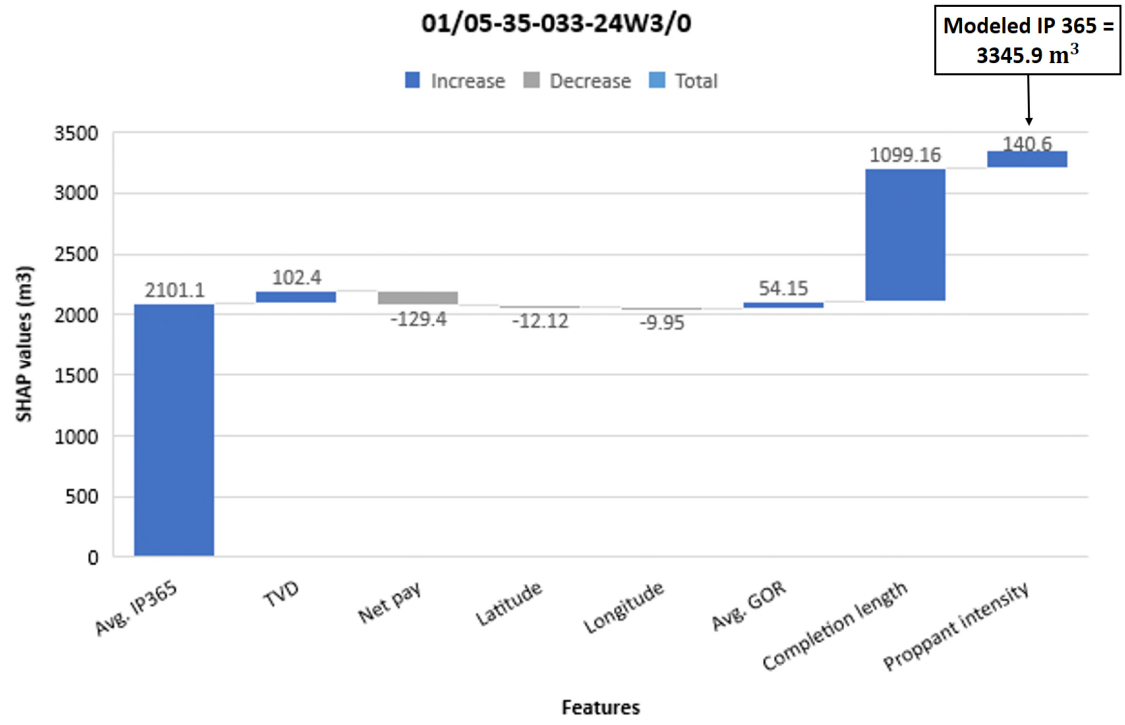

Figure 4.22. Feature contributions (SHAP values) for the well 01/05-35-033-24W3/0 in Kerrobert. The predicted IP 365 by the RF model was 3345.9 m^3 and the actual was 3695.9 m^3.

4.3.3.3 Case study: Whiteside

Whiteside has the highest production observed in this study. In spite of wells in Whiteside have the highest average GOR (275.9 m^3/m^3), the wells reported an average 365-day cumulative oil production of 2762.6 m^3. The case study presented in Table 4.8 compares the wells 03/10-35-029-25W3/0 and 02/07-35-029-25W3/0.

Both wells have long lateral lengths, which greatly affects production by adding more than 1000 m^3. Moreover, well geographic location, which is indicator of reservoir quality, provided more than 700 $m^3$of oil in both wells according to the SHAP values. These two wells were 150 % above the average well. Well 02/07-35-029-25W3/0 was treated with 0.06 t/m more proppant than well 03/10-35-029-25W3/0. This difference made a positive impact on production, contributing to 165.53 $m^3$of oil (Figure 4.24).

Table 4.8. Feature contributions and actual values for the wells 03/10-35-029-25W3/0 and 02/07-35-029-25W3/00 in Whiteside.

UWI	Values	TVD	Net pay	Lati-tude	Longi-tude	Average GOR	Completion length	Proppant intensity	IP365 (m^3)
03/10-35-029-25W3/0	Actual	715.9 m	5.7 m	51.53 °	-109.43 °	392.32 m^3/m^3	1148.4 m	0.35 t/m	5382.38
	Contribu-tion (m^3)	35.98	755.17	247.22	500.86	70.55	1162.7	-61.9	4811.9
02/07-35-029-25W3/0	Actual	718.3 m	5.7 m	51.52 °	-109.43 °	360.86 m^3/m^3	1104.2 m	0.41 t/m	5574.2
	Contribu-tion (m^3)	92.45	778.57	248.33	573.6	75.77	1259.4	165.53	5294.73

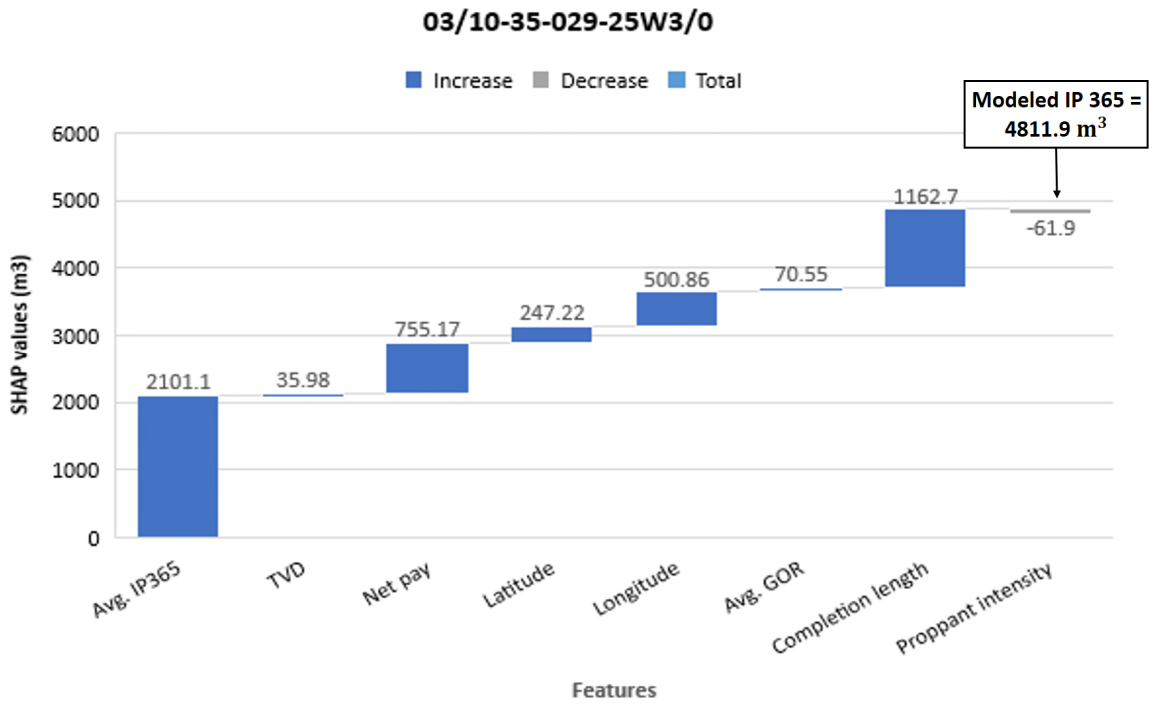

Figure 4.23. Feature contributions (SHAP values) for the well 03/10-35-029-25W3/0 in Whiteside. The predicted IP 365 by the RF model was 4811.9 m^3 and the actual was 5382.38 m^3.

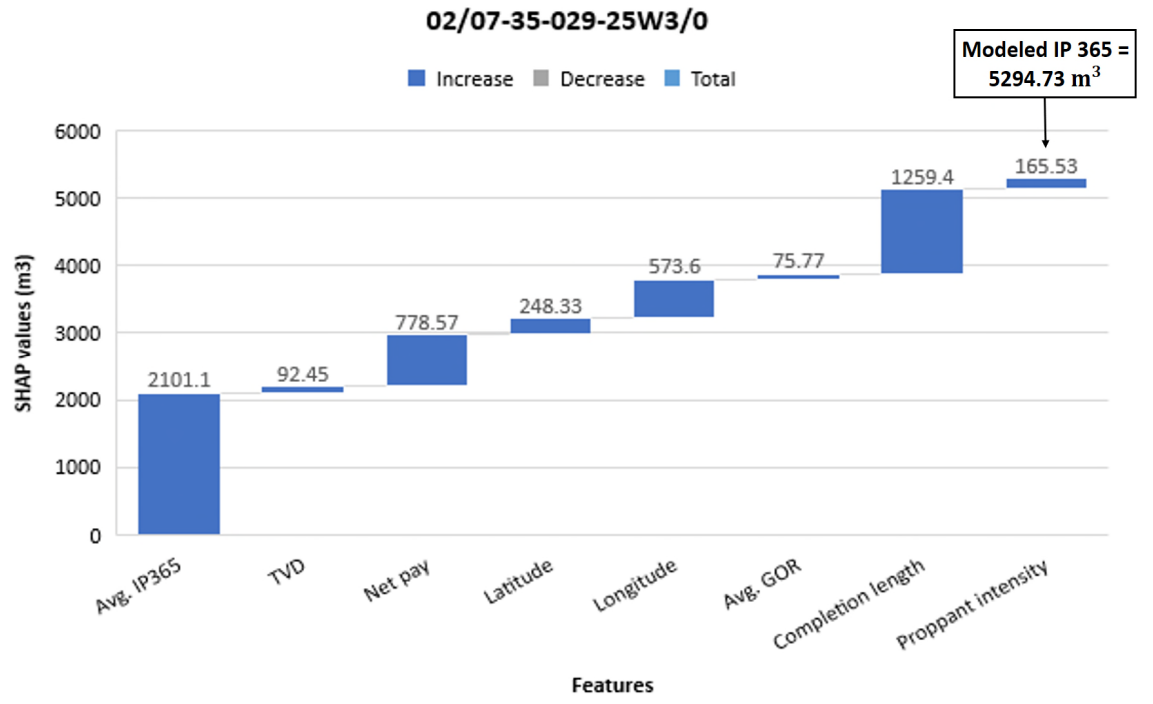

Figure 4.24. Feature contributions (SHAP values) for the well 02/07-35-029-25W3/0 in Whiteside. The predicted IP 365 by the RF model was 5294.73 m^3 and the actual was 5574.2 m^3.

4.3.3.4 Case study: Dodsland

Dodsland is considered one of the average areas in the study, reporting a mean 365-day cumulative oil production of 2268.1 m^3. Table 4.9 shows the comparison between wells 03/06-17-031-19W3/0 and 03/03-17-031-19W3/0. As seen in Figure 4.25 and Figure *4.26*, both wells reported oil productions greater than the average well, which can be mainly attributed to the long lateral lengths (more than 1500 m) and good well geographic location. Additionally, well 03/06-17-031-19W3/0 outperformed well 03/03-17-031-19W3/0 by 1601.2 m^3, primarily because of the higher proppant intensity used. The well was treated with 0.14 t/m more proppant, which added 443.5 m^3 of oil based on the SHAP values.

Table 4.9. Feature contributions and actual values for the wells 03/06-17-031-19W3/0 and 03/03-17-031-19W3/0 in Dodsland.

UWI	Values	TVD	Net pay	Lati-tude	Longi-tude	Average GOR	Completion length	Proppant intensity	IP365 (m^3)
03/06-17-031-19W3/0	Actual	696.6 m	3.8 m	51.66 °	-108.69 °	11.09 m^3/m^3	1543 m	0.51 t/m	5114.3
	Contribu-tion (m^3)	154.83	39.79	388.56	153.45	134.8	1343.9	443.5	4759.9
03/03-17-031-19W3/0	Actual	695.9 m	3.8 m	51.65 °	-108.69 °	14.36 m^3/m^3	1535.6 m	0.37 t/m	3513.1
	Contribu-tion (m^3)	89.87	0.66	234.74	82.25	93.46	1169.66	-41.27	3730.46

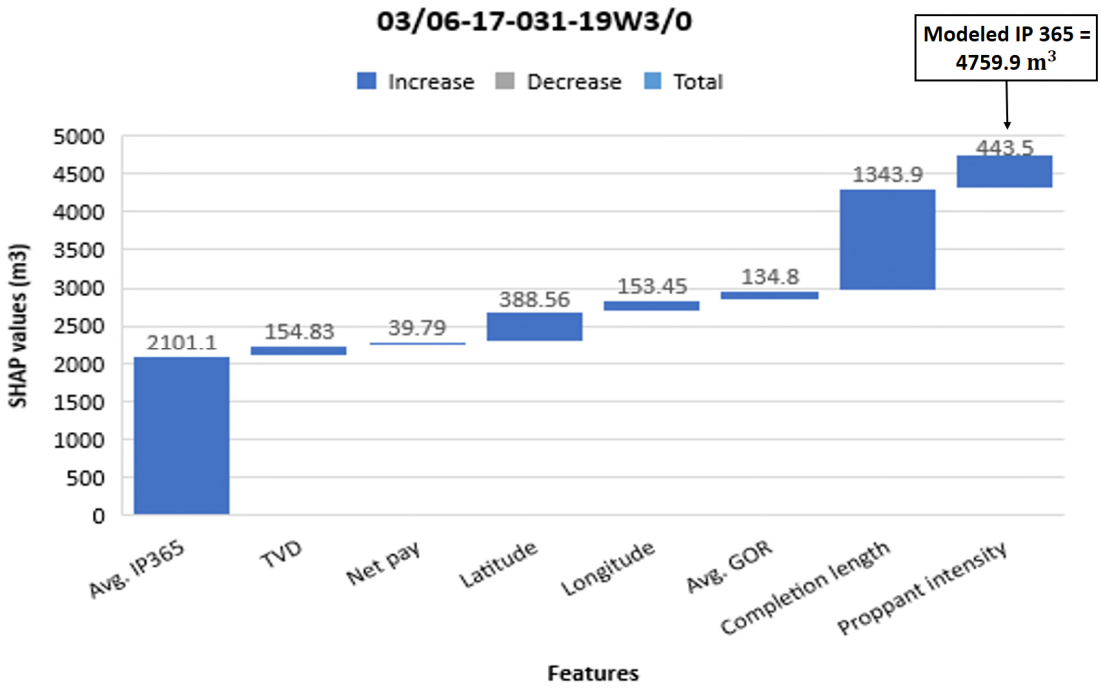

Figure 4.25. Feature contributions (SHAP values) for the well 03/06-17-031-19W3/0 in Dodsland. The predicted IP 365 by the RF model was 4759.9 m^3 and the actual was 5114.3 m^3.

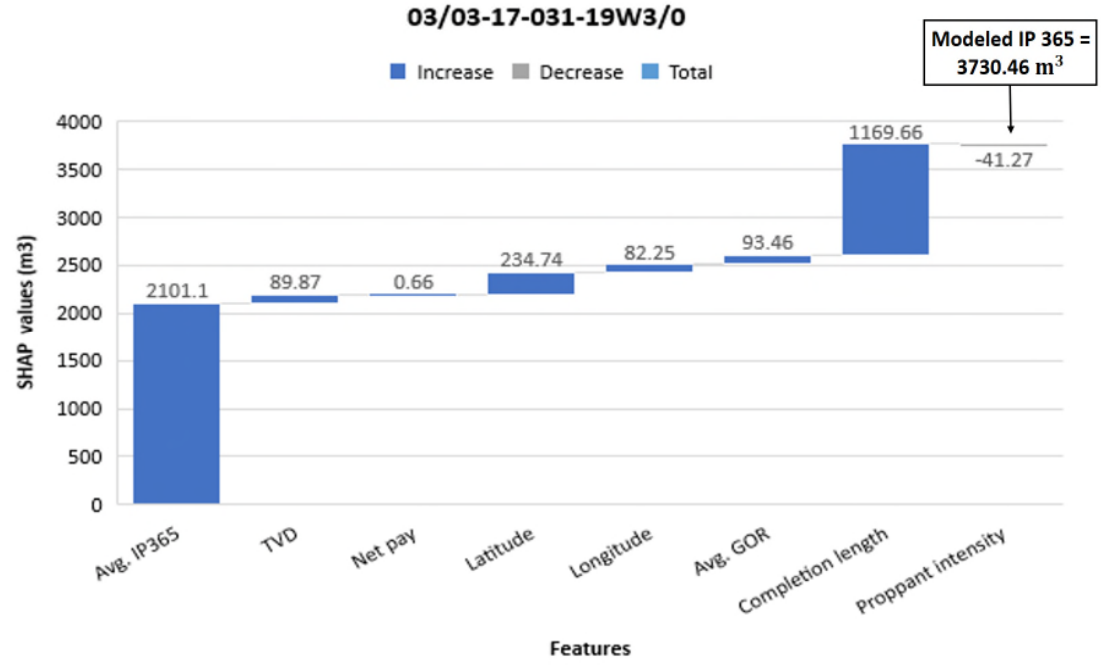

Figure 4.26. Feature contributions (SHAP values) for the well 03/03-17-031-19W3/0 in Dodsland. The predicted IP 365 by the RF model was 3730.46 m^3 and the actual was 3513.1 m^3.

SHAP values provided insights into how the machine learning model made the oil production predictions in each well. These values were useful to examine and understand well performance differences between wells. Additionally, the 365-day cumulative oil production predictions estimated using the Random forest model were close to the actual values. These results demonstrated the potential of the machine learning model for oil production forecasting in the Viking Formation. The SHAP values are available for all wells and features in the database (Appendix B).

4.3.3.5 True Vertical Depth SHAP values

The TVD contributions versus the actual values used in each well are presented in Figure 4.27. The values are color coded by operator. As shown, a specific TVD value does not provide the same contribution to well performance. These results are related to the fact that the feature contributions depend on the individual combination of features in the wells.

TVD values between ~688 m and ~730 m positively contribute to well performance for the majority of wells. Negative contributions from 0 to roughly -240 m^3 are observed for the deeper wells. Most of the wells from Teine Energy Ltd and Whitecap Resources, which are some of the top operators in the study area, are located within the best TVD interval. Therefore, this feature greatly contributed to the well performance of these operators.

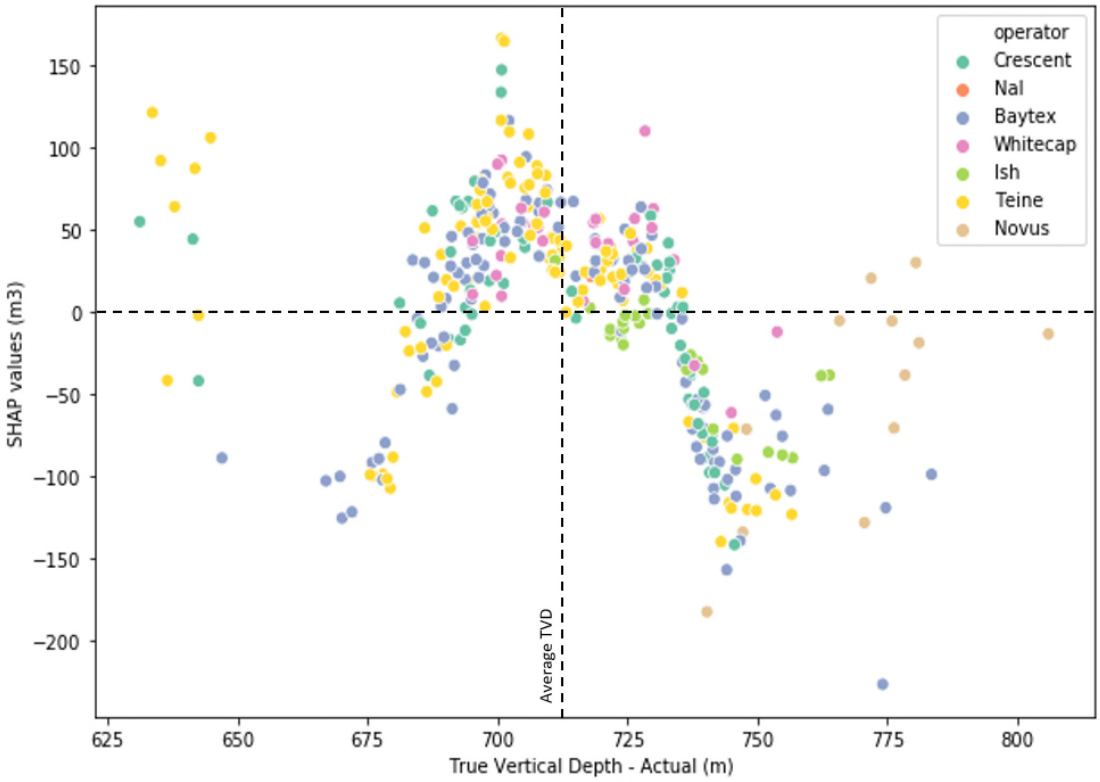

Figure 4.27. True Vertical Depth SHAP values versus actual values in each well. The dashed vertical line represents the average TVD (~ 714 m) in the test set, and the horizontal line at 0 corresponds to the average 365-day cumulative oil production in the test set (~ 2101m^3).

4.3.3.6 Average gas-oil ratio SHAP values

The average gas-oil ratio SHAP values plotted against the actual values in the dataset are shown in Figure 4.28. It can be observed that GOR values above the average (~86.7 m^3/m^3) have a detrimental impact on production, providing contributions from 0 m^3 to roughly -390 m^3. On the contrary, GOR values below the average can positively contribute to well performance, adding up to ~280 m^3 relative to the average well. More than ~90% of the wells from Baytex Energy Corp and Teine Energy Ltd reported a GOR below the average, meaning that this feature greatly contributed to the well productivity.

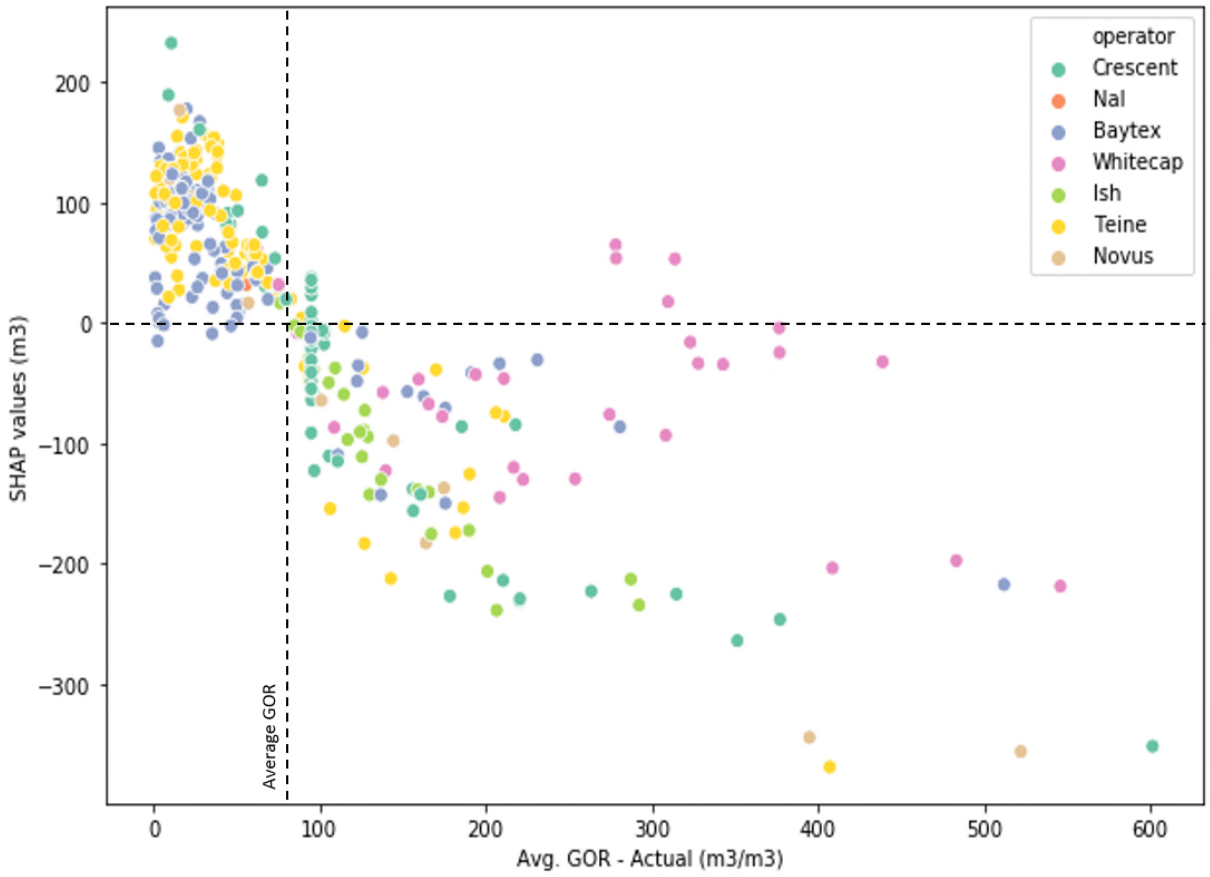

Figure 4.28. Average gas-oil ratio SHAP values versus actual values in each well. The dashed vertical line represents the average GOR (~86.7 m^3/m^3) in the test set, and the horizontal line at 0 corresponds to the average 365-day cumulative oil production in the test set.

4.3.3.7 Net pay SHAP values

The contributions of net pay to well performance versus the actual values in the dataset are shown in Figure 4.29. Net pay values higher than ~4.5 m tend to positively contribute to well performance for the majority of wells. Net pay has a negative impact on production for more than ~80% of the wells in the study area. Contributions to 365-day cumulative oil production range from roughly -280 m^3 to 650 m^3. As seen in Figure 4.29, all operators have their wells distributed across different zones. Teine Energy Ltd, Baytex Energy Corp, and Whitecap Resources Inc. own some of the wells with the highest net pays (more than 6 m).

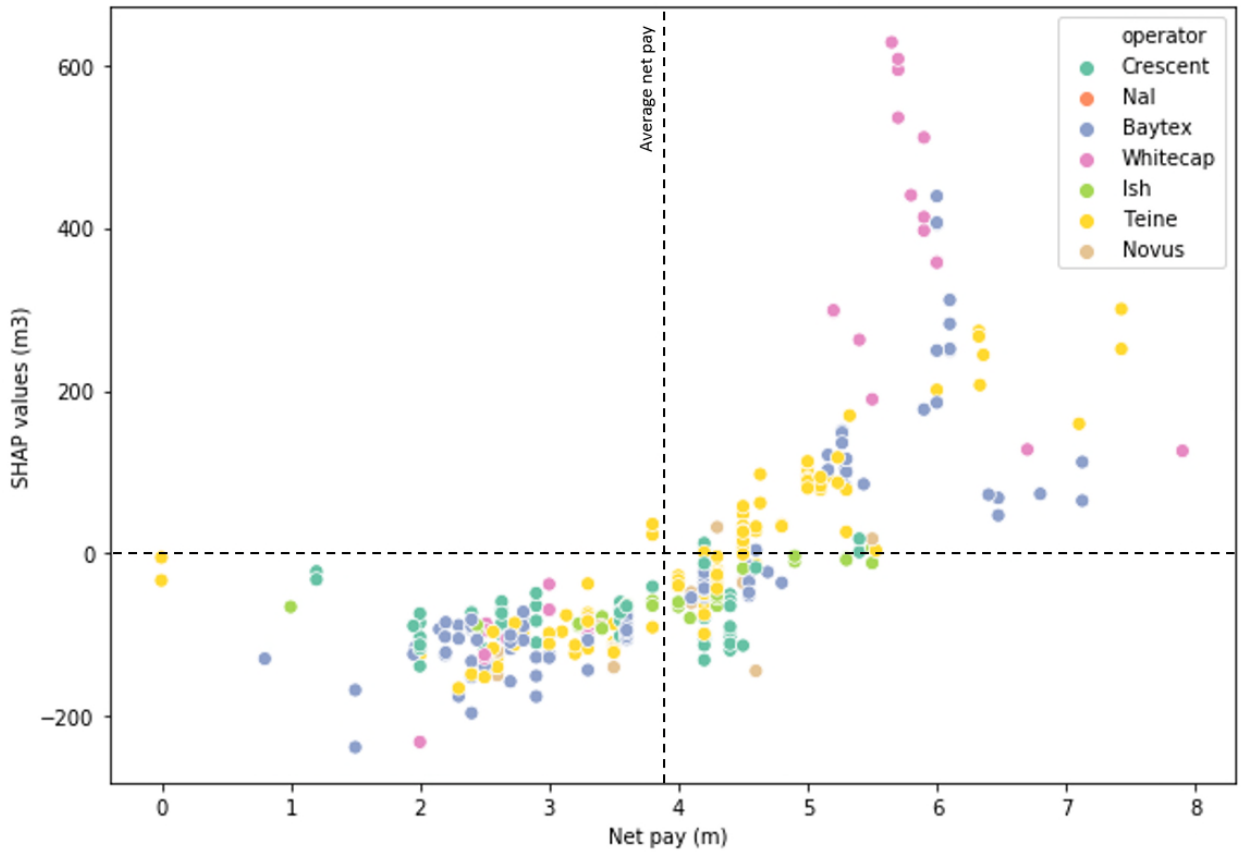

Figure 4.29. Net pay SHAP values versus actual values in each well. The dashed vertical line represents the average net pay (~3.8 m) in the test set, and the horizontal line at 0 corresponds to the average 365-day cumulative oil production in the test set.

4.3.3.8 Completion length SHAP values

The completion length contributions to productivity against the actual values in the wells are illustrated in Figure 4.30. As observed, this feature greatly contributes to well performance for the wells that have a lateral length above the average (~759.2 m). In contrast, a length below the average tends to have a detrimental effect on production. The feature contributions vary from roughly -280 m^3 to 1300 m^3 in the study area. Crescent Point Energy, Whitecap Resources Inc, Teine Energy and Baytex Energy have some of the wells with the longest lateral lengths, which greatly impacted the performance of these wells.

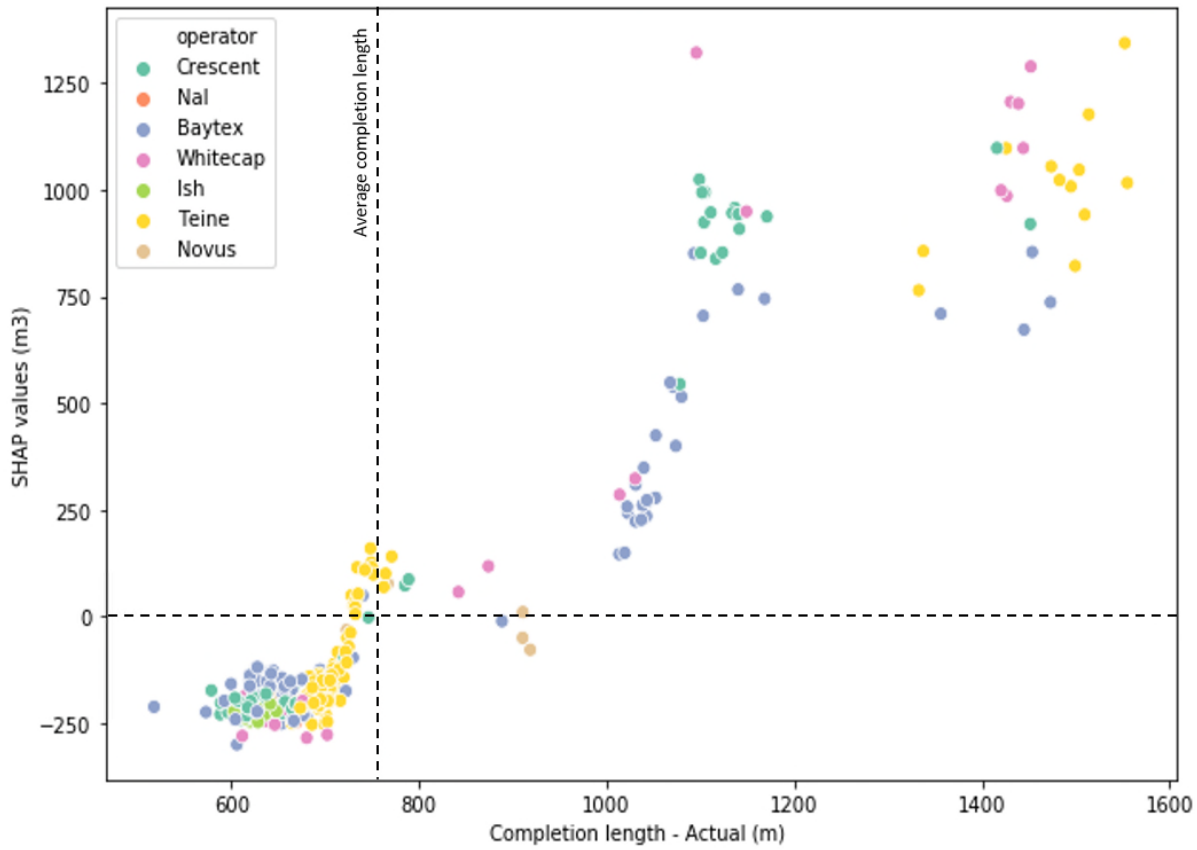

Figure 4.30. Completion length SHAP values versus actual values in each well. The dashed vertical line represents the average completion length (~759.2 m) in the test set, and the horizontal line at 0 corresponds to the average 365-day cumulative oil production in the test.

4.3.3.9 Proppant intensity SHAP values

The proppant intensity contributions versus the actual values are presented in Figure 4.31. The contributions range from roughly -690 m^3 to 500 m^3. All operators treated their wells with different intensities. Wells from Teine Energy had some of the highest proppant intensities (up to ~0.59 t/m), which added extra oil production in the first year. On the contrary, wells from Baytex Energy and Novus Energy used some of the lowest intensities (as low as ~0.20 t/m) in the study area.

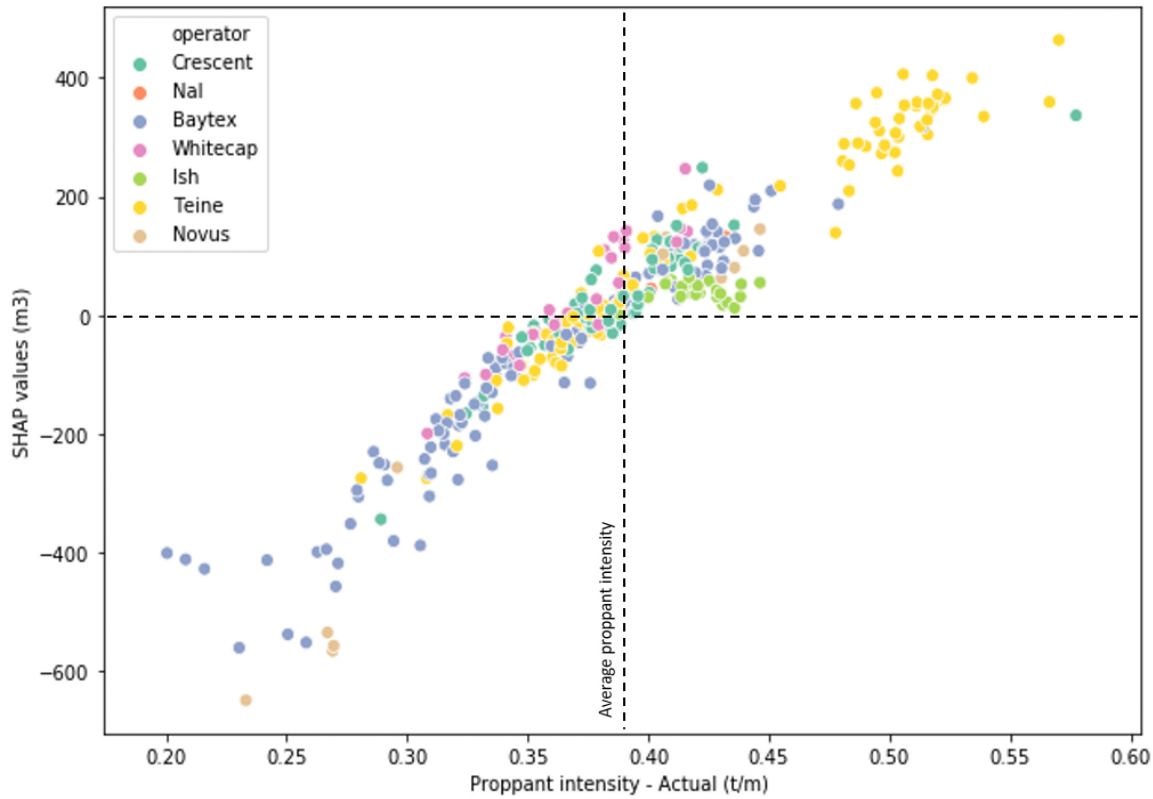

Figure 4.31. Proppant intensity SHAP values versus actual values in each well. The dashed vertical line represents the average proppant intensity (~0.38 m) in the test set, and the horizontal line at 0 corresponds to the average 365-day cumulative oil production in the test.

4.4 Summary of Results

The results from this work are divided into the following two categories:

1. Model performance: Two data-driven models, a multiple linear regression and random forest (RF) model, were developed to predict 365-day cumulative oil production. The RF model outperformed the multiple linear regression by 14%; therefore, this model was selected to examine the effect of reservoir and completion characteristics on well performance. The python code used to construct each regression model is presented in Appendix C.

   The major conclusions from the predictive model are as follows:

   a. The developed RF model B explained the relationships between seven input features and 365-day cumulative oil production. Additionally, the oil production predictions

estimated using the model were close to the actual values. These results demonstrated the potential of the RF model for oil production forecasting in the Viking Formation.

b. The performance of the machine learning model is highly affected by the selection of hyperparameters. As a result, it is key to find the optimum combination of hyperparameters for the model. In this case, random search and grid search were used to find the hypermeter's values that maximizes model's performance. Additionally, the results were validated using 5 k-fold cross validation method.

c. It is fundamental to split the dataset into two portions (training and test) to verify the prediction capabilities of the model. Furthermore, these two sets should have similar distributions because the model is only able to make accurate predictions within the range of the input features.

2. Model interpretation: three different interpretable machine learning techniques were applied to better understand and quantify the effects of reservoir and completion design parameters on well productivity. Results from these techniques are summarized as follows:

   a. The importance of the input features on explaining 365-day cumulative oil production variance was determined using a permutation feature importance technique. Results from RF model B indicated that completion length is the main oil production driver in the Viking Formation, followed by proppant intensity and net pay.

   b. The 365-day cumulative oil production response due to changes in the input features was visualized using ICE and PDP. Results suggested that wells with more than 750 m of lateral length tend to have oil production above an average well in the study area. A proppant intensity between 0.28 - 0.6 t/m greatly affects well performance. However, a diminishing effect is observed around 0.49 t/m, after this value, the contribution to productivity is minimal.

In terms of reservoirs, average gas-oil ratio has a detrimental impact on well productivity. The higher the GOR, the lower the production. Furthermore, net pays of ~5.5 m provide the highest contributions to performance based on the RF model. TVD ranging from ~690 m to ~710 m showed the highest contribution to performance.

SHAP values provided insights into how successful the machine learning model made the oil production predictions in each well. These values were useful to examine and understand well performance differences between wells. A given feature contribution did not provide the same well performance because the contributions were based on the individual combination of features in each well. Therefore, a successful stimulation design for a well might not provide the same performance in a different well. It is worth noting that the random forest model was able to explain only 59% of the 365-day cumulative oil production variance. As a result, caution should be taken when interpreting the feature contributions. The SHAP values are available for all wells and features in the database (Appendix B).

CHAPTER 5: CONCLUSIONS AND RECOMMENDATIONS

5.1 Conclusions

This work focused on evaluating hydraulic fracture performance in the Viking Formation using a data-driven approach. This study was conducted using an integrated data mining process which included data cleaning and preparation, exploratory data analysis, predictive modeling using a machine learning algorithm, and interpretation of the model predictions. The major conclusions of this study are summarized as follows:

1. Exploratory data analysis was useful to gain a general understanding of the dataset. Since this work was based on data-driven methods, data quality control was the most important step to ensure high-quality models and performance. Additionally, it is key to eliminate multicollinearity between the features for model performance and interpretation. Highly correlated predictor variables may lead to incorrect results when performing sensitivity analysis.

   In summary, completion length and number of the stages showed the highest positive correlation to well performance; however, these two variables were highly correlated. As a result, only completion length was used as an input feature in the data-driven model.

2. Comparing the two modelling techniques: multiple linear regression (MLR) and random forest (RF), RF outperformed MLR by 14%. The R^2 values of RF model B for the training and test sets were 0.95 and 0.59, respectively. Results indicated that RF was a suitable technique to capture the non-linear relationships between the predictor variables and the output.

3. The optimization of hyperparameters was critical to improve model performance. Random search and grid search were used to find the hyperparameters values. Results indicated that the optimum number of trees was 1785, the number of features was 3, the maximum depth of a tree was 15, and the number of data points to split in each internal node was 2.

4. Model interpretation was key to understanding how the random forest model made the 365-day cumulative oil production predictions. Understanding the predictions yielded insights into what drives oil production in the Viking Formation, including the following:

    a. The permutation feature importance technique indicated that completion length, proppant intensity and net pay are the most important features that contributes to the oil production variability.

    b. Partial dependence plots (PDP) showed the different well performance responses to changes in the input features. Based on RF model B, completion length could add up to 3050 m^3 , and proppant intensity up to 750 m^3 in the first year. Additionally, proppant intensity showed a diminishing effect on productivity around 0.49 t/m.

    c. According to the PDP, a well with a completion length greater than 750 m could produce above the average well in the study area. Moreover, a well treated with a proppant intensity higher than 0.40 t/m could also produce more than the average well.

    d. Net pay was one of the key predictors of 365-day cumulative oil production. PDP showed the positive effect of net pay on well performance. However, production decreased in wells that have highest values ranging from ~ 6 m to 7.32 m. This might be justified by the depletion effect induced by vertical wells in areas with such values.

    e. Shapley additive explanations (SHAP) values were helpful for understanding well performance on a well-by-well-basis. Additionally, this method provided insights about the interactions between the predictor variables. Well productivity could be compared across the play.

5. The increment of proppant intensity and completion length can increase oil production; however, it also increases the completion costs. As a result, it is key to find optimum values that maximize production without overspending on stimulation.

6. This is the first study that applied machine learning techniques to evaluate hydraulic fracture performance in the Viking Formation. Integrating different disciplines in the analysis is key to developing reliable production predictive models and optimizing well productivity. The results from this project are important for development planning and optimization of stimulation programs in the Viking Formation.

5.2 Recommendations

This study's findings have revealed opportunities for further investigation. The recommendations for future research are presented as follows:

1. The effect of proppant intensity was assessed in this work, but the importance of fluid intensity could be investigated further. A data-driven model including fluid instead of proppant intensity could be developed for this purpose.

2. The geographic location of wells were included to account for varying geologic and reservoir areas. However, the integration of parameters such as porosity, water saturation, and permeability could provide insights into how the reservoir quality influences well performance. The interactions between reservoir and completion parameters could be elucidated through additional research.

3. Gas-oil ratio (GOR) was taken from production data in this work due to data availability; however, GOR values obtained from well testing could provide a better understanding of how the percentage of gas impacts production. It is expected that high volumes of gas can lead to a drop in reservoir pressure, which negatively affects oil production.

4. Well spacing, parent and child relationships and time between wells play key roles in determining well performance. A future study could incorporate features that account for

well spacing relationships because they can increase model performance, consider depletion effects and provide insights for development planning.

5. In this work, only multiple linear regression and random forest were considered for predicting 365-day cumulative oil production. Different algorithms, such as Artificial Neural Networks, Extreme Gradient Boosting, and Support Vector Machine can be also used for regression tasks. It is suggested to apply these algorithms and compare the performances of the models.

6. A similar study can be conducted in future years to re-assess the production drivers (features importance) and sensitivities to determine if the dominant controls on well performance evolve with time.

REFERENCES

Abbas, A. K., Flori, R., Almubarak, H., Dawood, J., Abbas, H., & Alsaedi, A. (2019). Intelligent Prediction of Stuck Pipe Remediation Using Machine Learning Algorithms. *SPE Annual Technical Conference and Exhibition*. https://doi.org/10.2118/196229-ms

Al-Anazi, A. F., & Gates, I. D. (2012). Support Vector Regression to Predict Porosity and Permeability: Effect of sample size. *Computers and Geosciences*, *39*, 64–76. https://doi.org/10.1016/j.cageo.2011.06.011

Aulia, A., Rahman, A., & Quijano Velasco, J. J. (2014). Strategic Well Test Planning using Random Forest. *Society of Petroleum Engineers - SPE Intelligent Energy International 2014*, (April), 140–162. https://doi.org/10.2118/167827-ms

Baishev, T. B. (2017). Unconventional Oil Reserves Development in the Viking Play (Western Canada) Using Horizontal Wells and Hydraulic Fracturing. *Georesursy*, *19*(3), 182–185. https://doi.org/10.18599/grs.19.3.5

Balaji, K., Rabiei, M., Suicmez, V., Canbaz, H., Agharzeyva, Z., Tek, S., … Temizel, C. (2018). Status of data-driven methods and their applications in oil and gas industry. *Society of Petroleum Engineers - SPE Europec Featured at 80th EAGE Conference and Exhibition 2018*. https://doi.org/10.2118/190812-ms

Bataee, M., & Mohseni, S. (2011). Application of Artificial Intelligent Systems in ROP Optimization: a Case Study in Shadegan oil field. *Society of Petroleum Engineers - SPE Middle East Unconventional Gas Conference and Exhibition 2011, UGAS*, 13–22. https://doi.org/10.2118/140029-ms

Belyadi, H., Fathi, E., & Belyadi, F. (2016). Hydraulic Fracturing in Unconventional Reservoirs: Theories, Operations, and Economic Analysis. *Hydraulic Fracturing in Unconventional Reservoirs: Theories, Operations, and Economic Analysis*. Elsevier Inc.

Benyamin, D. (2012). A Gentle Introduction to Random Forests, Ensembles, and Performance Metrics in a Commercial System. Retrieved December 17, 2019, from https://blog.citizennet.com/blog/2012/11/10/random-forests-ensembles-and-performance-metrics

Biau, G., Devroye, L., & Lugosi, G. (2008). Consistency of Random Forests and Other Averaging Classifiers. *Machine Learning Research*, *9*(2008), 2016–2033.

Bowie, B. (2018). Machine learning applied to optimize duvernay well performance. *Society of Petroleum Engineers - SPE Canada Unconventional Resources Conference, URC 2018, 2018-March*(March), 13–14. https://doi.org/10.2118/189823-ms

Breiman, L. (2001). Random Forest. Univeristy of California, Technical Report 567, 33 p.

Brennan, B., & Schafer, L. (2014). Harness Oil and Gas Big Data with Analytics. *Harness Oil and Gas Big Data with Analytics*. https://doi.org/10.1002/9781118910948

Brown, J. B., Salehi, A., Benhallam, W., & Matringe, S. F. (2017). Using Data-Driven Technologies to Accelerate the Field Development Planning Process for Mature Field

Rejuvenation. *SPE Western Regional Meeting Proceedings*, *2017-April*, 1610–1629. https://doi.org/10.2118/185751-ms

Cho, H., & Shah, S. N. (2002). Optimization of Well Length for Horizontal Drilling. *Journal of Canadian Petroleum Technology*, *41*(5), 54–62. https://doi.org/10.2118/02-05-03

Clar, F. H., & Monaco, A. (2019). *Data-Driven Approach to Optimize Stimulation Design in Eagle Ford Formation*. 22–24. https://doi.org/10.15530/urtec-2019-224

Cunningham, C. F., Cooley, L., Wozniak, G., & Pancake, J. (2012). Using multiple linear regression to model EURs of horizontal Marcellus shale wells. *SPE Eastern Regional Meeting*, 223–243. https://doi.org/10.2118/161343-ms

Ebrahimi, A., & Khamehchi, E. (2016). Developing a Novel Workflow for Natural Gas lift Optimization using Advanced Support Vector Machine. *Journal of Natural Gas Science and Engineering*, *28*, 626–638. https://doi.org/10.1016/j.jngse.2015.12.031

Espinoza. (2019). Introduction to Energy Geomechanics. *Lecture notes, University of Texas at Austin.* Retrieved November 17, 2019, from https://dnicolasespinoza.github.io/node56.html

Fawzy, D., Moussa, S., & Badr, N. (2016). The Evolution of Data Mining Techniques to Big Data Analytics: An Extensive Study with Application to Renewable Energy Data Analytics. *Asian Journal of Applied Sciences*, 11.

Genuer, R., Poggi, J.-M., Tuleau-Malot, C., Vialaneix, N., & Villa-Vialaneix, N. (2017). Random Forests for Big Data. *Big Data Research*, (9). https://doi.org/10.1016/j.bdr.2017.07.003ï

Glaister, R. . (1959). Lower Cretaceous of Southern Alberta and Adjoining Areas. *AAPG Bulletin*, 590-620. http://archives.datapages.com/data/bulletns/1957-60/data/pg/0043/0003/0550/0590.htm

Gorunescu, F. (2011). Data Mining Concepts, Models and Techniques. *Springer*

Hirschmiller, J., Biryukov, A., Groulx, B., Emmerson, B., & Quinell, S. (2019). The Importance of Integrating Subsurface Disciplines with Machine Learning when Predicting and Optimizing Well Performance – Case Study from the Spirit River Formation. *SPE Annual Technical Conference and Exhibition***.** https://doi.org/10.2118/196089-ms

Hunt, W. (1954). The Joseph Lake-Armena-Camrose producing trend, Alberta. *AAPG SPECIAL PUBLICATION Western Canada Sedimentary Basin: A Symposium; Sponsored by the Alberta Society of Petroleum Geologists, and the Saskatchewan Society of Petroleum Geologists.* Editor: Leslie M. Clark. https://doi.org/10.1306/SV15347C27

IBM. (n.d.). CRISP-DM Help Overview. Retrieved November 23, 2019. https://www.ibm.com/support/knowledgecenter/en/SS3RA7_15.0.0/com.ibm.spss.crispdm.help/crisp_overview.htm

James, G., Daniela, W., Hastie, T., & Tibshirasni, R. (2013). An Introduction to Statistical Learning. *Springer Texts in Statistics*. http://books.google.com/books?id=9tv0taI8l6YC

Jans, P., Shepley, M., Magarian, G., Recsky, J., & Rugg, T. (2014). Rocking the Viking : Reservoir Quality and Net Pay Determination in the Bioturbated (Shaley Sand) Viking Formation of Western. *CSPG/CSEG/CWLS GeoConvention 2012*. 41340, 1–3.

Jensen, K. (2012). CRISP-DM process. *Stellar*. Retrieved November 23, 2019, from https://www.stellarconsulting.co.nz/data/crisp-dm-still-a-leader/

Jones, H. L. (1961). The Viking Formation in Southwestern Saskatchewan. *Journal of the Alberta Society of Petroleum Geologists,* 231-244

Kakar, K. (2018). Artificial Neural Network Modeling of Well Performance in the Garrington Field, Cardium Formation (Unpublished master's thesis). University of Calgary, Calgary, AB. http://hdl.handle.net/1880/109399.

Kamath, C. (2005). Scientific Data Mining and Pattern Recognition: Overview. Retrieved from https://computing.llnl.gov/projects/sapphire/overview.html

Kumar, A. (2012). Artificial Neural Network as a Tool for Reservoir Characterization and Its Application in the Petroleum Engineering. *Offshore Technology Conference*, 12. https://doi.org/10.4043/22967-MS

Li, X., Chan, C. W., & Nguyen, H. H. (2013). Application of the Neural Decision Tree Approach for Prediction of Petroleum Production. *Journal of Petroleum Science and Engineering* (Vol. 104). https://doi.org/10.1016/j.petrol.2013.03.018

Lundberg, S. M., Erion, G., Chen, H., DeGrave, A., Prutkin, J. M., Nair, B., … Lee, S.-I. (2020). From Local Explanations to Global Understanding with Explainable AI for Trees. *Nature Machine Intelligence*, *2*(1), 56–67. https://doi.org/10.1038/s42256-019-0138-9

Luo, G., Tian, Y., Sharma, A., & Ehlig-Economides, C. (2019). Eagle ford well insights using data-driven approaches. *International Petroleum Technology Conference 2019, IPTC 2019*. https://doi.org/10.2523/iptc-19260-ms

Ministry of Economy. (2014). Stratigraphic Correlation Chart. Retrieved from http://publications.gov.sk.ca/documents/310/9496-StratigraphicCorrelationChart.pdf

Mogensen, A. C., Bachman, R. C., & Singbeil, P. (2012). Case study - Evaluation of horizontal well multi-stage fracturing in the Viking oil formation. *Society of Petroleum Engineers - SPE Canadian Unconventional Resources Conference 2012, CURC 2012*, *2*(1993), 1346–1374. https://doi.org/10.2118/162813-ms

Mohaghegh, S. (2019). Traditional Statistics vs. Artificial Intelligence and Machine Learning. Retrieved November 23, 2019, from https://pubs.spe.org/en/dsde/dsde-article-detail-page/?art=6215

Mohaghegh, S. D. (2017). Shale Analytics. Springer, Cham. http://doi-org-443.webvpn.fjmu.edu.cn/10.1007/978-3-319-48753-3_3.

Mohammed, M., Khan, M., & Bashier, E. (2016). Machine Learning Algorithms and Applications. CRC Press. Retrieved from https://learning.oreilly.com/library/view/machine-learning/9781315354415/xhtml/cover.xhtml

Molnar, C. (2019). Interpretable Machine Learning. Github Repository. Retrieved November 12, 2019, from https://christophm.github.io/interpretable-ml-book/

NEB. (2014). Market Snapshot: Canadian Tight Oil Production Update. Retrieved November 18, 2019, from https://www.cer-rec.gc.ca/nrg/ntgrtd/mrkt/snpsht/2014/10-01tghtl-eng.html

Nejad, A. M., Sheludko, S., Hodgson, T., McFall, R., & Shelley, R. F. (2015). A case history: Evaluating well completions in the Eagle Ford Shale using a data-driven approach. *Society of Petroleum Engineers - SPE Hydraulic Fracturing Technology Conference 2015*, 164–182. https://doi.org/10.2118/173336-ms

NIST. (2012). NIST/SEMATECH e-Handbook of Statistical Methods. Retrieved from https://www.itl.nist.gov/div898/handbook/index.htm

Nwachukwu, A., Jeong, H., Pyrcz, M., & Lake, L. W. (2018). Fast Evaluation of Well Placements in Heterogeneous Reservoir Models using Machine Learning. *Journal of Petroleum Science and Engineering*, *163*(January), 463–475. https://doi.org/10.1016/j.petrol.2018.01.019

ODSC. (2019). Optimizing Hyperparameters for Random Forest Algorithms in scikit-learn. Retrieved November 14, 2019, from https://medium.com/@ODSC/optimizing-hyperparameters-for-random-forest-algorithms-in-scikit-learn-d60b7aa07ead

Pollock, J., Stoecker-Sylvia, Z., Veedu, V., Panchal, N., & Elshahawi, H. (2018). Machine Learning for Improved Directional Drilling. *Proceedings of the Annual Offshore Technology Conference*, *4*, 2496–2504. https://doi.org/10.4043/28633-ms

Pozzobon, J. (1987). Sedimentology and Stratigraphy of the Viking Formation, Eureka Field, Southwestern Saskatchewan. Master's thesis, McMaster University. http://hdl.handle.net/11375/19828

Reinson, G., Warters, W., Cox, J., & Price, P. (1994). Cretaceous Viking Formation of the Western Canada Sedimentary Basin. *Alberta Society of Petroleum Geologists.*

Rudkin, R. . (1964). Lower Cretaceous. Geological History of Western Canada. *Alberta Society of Petroleum Geologists*, 56–158.

Scikit-learn. (n.d.). Ensemble methods — scikit-learn 0.21.3 documentation. Retrieved November 14, 2019, from Scikit-learn website: https://scikit-learn.org/stable/modules/ensemble.html#random-forests

Scikit-learn. (2019). Cross-validation: evaluating estimator performance. Retrieved from https://scikit-learn.org/stable/modules/cross_validation.html

Shelley, B., Grieser, B., Johnson, B. J., Fielder, E. O., Heinze, J. R., & Werline, J. R. (2008). Data analysis of Barnett shale completions. *SPE Journal*, *13*(3), 366–374. https://doi.org/10.2118/100674-pa

Shelley, R., Nejad, A., Guliyev, N., Raleigh, M., & Matz, D. (2014). Understanding multi-fractured horizontal marcellus completions. *SPE Eastern Regional Meeting*, *2014-Janua*(January), 18–31. https://doi.org/10.2118/171003-ms

Simpson, F. (1982). Sedimentology, Palaeoecology and Economic Geology of Lower Colorado (Cretaceous) Strata of West central Saskatchewan. *Saskatchewan Energy and Mines, Saskatchewan Geological Survey, Report* 150, 183 p.

Slipper, S. (1918). Viking Gas Field, Structure of the Area. *Geological Survey of Canada Summary Report 1917, Part C*, p. 6-7.

Statistics Solutions. (n.d.). Missing Values in Data. Retrieved December 17, 2019, from https://www.statisticssolutions.com/missing-values-in-data

Stelck, C. (1958). Stratigraphic Position of the Viking Sand. *Alberta Society of Petroleum Geologists Journal*, *6*, 2–7.

STHDA. (2018). Multiple Linear Regression in R. Retrieved December 17, 2019, from http://www.sthda.com/english/articles/40-regression-analysis/168-multiple-linear-regression-in-r/

Swalin, A. (2018). How to Handle Missing Data. Retrieved December 17, 2019, from https://towardsdatascience.com/how-to-handle-missing-data-8646b18db0d4

Taylor, C. (2018). What Is the Interquartile Range Rule? Retrieved November 17, 2019, from https://www.thoughtco.com/what-is-the-interquartile-range-rule-3126244

Tecuci, G. (2012). Artificial intelligence. *Wiley Interdisciplinary Reviews: Computational Statistics*, *4*(2), 168–180. https://doi.org/10.1002/wics.200

Temizel, C., Energy, A., Nabizadeh, M., Kadkhodaei, N., Ranjith, R., Suhag, A., Dhannoon, D. (2017). Data-driven optimization of injection/production in waterflood operations. *Society of Petroleum Engineers - SPE Intelligent Oil and Gas Symposium 2017*. https://doi.org/10.2118/187468-ms

Walz, C. a, Pedersen, P. K., & Chi, G. (2005). Stratigraphy and petrography of Viking sandstones in the Bayhurst area, southwestern Saskatchewan. *Summary of Investigations 2005, Volume 1, Saskatchewan Geological Survey, Saskatchewan Industry Resources, Miscellaneous Report 2005-4.1*, *1*, 1–17.

Wang, S. (2018). Integrated Data Mining and Optimization in Hydraulically Fractured Tight Oil Reservoirs (Unpublished doctoral thesis). University of Calgary, Calgary, AB. doi:10.11575/PRISM/31896.

Wang, S., & Chen, S. (2016a). A comprehensive evaluation of well completion and production performance in Bakken shale using data-driven approaches. *Society of Petroleum Engineers - SPE Asia Pacific Hydraulic Fracturing Conference*. https://doi.org/10.2118/181803-ms

Wang, S., & Chen, S. (2016b). Evaluation and prediction of hydraulic fractured well performance in Montney formations using a data-driven approach. *Society of Petroleum Engineers - SPE Western Regional Meeting*. https://doi.org/10.2118/180416-ms

Wong, P. M., Henderson, D. J., & Brooks, L. J. (1998). Permeability Determination Using Neural Networks in the Ravva Field, Offshore India. *SPE Reservoir Engineering (Society of Petroleum Engineers)*, *1*(2), 99–104. https://doi.org/10.2118/38034-pa

Yanfang, W., & Salehi, S. (2014). Refracture Candidate Selection using Hybrid Simulation with

Neural Network and Data Analysis Techniques. *Journal of Petroleum Science and Engineering*, *123*, 138–146. https://doi.org/10.1016/j.petrol.2014.07.036

Yurkowski, M. (2019). Saskatchewan's Top Oil Play Opportunities. Saskatchewan Geological Survey.

APPENDIX A: DRILLING AND COMPLETION DATA EXTRACTED FROM ACCUMAP AND GEOVISTA IN JULY 2019

No.	UWI	Field	Operator	Completion date	Latitude	Longitude	Net pay	TVD	Avg. GOR	Completion length	Avg. stage spacing	Proppant intensity	Proppant concentration	IP365
1	02/04-21-024-14W3/0	Forgan	Baytex	8/3/2017	51.068388	-107.907142	2.6	666.9	1.79	1311.22	37.46	0.40	0.44	2235.9
2	01/05-21-024-14W3/0	Forgan	Baytex	3/12/2017	51.051469	-107.907762	2.6	658.4	1.10	642.1	35.67	0.40	0.43	1247.4
3	01/12-21-024-14W3/0	Forgan	Baytex	3/7/2017	51.068388	-107.906785	2.6	667	1.39	658.9	36.61	0.39	0.47	1349.9
4	01/14-21-024-14W3/0	Forgan	Teine	2/14/2016	51.058035	-107.899995	2.6	650.6	40.16	730.7	56.21	0.27	0.51	700.0
5	01/06-25-024-14W3/0	Forgan	Baytex	8/1/2017	51.084761	-107.833837	3.8	650.4	5.16	1216.6	46.79	0.31	0.45	2129.0
6	01/03-26-024-14W3/0	Forgan	Baytex	3/10/2018	51.082458	-107.854502	4.2	647	0.97	1168.3	41.73	0.35	0.41	2120.0
7	01/12-31-024-14W3/0	Forgan	Baytex	7/25/2017	51.080366	-107.953467	0.8	727.7	3.43	1021.8	37.84	0.37	0.38	1318.2
8	02/14-32-024-14W3/0	Forgan	Baytex	10/1/2016	51.083668	-107.923828	2.2	689.2	7.39	1038.1	43.25	0.21	0.42	3044.4
9	01/15-32-024-14W3/0	Forgan	Baytex	7/24/2017	51.083665	-107.923472	2.2	691.2	1.75	1054	37.64	0.40	0.42	2246.2
10	01/02-33-024-14W3/0	Forgan	Baytex	3/8/2017	51.084105	-107.911511	3.1	686	11.62	1013.9	36.21	0.40	0.46	2892.7
11	01/07-27-025-17W3/0	Plato	Teine	2/26/2017	51.153251	-108.292343	2.0	695.1	1.10	732.9	40.72	0.36	0.52	2166.0
12	01/10-27-025-17W3/0	Plato	Teine	2/26/2017	51.164247	-108.27991	2.0	690.4	4.33	716.5	39.81	0.38	0.47	1212.1

13	02/15-11-025-18W3/0	Plato	Crescent	7/19/2016	51.125856	-108.396343	2.0	642.5	94.99	603.7	33.54	0.42	0.45	1109.1
14	01/09-22-025-18W3/0	Plato	Crescent	3/5/2016	51.151091	-108.435609	3.0	677.8	94.95	642.2	35.68	0.39	0.5	1126.2
15	01/16-22-025-18W3/0	Plato	Crescent	3/5/2016	51.151226	-108.435609	3.0	679.6	94.82	610.2	33.9	0.40	0.51	1020.9
16	02/16-22-025-18W3/0	Plato	Crescent	3/5/2016	51.151361	-108.435609	3.0	675.5	95.06	609.6	33.87	0.41	0.5	1550.5
17	01/05-23-025-18W3/0	Plato	Teine	12/16/2016	51.146228	-108.397468	2.3	662.9	15.89	1492.3	37.31	0.40	0.42	1630.9
18	01/01-27-025-18W3/0	Plato	Teine	10/3/2016	51.1636	-108.423859	3.0	680.9	6.11	656.6	36.48	0.53	0.51	1881.9
19	01/05-27-025-18W3/0	Plato	Teine	9/30/2016	51.152988	-108.439681	3.0	675.5	16.48	667.7	37.09	0.54	0.61	2082.9
20	01/12-27-025-18W3/0	Plato	Teine	9/28/2016	51.170153	-108.441828	3.0	683.6	29.83	677.5	39.85	0.49	0.57	2563.2
21	01/01-28-025-18W3/0	Plato	Crescent	10/24/2017	51.156124	-108.459157	2.6	686.6	97.02	633.7	35.21	0.40	0.5	1337.1
22	02/01-28-025-18W3/0	Plato	Crescent	10/24/2017	51.156259	-108.459157	2.6	686	96.75	645.9	35.88	0.38	0.49	1442.2
23	01/04-28-025-18W3/0	Plato	Crescent	10/24/2017	51.156132	-108.454474	2.6	684.4	96.95	717	39.83	0.35	0.44	1689.6
24	02/04-28-025-18W3/0	Plato	Crescent	10/24/2017	51.156267	-108.454474	2.6	686.9	96.75	660	36.67	0.38	0.42	1779.4
25	02/05-28-025-18W3/0	Plato	Crescent	9/28/2017	51.170174	-108.46492	2.6	685.2	65.21	1077.9	35.93	0.39	0.41	4619.4
26	03/05-28-025-18W3/0	Plato	Crescent	9/28/2017	51.170175	-108.464705	2.6	681.2	73.10	1104.8	36.83	0.38	0.43	4797.0
27	03/06-28-025-18W3/0	Plato	Crescent	9/28/2017	51.170176	-108.464491	2.6	687.5	65.14	1078.1	35.94	0.39	0.42	3002.1
28	04/06-28-025-18W3/0	Plato	Crescent	10/22/2017	51.170202	-108.458107	2.6	688.4	56.57	1096	36.53	0.38	0.43	3893.8

29	05/06-28-025-18W3/0	Plato	Crescent	10/22/2017	51.170203	-108.457892	2.6	687.5	50.74	1101.6	36.72	0.37	0.51	3788.6
30	04/07-28-025-18W3/0	Plato	Crescent	11/3/2017	51.170204	-108.457678	2.6	692.7	43.98	1110.9	39.68	0.35	0.39	2729.1
31	07/07-28-025-18W3/0	Plato	Crescent	11/3/2017	51.170232	-108.450588	2.6	694.4	43.77	1170.7	39.02	0.36	0.41	3548.0
32	08/07-28-025-18W3/0	Plato	Crescent	11/3/2017	51.170233	-108.450373	2.6	692	44.85	1098.7	36.62	0.38	0.47	2673.5
33	04/08-28-025-18W3/0	Plato	Crescent	11/3/2017	51.170234	-108.450159	2.6	689.6	46.98	1104	36.8	0.36	0.47	3271.1
34	05/08-28-025-18W3/0	Plato	Crescent	11/3/2017	51.170235	-108.449944	2.6	693.2	46.25	1136.4	37.88	0.37	0.41	3070.9
35	04/12-30-025-18W3/0	Plato	Crescent	9/11/2017	51.164457	-108.495354	3.3	687.7	97.20	1061	35.37	0.39	0.44	1837.5
36	05/12-30-025-18W3/0	Plato	Crescent	9/11/2017	51.164322	-108.495354	3.3	687.4	96.61	1046.3	34.88	0.40	0.47	900.6
37	06/12-30-025-18W3/0	Plato	Crescent	9/11/2017	51.164187	-108.495354	3.3	686.8	97.26	1078.9	35.96	0.39	0.49	760.1
38	01/13-30-025-18W3/0	Plato	Crescent	8/29/2017	51.167198	-108.495069	3.3	694.7	96.44	1080.5	36.02	0.39	0.47	1735.3
39	02/13-30-025-18W3/0	Plato	Crescent	8/29/2017	51.167333	-108.495069	3.3	693.8	96.32	1077.8	35.93	0.38	0.45	1445.3
40	01/08-31-025-18W3/0	Plato	Teine	8/17/2016	51.181485	-108.494753	3.1	696.3	9.84	733.8	38.62	0.52	0.59	3367.2
41	01/16-31-025-18W3/0	Plato	Teine	8/2/2016	51.181201	-108.50655	3.1	686.7	28.47	692	40.71	0.48	0.57	1721.6
42	01/01-32-025-18W3/0	Plato	Crescent	11/14/2016	51.171662	-108.482058	2.0	692.9	94.99	657.1	36.51	0.38	0.5	1886.7
43	03/01-32-025-18W3/0	Plato	Crescent	11/14/2016	51.171797	-108.482916	2.0	692.9	95.02	614.8	34.16	0.40	0.4	1072.9
44	01/04-32-025-18W3/0	Plato	Crescent	11/13/2016	51.171596	-108.478573	2.0	690.2	95.05	602	33.44	0.42	0.47	1498.5

45	03/04-32-025-18W3/0	Plato	Crescent	11/13/2016	51.171731	-108.478573	2.0	690.7	94.94	596	33.11	0.42	0.47	2195.3
46	02/05-32-025-18W3/0	Plato	Crescent	11/8/2016	51.176662	-108.477993	2.0	701.8	94.95	702.1	39.01	0.36	0.44	2005.4
47	03/05-32-025-18W3/0	Plato	Crescent	11/13/2016	51.171865	-108.478573	2.0	690.5	95.11	585.4	32.52	0.42	0.48	2068.9
48	04/05-32-025-18W3/0	Plato	Crescent	11/8/2016	51.176797	-108.477993	2.0	700.5	95.01	629.1	34.95	0.39	0.47	1767.8
49	02/08-32-025-18W3/0	Plato	Crescent	11/14/2016	51.171932	-108.482058	2.0	695	95.03	641.6	35.64	0.39	0.46	2033.2
50	03/08-32-025-18W3/0	Plato	Crescent	10/5/2016	51.176596	-108.482059	2.0	699.5	95.04	720.3	40.02	0.38	0.5	1278.1
51	04/08-32-025-18W3/0	Plato	Crescent	10/5/2016	51.176731	-108.482059	2.0	691.5	94.87	643.9	35.77	0.39	0.48	1768.5
52	01/09-32-025-18W3/0	Plato	Crescent	9/28/2016	51.180282	-108.482059	2.0	693.8	94.98	622.8	34.6	0.39	0.46	1661.4
53	01/12-32-025-18W3/0	Plato	Crescent	9/22/2016	51.180212	-108.47713	2.0	697.2	95.13	616.9	34.27	0.40	0.44	964.9
54	02/12-32-025-18W3/0	Plato	Crescent	11/8/2016	51.177066	-108.477993	2.0	696.5	94.99	608.9	33.83	0.42	0.5	2144.9
55	03/12-32-025-18W3/0	Plato	Crescent	11/8/2016	51.176931	-108.477993	2.0	698.6	95.03	588.3	32.68	0.42	0.43	2093.4
56	01/13-32-025-18W3/0	Plato	Crescent	9/21/2016	51.180482	-108.477987	2.0	693.8	94.97	622.5	34.58	0.58	0.53	1859.3
57	02/13-32-025-18W3/0	Plato	Crescent	9/21/2016	51.180347	-108.477987	2.0	694.8	94.99	606.9	33.72	0.42	0.48	1638.2
58	02/16-32-025-18W3/0	Plato	Crescent	9/28/2016	51.180416	-108.482059	2.0	701.3	94.91	613.9	34.11	0.40	0.41	1684.0
59	03/16-32-025-18W3/0	Plato	Crescent	9/28/2016	51.180551	-108.482059	2.0	701.5	94.92	665.3	36.96	0.53	0.54	1906.8
60	01/02-33-025-18W3/0	Plato	Teine	9/13/2016	51.177841	-108.448396	2.7	680.6	39.03	724.5	40.25	0.46	0.5	2861.8

61	01/04-33-025-18W3/0	Plato	Teine	9/15/2016	51.178018	-108.465411	2.7	691.6	22.99	686	38.11	0.52	0.57	3091.8
62	01/10-33-025-18W3/0	Plato	Teine	9/15/2016	51.185164	-108.454375	2.7	688.7	38.55	676.7	37.59	0.51	0.53	3388.2
63	01/13-34-025-18W3/0	Plato	Teine	3/1/2017	51.174663	-108.44207	3.3	682.1	39.28	729.8	40.54	0.49	0.56	3540.4
64	02/13-34-025-18W3/0	Plato	Teine	2/27/2017	51.174662	-108.441856	3.3	679.9	42.02	694.1	38.56	0.52	0.59	3000.5
65	01/14-34-025-18W3/0	Plato	Teine	3/2/2017	51.174649	-108.436315	3.3	687.9	34.94	745.1	41.39	0.48	0.55	2967.9
66	02/14-34-025-18W3/0	Plato	Teine	3/2/2017	51.174649	-108.43653	3.3	682.3	38.78	699.1	38.84	0.49	0.57	2195.2
67	01/15-34-025-18W3/0	Plato	Teine	3/10/2017	51.174633	-108.429734	3.3	694.3	25.77	683.6	37.98	0.52	0.5	2439.2
68	02/15-34-025-18W3/0	Plato	Teine	3/10/2017	51.174633	-108.429519	3.3	696	19.75	727.6	40.42	0.49	0.59	3464.8
69	01/16-34-025-18W3/0	Plato	Teine	3/11/2017	51.174619	-108.424014	3.3	695.6	49.36	720.8	40.04	0.50	0.59	2833.6
70	02/16-34-025-18W3/0	Plato	Teine	3/11/2017	51.174618	-108.4238	3.3	697.9	33.58	689.9	38.33	0.52	0.56	2781.6
71	02/01-35-025-18W3/0	Plato	Teine	9/26/2016	51.177537	-108.406187	3.1	678	14.49	687.5	38.19	0.50	0.56	2435.9
72	01/12-05-026-17W3/0	Plato	Teine	3/3/2017	51.182375	-108.354102	1.2	682.2	1.11	748.4	37.42	0.40	0.51	2886.8
73	01/04-05-026-18W3/0	Plato	Teine	1/16/2017	51.192087	-108.488678	5.1	683	1.71	710.7	39.48	0.50	0.54	3247.6
74	01/08-05-026-18W3/0	Plato	Teine	2/27/2017	51.182052	-108.472553	5.1	690.2	1.19	703.8	39.1	0.51	0.55	2312.1
75	01/12-05-026-18W3/0	Plato	Teine	1/15/2017	51.19925	-108.488431	5.1	685.3	1.56	687.7	38.21	0.52	0.56	2778.6
76	01/05-06-026-18W3/0	Plato North	Baytex	8/18/2016	51.18941	-108.501015	4.5	689.7	6.80	667.1	37.06	0.40	0.5	1066.5

77	01/06-06-026-18W3/0	Plato North	Baytex	9/9/2017	51.182143	-108.506039	4.5	694.1	40.72	662.5	36.81	0.26	0.34	1859.9
78	02/06-06-026-18W3/0	Plato North	Baytex	9/9/2017	51.182145	-108.506754	4.5	692.4	36.93	642	35.67	0.28	0.35	1784.0
79	01/07-06-026-18W3/0	Plato North	Baytex	9/9/2017	51.182086	-108.501153	4.5	699.2	42.80	658.7	36.59	0.41	0.44	1979.6
80	01/08-06-026-18W3/0	Plato North	Baytex	8/26/2016	51.190353	-108.504532	4.5	684.6	10.15	517.4	28.74	0.51	0.51	1031.6
81	01/14-06-026-18W3/0	Plato North	Baytex	9/4/2017	51.189518	-108.507109	4.5	687.1	24.69	627.7	34.87	0.29	0.37	2027.5
82	02/14-06-026-18W3/0	Plato North	Baytex	9/5/2017	51.189517	-108.506751	4.5	690.1	27.97	626.1	34.78	0.29	0.37	1830.0
83	01/15-06-026-18W3/0	Plato North	Baytex	9/9/2017	51.189411	-108.500658	4.5	688.7	26.36	636.5	35.36	0.42	0.45	2065.0
84	02/15-06-026-18W3/0	Plato North	Baytex	9/7/2017	51.189365	-108.499942	4.5	685.7	29.15	626.2	34.79	0.43	0.46	2183.3
85	01/07-16-026-18W3/0	Plato North	Baytex	8/26/2016	51.214646	-108.443428	5.9	691.3	111.00	653	36.28	0.41	0.51	1317.5
86	01/10-16-026-18W3/0	Plato North	Baytex	12/2/2016	51.221245	-108.442824	5.9	689.8	262.91	604.8	33.6	0.45	0.47	483.3
87	01/03-17-026-18W3/0	Plato North	Teine	9/11/2016	51.215862	-108.493239	6.0	688.3	62.53	700.5	38.92	0.36	0.48	1302.0
88	01/15-17-026-18W3/0	Plato North	Teine	9/2/2016	51.218572	-108.473087	6.0	680.6	60.03	643.4	35.74	0.56	0.58	2604.8
89	01/16-17-026-18W3/0	Plato North	Teine	9/1/2016	51.218572	-108.472872	6.0	683.6	20.90	660.3	38.84	0.50	0.55	2622.2
90	01/08-18-026-18W3/0	Plato North	Baytex	8/25/2017	51.218467	-108.505735	6.0	698	37.25	676	37.56	0.26	0.37	2208.4
91	02/08-18-026-18W3/0	Plato North	Baytex	8/25/2017	51.218287	-108.505735	6.0	696.4	50.45	605.7	33.65	0.45	0.48	2029.6
92	01/09-18-026-18W3/0	Plato North	Baytex	8/23/2017	51.221967	-108.505376	6.0	692.1	48.75	629.2	34.96	0.29	0.38	1891.3

93	02/09-18-026-18W3/0	Plato North	Baytex	8/23/2017	51.222147	-108.505376	6.0	691.7	50.35	627.3	34.85	0.43	0.47	2476.3
94	01/12-18-026-18W3/0	Plato North	Baytex	8/23/2017	51.221918	-108.501267	6.0	692.6	30.82	613.6	34.09	0.29	0.38	1667.0
95	02/12-18-026-18W3/0	Plato North	Baytex	8/22/2017	51.222142	-108.501267	6.0	692.4	33.73	595.1	33.06	0.45	0.44	2414.7
96	01/13-18-026-18W3/0	Plato North	Baytex	8/27/2017	51.225271	-108.501274	6.0	690.8	51.65	620.5	34.47	0.29	0.39	2130.1
97	01/01-19-026-18W3/0	Plato North	Teine	5/16/2017	51.22981	-108.505801	5.0	690.2	49.63	748.1	41.56	0.48	0.58	2473.2
98	01/04-19-026-18W3/0	Plato North	Teine	5/16/2017	51.228906	-108.501068	5.0	698.5	85.28	749.1	41.62	0.48	0.57	2347.1
99	01/05-19-026-18W3/0	Plato North	Teine	5/15/2017	51.232546	-108.500934	5.0	694.1	101.88	753.1	44.3	0.45	0.55	2243.0
100	02/05-19-026-18W3/0	Plato North	Teine	5/15/2017	51.232681	-108.500934	5.0	698.7	72.16	737.9	40.99	0.49	0.59	2787.6
101	01/09-19-026-18W3/0	Plato North	Teine	3/9/2017	51.238745	-108.506013	5.0	695	142.53	734.5	40.81	0.47	0.57	2027.5
102	01/13-19-026-18W3/0	Plato North	Teine	5/15/2017	51.233239	-108.512301	5.0	702.3	17.28	770.7	42.82	0.45	0.56	3254.4
103	01/14-19-026-18W3/0	Plato North	Teine	5/12/2017	51.233372	-108.505792	5.0	693.3	85.55	741.8	41.21	0.49	0.55	3038.9
104	02/14-19-026-18W3/0	Plato North	Teine	5/12/2017	51.233507	-108.505792	5.0	695.4	36.45	743.9	41.33	0.48	0.56	3549.3
105	01/16-19-026-18W3/0	Plato North	Teine	3/9/2017	51.23888	-108.506013	5.0	697.7	142.85	742.1	41.23	0.48	0.56	2444.2
106	01/14-20-026-18W3/0	Plato North	Baytex	9/6/2016	51.239388	-108.493858	4.1	691	51.70	644.2	35.79	0.42	0.49	1112.2
107	01/02-01-026-19W3/0	Plato North	Teine	7/27/2016	51.192764	-108.520968	3.5	679.8	38.38	663.1	36.84	0.39	0.52	1349.3
108	01/04-01-026-19W3/0	Plato North	Teine	2/2/2017	51.185259	-108.521649	3.5	681.6	21.01	729.6	42.92	0.44	0.54	2495.8

109	02/04-01-026-19W3/0	Plato North	Teine	2/2/2017	51.185394	-108.521649	3.5	678.8	5.64	692.9	40.76	0.50	0.52	2778.7
110	01/05-01-026-19W3/0	Plato North	Teine	8/27/2016	51.188655	-108.522243	3.5	680.7	34.53	704	39.11	0.49	0.57	1852.2
111	04/05-01-026-19W3/0	Plato North	Teine	2/2/2017	51.18879	-108.522243	3.5	676.2	23.97	696.4	40.96	0.42	0.49	1966.8
112	01/12-01-026-19W3/0	Plato North	Teine	2/12/2017	51.19253	-108.522399	3.5	679.3	10.53	714.3	39.68	0.48	0.56	1659.7
113	04/12-01-026-19W3/0	Plato North	Teine	2/9/2017	51.19253	-108.522184	3.5	681.6	15.56	697.4	41.02	0.46	0.58	1787.0
114	01/10-03-026-19W3/0	Plato North	Teine	12/14/2016	51.192955	-108.55985	2.3	698	12.93	673.3	39.61	0.50	0.57	2119.4
115	92/01-10-026-19W3/0	Plato North	Crescent	5/8/2016	51.206634	-108.566259	4.2	691	27.66	636.8	35.38	0.40	0.56	2263.6
116	91/02-10-026-19W3/0	Plato North	Crescent	5/24/2016	51.206634	-108.566474	4.2	692	18.81	586.5	32.58	0.43	0.51	2452.9
117	92/02-10-026-19W3/0	Plato North	Crescent	2/10/2016	51.206644	-108.571732	4.2	701.6	10.94	623.4	34.63	0.39	0.48	2931.5
118	91/03-10-026-19W3/0	Plato North	Crescent	3/5/2016	51.206658	-108.579923	4.2	699.8	9.51	574.6	31.92	0.44	0.47	2811.7
119	92/03-10-026-19W3/0	Plato North	Crescent	2/10/2016	51.206644	-108.571947	4.2	700.8	10.65	624.3	34.68	0.40	0.48	2400.1
120	91/04-10-026-19W3/0	Plato North	Crescent	3/5/2016	51.206658	-108.580138	4.2	701.9	9.46	629.3	34.96	0.40	0.49	2785.3
121	92/04-10-026-19W3/0	Plato North	Crescent	3/5/2016	51.206658	-108.580352	4.2	700.7	8.91	578.5	32.14	0.44	0.49	2820.5
122	01/13-10-026-19W3/0	Plato North	Crescent	3/1/2016	51.204077	-108.580245	4.2	694	9.13	619.3	34.41	0.41	0.49	2504.6
123	02/13-10-026-19W3/0	Plato North	Crescent	3/1/2016	51.204076	-108.58003	4.2	688.9	13.55	637.5	35.42	0.40	0.54	2258.0
124	01/14-10-026-19W3/0	Plato North	Crescent	3/1/2016	51.204075	-108.579815	4.2	691.6	14.73	681.3	37.85	0.37	0.53	2533.9

125	91/14-10-026-19W3/0	Plato North	Crescent	2/17/2016	51.204055	-108.574202	4.2	693.8	21.69	616.3	34.24	0.40	0.46	1708.2
126	91/15-10-026-19W3/0	Plato North	Crescent	2/16/2016	51.204054	-108.573988	4.2	696.9	19.69	646.5	35.92	0.39	0.49	2673.4
127	92/15-10-026-19W3/0	Plato North	Crescent	2/10/2016	51.204026	-108.566583	4.2	689.9	14.14	603.8	33.54	0.41	0.46	2330.4
128	91/16-10-026-19W3/0	Plato North	Crescent	2/10/2016	51.204026	-108.566368	4.2	688.7	12.46	624.5	34.69	0.40	0.44	2688.6
129	02/02-11-026-19W3/0	Plato North	Crescent	8/4/2017	51.21483	-108.546862	4.1	703.4	25.12	1454.8	33.83	0.34	0.37	3484.2
130	01/16-12-026-19W3/0	Plato North	Crescent	12/18/2016	51.204434	-108.51862	4.4	694.2	99.66	617.1	30.86	0.41	0.43	1344.0
131	01/09-16-026-19W3/0	Plato North	Teine	1/14/2017	51.228405	-108.587805	5.0	709.2	15.86	757.1	42.06	0.45	0.57	3179.9
132	03/09-16-026-19W3/0	Plato North	Teine	3/13/2017	51.228405	-108.58802	5.0	707.7	11.38	725.1	40.28	0.50	0.56	2974.2
133	01/10-16-026-19W3/0	Plato North	Teine	3/13/2017	51.228924	-108.593483	5.0	706.3	106.36	700.3	38.91	0.51	0.59	2419.3
134	02/10-16-026-19W3/0	Plato North	Teine	3/13/2017	51.228789	-108.593484	5.0	709.3	34.71	634.6	35.26	0.57	0.59	2643.0
135	01/11-16-026-19W3/0	Plato North	Teine	1/24/2017	51.228792	-108.600116	5.0	709.8	5.35	714.9	42.05	0.47	0.55	3030.6
136	02/11-16-026-19W3/0	Plato North	Teine	1/24/2017	51.228657	-108.600116	5.0	709.2	4.29	714.6	39.7	0.50	0.57	2975.9
137	01/12-16-026-19W3/0	Plato North	Teine	1/21/2017	51.228254	-108.604654	5.0	711.9	8.51	695.3	40.9	0.49	0.56	2478.0
138	02/12-16-026-19W3/0	Plato North	Teine	1/21/2017	51.228254	-108.604869	5.0	710.6	14.93	721.5	40.08	0.49	0.55	2572.7
139	01/01-17-026-19W3/0	Plato North	Teine	11/21/2016	51.221583	-108.612392	4.5	710.5	6.48	793.7	46.69	0.43	0.56	2593.4
140	03/01-17-026-19W3/0	Plato North	Teine	11/21/2016	51.221583	-108.612607	4.5	709.1	7.66	697.8	38.77	0.52	0.54	2075.2

141	01/02-17-026-19W3/0	Plato North	Teine	11/30/2016	51.221371	-108.618132	4.5	712	7.20	695.5	40.91	0.42	0.44	2016.3
142	02/02-17-026-19W3/0	Plato North	Teine	11/30/2016	51.221371	-108.617917	4.5	714.1	7.02	708.4	39.36	0.50	0.53	2593.7
143	01/03-17-026-19W3/0	Plato North	Teine	11/30/2016	51.221371	-108.618347	4.5	712.3	7.60	661.9	36.77	0.53	0.54	2469.2
144	01/04-17-026-19W3/0	Plato North	Teine	12/1/2016	51.221404	-108.626674	4.5	724.9	6.50	645.2	35.84	0.52	0.58	2757.2
145	01/13-17-026-19W3/0	Plato North	Teine	11/10/2016	51.218632	-108.627109	4.5	714.2	8.13	704	39.11	0.41	0.48	2062.5
146	02/13-17-026-19W3/0	Plato North	Teine	11/10/2016	51.218632	-108.627323	4.5	715.5	6.60	682	40.12	0.50	0.55	2817.5
147	01/14-17-026-19W3/0	Plato North	Teine	11/14/2016	51.218396	-108.618764	4.5	711.1	7.56	698.8	38.82	0.51	0.58	2404.8
148	02/15-17-026-19W3/0	Plato North	Teine	11/15/2016	51.218396	-108.618335	4.5	709.8	12.86	710.7	39.48	0.50	0.58	2397.5
149	03/15-17-026-19W3/0	Plato North	Teine	11/15/2016	51.218396	-108.618549	4.5	710.7	4.95	704.9	41.46	0.48	0.61	2662.8
150	01/16-17-026-19W3/0	Plato North	Teine	11/19/2016	51.218797	-108.612252	4.5	713.8	7.45	706.1	39.23	0.49	0.53	2567.3
151	02/16-17-026-19W3/0	Plato North	Teine	11/20/2016	51.218797	-108.611822	4.5	715.9	6.14	695.4	40.91	0.48	0.53	2250.4
152	01/16-18-026-19W3/0	Plato North	Baytex	8/21/2016	51.225337	-108.645735	3.4	725.2	7.80	628.8	34.93	0.43	0.52	2054.6
153	02/16-18-026-19W3/0	Plato North	Baytex	5/29/2017	51.225203	-108.645735	3.4	722.9	4.92	618.7	34.37	0.40	0.42	1617.5
154	02/01-19-026-19W3/0	Plato North	Baytex	6/1/2017	51.236253	-108.634005	6.5	721.9	2.23	643.1	35.73	0.42	0.44	2569.8
155	03/01-19-026-19W3/0	Plato North	Baytex	6/1/2017	51.236253	-108.634435	6.5	720.1	2.47	653.5	36.31	0.41	0.41	2030.8
156	01/02-19-026-19W3/0	Plato North	Baytex	8/1/2016	51.235704	-108.64032	6.5	723.6	2.00	640.7	35.59	0.38	0.48	2500.6

157	02/02-19-026-19W3/0	Plato North	Baytex	8/1/2016	51.235704	-108.639962	6.5	726.5	4.47	644.8	35.82	0.41	0.5	2388.9
158	02/09-19-026-19W3/0	Plato North	Baytex	11/3/2017	51.243481	-108.634152	6.5	715.8	8.05	671.8	37.32	0.39	0.44	754.6
159	02/14-19-026-19W3/0	Plato North	Baytex	7/27/2016	51.239775	-108.634209	6.5	723.8	6.40	643.5	35.75	0.42	0.52	1482.3
160	03/14-19-026-19W3/0	Plato North	Baytex	7/24/2016	51.239999	-108.634209	6.5	724.7	9.87	643.1	35.73	0.41	0.51	1670.0
161	01/12-20-026-19W3/0	Plato North	Baytex	10/31/2017	51.243497	-108.628012	6.6	717.5	5.30	639.1	35.51	0.40	0.41	1348.6
162	02/08-22-026-19W3/0	Plato North	Crescent	9/11/2016	51.225698	-108.568575	6.3	700.1	38.25	624.3	34.68	0.39	0.45	3415.7
163	01/15-22-026-19W3/0	Plato North	Crescent	9/30/2016	51.233159	-108.568785	6.3	702.1	28.08	616.3	34.24	0.40	0.41	3459.2
164	01/01-25-026-19W3/0	Plato North	Teine	8/19/2016	51.244512	-108.52886	2.5	699	60.62	694.8	38.6	0.52	0.57	1960.6
165	01/14-26-026-19W3/0	Plato North	Teine	7/25/2016	51.253714	-108.562953	5.0	696.1	36.42	665.7	39.16	0.51	0.63	2137.4
166	02/03-28-026-19W3/0	Plato North	Teine	1/31/2017	51.258518	-108.598435	7.4	710.6	7.60	1554.9	37.92	0.50	0.47	3567.7
167	04/03-28-026-19W3/0	Plato North	Teine	1/31/2017	51.258383	-108.598435	7.4	718.4	10.94	1512.7	36.02	0.53	0.5	3328.2
168	03/04-28-026-19W3/0	Plato North	Teine	2/5/2017	51.258162	-108.604695	7.4	718.6	5.60	1525.9	35.49	0.56	0.5	5214.1
169	04/04-28-026-19W3/0	Plato North	Teine	2/7/2017	51.258162	-108.60448	7.4	719.6	10.72	1509.5	35.1	0.57	0.49	4001.1
170	02/11-29-026-19W3/0	Plato North	Baytex	1/14/2017	51.257479	-108.623142	7.6	707.3	14.49	629.2	34.96	0.44	0.52	3078.3
171	03/12-29-026-19W3/0	Plato North	Baytex	1/15/2017	51.257456	-108.628253	7.6	708.1	20.00	643.7	33.88	0.44	0.54	3198.8
172	02/06-32-026-19W3/0	Plato North	Baytex	3/1/2017	51.255101	-108.622231	7.1	703.6	40.32	609.2	33.84	0.43	0.46	1680.6

173	02/08-32-026-19W3/0	Plato North	Baytex	6/14/2017	51.26175	-108.622219	7.1	703.6	40.54	636.5	35.36	0.42	0.43	2369.1
174	01/15-32-026-19W3/0	Plato North	Baytex	6/22/2017	51.261757	-108.616306	7.1	698.6	9.69	665.1	36.95	0.41	0.44	1717.8
175	02/15-32-026-19W3/0	Plato North	Baytex	6/20/2017	51.261757	-108.616091	7.1	697.7	15.95	668.2	37.12	0.40	0.45	1296.9
176	01/16-32-026-19W3/0	Plato North	Baytex	6/10/2017	51.261742	-108.610719	7.1	701.9	24.21	614.1	34.12	0.43	0.44	3051.6
177	01/01-33-026-19W3/0	Plato North	Teine	7/23/2016	51.260001	-108.609898	7.1	711.1	9.04	1499.3	37.48	0.52	0.52	3808.9
178	02/15-23-026-20W3/0	Plato North	Baytex	11/4/2017	51.2399	-108.675397	4.7	731.7	19.81	639.6	35.53	0.39	0.42	1755.6
179	02/05-24-026-20W3/0	Plato North	Baytex	6/3/2017	51.232766	-108.664378	4.4	735.4	12.68	617.7	34.32	0.44	0.45	1892.9
180	02/10-24-026-20W3/0	Plato North	Baytex	8/1/2016	51.236143	-108.651475	4.4	727.5	7.39	641.9	35.66	0.42	0.5	1828.5
181	03/10-24-026-20W3/0	Plato North	Baytex	8/1/2016	51.236421	-108.651482	4.4	729.3	2.44	618.2	34.34	0.43	0.5	1947.9
182	02/01-25-026-20W3/0	Plato North	Teine	6/19/2017	51.249744	-108.65755	6.4	721.2	18.56	675	37.5	0.53	0.59	2714.4
183	02/07-26-026-20W3/0	Plato North	Baytex	9/1/2016	51.239886	-108.68659	6.4	728.3	3.27	666.4	37.02	0.37	0.5	2241.0
184	02/13-26-026-20W3/0	Plato North	Baytex	8/1/2016	51.255457	-108.686588	6.4	732.4	2.98	667	37.06	0.38	0.5	1759.0
185	03/13-26-026-20W3/0	Plato North	Baytex	8/1/2016	51.255682	-108.686589	6.4	737.1	20.08	639.3	35.52	0.41	0.5	2152.9
186	02/07-35-026-20W3/0	Plato North	Teine	6/27/2017	51.254559	-108.685656	6.2	727.1	15.56	694.7	38.59	0.52	0.56	3348.3
187	03/07-35-026-20W3/0	Plato North	Teine	6/27/2017	51.25456	-108.685441	6.2	728.9	23.93	679	37.72	0.52	0.53	3483.2
188	02/08-35-026-20W3/0	Plato North	Teine	7/8/2017	51.254567	-108.681144	6.2	735.2	18.37	780.1	43.34	0.46	0.74	3541.5

189	03/08-35-026-20W3/0	Plato North	Teine	7/8/2017	51.254566	-108.680929	6.2	732.2	18.52	707.2	39.29	0.51	0.61	3368.3
190	02/02-01-027-20W3/0	Plato North	Teine	7/26/2017	51.27999	-108.684162	6.3	722.2	25.24	694.3	38.57	0.52	0.56	3135.3
191	02/03-01-027-20W3/0	Plato North	Teine	7/24/2017	51.279956	-108.691075	6.3	720.5	30.24	707.5	39.31	0.51	0.59	2922.4
192	02/04-01-027-20W3/0	Plato North	Teine	7/27/2017	51.279957	-108.695538	6.3	723.9	23.28	699.6	38.87	0.51	0.58	2622.8
193	02/13-01-027-20W3/0	Plato North	Teine	7/27/2017	51.276078	-108.695427	6.3	718.9	55.46	687.4	38.19	0.52	0.59	2512.4
194	02/14-01-027-20W3/0	Plato North	Teine	7/31/2017	51.276089	-108.689917	6.3	723.8	58.70	680.5	37.81	0.50	0.57	2913.6
195	02/15-01-027-20W3/0	Plato North	Teine	7/31/2017	51.27569	-108.683803	6.3	721.1	58.49	676.6	39.8	0.40	0.55	2786.8
196	02/01-17-029-21W3/0	Avon Hill	Baytex	8/3/2017	51.478163	-108.935569	3.6	753.2	1.00	1455.9	34.66	0.43	0.45	3139.9
197	01/03-18-029-21W3/0	Avon Hill	Baytex	11/16/2017	51.476322	-108.930812	3.6	753.6	4.08	1030.6	34.35	0.27	0.3	1417.9
198	01/06-18-029-21W3/0	Avon Hill	Baytex	8/2/2017	51.480591	-108.93025	3.6	753.7	20.34	1040.2	31.52	0.43	0.42	2529.7
199	01/01-21-029-21W3/0	Avon Hill	Baytex	2/7/2016	51.491379	-108.899901	3.6	742.7	10.83	618.2	34.34	0.43	0.55	2551.9
200	02/01-21-029-21W3/0	Avon Hill	Baytex	1/18/2017	51.491604	-108.8999	3.6	744.2	22.85	675	37.5	0.24	0.31	1700.3
201	01/04-21-029-21W3/0	Avon Hill	Baytex	2/8/2016	51.491373	-108.895829	3.6	744.1	9.41	660.7	36.71	0.41	0.54	2655.3
202	02/04-21-029-21W3/0	Avon Hill	Baytex	1/15/2017	51.491598	-108.895828	3.6	743.2	44.10	619.2	34.4	0.29	0.35	1448.2
203	01/05-21-029-21W3/0	Avon Hill	Baytex	1/17/2017	51.491823	-108.895827	3.6	746.8	23.16	629.3	34.96	0.41	0.43	2005.7
204	02/05-21-029-21W3/0	Avon Hill	Baytex	1/16/2017	51.494744	-108.895818	3.6	740.6	17.56	634.3	35.24	0.28	0.36	1785.5

205	03/05-21-029-21W3/0	Avon Hill	Baytex	1/15/2017	51.494968	-108.895818	3.6	741.5	10.62	650.5	36.14	0.42	0.44	2020.1
206	01/08-21-029-21W3/0	Avon Hill	Baytex	1/18/2017	51.491828	-108.899898	3.6	743.7	11.16	678	37.67	0.39	0.42	1747.6
207	02/08-21-029-21W3/0	Avon Hill	Baytex	1/21/2017	51.494974	-108.899876	3.6	740.5	19.58	649.6	36.09	0.42	0.44	1707.3
208	03/08-21-029-21W3/0	Avon Hill	Baytex	1/18/2017	51.494749	-108.899878	3.6	737.9	14.37	645.8	35.88	0.21	0.27	1226.5
209	01/10-21-029-21W3/0	Avon Hill	Baytex	1/8/2017	51.504925	-108.898916	3.6	739	26.32	634.8	35.27	0.42	0.44	1728.0
210	02/10-21-029-21W3/0	Avon Hill	Baytex	1/10/2017	51.505388	-108.894231	3.6	739.6	8.74	694.4	38.58	0.22	0.29	1402.6
211	03/10-21-029-21W3/0	Avon Hill	Baytex	1/9/2017	51.505387	-108.89387	3.6	741.8	13.46	636.9	35.38	0.42	0.42	1428.1
212	01/11-21-029-21W3/0	Avon Hill	Baytex	1/11/2017	51.504926	-108.899276	3.6	739.9	21.28	644.7	35.82	0.28	0.35	1161.4
213	01/12-21-029-21W3/0	Avon Hill	Baytex	1/13/2017	51.504932	-108.905801	3.6	735.5	21.06	619.6	34.42	0.29	0.35	1990.7
214	02/12-21-029-21W3/0	Avon Hill	Baytex	1/11/2017	51.504933	-108.906161	3.6	736.2	17.31	615.3	34.18	0.43	0.43	1316.5
215	02/05-28-029-21W3/0	Avon Hill	Baytex	1/14/2018	51.502505	-108.90594	3.6	728.2	76.48	622.6	29.65	0.34	0.32	1919.7
216	01/06-28-029-21W3/0	Avon Hill	Baytex	1/14/2018	51.502499	-108.900684	3.6	728.1	26.48	637.3	30.35	0.32	0.31	1812.4
217	01/07-28-029-21W3/0	Avon Hill	Baytex	1/14/2018	51.502561	-108.895169	3.6	731.5	57.19	625.3	29.78	0.34	0.33	1326.9
218	01/13-28-029-21W3/0	Avon Hill	Baytex	9/6/2017	51.509696	-108.906154	3.6	727.2	13.70	627.7	31.39	0.31	0.36	1640.8
219	02/13-28-029-21W3/0	Avon Hill	Baytex	1/7/2018	51.509696	-108.905794	3.6	724.4	16.99	627.5	31.38	0.31	0.3	1241.0
220	01/15-28-029-21W3/0	Avon Hill	Baytex	1/8/2018	51.509864	-108.894476	3.6	720.9	17.94	621.7	29.6	0.30	0.26	1666.3

221	02/15-28-029-21W3/0	Avon Hill	Baytex	1/7/2018	51.509865	-108.895196	3.6	725.2	19.51	637.5	30.36	0.27	0.28	964.0
222	01/16-28-029-21W3/0	Avon Hill	Baytex	1/9/2018	51.502487	-108.889026	3.6	729.2	17.90	1443.5	33.57	0.24	0.25	2395.9
223	02/16-28-029-21W3/0	Avon Hill	Baytex	1/12/2018	51.502487	-108.888666	3.6	729.6	6.05	1430.7	33.27	0.21	0.25	1230.4
224	02/11-29-029-21W3/0	Avon Hill	Baytex	10/23/2017	51.519694	-108.92495	4.1	725.9	11.19	627.6	31.38	0.29	0.32	2182.1
225	03/11-29-029-21W3/0	Avon Hill	Baytex	10/24/2017	51.519694	-108.92459	4.1	727	10.41	616.2	30.81	0.29	0.31	1979.6
226	02/12-29-029-21W3/0	Avon Hill	Baytex	10/26/2017	51.52051	-108.930453	4.1	724.6	16.31	744.1	39.16	0.22	0.31	1605.6
227	03/06-31-029-21W3/0	Avon Hill	Baytex	1/7/2017	51.516574	-108.947771	4.6	717.7	16.83	698.4	38.8	0.19	0.24	1339.4
228	04/06-31-029-21W3/0	Avon Hill	Baytex	1/9/2017	51.516574	-108.948131	4.6	715.1	19.75	696.8	38.71	0.38	0.39	1646.4
229	01/07-31-029-21W3/0	Avon Hill	Baytex	1/8/2017	51.517197	-108.942011	4.6	718	20.48	627.7	34.87	0.28	0.33	1869.0
230	02/07-31-029-21W3/0	Avon Hill	Baytex	1/9/2017	51.517198	-108.942371	4.6	717.9	18.38	628.5	34.92	0.39	0.39	2055.7
231	03/07-31-029-21W3/0	Avon Hill	Baytex	1/14/2017	51.517197	-108.94165	4.6	718.7	18.53	640	35.56	0.35	0.4	1506.6
232	01/09-31-029-21W3/0	Avon Hill	Baytex	9/5/2017	51.534371	-108.936932	4.6	705.5	3.08	626.5	31.33	0.48	0.45	2426.1
233	01/11-31-029-21W3/0	Avon Hill	Baytex	9/1/2017	51.533981	-108.948217	4.6	709.4	5.86	627.4	29.88	0.33	0.37	2725.5
234	01/01-33-029-21W3/0	Avon Hill	Teine	9/3/2017	51.520313	-108.9014	4.2	720.8	36.08	762.4	42.36	0.35	0.41	1830.2
235	02/01-33-029-21W3/0	Avon Hill	Teine	9/1/2017	51.520448	-108.9014	4.2	719.8	49.07	764.2	42.46	0.34	0.45	1464.6
236	01/04-33-029-21W3/0	Avon Hill	Teine	9/3/2016	51.520444	-108.896402	4.2	723.2	20.94	699.1	38.84	0.39	0.55	1361.4

237	02/04-33-029-21W3/0	Avon Hill	Teine	9/5/2017	51.520309	-108.896402	4.2	723.1	53.70	722.2	40.12	0.37	0.45	1392.0
238	01/05-33-029-21W3/0	Avon Hill	Teine	9/10/2017	51.523719	-108.895764	4.2	717.5	72.51	721	40.06	0.37	0.42	2036.4
239	02/05-33-029-21W3/0	Avon Hill	Teine	9/10/2017	51.523863	-108.895764	4.2	715.8	46.99	715.2	39.73	0.38	0.44	1859.0
240	01/08-33-029-21W3/0	Avon Hill	Teine	9/4/2016	51.523726	-108.899076	4.2	711.9	91.06	683.7	37.98	0.39	0.52	1731.1
241	02/08-33-029-21W3/0	Avon Hill	Teine	9/11/2017	51.523861	-108.899076	4.2	715.5	43.80	720.7	40.04	0.37	0.43	1647.8
242	01/15-33-029-21W3/0	Avon Hill	Teine	9/9/2017	51.530186	-108.881546	4.2	709.3	135.12	698.9	31.77	0.33	0.42	705.5
243	01/09-13-029-22W3/0	Avon Hill	Teine	8/19/2017	51.483872	-108.971054	3.5	752.5	69.08	713.9	39.66	0.38	0.49	1705.7
244	02/09-13-029-22W3/0	Avon Hill	Teine	8/18/2017	51.484007	-108.971054	3.5	751.2	56.27	710.9	39.49	0.38	0.47	2040.2
245	01/12-13-029-22W3/0	Avon Hill	Teine	8/14/2017	51.483865	-108.965336	3.5	744.6	44.33	707.1	39.28	0.38	0.47	1712.4
246	02/12-13-029-22W3/0	Avon Hill	Teine	8/14/2017	51.484	-108.965337	3.5	746.5	72.33	710.5	39.47	0.37	0.44	1362.5
247	01/13-13-029-22W3/0	Avon Hill	Teine	8/13/2017	51.486404	-108.965343	3.5	744.5	56.56	682.9	37.94	0.39	0.43	1480.1
248	01/16-13-029-22W3/0	Avon Hill	Teine	8/23/2017	51.486681	-108.971046	3.5	753.5	56.48	751.1	41.73	0.36	0.47	1810.1
249	01/01-14-029-22W3/0	Avon Hill	Baytex	8/2/2017	51.477239	-109.005466	3.0	754.8	6.10	1453.5	33.8	0.43	0.41	1251.8
250	01/06-14-029-22W3/0	Avon Hill	Baytex	8/1/2017	51.490244	-108.994669	3.0	742.8	18.06	1030.6	32.21	0.31	0.34	2294.8
251	01/13-14-029-22W3/0	Avon Hill	Baytex	7/25/2017	51.477238	-108.999635	3.0	752.5	13.25	1030.9	32.22	0.45	0.42	2957.9
252	01/16-15-029-22W3/0	Avon Hill	Baytex	8/17/2017	51.480834	-109.006187	3.3	747.3	30.78	649.5	30.93	0.31	0.39	1697.5

253	02/16-15-029-22W3/0	Avon Hill	Baytex	8/21/2017	51.480834	-109.006547	3.3	746.7	17.91	633.7	30.18	0.33	0.38	1058.7
254	02/03-16-029-22W3/0	Avon Hill	Baytex	11/16/2017	51.476076	-109.023029	3.3	771.8	28.84	1142.7	38.09	0.25	0.31	2524.4
255	01/06-16-029-22W3/0	Avon Hill	Baytex	8/6/2017	51.479601	-109.024609	3.3	756.4	10.37	1039.5	33.53	0.44	0.45	3387.5
256	01/09-16-029-22W3/0	Avon Hill	Baytex	5/28/2017	51.49061	-109.029639	3.3	744.9	8.05	629	29.95	0.33	0.34	1806.6
257	02/09-16-029-22W3/0	Avon Hill	Baytex	5/25/2017	51.49061	-109.029999	3.3	745.3	19.57	617	30.85	0.29	0.32	1802.1
258	01/11-16-029-22W3/0	Avon Hill	Baytex	6/1/2017	51.490881	-109.041459	3.3	747.3	49.52	655.7	31.22	0.30	0.32	1311.9
259	02/11-16-029-22W3/0	Avon Hill	Baytex	6/1/2017	51.490657	-109.041459	3.3	746.2	27.00	636.7	33.51	0.27	0.33	1114.3
260	02/12-16-029-22W3/0	Avon Hill	Baytex	5/25/2017	51.490163	-109.047722	3.3	745.8	20.86	599.5	29.98	0.31	0.33	1644.4
261	01/10-17-029-22W3/0	Avon Hill	Teine	7/29/2017	51.483755	-109.048014	3.3	748.1	10.90	693.1	38.51	0.39	0.5	2602.6
262	02/08-18-029-22W3/0	Avon Hill	Baytex	1/3/2018	51.480832	-109.093888	2.5	738.9	17.53	1038.5	33.5	0.45	0.41	2556.8
263	01/16-18-029-22W3/0	Avon Hill	Baytex	1/16/2018	51.48037	-109.076267	2.5	735.2	14.36	624.5	32.87	0.36	0.31	1700.8
264	01/06-19-029-22W3/0	Avon Hill	Baytex	9/1/2017	51.495801	-109.098848	2.8	745.1	36.89	625.6	32.93	0.45	0.45	1911.1
265	02/07-19-029-22W3/0	Avon Hill	Baytex	3/10/2017	51.49552	-109.070645	2.8	738.3	23.72	621.1	34.51	0.43	0.46	1514.1
266	01/09-19-029-22W3/0	Avon Hill	Baytex	5/22/2017	51.50584	-109.078127	2.8	737.3	61.78	739.9	37	0.23	0.28	1157.7
267	02/09-19-029-22W3/0	Avon Hill	Baytex	5/22/2017	51.50584	-109.078487	2.8	738.5	59.89	633.5	30.17	0.34	0.35	1719.2
268	01/10-19-029-22W3/0	Avon Hill	Baytex	5/23/2017	51.505253	-109.082447	2.8	737.3	86.24	644.6	32.23	0.30	0.32	1165.5

269	01/12-19-029-22W3/0	Avon Hill	Baytex	9/1/2017	51.505551	-109.09459	2.8	748	38.61	664.9	33.25	0.30	0.37	1501.8
270	03/01-20-029-22W3/0	Avon Hill	Crescent	9/11/2016	51.490393	-109.069498	2.9	738.2	70.27	1036.3	34.54	0.41	0.44	2975.1
271	04/01-20-029-22W3/0	Avon Hill	Crescent	9/11/2016	51.490528	-109.069498	2.9	736.2	70.82	1040.7	34.69	0.40	0.38	3387.2
272	01/05-20-029-22W3/0	Avon Hill	Crescent	10/1/2016	51.487697	-109.070653	2.9	731.1	75.49	661.9	36.77	0.38	0.37	2243.1
273	02/05-20-029-22W3/0	Avon Hill	Crescent	10/1/2016	51.487697	-109.070437	2.9	733.1	65.43	668.1	37.12	0.38	0.45	2344.7
274	01/08-20-029-22W3/0	Avon Hill	Crescent	10/1/2016	51.495114	-109.069206	2.9	736.7	70.39	1019.8	33.99	0.40	0.42	2927.7
275	02/08-20-029-22W3/0	Avon Hill	Crescent	10/1/2016	51.495249	-109.069205	2.9	733.5	66.83	1015.8	33.86	0.40	0.38	3585.5
276	01/09-20-029-22W3/0	Avon Hill	Crescent	11/15/2016	51.497756	-109.064019	2.9	732.6	58.03	653.7	36.32	0.39	0.41	1714.9
277	02/09-20-029-22W3/0	Avon Hill	Crescent	11/15/2016	51.497621	-109.064019	2.9	735.2	60.49	615.7	34.21	0.40	0.4	1778.6
278	03/09-20-029-22W3/0	Avon Hill	Crescent	11/21/2016	51.501845	-109.064014	2.9	739.8	94.95	686.1	38.12	0.37	0.38	2009.6
279	01/12-20-029-22W3/0	Avon Hill	Crescent	11/18/2016	51.50177	-109.059885	2.9	736.2	122.16	612.2	34.01	0.41	0.42	1603.0
280	02/12-20-029-22W3/0	Avon Hill	Crescent	11/21/2016	51.49768	-109.059886	2.9	739.3	65.49	627.3	34.85	0.39	0.37	1725.5
281	03/12-20-029-22W3/0	Avon Hill	Crescent	11/21/2016	51.497815	-109.059886	2.9	737	75.11	619.2	34.4	0.42	0.42	1900.7
282	01/13-20-029-22W3/0	Avon Hill	Crescent	11/18/2016	51.502039	-109.059884	2.9	734.7	110.87	617.1	34.28	0.41	0.46	2003.4
283	02/13-20-029-22W3/0	Avon Hill	Crescent	11/18/2016	51.501905	-109.059885	2.9	735.9	120.16	616.1	34.23	0.41	0.45	1318.6
284	01/16-20-029-22W3/0	Avon Hill	Crescent	11/21/2016	51.502115	-109.064014	2.9	737.4	93.16	612.7	34.04	0.41	0.46	2072.7

285	02/16-20-029-22W3/0	Avon Hill	Crescent	11/21/2016	51.50198	-109.064014	2.9	736.5	83.87	640.2	35.57	0.39	0.43	2173.5
286	02/05-21-029-22W3/0	Avon Hill	Baytex	3/7/2017	51.488455	-109.046788	3.6	730.7	18.12	604.1	33.56	0.42	0.45	2240.7
287	01/12-21-029-22W3/0	Avon Hill	Baytex	3/9/2017	51.505262	-109.046992	3.6	737.5	22.52	639.6	35.53	0.34	0.4	1732.9
288	02/01-22-029-22W3/0	Avon Hill	Baytex	3/13/2017	51.497468	-109.007552	4.1	737.6	22.65	613.4	34.08	0.42	0.45	1797.9
289	92/05-24-029-22W3/0	Avon Hill	Baytex	5/7/2016	51.48808	-108.9765	4.2	742.3	17.63	637.6	30.36	0.33	0.42	2014.1
290	92/06-24-029-22W3/0	Avon Hill	Baytex	5/5/2016	51.488343	-108.970683	4.2	743.6	25.20	617.4	34.3	0.34	0.45	1650.4
291	92/07-24-029-22W3/0	Avon Hill	Baytex	5/5/2016	51.488247	-108.964984	4.2	746.7	25.78	611.1	33.95	0.39	0.49	1685.6
292	93/07-24-029-22W3/0	Avon Hill	Baytex	5/5/2016	51.488247	-108.965704	4.2	741.7	16.92	630.8	35.04	0.43	0.5	1924.8
293	92/08-24-029-22W3/0	Avon Hill	Baytex	5/2/2016	51.48824	-108.959729	4.2	745.9	24.59	627.7	29.89	0.33	0.42	1991.7
294	92/09-24-029-22W3/0	Avon Hill	Baytex	4/24/2016	51.505244	-108.960266	4.2	750.4	20.39	653.8	43.59	0.24	0.42	1425.0
295	91/10-24-029-22W3/0	Avon Hill	Baytex	4/24/2016	51.505249	-108.965263	4.2	741.6	33.51	636.5	35.36	0.41	0.48	1789.5
296	92/10-24-029-22W3/0	Avon Hill	Baytex	4/23/2016	51.505248	-108.964543	4.2	742.2	30.33	638.7	35.48	0.40	0.47	1770.4
297	93/10-24-029-22W3/0	Avon Hill	Baytex	4/23/2016	51.505248	-108.964903	4.2	739.8	33.00	650.9	43.39	0.35	0.51	1810.1
298	91/11-24-029-22W3/0	Avon Hill	Baytex	4/26/2016	51.505254	-108.971384	4.2	737.9	13.76	607.2	33.73	0.36	0.43	1701.9
299	92/11-24-029-22W3/0	Avon Hill	Baytex	4/25/2016	51.505253	-108.970664	4.2	739.3	13.90	638.6	30.41	0.32	0.39	1857.9
300	93/11-24-029-22W3/0	Avon Hill	Baytex	4/26/2016	51.505253	-108.971024	4.2	737.5	8.90	664.1	36.89	0.38	0.49	1876.5

301	91/12-24-029-22W3/0	Avon Hill	Baytex	5/3/2016	51.505258	-108.976656	4.2	735.6	15.81	633.6	35.2	0.37	0.48	1735.3
302	92/12-24-029-22W3/0	Avon Hill	Baytex	5/2/2016	51.505258	-108.977016	4.2	742.9	14.15	637.5	30.36	0.33	0.42	1984.0
303	01/01-25-029-22W3/0	Avon Hill	Teine	9/17/2017	51.506926	-108.970717	4.0	739.9	25.75	699.3	38.85	0.39	0.51	2063.6
304	02/01-25-029-22W3/0	Avon Hill	Teine	9/15/2017	51.507061	-108.970717	4.0	732.9	19.71	712.2	39.57	0.38	0.51	1755.3
305	01/04-25-029-22W3/0	Avon Hill	Teine	9/1/2017	51.507723	-108.96581	4.0	734.2	36.42	718.6	39.92	0.37	0.5	2274.6
306	02/04-25-029-22W3/0	Avon Hill	Teine	9/1/2017	51.507858	-108.965809	4.0	728.9	45.07	686.1	38.12	0.39	0.47	1917.0
307	01/05-25-029-22W3/0	Avon Hill	Teine	9/1/2017	51.507993	-108.965809	4.0	730.5	58.91	713.3	39.63	0.38	0.49	1900.0
308	02/05-25-029-22W3/0	Avon Hill	Teine	9/1/2017	51.508128	-108.965808	4.0	727.6	28.56	713.9	39.66	0.38	0.43	2189.9
309	01/08-25-029-22W3/0	Avon Hill	Teine	9/15/2017	51.509509	-108.970717	4.0	727.9	26.54	724.5	40.25	0.37	0.48	2265.5
310	02/08-25-029-22W3/0	Avon Hill	Teine	9/15/2017	51.509644	-108.970717	4.0	728.8	33.58	704.5	39.14	0.36	0.41	1374.0
311	01/09-25-029-22W3/0	Avon Hill	Teine	9/19/2017	51.514649	-108.970717	4.0	725.9	15.34	711.3	39.52	0.38	0.43	1892.6
312	02/09-25-029-22W3/0	Avon Hill	Teine	9/19/2017	51.514784	-108.970717	4.0	722.1	17.51	697.1	38.73	0.39	0.43	1905.1
313	01/12-25-029-22W3/0	Avon Hill	Teine	9/18/2017	51.512877	-108.966514	4.0	725.6	30.93	693.7	38.54	0.39	0.47	2556.8
314	02/12-25-029-22W3/0	Avon Hill	Teine	9/18/2017	51.513011	-108.966514	4.0	724.5	23.67	721.6	40.09	0.37	0.47	2300.3
315	01/13-25-029-22W3/0	Avon Hill	Teine	9/22/2017	51.516494	-108.966507	4.0	721.8	18.37	698.6	38.81	0.39	0.49	2367.4
316	02/13-25-029-22W3/0	Avon Hill	Teine	9/22/2017	51.516629	-108.966507	4.0	721.1	38.98	696.6	38.7	0.39	0.48	2413.0

317	01/16-25-029-22W3/0	Avon Hill	Teine	6/27/2017	51.515054	-108.970717	4.0	719.9	12.47	720.4	40.02	0.37	0.46	2290.7
318	02/16-25-029-22W3/0	Avon Hill	Teine	9/19/2017	51.514919	-108.970717	4.0	725.8	33.02	706.4	39.24	0.38	0.43	2307.5
319	02/14-26-029-22W3/0	Avon Hill	Teine	3/7/2016	51.516698	-109.004836	4.2	726.1	34.56	662.7	36.82	0.41	0.53	2401.7
320	02/15-26-029-22W3/0	Avon Hill	Nal	6/9/2016	51.510305	-108.988795	4.2	718	55.54	640.7	33.72	0.43	0.33	1902.7
321	03/15-26-029-22W3/0	Avon Hill	Nal	2/23/2017	51.510304	-108.988506	4.2	721.8	8.91	622.2	34.57	0.41	0.33	2511.8
322	01/16-26-029-22W3/0	Avon Hill	Nal	2/23/2017	51.509892	-108.982745	4.2	727.4	8.78	644.3	35.79	0.41	0.31	2311.8
323	01/01-28-029-22W3/0	Avon Hill	Crescent	12/6/2016	51.505946	-109.039361	4.4	736.7	71.36	568.4	31.58	0.44	0.42	1753.5
324	02/01-28-029-22W3/0	Avon Hill	Crescent	12/2/2016	51.505946	-109.039577	4.4	740.6	67.17	587.9	32.66	0.43	0.41	1908.1
325	91/13-28-029-22W3/0	Avon Hill	Crescent	2/1/2016	51.509937	-109.046081	4.4	731.4	262.90	694.3	38.57	0.36	0.4	1398.9
326	92/13-28-029-22W3/0	Avon Hill	Crescent	2/1/2016	51.509937	-109.045865	4.4	730.6	194.84	633.1	35.17	0.38	0.42	1624.9
327	01/14-28-029-22W3/0	Avon Hill	Crescent	2/9/2016	51.509941	-109.042991	4.4	730.7	263.53	629.5	34.97	0.38	0.41	1078.3
328	91/14-28-029-22W3/0	Avon Hill	Crescent	2/1/2016	51.509941	-109.042775	4.4	733.1	314.86	692.1	38.45	0.36	0.42	1606.8
329	02/15-28-029-22W3/0	Avon Hill	Crescent	11/27/2016	51.505951	-109.036055	4.4	733.5	185.54	1116.1	37.2	0.35	0.35	2023.5
330	03/15-28-029-22W3/0	Avon Hill	Crescent	12/2/2016	51.505958	-109.030798	4.4	734.3	172.35	1123.2	37.44	0.37	0.43	2416.5
331	04/15-28-029-22W3/0	Avon Hill	Crescent	11/27/2016	51.50595	-109.036271	4.4	734.3	180.86	1105.9	36.86	0.37	0.42	2156.6
332	01/16-28-029-22W3/0	Avon Hill	Crescent	12/2/2016	51.505958	-109.030582	4.4	735.2	218.00	1123.3	37.44	0.37	0.42	2162.0

333	02/16-28-029-22W3/0	Avon Hill	Crescent	12/2/2016	51.505958	-109.030366	4.4	737.1	156.11	1100.2	36.67	0.39	0.44	2394.7
334	92/01-29-029-22W3/0	Avon Hill	Crescent	2/23/2016	51.506722	-109.06401	4.4	736.8	44.16	628.7	34.93	0.40	0.42	1836.3
335	91/03-29-029-22W3/0	Avon Hill	Crescent	2/17/2016	51.512076	-109.064008	4.4	736.1	79.83	618.9	34.38	0.40	0.44	1527.7
336	92/04-29-029-22W3/0	Avon Hill	Crescent	2/27/2016	51.512179	-109.070633	4.4	739.5	127.64	571.5	31.75	0.45	0.45	1908.6
337	91/08-29-029-22W3/0	Avon Hill	Crescent	2/17/2016	51.506857	-109.06401	4.4	737	47.03	623	34.61	0.40	0.4	1760.8
338	92/08-29-029-22W3/0	Avon Hill	Crescent	2/23/2016	51.512346	-109.064008	4.4	734.1	195.25	695.5	38.64	0.34	0.41	1796.8
339	91/09-29-029-22W3/0	Avon Hill	Crescent	2/17/2016	51.512481	-109.064007	4.4	735.5	220.20	631.3	35.07	0.39	0.44	1503.7
340	92/09-29-029-22W3/0	Avon Hill	Crescent	3/1/2016	51.515676	-109.064006	4.4	734.2	218.45	688.7	38.26	0.37	0.43	1534.5
341	92/16-29-029-22W3/0	Avon Hill	Crescent	2/25/2016	51.515946	-109.064006	4.4	736.8	403.90	654	36.33	0.36	0.4	1073.0
342	91/01-30-029-22W3/0	Avon Hill	Crescent	3/1/2016	51.512589	-109.076613	4.2	741.9	155.15	634.6	35.26	0.39	0.45	1718.0
343	92/01-30-029-22W3/0	Avon Hill	Crescent	3/1/2016	51.512589	-109.076397	4.2	741.3	156.36	606.1	33.67	0.41	0.41	2056.8
344	01/02-30-029-22W3/0	Avon Hill	Crescent	8/18/2017	51.51258	-109.083887	4.2	742.7	171.11	633.5	35.19	0.39	0.4	1239.9
345	02/02-30-029-22W3/0	Avon Hill	Crescent	8/18/2017	51.51258	-109.083671	4.2	743.7	105.58	620.4	34.47	0.34	0.34	1126.6
346	01/03-30-029-22W3/0	Avon Hill	Crescent	6/12/2017	51.512568	-109.09243	4.2	740.2	166.02	658.5	36.58	0.37	0.4	956.5
347	02/03-30-029-22W3/0	Avon Hill	Crescent	6/12/2017	51.512569	-109.092214	4.2	741.8	178.40	616.7	34.26	0.41	0.43	1112.4
348	03/03-30-029-22W3/0	Avon Hill	Crescent	8/18/2017	51.512579	-109.084103	4.2	743	164.29	639.9	35.55	0.39	0.33	1318.1

349	01/04-30-029-22W3/0	Avon Hill	Crescent	6/19/2017	51.512568	-109.092862	4.2	738.4	477.03	631	35.06	0.35	0.32	937.4
350	02/04-30-029-22W3/0	Avon Hill	Crescent	6/12/2017	51.512568	-109.092646	4.2	738.6	297.04	614.5	34.14	0.40	0.37	1090.5
351	01/13-30-029-22W3/0	Avon Hill	Crescent	7/24/2017	51.509959	-109.092754	4.2	738.6	601.61	680.4	37.8	0.37	0.43	963.6
352	02/13-30-029-22W3/0	Avon Hill	Crescent	7/24/2017	51.509959	-109.092538	4.2	735.7	377.17	617.3	34.29	0.35	0.37	988.5
353	01/14-30-029-22W3/0	Avon Hill	Crescent	7/24/2017	51.509959	-109.092322	4.2	740.8	220.59	654.3	36.35	0.39	0.46	1379.9
354	02/14-30-029-22W3/0	Avon Hill	Crescent	8/2/2017	51.50997	-109.084427	4.2	739.8	276.60	724.3	40.24	0.34	0.37	1578.0
355	04/14-30-029-22W3/0	Avon Hill	Crescent	8/2/2017	51.50997	-109.084211	4.2	737.5	266.62	648.7	36.04	0.39	0.45	1445.1
356	01/15-30-029-22W3/0	Avon Hill	Crescent	8/2/2017	51.509971	-109.083995	4.2	741.3	351.59	616	34.22	0.41	0.47	1375.2
357	02/15-30-029-22W3/0	Avon Hill	Crescent	8/2/2017	51.509971	-109.083779	4.2	740.7	335.88	693.9	38.55	0.38	0.47	1414.5
358	91/16-30-029-22W3/0	Avon Hill	Crescent	3/1/2016	51.509976	-109.075245	4.2	739.6	210.45	616.3	34.24	0.40	0.47	1467.7
359	92/16-30-029-22W3/0	Avon Hill	Crescent	3/1/2016	51.509976	-109.075461	4.2	738.6	186.98	680.4	37.8	0.33	0.37	1521.7
360	01/03-34-029-22W3/0	Avon Hill	Crescent	2/11/2018	51.534016	-109.016075	4.5	739.4	160.80	1451.5	33.76	0.41	0.41	2029.7
361	03/01-35-029-22W3/0	Avon Hill	Teine	7/30/2017	51.526473	-108.983561	4.5	716.4	11.90	731.7	40.65	0.36	0.49	2798.5
362	05/02-35-029-22W3/0	Avon Hill	Teine	8/1/2017	51.52648	-108.988674	4.5	721.4	36.82	687.9	38.22	0.35	0.38	2270.4
363	01/04-35-029-22W3/0	Avon Hill	Teine	8/10/2017	51.527619	-108.999014	4.5	731.3	25.71	709.3	39.41	0.38	0.48	2307.0
364	02/04-35-029-22W3/0	Avon Hill	Teine	8/14/2017	51.527619	-108.99923	4.5	726.9	21.62	726.9	42.76	0.35	0.48	2376.1

365	01/12-35-029-22W3/0	Avon Hill	Teine	7/9/2016	51.534746	-108.998348	4.5	737	37.07	684.5	38.03	0.39	0.51	2909.7
366	03/12-35-029-22W3/0	Avon Hill	Teine	8/13/2017	51.534746	-108.998131	4.5	735.5	14.23	693.5	38.53	0.39	0.52	2482.5
367	03/15-35-029-22W3/0	Avon Hill	Teine	8/3/2017	51.524215	-108.988687	4.5	723.2	23.41	718.6	42.27	0.35	0.47	2540.4
368	04/15-35-029-22W3/0	Avon Hill	Teine	8/3/2017	51.524216	-108.98847	4.5	720.9	24.42	705	41.47	0.36	0.48	2732.7
369	01/16-35-029-22W3/0	Avon Hill	Teine	7/17/2016	51.524218	-108.983789	4.5	716.9	44.76	683.1	37.95	0.31	0.32	2460.1
370	03/16-35-029-22W3/0	Avon Hill	Teine	8/1/2017	51.524218	-108.983573	4.5	717	33.58	712.8	39.6	0.38	0.5	2543.0
371	91/16-19-029-24W3/0	Whitesi de	Baytex	2/5/2016	51.502233	-109.369686	6.5	717.9	652.01	686.3	38.13	0.38	0.47	892.8
372	91/09-21-029-24W3/0	Whitesi de	Baytex	9/4/2016	51.505724	-109.3117	4.8	713.1	338.21	690	38.33	0.38	0.44	1468.9
373	01/10-21-029-24W3/0	Whitesi de	Baytex	9/20/2016	51.504998	-109.316741	4.8	713.9	270.66	617.2	34.29	0.35	0.37	1053.0
374	01/11-21-029-24W3/0	Whitesi de	Baytex	9/4/2016	51.504989	-109.322543	4.8	725.9	300.49	633.4	37.26	0.39	0.46	1063.1
375	01/12-21-029-24W3/0	Whitesi de	Baytex	9/4/2016	51.505204	-109.328664	4.8	723.9	219.20	632.2	35.12	0.39	0.44	1387.3
376	91/12-21-029-24W3/0	Whitesi de	Baytex	1/14/2016	51.505204	-109.329024	4.8	728.7	136.83	617.9	34.33	0.34	0.39	1643.5
377	01/02-28-029-24W3/0	Whitesi de	Whiteca p	8/24/2017	51.512389	-109.317064	5.9	716.2	424.40	621.4	34.52	0.38	0.39	2047.7
378	01/03-28-029-24W3/0	Whitesi de	Whiteca p	1/21/2017	51.512385	-109.32295	5.9	721.3	274.60	634.6	35.26	0.37	0.37	2191.6
379	01/04-29-029-24W3/0	Whitesi de	Whiteca p	8/9/2017	51.506309	-109.329097	5.8	721.8	607.09	1495.8	34	0.38	0.39	1705.1
380	02/04-29-029-24W3/0	Whitesi de	Whiteca p	8/9/2017	51.506534	-109.329097	5.8	726.2	371.16	1419.5	32.26	0.40	0.38	1996.0

381	01/01-30-029-24W3/0	Whitesi de	Baytex	1/6/2017	51.505308	-109.37099	6.1	718.6	175.70	676.3	37.57	0.37	0.37	1483.4
382	91/01-30-029-24W3/0	Whitesi de	Baytex	1/10/2016	51.505533	-109.370989	6.1	722	512.12	729.5	40.53	0.33	0.41	789.5
383	01/04-30-029-24W3/0	Whitesi de	Baytex	1/7/2017	51.51317	-109.37589	6.1	719.2	162.61	680.6	37.81	0.37	0.41	2069.9
384	02/04-30-029-24W3/0	Whitesi de	Baytex	1/7/2017	51.513169	-109.37553	6.1	718.9	123.21	721.9	40.11	0.36	0.42	2139.5
385	01/08-30-029-24W3/0	Whitesi de	Baytex	1/6/2017	51.508523	-109.370914	6.1	722.3	250.26	633.8	35.21	0.42	0.41	1685.8
386	91/08-30-029-24W3/0	Whitesi de	Baytex	1/13/2016	51.508747	-109.370913	6.1	724.5	133.55	671.4	37.3	0.40	0.46	2135.9
387	01/02-31-029-24W3/0	Whitesi de	Whiteca p	2/4/2017	51.526757	-109.360363	6.2	720.5	262.55	613.6	34.09	0.35	0.35	3491.5
388	01/11-32-029-24W3/0	Whitesi de	Whiteca p	12/15/2016	51.526891	-109.361084	5.7	719.6	320.90	952.7	32.85	0.40	0.4	3449.1
389	03/11-32-029-24W3/0	Whitesi de	Whiteca p	12/15/2016	51.526621	-109.361084	5.7	718.5	323.18	873.8	32.36	0.42	0.4	3104.0
390	01/04-34-029-24W3/0	Whitesi de	Baytex	1/9/2017	51.520624	-109.295497	5.4	706.6	156.54	594.6	33.03	0.45	0.43	1616.9
391	01/05-34-029-24W3/0	Whitesi de	Baytex	1/8/2017	51.52377	-109.29549	5.4	708	175.72	592.4	32.91	0.32	0.34	1601.1
392	91/11-34-029-24W3/0	Whitesi de	Baytex	1/13/2016	51.527599	-109.309531	5.4	715.4	165.77	599.1	33.28	0.44	0.44	1910.2
393	92/11-34-029-24W3/0	Whitesi de	Baytex	1/16/2016	51.527374	-109.30953	5.4	714.5	137.30	622.1	34.56	0.43	0.45	2453.5
394	01/12-21-029-25W3/0	Whitesi de	Whiteca p	6/4/2017	51.499229	-109.446196	2.0	745	439.01	1444	32.82	0.38	0.31	3097.8
395	01/01-23-029-25W3/0	Whitesi de	Teine	7/29/2017	51.491132	-109.42792	2.0	718.2	29.56	1483.5	35.32	0.34	0.37	885.5
396	01/05-26-029-25W3/0	Whitesi de	Teine	6/29/2017	51.501826	-109.420127	5.3	710.5	18.49	722.4	40.13	0.50	0.55	1514.6

397	01/06-26-029-25W3/0	Whitesi de	Teine	6/29/2017	51.501826	-109.419911	5.3	713.2	14.29	716	39.78	0.48	0.53	1958.5
398	92/10-26-029-25W3/0	Whitesi de	Baytex	1/9/2016	51.512666	-109.400136	5.3	707.1	81.18	611.7	33.98	0.41	0.41	2375.7
399	02/11-26-029-25W3/0	Whitesi de	Teine	6/28/2017	51.513004	-109.426237	5.3	722.2	15.34	685.7	40.34	0.36	0.49	1728.3
400	02/14-26-029-25W3/0	Whitesi de	Teine	6/28/2017	51.516554	-109.426227	5.3	722	13.11	685.7	40.34	0.37	0.5	1983.0
401	92/15-26-029-25W3/0	Whitesi de	Baytex	1/7/2016	51.516531	-109.400131	5.3	709.3	98.83	625.9	34.77	0.41	0.45	2209.1
402	01/01-27-029-25W3/0	Whitesi de	Whiteca p	10/31/2016	51.506459	-109.451235	5.2	726	188.52	1434.3	32.6	0.38	0.3	4875.2
403	01/08-27-029-25W3/0	Whitesi de	Whiteca p	10/31/2016	51.506594	-109.451234	5.2	728	100.14	1429.2	32.48	0.40	0.35	4386.5
404	01/09-27-029-25W3/0	Whitesi de	Whiteca p	7/30/2017	51.520142	-109.427946	5.2	724.3	271.83	622.5	34.58	0.38	0.4	2791.9
405	01/16-27-029-25W3/0	Whitesi de	Whiteca p	2/15/2017	51.516627	-109.447737	5.2	726.1	278.26	1095.5	31.3	0.42	0.38	4497.5
406	01/12-28-029-25W3/0	Whitesi de	Whiteca p	7/4/2017	51.513916	-109.446029	5.2	734	309.84	1430.5	32.51	0.39	0.37	4348.5
407	01/16-31-029-25W3/0	Whitesi de	Whiteca p	10/2/2016	51.524712	-109.500213	6.7	733.5	998.74	623.8	34.66	0.37	0.37	1064.7
408	02/01-32-029-25W3/0	Whitesi de	Whiteca p	2/15/2017	51.522344	-109.486529	6.0	752.2	255.92	654.1	36.34	0.36	0.41	2391.2
409	01/08-32-029-25W3/0	Whitesi de	Whiteca p	9/20/2016	51.52704	-109.486014	6.0	730	193.90	637.9	35.44	0.37	0.39	1378.3
410	01/09-32-029-25W3/0	Whitesi de	Whiteca p	9/21/2016	51.527175	-109.486014	6.0	737.9	210.97	646.1	35.89	0.36	0.41	1783.6
411	92/07-33-029-25W3/0	Whitesi de	Whiteca p	9/3/2016	51.524045	-109.446556	5.9	729.5	394.63	617.5	34.31	0.37	0.33	3417.9
412	01/14-33-029-25W3/0	Whitesi de	Whiteca p	8/8/2017	51.531575	-109.473547	5.9	731.9	406.68	651	36.17	0.35	0.44	1588.5

413	91/15-33-029-25W3/0	Whitesi de	Whiteca p	2/6/2016	51.523872	-109.4564	5.9	728.4	313.96	627.9	34.88	0.36	0.42	3374.7
414	92/15-33-029-25W3/0	Whitesi de	Whiteca p	2/7/2016	51.523764	-109.456716	5.9	730	311.30	631.8	35.1	0.37	0.39	3310.8
415	93/15-33-029-25W3/0	Whitesi de	Whiteca p	2/8/2016	51.523658	-109.457032	5.9	731.6	343.56	626	34.78	0.37	0.39	3247.0
416	02/08-34-029-25W3/0	Whitesi de	Whiteca p	7/9/2017	51.524371	-109.439639	5.8	725.5	327.17	646.3	35.91	0.35	0.46	3016.4
417	03/08-34-029-25W3/0	Whitesi de	Whiteca p	7/10/2017	51.520956	-109.439076	5.8	726.4	546.09	611.5	33.97	0.38	0.4	2961.6
418	01/15-34-029-25W3/0	Whitesi de	Whiteca p	1/26/2018	51.52384	-109.433987	5.8	726.4	308.99	684.7	38.04	0.34	0.41	3065.4
419	02/07-35-029-25W3/0	Whitesi de	Whiteca p	9/5/2016	51.523401	-109.427361	5.7	718.3	360.86	1104.2	31.55	0.41	0.34	5574.2
420	01/10-35-029-25W3/0	Whitesi de	Whiteca p	3/12/2017	51.529027	-109.427706	5.7	719.8	284.80	1123.9	32.11	0.41	0.39	7023.4
421	02/10-35-029-25W3/0	Whitesi de	Whiteca p	3/12/2017	51.528757	-109.427706	5.7	719.4	296.43	1147.7	32.79	0.38	0.38	5270.5
422	03/10-35-029-25W3/0	Whitesi de	Whiteca p	3/11/2017	51.528488	-109.427707	5.7	715.9	392.32	1148.4	32.81	0.35	0.34	5382.4
423	91/16-35-029-25W3/0	Whitesi de	Whiteca p	1/22/2016	51.524577	-109.399343	5.7	700.9	376.93	680.1	37.78	0.34	0.36	3137.2
424	03/05-36-029-25W3/0	Whitesi de	Whiteca p	1/30/2017	51.523932	-109.381478	5.5	716.6	307.98	838	41.9	0.31	0.41	3113.8
425	04/05-36-029-25W3/0	Whitesi de	Whiteca p	1/30/2017	51.523798	-109.381478	5.5	718.9	342.87	841.9	42.1	0.31	0.38	2843.7
426	01/02-24-029-26W3/0	Whitesi de	Novus	6/20/2017	51.490475	-109.517053	2.6	781.1	22.33	650.7	29.58	0.44	0.34	483.3
427	02/11-24-029-26W3/0	Whitesi de	Novus	6/1/2017	51.501126	-109.544782	2.6	778.4	45.19	722.7	32.85	0.41	0.36	1107.5
428	02/14-24-029-26W3/0	Whitesi de	Novus	6/1/2017	51.501306	-109.544782	2.6	777	41.22	670.6	30.48	0.43	0.36	1195.5

429	02/06-25-029-26W3/0	Whitesi de	Novus	8/27/2017	51.502175	-109.534613	2.8	806	144.45	716.3	32.56	0.38	0.33	1207.6
430	02/12-26-029-26W3/0	Whitesi de	Novus	5/25/2017	51.502893	-109.564387	3.4	776.3	9.37	766.6	34.85	0.37	0.39	2494.5
431	01/03-27-029-26W3/0	Whitesi de	Novus	7/8/2017	51.509829	-109.591376	5.5	775.9	10.06	704.3	32.01	0.41	0.33	2342.7
432	01/14-27-029-26W3/0	Whitesi de	Novus	7/31/2017	51.516672	-109.591702	5.5	770	9.18	625	28.41	0.46	0.36	1417.2
433	01/10-28-029-26W3/0	Whitesi de	Novus	8/2/2017	51.515391	-109.58753	4.3	771.4	17.62	650.3	29.56	0.44	0.38	2927.6
434	01/15-28-029-26W3/0	Whitesi de	Novus	8/2/2017	51.515526	-109.58753	4.3	771.9	15.72	640.8	29.13	0.45	0.37	1740.6
435	01/05-32-029-26W3/0	Whitesi de	Novus	7/7/2017	51.526368	-109.622001	4.1	765.8	164.01	662.1	30.1	0.43	0.3	2720.9
436	01/14-32-029-26W3/0	Whitesi de	Novus	8/25/2017	51.532025	-109.638039	4.1	765.5	57.04	627.9	28.54	0.46	0.35	2487.9
437	01/03-33-029-26W3/0	Whitesi de	Novus	8/3/2017	51.526748	-109.606647	4.1	780.5	101.01	642.2	29.19	0.44	0.3	2408.3
438	01/02-35-029-26W3/0	Whitesi de	Novus	12/14/2016	51.527286	-109.548587	4.3	765.5	51.24	706.8	32.13	0.40	0.42	3126.8
439	02/02-35-029-26W3/0	Whitesi de	Novus	8/26/2017	51.527286	-109.548298	4.3	780.1	58.17	651.6	29.62	0.42	0.32	2760.8
440	01/16-02-030-19W3/0	Dodsla nd	Baytex	9/1/2016	51.545276	-108.583499	1.5	763.6	2.49	1444.8	46.61	0.29	0.42	380.1
441	01/02-07-030-19W3/0	Dodsla nd	Teine	6/18/2016	51.54917	-108.670906	3.2	749.7	186.49	674.3	37.46	0.36	0.47	706.3
442	01/09-07-030-19W3/0	Dodsla nd	Teine	6/24/2016	51.563486	-108.65463	3.2	748	19.80	706.2	39.23	0.38	0.54	1713.0
443	01/12-07-030-19W3/0	Dodsla nd	Teine	6/16/2016	51.563599	-108.672045	3.2	756.6	25.88	721.4	40.08	0.36	0.47	1931.7
444	01/01-08-030-19W3/0	Dodsla nd	Baytex	12/2/2016	51.55036	-108.653807	3.1	743.8	6.18	1487.2	33.05	0.38	0.41	1638.0

445	01/14-13-030-19W3/0	Dodsland	Baytex	12/1/2016	51.573924	-108.532375	2.4	762.9	2.48	1092.9	32.14	0.39	0.42	1782.4
446	01/10-14-030-19W3/0	Dodsland	Baytex	7/15/2017	51.577785	-108.567571	3.0	783.5	2.24	651	36.17	0.35	0.41	1665.6
447	01/13-14-030-19W3/0	Dodsland	Baytex	7/15/2017	51.567993	-108.578069	3.0	786.9	1.86	618.5	34.36	0.36	0.4	1745.7
448	01/04-15-030-19W3/0	Dodsland	Baytex	7/15/2017	51.56365	-108.586508	2.9	769.5	2.87	863.1	33.2	0.37	0.4	1097.3
449	01/05-15-030-19W3/0	Dodsland	Baytex	7/14/2017	51.56774	-108.586507	2.9	774.1	3.08	888.3	34.17	0.37	0.37	1180.5
450	01/08-15-030-19W3/0	Dodsland	Baytex	11/8/2016	51.560633	-108.584203	2.9	774.7	1.40	637.1	35.39	0.37	0.42	898.1
451	01/12-15-030-19W3/0	Dodsland	Baytex	2/13/2016	51.577852	-108.601878	2.9	744.3	5.37	642.6	35.7	0.42	0.52	1724.1
452	01/01-16-030-19W3/0	Dodsland	Baytex	11/13/2017	51.563642	-108.62446	3.3	744.1	8.32	1022.5	31.95	0.39	0.4	1539.9
453	01/08-16-030-19W3/0	Dodsland	Baytex	11/12/2017	51.567685	-108.623737	3.3	744.4	4.02	1006.4	31.45	0.40	0.42	1680.6
454	01/13-18-030-19W3/0	Dodsland	Baytex	7/22/2017	51.560857	-108.672192	4.2	747.3	1.34	1437.8	31.95	0.39	0.37	3370.7
455	01/16-19-030-19W3/0	Dodsland	Baytex	7/3/2016	51.582991	-108.654624	3.0	734.5	13.27	659.1	36.62	0.41	0.46	2163.5
456	01/01-21-030-19W3/0	Dodsland	Teine	6/20/2016	51.578416	-108.617945	3.0	740	79.92	673.2	37.4	0.40	0.5	2051.6
457	01/04-21-030-19W3/0	Dodsland	Teine	6/21/2016	51.578406	-108.614285	3.0	743	46.67	670.4	37.24	0.38	0.47	1145.9
458	01/01-22-030-19W3/0	Dodsland	Teine	6/14/2016	51.578777	-108.59574	2.8	749.8	89.18	721.8	40.1	0.37	0.49	1561.5
459	01/03-27-030-19W3/0	Dodsland	Teine	6/30/2016	51.593255	-108.606712	3.2	735.8	58.57	660.5	36.69	0.40	0.5	2329.8
460	01/03-28-030-19W3/0	Dodsland	Crescent	9/22/2017	51.593328	-108.636419	3.8	730.2	107.52	1094.2	25.45	0.53	0.34	3456.4

461	02/03-28-030-19W3/0	Dodsland	Crescent	9/22/2017	51.593193	-108.636419	3.8	726.5	112.66	1133.3	37.78	0.37	0.44	3252.9
462	02/06-28-030-19W3/0	Dodsland	Crescent	9/21/2017	51.596343	-108.630363	3.8	728.6	104.92	683.8	37.99	0.37	0.47	1966.8
463	03/11-28-030-19W3/0	Dodsland	Crescent	9/18/2017	51.599384	-108.635634	3.8	732.1	102.59	1103.6	36.79	0.35	0.4	2307.4
464	04/11-28-030-19W3/0	Dodsland	Crescent	9/18/2017	51.599249	-108.635634	3.8	731.7	104.72	1073.6	35.79	0.39	0.46	3356.8
465	01/12-29-030-19W3/0	Dodsland	Crescent	9/13/2017	51.601263	-108.631957	3.6	725.4	105.77	1132.1	37.74	0.36	0.36	3384.4
466	03/12-29-030-19W3/0	Dodsland	Crescent	9/13/2017	51.600993	-108.631956	3.6	733.5	102.76	1141.3	38.04	0.35	0.3	1792.8
467	04/12-29-030-19W3/0	Dodsland	Crescent	9/13/2017	51.601128	-108.631956	3.6	728.7	105.91	1117.6	37.25	0.39	0.34	3276.5
468	01/13-29-030-19W3/0	Dodsland	Crescent	8/19/2017	51.603819	-108.629867	3.6	726.6	101.52	1140.1	38	0.38	0.4	2762.2
469	02/13-29-030-19W3/0	Dodsland	Crescent	8/19/2017	51.603684	-108.629867	3.6	727.8	102.76	1133.6	37.79	0.37	0.42	3077.5
470	01/01-30-030-19W3/0	Dodsland	Crescent	10/1/2016	51.593393	-108.666098	3.6	737.1	94.97	618.6	34.37	0.40	0.45	2051.1
471	02/01-30-030-19W3/0	Dodsland	Crescent	10/1/2016	51.593258	-108.666098	3.6	736.2	94.93	728.5	40.47	0.35	0.45	2468.9
472	01/04-30-030-19W3/0	Dodsland	Crescent	9/15/2016	51.592611	-108.660647	3.6	743.9	95.05	685.4	38.08	0.37	0.46	1845.0
473	02/04-30-030-19W3/0	Dodsland	Crescent	9/15/2016	51.592476	-108.660647	3.6	743	95.19	670.4	37.24	0.38	0.47	971.8
474	01/05-30-030-19W3/0	Dodsland	Crescent	11/3/2016	51.596656	-108.660647	3.6	745.6	95.01	648.7	36.04	0.39	0.45	1642.1
475	02/05-30-030-19W3/0	Dodsland	Crescent	11/3/2016	51.596926	-108.660647	3.6	739.4	95.08	639.9	35.55	0.39	0.45	1205.6
476	03/05-30-030-19W3/0	Dodsland	Crescent	11/3/2016	51.596791	-108.660647	3.6	745.8	94.90	611.6	33.98	0.41	0.48	1409.5

477	01/08-30-030-19W3/0	Dodsland	Crescent	11/5/2016	51.596786	-108.666094	3.6	739.9	94.93	637.6	35.42	0.40	0.39	2561.2
478	02/08-30-030-19W3/0	Dodsland	Crescent	11/5/2016	51.597056	-108.666093	3.6	737.9	94.97	608.9	33.83	0.40	0.44	2074.4
479	03/08-30-030-19W3/0	Dodsland	Crescent	11/5/2016	51.596921	-108.666093	3.6	739.7	94.96	627.7	34.87	0.40	0.41	2458.1
480	01/12-30-030-19W3/0	Dodsland	Crescent	11/23/2016	51.600297	-108.660646	3.6	732.9	95.01	663.8	36.88	0.38	0.43	2097.0
481	02/12-30-030-19W3/0	Dodsland	Crescent	11/23/2016	51.600567	-108.660646	3.6	726.9	94.95	697.4	38.74	0.35	0.45	2710.9
482	03/12-30-030-19W3/0	Dodsland	Crescent	11/23/2016	51.600432	-108.660646	3.6	729.5	95.03	637.1	35.39	0.38	0.46	2287.7
483	01/13-30-030-19W3/0	Dodsland	Crescent	11/16/2016	51.603938	-108.660646	3.6	730.4	94.92	617.8	34.32	0.41	0.44	2461.3
484	02/13-30-030-19W3/0	Dodsland	Crescent	11/16/2016	51.604073	-108.660646	3.6	729.2	95.00	609.9	33.88	0.41	0.45	2193.6
485	01/14-34-030-19W3/0	Dodsland	Crescent	12/14/2017	51.604344	-108.592191	3.4	747.4	128.37	1435.4	33.38	0.41	0.39	3932.1
486	91/01-01-030-20W3/0	Dodsland	Novus	8/22/2014	51.536575	-108.696363	3.5	773.5	346.95	910.6	50.59	0.26	0.38	685.0
487	91/08-01-030-20W3/0	Dodsland	Novus	8/22/2014	51.536755	-108.696363	3.5	770.6	522.27	910.3	50.57	0.27	0.4	376.3
488	92/16-01-030-20W3/0	Dodsland	Novus	8/15/2014	51.544715	-108.696039	3.5	747.2	93.32	910.5	50.58	0.27	0.42	2093.7
489	91/01-03-030-20W3/0	Dodsland	Novus	8/2/2014	51.536573	-108.74324	4.6	740.1	312.90	923	54.29	0.26	0.45	353.9
490	91/08-03-030-20W3/0	Dodsland	Novus	8/3/2014	51.536753	-108.743239	4.6	742	408.51	923.4	51.3	0.27	0.42	382.0
491	91/09-03-030-20W3/0	Dodsland	Novus	7/24/2014	51.543825	-108.743226	4.6	740.3	394.92	918.4	57.4	0.23	0.41	461.4
492	91/16-03-030-20W3/0	Dodsland	Novus	7/23/2014	51.544005	-108.743226	4.6	738.3	436.78	936.7	52.04	0.24	0.42	418.7

493	01/03-11-030-20W3/0	Dodsland	Crescent	11/4/2017	51.563449	-108.712387	4.0	732.1	85.61	1434	33.35	0.41	0.38	3035.7
494	01/08-11-030-20W3/0	Dodsland	Crescent	8/18/2016	51.563517	-108.70145	4.0	736.1	4.05	1031.8	32.24	0.37	0.37	3234.5
495	91/01-13-030-20W3/0	Dodsland	Novus	2/16/2014	51.565248	-108.689333	4.5	747	117.27	646.3	46.16	0.28	0.42	1493.3
496	91/06-13-030-20W3/0	Dodsland	Novus	9/10/2013	51.570291	-108.700432	4.5	726.5	57.08	707.1	50.51	0.27	0.48	1223.9
497	92/06-13-030-20W3/0	Dodsland	Novus	2/25/2014	51.565876	-108.700799	4.5	736.4	94.19	683.9	48.85	0.28	0.4	942.3
498	91/08-13-030-20W3/0	Dodsland	Novus	2/15/2014	51.565428	-108.689333	4.5	747.9	174.86	662.4	47.31	0.30	0.4	967.6
499	01/04-14-030-20W3/0	Dodsland	Teine	2/19/2017	51.564607	-108.696256	4.2	747	39.31	1340.6	36.23	0.41	0.47	2797.9
500	02/04-14-030-20W3/0	Dodsland	Teine	2/22/2017	51.564741	-108.696256	4.2	745	45.54	1337.4	36.15	0.42	0.47	2976.2
501	01/05-14-030-20W3/0	Dodsland	Teine	2/13/2017	51.567504	-108.696252	4.2	736.4	12.61	1339.2	34.34	0.43	0.47	2865.0
502	02/05-14-030-20W3/0	Dodsland	Teine	2/18/2017	51.567639	-108.696252	4.2	736.8	13.14	1332.6	37.02	0.40	0.48	3029.4
503	03/01-16-030-20W3/0	Dodsland	Crescent	12/16/2016	51.563891	-108.758579	5.4	716.4	94.97	611.2	33.96	0.41	0.44	1905.2
504	04/01-16-030-20W3/0	Dodsland	Crescent	12/16/2016	51.564026	-108.758579	5.4	715	94.95	587.3	32.63	0.43	0.43	1765.8
505	03/04-16-030-20W3/0	Dodsland	Crescent	12/21/2016	51.563965	-108.75565	5.4	717.2	94.99	608.2	33.79	0.41	0.47	2057.2
506	04/04-16-030-20W3/0	Dodsland	Crescent	12/21/2016	51.5641	-108.75565	5.4	713.8	95.08	592.2	32.9	0.43	0.47	2061.5
507	03/05-16-030-20W3/0	Dodsland	Crescent	12/14/2016	51.568526	-108.755659	5.4	711.1	95.03	586.1	32.56	0.43	0.44	1950.7
508	02/08-16-030-20W3/0	Dodsland	Crescent	12/16/2016	51.564161	-108.758579	5.4	715.1	94.90	613.3	34.07	0.41	0.38	1643.1

509	91/08-16-030-20W3/0	Dodsland	Crescent	12/19/2016	51.568453	-108.758576	5.4	715	94.90	602	33.44	0.42	0.45	1646.9
510	01/09-16-030-20W3/0	Dodsland	Crescent	12/16/2016	51.573692	-108.758574	5.4	719.5	95.03	717.8	39.88	0.35	0.44	1935.2
511	91/09-16-030-20W3/0	Dodsland	Crescent	12/19/2016	51.568587	-108.758576	5.4	716.2	94.87	598.7	33.26	0.41	0.4	1856.8
512	02/12-16-030-20W3/0	Dodsland	Crescent	12/14/2016	51.570174	-108.755662	5.4	711	94.86	581.2	32.29	0.43	0.47	1647.2
513	03/12-16-030-20W3/0	Dodsland	Crescent	12/16/2016	51.573769	-108.755669	5.4	714.3	94.97	620.6	34.48	0.40	0.43	1712.4
514	02/02-18-030-20W3/0	Dodsland	Baytex	8/2/2017	51.570983	-108.803538	5.3	693.8	54.04	637.8	35.43	0.42	0.45	2145.1
515	03/02-18-030-20W3/0	Dodsland	Baytex	8/6/2017	51.570974	-108.797624	5.3	702.2	27.78	674.5	37.47	0.40	0.45	2501.6
516	01/03-18-030-20W3/0	Dodsland	Baytex	8/3/2017	51.570983	-108.803898	5.3	696.3	44.62	653	36.28	0.41	0.44	2070.1
517	01/08-20-030-20W3/0	Dodsland	Crescent	1/6/2017	51.581389	-108.794161	5.8	697.7	47.05	1475.3	32.78	0.42	0.42	5204.9
518	02/15-30-030-20W3/0	Dodsland	Baytex	1/19/2017	51.597513	-108.801361	4.9	699.2	27.69	614.3	34.13	0.44	0.44	2922.7
519	01/13-01-030-21W3/0	Dodsland	Crescent	12/1/2016	51.531559	-108.836903	4.0	707.8	94.96	1434.4	36.78	0.37	0.38	2317.9
520	01/05-05-030-21W3/0	Avon Hill	Teine	11/15/2016	51.531617	-108.928574	4.3	696.5	68.60	707.9	41.64	0.37	0.47	2593.6
521	02/05-05-030-21W3/0	Avon Hill	Teine	11/14/2016	51.531617	-108.928358	4.3	701	51.18	699.7	38.87	0.35	0.43	1727.1
522	01/06-05-030-21W3/0	Avon Hill	Teine	9/8/2016	51.531336	-108.92051	4.3	696.9	82.63	706.2	39.23	0.38	0.49	2040.0
523	02/06-05-030-21W3/0	Avon Hill	Teine	11/15/2016	51.531616	-108.928142	4.3	696.7	40.41	702.8	41.34	0.36	0.47	2057.5
524	01/07-05-030-21W3/0	Avon Hill	Teine	9/9/2016	51.531335	-108.920294	4.3	696.5	93.79	676.6	39.8	0.38	0.53	1952.1

525	03/07-05-030-21W3/0	Avon Hill	Teine	8/30/2016	51.531596	-108.914342	4.3	694.7	95.99	698.9	38.83	0.36	0.42	1427.4
526	01/08-05-030-21W3/0	Avon Hill	Teine	8/29/2016	51.531596	-108.914125	4.3	700	85.34	703.2	41.36	0.36	0.43	1787.7
527	02/08-05-030-21W3/0	Avon Hill	Teine	8/28/2016	51.531596	-108.91391	4.3	696.1	92.77	711.1	39.51	0.37	0.46	1561.2
528	01/12-05-030-21W3/0	Avon Hill	Teine	9/13/2016	51.549104	-108.934191	4.3	693	42.71	723.2	40.18	0.37	0.5	1902.7
529	01/13-05-030-21W3/0	Avon Hill	Teine	11/19/2016	51.538572	-108.92515	4.3	696.3	37.66	714.9	42.05	0.33	0.43	2199.6
530	01/14-05-030-21W3/0	Avon Hill	Teine	11/20/2016	51.538707	-108.92515	4.3	702	38.38	700	38.89	0.38	0.47	2328.1
531	02/14-05-030-21W3/0	Avon Hill	Teine	11/19/2016	51.538842	-108.92515	4.3	705.3	38.16	694.4	40.85	0.37	0.49	2055.4
532	01/15-05-030-21W3/0	Avon Hill	Teine	8/23/2016	51.538933	-108.918268	4.3	705.5	38.52	697.6	41.04	0.32	0.46	1724.5
533	02/15-05-030-21W3/0	Avon Hill	Teine	8/22/2016	51.538933	-108.918052	4.3	706.1	47.45	692.4	38.47	0.39	0.48	2532.2
534	01/16-05-030-21W3/0	Avon Hill	Teine	8/3/2016	51.53893	-108.913463	4.3	705.8	61.32	687.8	38.21	0.35	0.44	2176.7
535	01/09-07-030-21W3/0	Avon Hill	Teine	7/28/2016	51.556741	-108.948402	4.6	696.1	62.69	722.8	40.16	0.36	0.48	2241.2
536	01/11-07-030-21W3/0	Avon Hill	Teine	1/17/2018	51.556317	-108.95749	4.6	706	34.66	706.9	39.27	0.35	0.45	1962.8
537	02/11-07-030-21W3/0	Avon Hill	Teine	1/22/2018	51.556452	-108.95749	4.6	708.2	34.44	708.7	37.3	0.40	0.5	2844.5
538	91/11-07-030-21W3/0	Avon Hill	Teine	3/4/2016	51.556722	-108.95749	4.6	703	39.74	679.7	37.76	0.39	0.53	3266.5
539	03/01-13-030-21W3/0	Dodsland	Baytex	7/17/2017	51.576027	-108.819005	4.7	689.3	31.27	1159.1	38.64	0.36	0.44	3610.5
540	02/02-13-030-21W3/0	Dodsland	Baytex	7/17/2017	51.575186	-108.824774	4.7	689.2	33.24	1143.7	38.12	0.39	0.46	2459.9

541	02/03-13-030-21W3/0	Dodsland	Baytex	8/1/2017	51.5743	-108.831279	4.7	685.9	24.57	1063.1	35.44	0.40	0.43	3372.8
542	91/03-13-030-21W3/0	Dodsland	Novus	9/24/2010	51.566177	-108.832059	4.7	684.8	37.09	212	30.29	0.30	0.36	326.2
543	02/04-13-030-21W3/0	Dodsland	Baytex	8/2/2017	51.575426	-108.836727	4.7	683.7	24.99	1140	38	0.39	0.45	3203.0
544	91/12-13-030-21W3/0	Dodsland	Novus	9/28/2010	51.574393	-108.836659	4.7	687	24.59	304.4	27.67	0.28	0.39	402.2
545	02/01-16-030-21W3/0	Dodsland	Baytex	1/24/2016	51.570767	-108.889039	5.2	694.4	19.88	610.1	33.89	0.44	0.53	2447.2
546	03/01-16-030-21W3/0	Dodsland	Baytex	1/23/2016	51.570764	-108.889399	5.2	695.5	19.50	651.1	36.17	0.27	0.45	2081.0
547	04/02-16-030-21W3/0	Dodsland	Baytex	1/21/2016	51.57042	-108.894217	5.2	693.3	20.56	632.9	35.16	0.40	0.53	2611.0
548	05/02-16-030-21W3/0	Dodsland	Baytex	1/21/2016	51.570408	-108.894577	5.2	695.2	21.07	626.2	34.79	0.43	0.54	2234.1
549	02/09-16-030-21W3/0	Dodsland	Baytex	1/21/2016	51.578003	-108.890537	5.2	686	22.45	621.3	34.52	0.42	0.53	2381.8
550	01/12-16-030-21W3/0	Dodsland	Teine	1/25/2017	51.570992	-108.895796	5.2	689.2	60.26	709.6	39.42	0.38	0.52	2440.9
551	02/13-16-030-21W3/0	Dodsland	Teine	1/26/2017	51.575311	-108.896322	5.2	687.1	62.19	712.1	39.56	0.38	0.49	2261.5
552	03/09-18-030-21W3/0	Avon Hill	Teine	2/1/2017	51.571725	-108.946848	5.5	697.6	127.01	664.4	36.91	0.41	0.52	1618.0
553	02/11-18-030-21W3/0	Avon Hill	Teine	2/4/2017	51.571969	-108.959223	5.5	695.6	190.13	697.7	38.76	0.39	0.53	1141.5
554	02/14-18-030-21W3/0	Avon Hill	Teine	1/27/2017	51.575329	-108.957379	5.5	698	158.35	675.8	37.54	0.40	0.49	1479.2
555	03/16-18-030-21W3/0	Avon Hill	Teine	2/9/2017	51.576057	-108.946628	5.5	696.5	142.11	726.8	40.38	0.35	0.48	1351.0
556	01/09-19-030-21W3/0	Avon Hill	Teine	1/2/2018	51.58548	-108.959908	6.0	679.8	97.60	1327.1	39.03	0.38	0.47	3628.0

557	02/05-22-030-21W3/0	Dodsland	Baytex	2/1/2016	51.575608	-108.880944	5.3	685.7	18.32	628.5	34.92	0.43	0.54	2527.4
558	03/06-22-030-21W3/0	Dodsland	Baytex	3/1/2016	51.575478	-108.875319	5.3	687.7	34.04	641	35.61	0.33	0.46	2215.6
559	02/07-22-030-21W3/0	Dodsland	Baytex	3/1/2016	51.575587	-108.871898	5.3	697.2	32.73	619.5	34.42	0.34	0.45	2342.8
560	02/08-22-030-21W3/0	Dodsland	Baytex	3/1/2016	51.575516	-108.864686	5.3	691.2	32.98	639.6	35.53	0.34	0.45	2555.9
561	02/09-22-030-21W3/0	Dodsland	Baytex	2/1/2016	51.592627	-108.864372	5.3	692.8	12.01	632.6	35.14	0.34	0.46	2491.0
562	02/10-22-030-21W3/0	Dodsland	Baytex	2/1/2016	51.592431	-108.870331	5.3	691	13.78	628.8	34.93	0.33	0.48	2504.0
563	03/11-22-030-21W3/0	Dodsland	Baytex	2/1/2016	51.591995	-108.878477	5.3	682	13.43	574.9	31.94	0.47	0.53	2459.8
564	01/01-24-030-21W3/0	Dodsland	Baytex	7/11/2017	51.577445	-108.830561	4.7	687.1	18.26	655.8	36.43	0.41	0.42	2294.6
565	01/08-24-030-21W3/0	Dodsland	Baytex	7/12/2017	51.582569	-108.830921	4.7	690.9	48.37	627.3	34.85	0.43	0.45	2309.9
566	02/10-24-030-21W3/0	Dodsland	Baytex	7/9/2017	51.584763	-108.81425	4.7	704.2	27.69	627.5	34.86	0.43	0.52	2655.3
567	03/15-24-030-21W3/0	Dodsland	Baytex	7/10/2017	51.589167	-108.813845	4.7	708.9	22.41	619.7	34.43	0.44	0.44	3131.7
568	02/14-26-030-21W3/0	Dodsland	Teine	7/15/2016	51.588896	-108.855395	5.3	686	17.43	1494.8	36.46	0.40	0.44	6060.2
569	02/01-01-030-22W3/0	Avon Hill	Teine	7/4/2017	51.534492	-108.970346	4.3	710.1	44.95	702.6	39.03	0.38	0.46	1728.3
570	01/08-01-030-22W3/0	Avon Hill	Teine	7/5/2017	51.538196	-108.969531	4.3	713.3	33.96	762.3	42.35	0.32	0.45	1788.1
571	02/08-01-030-22W3/0	Avon Hill	Teine	7/7/2017	51.538421	-108.96953	4.3	709.3	37.59	710.4	39.47	0.38	0.46	1871.5
572	02/14-02-030-22W3/0	Avon Hill	Crescent	2/14/2018	51.531848	-108.992384	4.1	725.1	135.31	1421.3	33.05	0.41	0.4	2273.7

573	01/04-03-030-22W3/0	Avon Hill	Teine	2/28/2016	51.534757	-109.013392	5.4	735	88.54	674.1	37.45	0.40	0.54	1712.7
574	01/05-03-030-22W3/0	Avon Hill	Teine	11/20/2016	51.538891	-109.013516	5.4	733.2	40.76	702.3	43.89	0.33	0.47	1931.0
575	02/05-03-030-22W3/0	Avon Hill	Teine	11/20/2016	51.539026	-109.013516	5.4	729.1	55.74	683.4	40.2	0.38	0.48	1347.4
576	01/15-03-030-22W3/0	Avon Hill	Teine	2/17/2018	51.54546	-109.001083	5.4	728.8	61.28	706.7	37.19	0.27	0.43	989.1
577	02/09-12-030-22W3/0	Avon Hill	Teine	7/18/2016	51.556147	-108.970135	4.8	712.4	65.06	734.9	40.83	0.34	0.43	2298.7
578	03/09-12-030-22W3/0	Avon Hill	Teine	7/19/2016	51.556012	-108.970135	4.8	710.7	58.74	708.6	39.37	0.32	0.38	1994.8
579	04/09-12-030-22W3/0	Avon Hill	Teine	7/18/2016	51.556282	-108.970134	4.8	707.6	68.81	692.9	40.76	0.35	0.44	2612.3
580	02/04-24-030-22W3/0	Avon Hill	Teine	11/26/2016	51.579205	-108.966636	6.5	694.9	30.07	705.1	41.48	0.36	0.53	1246.1
581	02/05-24-030-22W3/0	Avon Hill	Teine	11/27/2016	51.58288	-108.96664	6.5	693.5	26.73	726.5	45.41	0.32	0.5	1142.6
582	02/13-25-030-22W3/0	Dodsland	Teine	12/3/2016	51.600911	-108.965184	6.0	677.5	25.34	700.6	41.21	0.37	0.51	1253.2
583	01/11-30-030-22W3/0	Eureka	Baytex	7/9/2017	51.600447	-109.099263	5.3	729.7	122.47	633	35.17	0.43	0.5	1862.5
584	02/11-30-030-22W3/0	Eureka	Baytex	7/8/2017	51.600672	-109.099263	5.3	728.4	102.74	639	35.5	0.42	0.51	2867.7
585	02/14-30-030-22W3/0	Eureka	Baytex	7/1/2016	51.60528	-109.098762	5.3	726.6	2.00	641.1	35.62	0.41	0.46	2650.2
586	03/14-30-030-22W3/0	Eureka	Baytex	7/1/2016	51.605055	-109.098761	5.3	730.5	3.68	617	34.28	0.43	0.45	2514.4
587	03/03-35-030-22W3/0	Dodsland	Baytex	6/20/2016	51.607076	-109.004906	4.8	683.6	17.17	631.1	35.06	0.57	0.62	2843.1
588	02/08-36-030-23W3/0	Eureka	Baytex	7/14/2017	51.60492	-109.098731	6.8	722.3	280.87	636	35.33	0.42	0.51	1349.2

589	01/12-05-030-24W3/0	Whitesi de	Whiteca p	8/12/2017	51.5427	-109.328018	5.7	695.2	278.54	1438.8	32.7	0.39	0.37	8272.1
590	02/12-05-030-24W3/0	Whitesi de	Whiteca p	8/1/2017	51.542475	-109.327961	5.7	701	303.84	1462.8	33.25	0.38	0.37	5308.7
591	01/14-06-030-24W3/0	Whitesi de	Whiteca p	1/26/2016	51.538687	-109.36934	5.7	719.6	294.29	645.1	35.84	0.36	0.35	2535.6
592	02/14-06-030-24W3/0	Whitesi de	Whiteca p	12/2/2016	51.538687	-109.368908	5.7	718.9	328.00	702	39	0.33	0.43	3380.4
593	02/07-09-030-24W3/0	Whitesi de	Whiteca p	7/31/2017	51.546176	-109.317984	5.9	725.5	330.58	644.6	35.81	0.36	0.45	2643.5
594	93/13-09-030-24W3/0	Whitesi de	Whiteca p	1/18/2016	51.553709	-109.327161	5.9	716.5	483.43	627.9	34.88	0.37	0.43	1890.8
595	01/06-15-030-24W3/0	Whitesi de	Whiteca p	11/9/2016	51.567796	-109.310757	6.4	706	348.19	631.1	35.06	0.37	0.29	2195.8
596	01/03-16-030-24W3/0	Whitesi de	Whiteca p	9/5/2017	51.570694	-109.321351	7.0	717.6	395.61	613.1	34.06	0.38	0.36	1825.4
597	01/12-17-030-24W3/0	Whitesi de	Whiteca p	9/5/2017	51.571276	-109.328647	6.2	718.9	864.75	1433.7	32.58	0.39	0.34	1836.5
598	02/16-18-030-24W3/0	Whitesi de	Teine	7/28/2017	51.574039	-109.368974	6.3	679.4	75.62	694.3	40.84	0.28	0.45	333.5
599	01/13-21-030-24W3/0	Whitesi de	Whiteca p	11/8/2016	51.589196	-109.317605	6.7	708.7	408.80	615.4	34.19	0.38	0.4	2289.3
600	03/04-01-030-25W3/0	Whitesi de	Baytex	1/25/2018	51.534896	-109.382151	6.0	724.5	152.80	1052.3	38.97	0.39	0.42	4691.8
601	01/05-01-030-25W3/0	Whitesi de	Baytex	1/29/2018	51.538981	-109.380612	6.0	722.3	250.03	1087.1	38.83	0.30	0.33	3969.0
602	01/03-02-030-25W3/0	Whitesi de	Baytex	1/29/2018	51.533697	-109.398635	6.0	727.6	231.13	1067.6	41.06	0.37	0.42	3900.1
603	01/04-02-030-25W3/0	Whitesi de	Baytex	1/24/2018	51.545899	-109.423012	6.0	751.5	208.40	1071.1	39.67	0.32	0.39	4354.8
604	01/03-03-030-25W3/0	Whitesi de	Whiteca p	3/19/2017	51.536323	-109.462102	6.0	727.9	601.97	1489.3	33.85	0.37	0.31	4160.5

605	02/03-03-030-25W3/0	Whitesi de	Whiteca p	1/14/2018	51.536096	-109.462113	6.0	731	480.36	1496.4	34.01	0.38	0.34	5380.5
606	01/06-03-030-25W3/0	Whitesi de	Whiteca p	3/19/2017	51.536458	-109.462102	6.0	729.5	554.75	1503	34.16	0.38	0.3	4179.0
607	02/06-03-030-25W3/0	Whitesi de	Whiteca p	1/14/2018	51.537511	-109.464186	6.0	733.1	629.13	1447.4	32.9	0.40	0.34	5565.6
608	02/06-04-030-25W3/0	Whitesi de	Whiteca p	8/23/2017	51.538902	-109.474649	6.1	746.5	346.63	672.7	37.37	0.35	0.4	1773.0
609	03/06-04-030-25W3/0	Whitesi de	Whiteca p	8/23/2017	51.539127	-109.474649	6.1	748.4	343.25	635.2	35.29	0.37	0.45	2876.3
610	01/11-04-030-25W3/0	Whitesi de	Whiteca p	7/26/2017	51.545079	-109.474512	6.1	738.1	390.75	662.5	36.81	0.35	0.42	2235.2
611	01/14-04-030-25W3/0	Whitesi de	Whiteca p	7/26/2017	51.545213	-109.474512	6.1	739	479.32	644.1	35.78	0.37	0.44	2303.9
612	02/14-04-030-25W3/0	Whitesi de	Whiteca p	7/26/2017	51.545348	-109.474512	6.1	748.4	385.78	630.1	35.01	0.37	0.34	2289.9
613	01/13-05-030-25W3/0	Whitesi de	Whiteca p	2/9/2017	51.534413	-109.492559	5.3	747.5	323.21	1140.5	33.54	0.39	0.37	4703.8
614	02/13-05-030-25W3/0	Whitesi de	Whiteca p	8/11/2017	51.534413	-109.492198	5.3	742.2	336.20	1147.1	33.74	0.39	0.37	5127.3
615	01/14-05-030-25W3/0	Whitesi de	Whiteca p	8/11/2017	51.534413	-109.491982	5.3	744.5	340.09	1088.9	32.03	0.41	0.38	4113.0
616	01/04-07-030-25W3/0	Whitesi de	Whiteca p	9/26/2017	51.550806	-109.493209	5.4	753.8	376.77	1452	33	0.39	0.38	3099.7
617	91/01-08-030-25W3/0	Whitesi de	Whiteca p	1/27/2016	51.549257	-109.491912	7.9	729.7	173.88	1013.7	30.72	0.41	0.36	5448.6
618	01/01-09-030-25W3/0	Whitesi de	Novus	1/17/2017	51.549348	-109.474685	6.6	716.2	311.63	1335.4	31.06	0.36	0.33	1329.0
619	02/06-09-030-25W3/0	Whitesi de	Novus	8/29/2017	51.553838	-109.474294	6.6	728.2	488.68	654.7	29.76	0.44	0.34	852.0
620	01/06-08-031-18W3/0	Dodsla nd	Nal	1/31/2017	51.63766	-108.533469	4.2	701.7	8.88	670.3	37.24	0.42	0.46	1956.3

621	01/07-08-031-18W3/0	Dodsland	Nal	1/27/2017	51.637085	-108.505116	4.2	697.1	8.92	669	37.17	0.40	0.38	1046.2
622	01/13-10-031-18W3/0	Dodsland	Crescent	11/28/2016	51.632922	-108.482325	4.6	695.6	95.01	1415.9	32.93	0.42	0.4	4254.9
623	01/03-20-031-18W3/0	Dodsland	Crescent	11/14/2017	51.665058	-108.506474	3.5	718.3	89.39	1021.4	34.05	0.41	0.42	1899.5
624	02/02-06-031-19W3/0	Dodsland	Teine	1/19/2017	51.622284	-108.671968	5.2	702.5	94.87	719.6	39.98	0.38	0.51	2675.8
625	02/07-06-031-19W3/0	Dodsland	Teine	1/20/2017	51.627601	-108.668937	5.2	703.5	22.02	736.9	40.94	0.37	0.52	3013.7
626	02/11-06-031-19W3/0	Dodsland	Teine	3/17/2017	51.626409	-108.699079	5.2	696.3	10.04	732	40.67	0.37	0.53	2644.0
627	02/14-06-031-19W3/0	Dodsland	Teine	11/11/2017	51.632719	-108.698675	5.2	692.6	30.85	717.1	39.84	0.38	0.5	2197.2
628	02/03-17-031-19W3/0	Dodsland	Teine	10/14/2016	51.650025	-108.686857	3.8	700.2	14.63	1515.3	48.88	0.41	0.57	4269.1
629	03/03-17-031-19W3/0	Dodsland	Teine	10/3/2016	51.650159	-108.686857	3.8	695.9	14.36	1535.6	51.19	0.37	0.56	3513.1
630	02/06-17-031-19W3/0	Dodsland	Teine	11/7/2016	51.655082	-108.68779	3.8	701.3	11.95	1552.3	39.8	0.51	0.58	4899.9
631	03/06-17-031-19W3/0	Dodsland	Teine	11/5/2016	51.655083	-108.687574	3.8	696.6	11.09	1543	38.58	0.51	0.56	5114.3
632	03/11-17-031-19W3/0	Dodsland	Teine	3/12/2017	51.65863	-108.688169	3.8	700.8	16.60	1425.8	38.54	0.39	0.51	4888.7
633	03/14-17-031-19W3/0	Dodsland	Teine	5/24/2017	51.661269	-108.689437	3.8	701.1	23.27	1379.3	36.3	0.42	0.46	5265.1
634	01/16-22-031-19W3/0	Dodsland	Teine	5/21/2017	51.676604	-108.627259	3.8	683.7	19.82	1509.5	39.72	0.38	0.45	4888.3
635	01/01-30-031-19W3/0	Dodsland	Teine	11/14/2017	51.67709	-108.687314	3.8	722	533.92	682.2	37.9	0.40	0.46	718.9
636	02/01-30-031-19W3/0	Dodsland	Teine	11/11/2017	51.67709	-108.68753	3.8	724.1	407.18	730.1	40.56	0.37	0.53	936.7

637	01/07-30-031-19W3/0	Dodsland	Teine	10/16/2017	51.68944	-108.681853	3.8	654.1	425.78	710.5	39.47	0.38	0.52	1321.5
638	01/01-32-031-19W3/0	Dodsland	Teine	12/11/2016	51.701807	-108.653035	0.0	635.6	201.28	763.5	42.42	0.35	0.52	2761.0
639	02/01-32-031-19W3/0	Dodsland	Teine	12/11/2016	51.701807	-108.653252	0.0	635.2	170.10	749.8	44.11	0.34	0.51	2714.7
640	01/02-32-031-19W3/0	Dodsland	Teine	12/11/2016	51.700825	-108.658174	0.0	631.1	120.14	696.7	38.71	0.38	0.49	2856.3
641	02/02-32-031-19W3/0	Dodsland	Teine	12/16/2016	51.700825	-108.658391	0.0	633.6	211.13	679.7	39.98	0.37	0.5	2258.0
642	01/04-32-031-19W3/0	Dodsland	Teine	7/8/2016	51.700823	-108.669877	0.0	647.4	327.57	700.2	38.9	0.38	0.52	1295.6
643	02/04-26-031-23W3/0	Eureka	Baytex	9/2/2016	51.679553	-109.149476	5.7	713.6	44.89	1073.4	35.78	0.34	0.4	3830.2
644	02/13-32-031-25W3/0	Prairiedale	Ish	10/28/2017	51.698203	-109.522133	2.9	754.4	65.33	630.7	35.04	0.43	0.41	1657.3
646	02/02-28-031-26W3/0	Prairiedale	Ish	1/29/2017	51.686514	-109.628832	5.4	752.1	1028.97	635.5	35.31	0.42	0.4	452.6
649	03/13-28-031-26W3/0	Prairiedale	Ish	12/4/2016	51.683444	-109.640342	5.4	762.6	190.56	640.75	35.6	0.42	0.37	906.8
650	04/14-28-031-26W3/0	Prairiedale	Ish	12/4/2016	51.683453	-109.634775	5.4	763.8	116.64	640.7	35.59	0.42	0.4	1574.9
651	02/15-28-031-26W3/0	Prairiedale	Ish	12/14/2016	51.683463	-109.62854	5.4	766.8	250.77	611.1	33.95	0.44	0.4	1024.0
652	03/16-28-031-26W3/0	Prairiedale	Ish	12/14/2016	51.683472	-109.622757	5.4	761.1	104.92	648.2	36.01	0.41	0.36	1225.6
653	01/09-34-032-19W3/0	Plenty	Teine	9/16/2017	51.795801	-108.606368	3.0	597.2	320.15	698.5	34.93	0.31	0.43	719.2
654	01/13-32-032-20W3/0	Plenty	Teine	3/11/2018	51.793316	-108.801207	3.2	657.4	50.83	725.1	38.16	0.39	0.5	2557.3
655	01/07-33-032-20W3/0	Plenty	Teine	6/17/2016	51.778457	-108.777312	4.2	641.8	126.05	692.6	40.74	0.35	0.44	2653.6

656	01/12-33-032-20W3/0	Plenty	Teine	1/4/2018	51.788585	-108.765184	4.2	636.5	10.79	1503.6	34.97	0.43	0.49	2983.5
657	01/07-34-032-20W3/0	Plenty	Teine	3/5/2018	51.777724	-108.752865	4.6	642	178.50	708.6	37.29	0.39	0.48	2205.4
658	01/08-34-032-20W3/0	Plenty	Teine	2/19/2018	51.777589	-108.74736	4.6	647	122.52	714.7	39.71	0.37	0.51	2815.8
659	02/08-34-032-20W3/0	Plenty	Teine	2/23/2018	51.777589	-108.747142	4.6	645.7	112.26	730.7	40.59	0.36	0.51	3311.3
660	01/09-34-032-20W3/0	Plenty	Teine	3/7/2018	51.79532	-108.746791	4.6	642.5	37.18	722.9	40.16	0.37	0.44	1864.8
661	02/09-34-032-20W3/0	Plenty	Teine	3/8/2018	51.79532	-108.747008	4.6	644.8	115.11	713	41.94	0.34	0.43	1520.4
662	01/10-34-032-20W3/0	Plenty	Teine	3/5/2018	51.795272	-108.752755	4.6	640.4	52.31	707.6	39.31	0.37	0.48	1122.1
663	02/10-34-032-20W3/0	Plenty	Teine	3/5/2018	51.795272	-108.752972	4.6	637.9	190.34	698.7	38.82	0.39	0.49	1137.5
664	01/13-03-032-25W3/0	Prairiedale	Ish	10/18/2017	51.71273	-109.472026	2.3	705.7	74.64	642.2	35.68	0.41	0.37	1609.3
665	01/12-04-032-25W3/0	Prairiedale	Ish	10/29/2017	51.722679	-109.496343	3.9	715.6	93.20	639.5	35.53	0.42	0.41	1726.7
666	01/15-05-032-25W3/0	Prairiedale	Ish	10/20/2017	51.712788	-109.507537	3.6	736.9	79.16	638.9	35.49	0.42	0.38	1559.1
667	02/16-07-032-25W3/0	Prairiedale	Ish	10/22/2017	51.727217	-109.528296	4.1	741.1	94.68	634.6	31.73	0.42	0.34	1940.4
668	02/14-17-032-25W3/0	Prairiedale	Ish	10/12/2017	51.741861	-109.516426	2.8	734.2	75.84	637.5	33.55	0.42	0.34	1671.9
669	01/06-30-032-25W3/0	Prairiedale	Ish	10/22/2017	51.763586	-109.540218	3.8	737.2	126.69	633.6	35.2	0.43	0.39	1564.2
670	02/10-30-032-25W3/0	Prairiedale	Ish	10/1/2017	51.780969	-109.534122	3.8	724.6	136.98	647.7	35.98	0.42	0.35	1555.4
671	03/12-30-032-25W3/0	Prairiedale	Ish	12/19/2016	51.781467	-109.54294	3.8	730.9	111.31	652.5	36.25	0.42	0.4	1616.2

672	02/16-30-032-25W3/0	Prairiedale	Ish	3/1/2017	51.770995	-109.528322	3.8	726.1	115.59	613.8	34.1	0.44	0.39	1491.1
673	01/03-32-032-25W3/0	Prairiedale	Ish	8/1/2017	51.78815	-109.516444	3.6	719.2	116.85	634.7	35.26	0.43	0.4	1411.0
674	02/04-32-032-25W3/0	Prairiedale	Ish	8/3/2017	51.788145	-109.522168	3.6	724.1	88.65	602.5	33.47	0.45	0.39	1821.4
675	01/11-07-032-26W3/0	Prairiedale	Ish	4/1/2017	51.737176	-109.681752	3.8	746.1	185.12	620.5	31.03	0.48	0.38	528.9
676	02/05-09-032-26W3/0	Prairiedale	Ish	12/7/2017	51.720017	-109.640348	4.3	763.9	125.52	628	34.89	0.43	0.38	1493.9
677	02/06-09-032-26W3/0	Prairiedale	Ish	12/15/2017	51.720036	-109.634635	4.3	762.3	116.82	641.3	33.75	0.40	0.31	1422.6
678	02/08-09-032-26W3/0	Prairiedale	Ish	12/19/2017	51.720047	-109.622851	4.3	756.4	232.44	627	34.83	0.43	0.41	568.8
679	02/05-10-032-26W3/0	Prairiedale	Ish	12/15/2017	51.720049	-109.6167	4.1	754.8	292.42	619.6	34.42	0.44	0.38	749.6
680	02/06-10-032-26W3/0	Prairiedale	Ish	11/12/2017	51.720035	-109.610984	4.1	755	242.51	620.6	34.48	0.43	0.41	927.7
681	02/07-10-032-26W3/0	Prairiedale	Ish	11/12/2017	51.72002	-109.604996	4.1	757.5	153.66	642.1	35.67	0.42	0.41	1478.7
682	01/08-10-032-26W3/0	Prairiedale	Ish	11/12/2017	51.720005	-109.599208	4.1	756.2	97.48	639.2	35.51	0.42	0.38	1867.1
683	02/01-16-032-26W3/0	Prairiedale	Ish	12/21/2017	51.744639	-109.62284	4.9	750.2	182.39	611.4	33.97	0.44	0.4	1266.5
684	02/02-16-032-26W3/0	Prairiedale	Ish	12/10/2017	51.744629	-109.628631	4.9	746.1	287.41	614.9	34.16	0.44	0.37	933.1
685	02/06-17-032-26W3/0	Prairiedale	Ish	5/31/2017	51.734532	-109.65812	4.3	751.1	113.83	630.8	35.04	0.43	0.4	1136.7
686	03/11-17-032-26W3/0	Prairiedale	Ish	1/18/2017	51.751766	-109.658053	4.3	756.8	206.58	631	35.06	0.42	0.35	795.8
687	02/16-20-032-26W3/0	Prairiedale	Ish	3/15/2017	51.755492	-109.646293	5.5	746.5	73.17	648.7	36.04	0.41	0.36	1706.7

688	01/02-21-032-26W3/0	Prairiedale	Teine	12/8/2016	51.753232	-109.616113	4.1	745.4	181.74	707.7	39.32	0.38	0.52	1011.8
689	01/06-22-032-26W3/0	Prairiedale	Ish	3/17/2017	51.749162	-109.610825	4.9	752.1	200.99	638.5	35.47	0.42	0.38	1211.3
690	02/08-25-032-26W3/0	Prairiedale	Ish	12/19/2016	51.762868	-109.551807	4.2	729	118.85	644.3	37.9	0.39	0.37	1407.3
691	01/01-12-033-20W3/0	Plenty	Crescent	2/2/2017	51.812361	-108.710668	1.2	631.2	95.06	665.8	41.61	0.33	0.48	1546.1
692	01/04-12-033-20W3/0	Plenty	Crescent	2/6/2017	51.812359	-108.706456	1.2	638.7	95.02	625.7	34.76	0.40	0.42	2083.8
693	01/05-12-033-20W3/0	Plenty	Crescent	2/24/2017	51.812494	-108.706456	1.2	635.9	94.95	619	34.39	0.39	0.37	1774.6
694	02/05-12-033-20W3/0	Plenty	Crescent	2/6/2017	51.812629	-108.706457	1.2	636.9	94.90	613.3	34.07	0.42	0.45	2207.7
695	01/08-12-033-20W3/0	Plenty	Crescent	2/2/2017	51.812631	-108.710668	1.2	641.4	95.01	671.5	37.31	0.37	0.45	2052.1
696	02/08-12-033-20W3/0	Plenty	Crescent	2/2/2017	51.812496	-108.710668	1.2	641.1	94.98	626	34.78	0.40	0.47	2430.5
697	01/01-20-033-23W3/0	Kerrobert	Teine	6/18/2016	51.839554	-109.231473	2.6	710.5	53.73	716.7	39.82	0.36	0.48	1219.7
698	02/04-20-033-23W3/0	Kerrobert	Teine	6/30/2016	51.83954	-109.226158	2.6	705	122.70	688.2	40.48	0.37	0.52	1210.9
699	01/05-20-033-23W3/0	Kerrobert	Teine	6/30/2016	51.841077	-109.22616	2.6	694.6	88.48	701.7	43.86	0.34	0.53	1307.0
700	01/08-20-033-23W3/0	Kerrobert	Teine	6/22/2016	51.843423	-109.231417	2.6	702.5	61.59	702.2	39.01	0.36	0.49	1544.9
701	02/09-20-033-23W3/0	Kerrobert	Teine	6/21/2016	51.846843	-109.231405	2.6	693.3	42.87	702.2	39.01	0.32	0.46	1645.9
702	02/11-20-033-23W3/0	Kerrobert	Teine	6/23/2016	51.845996	-109.242451	2.6	700.9	105.69	688.2	38.23	0.36	0.49	1141.5
703	02/13-20-033-23W3/0	Kerrobert	Teine	6/23/2016	51.850343	-109.227572	2.6	695.1	85.78	713.2	39.62	0.37	0.5	1488.3

704	01/16-20-033-23W3/0	Kerrobert	Teine	6/24/2016	51.850432	-109.231117	2.6	689.3	67.48	711.1	39.51	0.32	0.4	2044.3
705	91/01-21-033-23W3/0	Kerrobert	Whitecap	11/19/2015	51.840446	-109.207072	2.5	706.5	83.21	736.9	40.94	0.32	0.37	2715.7
706	01/08-21-033-23W3/0	Kerrobert	Whitecap	12/7/2016	51.842873	-109.207357	2.5	703.9	176.04	621.8	34.54	0.36	0.41	1867.2
707	91/08-21-033-23W3/0	Kerrobert	Whitecap	11/18/2015	51.840581	-109.207071	2.5	704.8	62.15	648.5	36.03	0.35	0.38	2485.5
708	01/09-21-033-23W3/0	Kerrobert	Whitecap	2/18/2016	51.849661	-109.207052	2.5	711.1	222.55	642.3	40.14	0.32	0.38	1696.5
709	01/03-27-033-23W3/0	Kerrobert	Baytex	8/29/2017	51.868286	-109.184929	2.8	713.7	39.61	1466.1	40.73	0.34	0.42	3169.8
710	01/05-27-033-23W3/0	Kerrobert	Baytex	9/7/2017	51.85131	-109.188111	2.8	707.7	95.95	644.2	35.79	0.42	0.39	2312.2
711	01/12-27-033-23W3/0	Kerrobert	Baytex	8/23/2017	51.86874	-109.190716	2.8	714.6	58.86	572.7	33.69	0.44	0.43	1731.4
712	02/01-28-033-23W3/0	Kerrobert	Whitecap	5/29/2017	51.854307	-109.219096	2.7	704.6	308.40	1426.5	35.66	0.36	0.35	2576.8
713	06/08-28-033-23W3/0	Kerrobert	Whitecap	10/6/2017	51.869276	-109.196016	2.7	722.4	163.01	1157.8	41.35	0.32	0.35	1205.2
714	01/05-29-033-23W3/0	Kerrobert	Baytex	8/6/2016	51.851248	-109.23849	2.7	695.5	11.14	634.9	35.27	0.42	0.48	1996.7
715	01/06-29-033-23W3/0	Kerrobert	Baytex	8/1/2016	51.850885	-109.233062	2.7	697.9	25.96	652.6	36.26	0.33	0.44	2090.8
716	02/06-29-033-23W3/0	Kerrobert	Baytex	8/3/2016	51.850885	-109.233425	2.7	697	16.99	662.7	36.82	0.31	0.41	2126.4
717	01/07-29-033-23W3/0	Kerrobert	Baytex	8/1/2016	51.851312	-109.225137	2.7	695.3	17.89	626.2	41.75	0.29	0.44	2076.6
718	01/08-29-033-23W3/0	Kerrobert	Baytex	8/1/2016	51.851116	-109.218051	2.7	709.5	16.89	654.2	36.34	0.41	0.49	2542.9
719	02/08-29-033-23W3/0	Kerrobert	Baytex	8/1/2016	51.851116	-109.218414	2.7	710.1	18.38	638.9	35.49	0.34	0.44	2190.2

720	01/09-29-033-23W3/0	Kerrobert	Baytex	2/10/2017	51.868211	-109.219913	2.7	718.8	44.76	619.3	36.43	0.33	0.38	1694.9
721	01/10-29-033-23W3/0	Kerrobert	Baytex	2/21/2017	51.868261	-109.224922	2.7	711.7	34.04	642.3	37.78	0.31	0.37	2008.4
722	02/10-29-033-23W3/0	Kerrobert	Baytex	2/21/2017	51.868261	-109.224559	2.7	715.4	21.95	646.3	35.91	0.35	0.39	2452.4
723	01/12-29-033-23W3/0	Kerrobert	Baytex	2/24/2017	51.861387	-109.226	2.7	712.9	35.55	537.8	41.37	0.29	0.38	1387.6
724	02/12-29-033-23W3/0	Kerrobert	Baytex	2/22/2017	51.861612	-109.226001	2.7	708.1	40.47	631.9	39.49	0.32	0.38	1700.2
725	02/14-29-033-23W3/0	Kerrobert	Baytex	2/8/2017	51.865402	-109.242817	2.7	678.4	20.64	668.1	37.12	0.34	0.39	1843.5
726	01/09-30-033-23W3/0	Kerrobert	Teine	7/8/2017	51.86234	-109.26573	2.4	703	16.08	1488.8	36.31	0.41	0.48	3553.3
727	02/09-30-033-23W3/0	Kerrobert	Teine	7/8/2017	51.862474	-109.26573	2.4	700.7	15.10	1513.9	36.92	0.38	0.45	3221.2
728	01/16-30-033-23W3/0	Kerrobert	Teine	7/9/2017	51.862609	-109.26573	2.4	699.8	21.16	1509.1	36.81	0.41	0.49	2961.9
729	01/01-31-033-23W3/0	Kerrobert	Baytex	6/16/2017	51.875425	-109.243594	2.5	679.4	43.51	629	37	0.33	0.37	1477.0
730	01/02-31-033-23W3/0	Kerrobert	Baytex	6/19/2017	51.874932	-109.248867	2.5	688.3	38.71	597.9	33.22	0.38	0.38	1703.2
731	01/03-31-033-23W3/0	Kerrobert	Baytex	6/18/2017	51.875247	-109.2549	2.5	691.5	62.27	630	35	0.35	0.38	1791.6
732	01/04-31-033-23W3/0	Kerrobert	Baytex	6/16/2017	51.875021	-109.259391	2.5	691.6	83.80	610.4	33.91	0.36	0.38	1884.9
733	02/09-31-033-23W3/0	Kerrobert	Baytex	6/14/2017	51.882894	-109.243657	2.5	673	46.25	649.1	36.06	0.28	0.32	910.4
734	02/13-31-033-23W3/0	Kerrobert	Baytex	6/19/2017	51.873719	-109.259682	2.5	688.9	34.49	590.6	34.74	0.34	0.37	1498.4
735	01/14-31-033-23W3/0	Kerrobert	Baytex	6/20/2017	51.872949	-109.255161	2.5	685.4	42.42	610.4	33.91	0.31	0.32	1205.1

736	01/15-31-033-23W3/0	Kerrobert	Baytex	6/14/2017	51.873497	-109.249232	2.5	687.3	36.33	602.4	33.47	0.37	0.39	1603.5
737	01/01-34-033-23W3/0	Kerrobert	Baytex	8/9/2016	51.868735	-109.182876	2.7	712.2	21.92	619.6	36.45	0.32	0.42	891.7
738	01/04-34-033-23W3/0	Kerrobert	Baytex	8/7/2016	51.868103	-109.178883	2.7	703.7	11.57	653.9	38.46	0.33	0.43	1164.4
739	02/04-34-033-23W3/0	Kerrobert	Baytex	8/7/2016	51.868102	-109.178521	2.7	700.4	13.78	660.5	44.03	0.28	0.43	1571.3
740	01/05-34-033-23W3/0	Kerrobert	Baytex	1/23/2017	51.882932	-109.189963	2.7	707.9	17.13	1052.1	40.47	0.31	0.41	2590.7
741	01/06-34-033-23W3/0	Kerrobert	Baytex	1/12/2018	51.883473	-109.184517	2.7	725.3	24.67	1102.8	45.95	0.25	0.4	2105.6
742	01/06-03-033-24W3/0	Kerrobert	Whitecap	1/28/2018	51.80002	-109.340607	4.2	734	393.59	651.8	36.21	0.36	0.47	1743.5
743	01/02-04-033-24W3/0	Kerrobert	Whitecap	1/26/2018	51.804169	-109.342782	3.2	726.5	135.88	761.2	42.29	0.31	0.43	1250.5
744	01/04-04-033-24W3/0	Kerrobert	Whitecap	1/11/2018	51.797275	-109.342848	3.2	724	299.29	663.8	36.88	0.35	0.45	1245.1
745	01/05-04-033-24W3/0	Kerrobert	Whitecap	1/11/2018	51.7974	-109.342764	3.2	727.2	146.73	765.8	42.54	0.29	0.42	1378.2
746	01/12-04-033-24W3/0	Kerrobert	Whitecap	1/26/2018	51.804304	-109.342782	3.2	727.5	188.41	656.1	36.45	0.35	0.42	1485.3
747	01/13-04-033-24W3/0	Kerrobert	Whitecap	1/31/2018	51.807168	-109.342969	3.2	730.4	165.64	676.2	37.57	0.34	0.43	2242.9
748	01/15-04-033-24W3/0	Kerrobert	Whitecap	1/28/2018	51.799895	-109.340685	3.2	724.9	254.39	752.3	41.79	0.31	0.43	2051.3
749	01/16-04-033-24W3/0	Kerrobert	Whitecap	1/28/2018	51.800398	-109.340371	3.2	726.6	376.36	656.4	36.47	0.35	0.45	1395.0
750	91/10-05-033-24W3/0	Kerrobert	Baytex	1/21/2016	51.811141	-109.366253	2.2	728.4	125.77	776.5	43.14	0.34	0.5	2595.5
751	91/12-05-033-24W3/0	Kerrobert	Baytex	1/18/2016	51.811446	-109.377796	2.2	732.7	146.12	777.6	43.2	0.35	0.51	2661.5

752	01/13-05-033-24W3/0	Kerrobert	Baytex	1/23/2018	51.792858	-109.376663	2.2	724.2	443.18	1457.7	40.49	0.35	0.4	3058.8
753	01/10-07-033-24W3/0	Kerrobert	Baytex	1/28/2017	51.82464	-109.390897	2.4	715.2	125.80	628	34.89	0.43	0.44	2486.2
754	01/11-09-033-24W3/0	Kerrobert	Whitecap	1/20/2017	51.807087	-109.347991	3.0	727.3	166.45	1069.6	33.43	0.34	0.44	2976.9
755	01/12-09-033-24W3/0	Kerrobert	Whitecap	1/20/2017	51.807087	-109.348209	3.0	724.4	138.01	1148.9	33.79	0.38	0.37	3258.8
756	01/13-09-033-24W3/0	Kerrobert	Whitecap	6/18/2017	51.831497	-109.353662	3.0	704	156.92	1054.9	31.03	0.42	0.4	3728.3
757	01/14-09-033-24W3/0	Kerrobert	Whitecap	6/18/2017	51.831497	-109.353225	3.0	709	159.59	1030.3	31.22	0.41	0.38	3520.0
758	02/15-09-033-24W3/0	Kerrobert	Whitecap	1/31/2018	51.807168	-109.342752	3.0	725.3	233.05	1429.2	32.48	0.40	0.41	3784.0
759	01/12-10-033-24W3/0	Kerrobert	Whitecap	9/30/2017	51.818729	-109.319713	3.6	710.3	294.34	658.9	36.61	0.36	0.33	1263.6
760	02/12-13-033-24W3/0	Kerrobert	Teine	7/1/2017	51.835389	-109.262286	2.6	704.3	81.77	1473.8	35.95	0.40	0.63	3325.6
761	02/13-13-033-24W3/0	Kerrobert	Teine	7/1/2017	51.835524	-109.262286	2.6	707.6	206.17	1482.7	36.16	0.41	0.48	2711.9
762	02/03-16-033-24W3/0	Kerrobert	Whitecap	6/18/2017	51.831497	-109.353444	3.3	699.8	165.71	663.5	34.92	0.34	0.38	1872.6
763	01/08-16-033-24W3/0	Kerrobert	Whitecap	6/12/2017	51.828144	-109.349896	3.3	704.2	176.94	725.7	40.32	0.32	0.44	2592.9
764	02/08-16-033-24W3/0	Kerrobert	Whitecap	6/12/2017	51.828278	-109.349896	3.3	701.5	176.76	742.2	41.23	0.32	0.42	1910.5
765	01/09-16-033-24W3/0	Kerrobert	Whitecap	9/18/2017	51.839397	-109.339492	3.3	707	208.48	641.9	35.66	0.36	0.36	903.7
766	01/10-16-033-24W3/0	Kerrobert	Whitecap	9/19/2017	51.839893	-109.341232	3.3	709.4	206.52	721.8	40.1	0.32	0.35	1573.4
767	01/13-16-033-24W3/0	Kerrobert	Whitecap	6/20/2017	51.829214	-109.353687	3.3	700.8	246.85	685.9	38.11	0.34	0.43	1682.1

768	01/14-16-033-24W3/0	Kerrobert	Whitecap	6/20/2017	51.829214	-109.35347	3.3	700.7	216.86	648.8	36.04	0.35	0.4	1923.5
769	01/01-17-033-24W3/0	Kerrobert	Crescent	12/12/2016	51.831918	-109.364252	2.4	707	94.99	616.1	34.23	0.41	0.4	2077.2
770	01/02-17-033-24W3/0	Kerrobert	Crescent	12/12/2016	51.831919	-109.364687	2.4	706.7	94.91	725.4	40.3	0.35	0.4	2203.1
771	03/02-17-033-24W3/0	Kerrobert	Crescent	12/12/2016	51.831918	-109.36447	2.4	709.6	95.05	626	34.78	0.40	0.4	2229.3
772	01/15-17-033-24W3/0	Kerrobert	Crescent	12/9/2016	51.829307	-109.366069	2.4	706.9	95.02	640.2	35.57	0.38	0.39	2072.1
773	02/15-17-033-24W3/0	Kerrobert	Crescent	12/9/2016	51.829307	-109.365851	2.4	705.9	95.01	623.2	34.62	0.40	0.38	2013.7
774	01/16-17-033-24W3/0	Kerrobert	Crescent	12/9/2016	51.829307	-109.365634	2.4	705	95.01	673.3	37.41	0.37	0.42	1351.1
775	01/13-21-033-24W3/0	Kerrobert	Teine	6/10/2017	51.850803	-109.344691	2.2	692.4	80.39	700.4	38.91	0.38	0.52	1594.8
776	01/15-21-033-24W3/0	Kerrobert	Baytex	8/28/2017	51.843894	-109.343122	2.2	704.4	94.82	643.3	35.74	0.41	0.46	2200.7
777	03/10-22-033-24W3/0	Kerrobert	Whitecap	11/25/2016	51.847685	-109.309152	3.0	695.2	253.82	675.8	37.54	0.34	0.4	994.4
778	02/12-22-033-24W3/0	Kerrobert	Whitecap	5/31/2017	51.849486	-109.320618	3.0	704.5	183.65	697.9	38.77	0.31	0.33	1680.2
779	01/13-22-033-24W3/0	Kerrobert	Whitecap	5/31/2017	51.849621	-109.320618	3.0	703.6	230.85	646.7	35.93	0.34	0.34	1367.0
780	01/15-22-033-24W3/0	Kerrobert	Whitecap	11/25/2016	51.84782	-109.309152	3.0	696.4	184.60	670.7	37.26	0.35	0.44	1940.9
781	04/03-24-033-24W3/0	Kerrobert	Whitecap	2/26/2017	51.839215	-109.295819	2.6	704.5	205.99	1061.9	31.23	0.41	0.39	2196.3
782	05/03-24-033-24W3/0	Kerrobert	Whitecap	2/26/2017	51.839349	-109.295818	2.6	705.8	213.03	1069.3	31.45	0.41	0.37	2525.6
783	91/13-25-033-24W3/0	Kerrobert	Teine	7/7/2016	51.86486	-109.274018	2.5	686.4	25.84	698.8	46.59	0.32	0.49	1117.1

784	01/02-27-033-24W3/0	Kerrobert	Baytex	2/11/2017	51.860963	-109.320233	2.4	701.3	51.41	635.1	35.28	0.20	0.38	1388.2
785	01/03-27-033-24W3/0	Kerrobert	Baytex	2/8/2017	51.860884	-109.325866	2.4	701.4	62.43	655.8	38.58	0.32	0.4	2287.9
786	02/04-27-033-24W3/0	Kerrobert	Baytex	2/7/2017	51.860895	-109.331846	2.4	702.8	61.16	631.7	39.48	0.32	0.38	1737.6
787	01/08-27-033-24W3/0	Kerrobert	Baytex	2/5/2017	51.851778	-109.313213	2.4	697.6	91.10	635.9	37.41	0.31	0.38	1648.1
788	01/09-27-033-24W3/0	Kerrobert	Baytex	2/5/2017	51.861333	-109.325895	2.4	695.3	83.74	683.6	40.21	0.31	0.38	1683.0
789	01/12-27-033-24W3/0	Kerrobert	Baytex	2/5/2017	51.860964	-109.320596	2.4	697.4	36.64	626.5	36.85	0.34	0.37	1900.4
790	01/13-27-033-24W3/0	Kerrobert	Baytex	2/4/2017	51.865234	-109.320798	2.4	697.1	68.44	628	36.94	0.34	0.4	1936.2
791	01/16-27-033-24W3/0	Kerrobert	Baytex	2/4/2017	51.865242	-109.325201	2.4	695.9	44.26	653.8	38.46	0.31	0.37	1595.8
792	01/02-28-033-24W3/0	Kerrobert	Whitecap	7/18/2017	51.85672	-109.331634	2.5	707.8	108.77	677.8	37.66	0.34	0.42	1852.8
793	01/04-28-033-24W3/0	Kerrobert	Crescent	3/11/2017	51.856026	-109.34147	2.5	694.7	95.04	733.5	40.75	0.34	0.49	1484.2
794	01/05-28-033-24W3/0	Kerrobert	Crescent	3/11/2017	51.856296	-109.341469	2.5	698.4	94.73	784.8	43.6	0.33	0.49	1620.4
795	02/05-28-033-24W3/0	Kerrobert	Crescent	3/11/2017	51.856161	-109.34147	2.5	695.1	94.95	664.6	36.92	0.36	0.43	1683.7
796	01/07-28-033-24W3/0	Kerrobert	Whitecap	7/18/2017	51.856855	-109.331634	2.5	700.8	139.82	660.1	36.67	0.35	0.37	1470.7
797	01/12-28-033-24W3/0	Kerrobert	Crescent	3/11/2017	51.856431	-109.341469	2.5	699.5	94.86	831.7	46.21	0.29	0.43	1294.4
798	02/12-28-033-24W3/0	Kerrobert	Crescent	10/19/2017	51.863864	-109.3407	2.5	701.2	95.91	788.8	43.82	0.32	0.45	1630.0
799	03/12-28-033-24W3/0	Kerrobert	Crescent	10/19/2017	51.863999	-109.3407	2.5	700	97.35	702.3	39.02	0.35	0.35	827.7

800	01/13-28-033-24W3/0	Kerrobert	Crescent	10/19/2017	51.864268	-109.3407	2.5	701	97.88	692.9	38.49	0.36	0.4	1545.4
801	02/13-28-033-24W3/0	Kerrobert	Crescent	10/19/2017	51.864134	-109.3407	2.5	705.3	96.85	745.9	41.44	0.29	0.29	855.1
802	01/05-35-033-24W3/0	Kerrobert	Whitecap	11/28/2016	51.873401	-109.285012	2.5	697.5	73.33	1452.2	33	0.38	0.37	3695.9
803	02/05-35-033-24W3/0	Kerrobert	Whitecap	3/3/2017	51.873266	-109.285012	2.5	700	75.28	1420.4	32.28	0.39	0.33	3009.4
804	02/12-35-033-24W3/0	Kerrobert	Whitecap	3/3/2017	51.873536	-109.285011	2.5	700.8	86.65	1422.9	32.34	0.39	0.31	3201.5
805	02/02-36-033-24W3/0	Kerrobert	Baytex	9/4/2017	51.876037	-109.272969	2.4	695.1	69.17	654.9	36.38	0.41	0.45	1889.2
806	03/02-36-033-24W3/0	Kerrobert	Baytex	9/3/2017	51.876038	-109.272533	2.4	695	94.56	656.5	36.47	0.33	0.37	1535.5
807	02/15-36-033-24W3/0	Kerrobert	Baytex	6/4/2017	51.871922	-109.273257	2.4	692.1	30.01	727.9	42.82	0.29	0.39	808.2
808	02/16-36-033-24W3/0	Kerrobert	Baytex	6/4/2017	51.872434	-109.267126	2.4	695	44.65	676	39.76	0.31	0.38	1539.5
809	03/16-36-033-24W3/0	Kerrobert	Baytex	6/4/2017	51.872436	-109.26669	2.4	694.4	45.67	667.2	37.07	0.34	0.4	1447.2
810	02/15-04-033-25W3/0	Prairiedale	Ish	2/25/2017	51.800083	-109.48673	3.2	717.8	114.56	645.8	40.36	0.37	0.39	1769.9
811	02/16-04-033-25W3/0	Prairiedale	Ish	7/26/2017	51.800132	-109.481077	3.2	711.1	127.17	655.1	40.94	0.36	0.38	1324.3
812	02/01-06-033-25W3/0	Prairiedale	Ish	11/20/2016	51.80273	-109.527462	5.3	729	189.92	628.2	34.9	0.41	0.36	636.1
813	02/02-06-033-25W3/0	Prairiedale	Ish	8/7/2017	51.802811	-109.534087	5.3	728.6	155.85	620.5	34.47	0.44	0.4	1304.1
814	02/04-06-033-25W3/0	Prairiedale	Ish	8/6/2017	51.802821	-109.54581	5.3	717.6	168.45	646.1	35.89	0.42	0.4	1003.1
815	02/13-06-033-25W3/0	Prairiedale	Ish	1/20/2018	51.800117	-109.542982	5.3	717	170.55	625.5	34.75	0.43	0.38	827.4

816	02/14-06-033-25W3/0	Prairiedale	Ish	1/22/2018	51.800114	-109.537184	5.3	717.6	223.48	623.5	34.64	0.43	0.4	928.7
817	02/15-06-033-25W3/0	Prairiedale	Ish	1/25/2018	51.800111	-109.531231	5.3	721.7	159.04	643.3	35.74	0.42	0.38	1080.6
818	02/09-08-033-25W3/0	Prairiedale	Ish	9/6/2016	51.824781	-109.501937	3.6	727.1	86.01	671.2	41.95	0.36	0.42	1701.6
819	02/04-09-033-25W3/0	Prairiedale	Ish	7/27/2017	51.817311	-109.495544	4.5	741.5	84.95	622.8	34.6	0.43	0.38	1842.2
820	02/04-16-033-25W3/0	Prairiedale	Ish	6/1/2017	51.831959	-109.498322	1.0	724.3	109.29	621.8	34.54	0.44	0.38	1142.7
821	02/12-16-033-25W3/0	Prairiedale	Ish	5/30/2017	51.839196	-109.498334	1.0	731.1	74.58	623.6	34.64	0.43	0.39	1370.8
822	02/05-18-033-25W3/0	Prairiedale	Ish	8/24/2017	51.821508	-109.545816	2.4	721.9	84.27	625.1	34.73	0.43	0.36	1389.2
823	02/06-18-033-25W3/0	Prairiedale	Ish	8/22/2017	51.821011	-109.540363	2.4	726.5	76.10	640.5	35.58	0.41	0.33	1501.0
824	02/08-18-033-25W3/0	Prairiedale	Ish	2/26/2017	51.82183	-109.528187	2.4	728.2	129.00	621.9	38.87	0.39	0.4	900.7
825	01/10-18-033-25W3/0	Prairiedale	Ish	12/29/2016	51.838806	-109.533991	2.4	721.7	96.40	621.5	34.53	0.43	0.38	1215.0
826	01/13-18-033-25W3/0	Prairiedale	Ish	1/18/2018	51.829292	-109.545819	2.4	719	125.43	644.3	33.91	0.42	0.35	1274.9
827	02/05-01-033-26W3/0	Prairiedale	Ish	3/1/2017	51.792444	-109.569441	2.1	737	165.62	636.8	37.46	0.40	0.34	1263.7
828	02/06-01-033-26W3/0	Prairiedale	Ish	8/21/2017	51.792702	-109.562992	2.1	734.1	113.83	657.6	36.53	0.41	0.4	1908.7
829	02/07-01-033-26W3/0	Prairiedale	Ish	2/27/2017	51.792699	-109.55762	2.1	727.2	148.20	632.9	35.16	0.42	0.33	1595.1
830	01/08-01-033-26W3/0	Prairiedale	Ish	8/10/2017	51.792517	-109.552287	2.1	721	177.99	623.9	34.66	0.43	0.36	1330.1
831	02/01-02-033-26W3/0	Prairiedale	Ish	9/21/2017	51.802897	-109.575585	5.5	739.5	165.79	653.9	36.33	0.41	0.35	1030.7

832	02/03-02-033-26W3/0	Prairiedale	Ish	9/25/2017	51.803393	-109.58821	5.5	738.5	93.94	655.3	36.41	0.41	0.36	1356.1
833	02/09-02-033-26W3/0	Prairiedale	Ish	5/27/2017	51.810135	-109.573031	5.5	731.3	93.69	654.4	36.36	0.41	0.42	1188.7
834	01/03-03-033-26W3/0	Prairiedale	Ish	9/22/2017	51.802914	-109.611299	4.0	741.4	129.20	635.2	37.36	0.42	0.37	926.2
835	02/04-03-033-26W3/0	Prairiedale	Ish	9/24/2017	51.802927	-109.616735	4.0	743.6	73.27	617.1	34.28	0.43	0.36	1469.1
836	02/07-03-033-26W3/0	Prairiedale	Ish	12/20/2017	51.792534	-109.604752	4.0	736.8	130.05	647.3	35.96	0.41	0.35	729.7
837	01/08-03-033-26W3/0	Prairiedale	Ish	1/7/2018	51.792264	-109.599591	4.0	736.4	167.24	636.2	35.34	0.42	0.34	1252.0
838	02/06-04-033-26W3/0	Prairiedale	Ish	4/1/2017	51.792708	-109.634486	2.6	726.1	138.22	625.9	34.77	0.43	0.38	417.7
839	01/08-05-033-26W3/0	Prairiedale	Ish	3/16/2017	51.792759	-109.646952	1.4	736.4	88.48	633.1	35.17	0.43	0.37	1225.8
840	01/13-11-033-26W3/0	Prairiedale	Ish	9/23/2017	51.813247	-109.591262	3.4	729.3	116.05	649.8	36.1	0.41	0.32	1013.4
841	01/14-11-033-26W3/0	Prairiedale	Ish	9/23/2017	51.814655	-109.588234	3.4	727.3	94.00	636.7	35.37	0.42	0.34	1262.2
842	03/15-11-033-26W3/0	Prairiedale	Ish	1/6/2017	51.814664	-109.581359	3.4	724.2	124.26	628	34.89	0.43	0.42	1321.7
843	03/16-11-033-26W3/0	Prairiedale	Ish	12/28/2016	51.814671	-109.575558	3.4	723.9	105.48	623.9	34.66	0.43	0.42	1330.3
844	02/04-12-033-26W3/0	Prairiedale	Ish	5/29/2017	51.817364	-109.569097	4.1	724.2	98.18	632.1	35.12	0.43	0.37	1283.6
845	02/06-12-033-26W3/0	Prairiedale	Ish	12/21/2017	51.807421	-109.563685	4.1	722.1	121.83	645.7	35.87	0.42	0.4	1602.8
846	02/07-12-033-26W3/0	Prairiedale	Ish	1/5/2018	51.807399	-109.555831	4.1	721.4	128.58	627.6	34.87	0.43	0.36	1395.9
847	02/08-12-033-26W3/0	Prairiedale	Ish	1/5/2018	51.807388	-109.551975	4.1	719.5	187.65	626.82	34.82	0.43	0.35	1269.5

848	02/13-12-033-26W3/0	Prairiedale	Ish	5/30/2017	51.814672	-109.569394	4.1	723.3	131.81	627.2	34.84	0.43	0.37	1140.3
849	02/14-12-033-26W3/0	Prairiedale	Ish	9/12/2017	51.814654	-109.563086	4.1	719.4	159.16	615.3	34.18	0.44	0.39	1495.9
850	02/15-12-033-26W3/0	Prairiedale	Ish	8/30/2017	51.81464	-109.557778	4.1	718.3	92.98	630.1	35.01	0.42	0.39	1795.0
851	02/16-12-033-26W3/0	Prairiedale	Ish	9/17/2017	51.814623	-109.551978	4.1	720.1	126.94	642.4	35.69	0.41	0.31	1226.6
852	01/01-14-033-26W3/0	Prairiedale	Ish	12/20/2017	51.832022	-109.573853	3.7	726	112.98	619.5	34.42	0.44	0.37	1663.1
853	91/06-06-034-23W3/0	Kerrobert	Baytex	1/16/2016	51.887917	-109.267048	2.3	691.9	30.09	666.4	37.02	0.40	0.5	1469.3
854	01/16-06-034-23W3/0	Kerrobert	Baytex	3/1/2017	51.896559	-109.262158	2.3	691	35.71	1356.1	48.43	0.26	0.39	2053.9
855	01/07-03-034-24W3/0	Kerrobert	Baytex	1/21/2017	51.888017	-109.337417	1.5	698.3	41.19	1079.7	37.23	0.40	0.44	2022.2
856	01/08-03-034-24W3/0	Kerrobert	Baytex	9/17/2016	51.88018	-109.313391	1.5	702.9	49.99	627.1	36.89	0.34	0.44	1948.9
857	01/16-04-034-24W3/0	Kerrobert	Baytex	1/23/2017	51.895622	-109.354453	2.0	703.8	23.08	1019.2	36.4	0.31	0.39	1772.8
858	01/15-05-034-24W3/0	Kerrobert	Baytex	6/7/2017	51.88358	-109.368179	2.2	697.4	191.49	1042.8	38.62	0.32	0.37	1947.7
859	01/01-09-034-24W3/0	Kerrobert	Baytex	8/28/2017	51.898248	-109.360556	2.3	705.5	68.83	1473	39.81	0.34	0.44	2584.9
860	01/05-09-034-24W3/0	Kerrobert	Baytex	9/4/2016	51.911658	-109.356195	2.3	692.4	50.04	1049.7	43.74	0.28	0.4	2440.7
861	01/06-09-034-24W3/0	Kerrobert	Baytex	1/16/2017	51.91203	-109.34951	2.3	694	23.07	1030.6	38.17	0.21	0.25	1142.1
862	02/06-09-034-24W3/0	Kerrobert	Baytex	1/14/2018	51.912031	-109.349147	2.3	693.6	61.61	1043.8	41.75	0.35	0.42	2458.2
863	02/07-10-034-24W3/0	Kerrobert	Baytex	11/17/2016	51.900813	-109.336461	2.0	693.2	25.86	1041	40.04	0.30	0.37	1628.5

864	01/11-10-034-24W3/0	Kerrobert	Baytex	11/25/2016	51.912048	-109.325986	2.0	686.2	46.08	639.1	35.51	0.35	0.39	1661.4
865	02/11-10-034-24W3/0	Kerrobert	Baytex	11/19/2016	51.912048	-109.325623	2.0	681.3	29.46	626	36.82	0.34	0.4	1056.9
866	01/12-10-034-24W3/0	Kerrobert	Baytex	11/25/2016	51.911742	-109.331408	2.0	689.7	27.36	657.4	36.52	0.34	0.39	1620.5
867	01/02-14-034-24W3/0	Kerrobert	Baytex	9/27/2016	51.912573	-109.313274	2.5	679.3	50.20	1026.5	39.48	0.30	0.37	1183.3
868	01/02-15-034-24W3/0	Kerrobert	Baytex	1/17/2017	51.912593	-109.336886	2.4	689.7	26.41	1073.6	38.34	0.32	0.37	1889.3
869	01/04-15-034-24W3/0	Kerrobert	Baytex	6/3/2017	51.924334	-109.330744	2.4	680.1	94.80	1023.2	42.63	0.28	0.38	1455.5
870	02/14-15-034-24W3/0	Kerrobert	Baytex	9/23/2016	51.924072	-109.3363	2.4	677.2	50.15	644.4	37.91	0.28	0.36	1401.5
871	01/16-15-034-24W3/0	Kerrobert	Baytex	9/24/2016	51.924184	-109.3363	2.4	676.2	49.96	1433	38.73	0.32	0.37	884.8
872	01/08-20-034-24W3/0	Kerrobert	Baytex	12/1/2016	51.940836	-109.360559	2.4	672	35.30	1042.3	37.23	0.33	0.38	1654.5
873	01/09-21-034-24W3/0	Kerrobert	Baytex	9/24/2016	51.924296	-109.3363	2.3	677.9	50.05	1013.2	38.97	0.31	0.4	2342.4
874	01/11-21-034-24W3/0	Kerrobert	Baytex	12/18/2017	51.923898	-109.350199	2.3	675.9	125.62	1042.4	41.7	0.32	0.39	2640.9
875	01/12-21-034-24W3/0	Kerrobert	Baytex	6/10/2017	51.923883	-109.355758	2.3	675.3	105.29	1040.9	41.64	0.29	0.38	2238.8
876	01/09-22-034-24W3/0	Kerrobert	Baytex	11/22/2016	51.923711	-109.314282	2.2	670.1	35.59	1038.4	38.46	0.32	0.38	2956.0
877	01/11-22-034-24W3/0	Kerrobert	Baytex	11/22/2016	51.923931	-109.325542	2.2	669.7	46.61	1036.8	43.2	0.27	0.38	2628.5
878	01/02-28-034-24W3/0	Kerrobert	Baytex	12/1/2016	51.940948	-109.360559	1.5	673.6	41.62	1062.3	36.63	0.34	0.4	1536.6

APPENDIX B: SHAP VALUES ESTIMATED USING THE RANDOM FOREST MODEL B

UWI	Operator	TVD shap	Net pay shap	Latitude shap	Longitude shap	Completion length shap	Proppant completion shap	Avg. GOR shap
02/13-28-033-24W3/0	Crescent	38.93	-122.08	-131.68	-46.70	-1.72	-344.51	-60.22
02/15-26-029-22W3/0	Nal	21.15	-43.23	37.33	20.33	-192.44	132.24	31.28
01/04-30-029-24W3/0	Baytex	40.94	311.29	15.46	124.56	-236.92	-31.89	-61.42
01/05-28-033-24W3/0	Crescent	18.53	-119.25	-110.26	-45.33	73.45	-154.77	-33.54
91/16-35-029-25W3/0	Whitecap	52.93	593.73	166.04	218.04	-283.57	-36.04	-24.83
91/14-28-029-22W3/0	Crescent	25.02	-100.41	-5.49	-49.39	-200.57	-50.34	-225.34
02/15-04-033-25W3/0	Ish	2.16	-88.91	-107.97	140.97	-217.96	-12.13	-59.64
01/12-16-026-19W3/0	Teine	33.05	94.00	83.68	94.22	-174.38	284.42	112.95
01/06-22-032-26W3/0	Ish	-85.77	-9.69	-166.03	-330.86	-223.16	36.57	-206.40
91/13-25-033-24W3/0	Teine	-48.93	-117.12	-114.53	-60.77	-172.36	-168.86	63.27
02/01-28-029-22W3/0	Crescent	-88.86	-49.92	-16.07	-21.14	-228.55	113.34	30.18
02/02-30-029-22W3/0	Crescent	-105.61	-101.33	-34.86	-47.70	-187.06	-99.19	-110.72
91/08-13-030-20W3/0	Novus	-71.70	-33.26	-1.42	-12.33	-170.70	-257.08	-137.32
04/06-31-029-21W3/0	Baytex	21.44	4.44	13.47	-13.71	-177.22	-26.61	121.79
03/04-32-025-18W3/0	Crescent	-17.03	-105.41	-75.88	-21.13	-223.49	72.26	-31.86
01/16-27-029-25W3/0	Whitecap	42.68	297.09	150.31	532.99	1320.61	246.61	64.47
03/10-21-029-21W3/0	Baytex	-91.80	-82.93	-9.41	4.93	-183.80	136.74	114.09
02/06-25-029-26W3/0	Novus	-13.73	-100.57	10.96	32.65	-89.47	-0.20	-98.06
01/14-13-030-19W3/0	Baytex	-96.89	-195.66	13.76	-5.51	850.42	41.61	-15.32
02/15-32-026-19W3/0	Baytex	83.01	112.49	63.09	107.31	-233.74	76.98	141.04
02/01-35-025-18W3/0	Teine	-99.21	-95.64	10.83	11.52	-203.65	299.46	91.91
03/11-28-030-19W3/0	Crescent	11.71	-40.46	176.38	70.07	923.43	-36.18	-18.02
03/12-29-030-19W3/0	Crescent	-1.34	-69.52	183.48	67.58	907.95	-18.15	-5.77
02/08-25-029-22W3/0	Teine	38.23	-32.66	20.35	-6.62	-154.07	-73.56	122.99
01/15-34-025-18W3/0	Teine	18.93	-80.90	34.90	29.73	-195.43	362.23	135.35
03/04-01-030-25W3/0	Baytex	49.97	404.45	131.45	180.19	424.58	23.83	-57.40
02/04-28-025-18W3/0	Crescent	-39.02	-100.17	-122.08	-50.03	-193.34	-21.57	-122.90
07/07-28-025-18W3/0	Crescent	66.83	-73.97	6.62	54.48	937.01	-6.58	79.50
02/04-13-030-21W3/0	Baytex	31.15	-22.58	24.28	-95.88	766.30	63.53	83.94

02/15-34-025-18W3/0	Teine	44.55	-36.91	54.29	46.00	49.92	374.76	133.23
01/05-34-033-23W3/0	Baytex	61.08	-116.63	-135.69	-32.20	278.42	-388.76	81.06
02/15-28-029-22W3/0	Crescent	-10.45	-101.41	-72.17	-89.72	838.37	-55.44	-86.39
92/01-29-029-22W3/0	Crescent	-53.52	-57.31	-19.64	-24.60	-208.03	20.90	62.04
02/12-35-033-24W3/0	Whitecap	92.02	-126.57	-30.52	-26.19	991.91	125.20	-8.65
02/08-36-030-23W3/0	Baytex	32.11	73.33	93.95	-5.22	-236.08	83.94	-86.59
01/12-13-029-22W3/0	Teine	-116.48	-108.50	-16.21	-32.34	-148.93	-33.58	58.91
91/12-24-029-22W3/0	Baytex	-31.09	-37.00	-39.57	-6.51	-182.35	-34.79	112.99
01/06-06-026-18W3/0	Baytex	29.50	-36.38	31.60	-8.85	-169.87	-399.63	49.04
01/13-14-029-22W3/0	Baytex	-107.85	-100.61	48.47	8.40	309.31	209.50	100.06
01/09-29-033-23W3/0	Baytex	43.92	-94.22	-58.26	0.36	-148.05	-146.75	40.00
02/10-34-032-20W3/0	Teine	63.69	-13.40	-17.58	33.68	-251.02	23.43	-125.74
93/13-09-030-24W3/0	Whitecap	6.29	396.51	33.63	-7.95	-167.59	10.76	-197.57
02/12-28-033-24W3/0	Crescent	17.01	-122.47	-138.91	-46.19	87.52	-166.02	-63.96
01/04-05-026-18W3/0	Teine	-24.16	78.61	-22.60	-35.56	-165.55	310.79	93.13
01/12-05-030-21W3/0	Teine	51.69	-3.53	49.79	-8.20	-101.68	-21.30	62.52
02/14-26-030-21W3/0	Teine	50.69	169.49	123.81	-15.85	1007.55	132.34	85.40
91/10-24-029-22W3/0	Baytex	-107.88	-43.48	-21.31	-6.89	-180.33	112.28	108.57
01/08-29-033-23W3/0	Baytex	73.88	-92.66	-38.15	22.40	-203.91	110.73	132.27
02/08-05-030-21W3/0	Teine	55.39	-20.03	59.97	-22.55	-126.08	1.93	-40.23
03/01-17-026-19W3/0	Teine	63.89	5.09	57.58	75.77	-170.29	304.60	123.19
01/10-18-033-25W3/0	Ish	-14.62	-97.48	-118.78	-205.94	-199.97	16.85	-38.80
01/06-34-033-23W3/0	Baytex	23.73	-156.82	-121.01	-55.17	704.49	-538.60	52.88
01/09-21-033-23W3/0	Whitecap	45.16	-85.84	14.88	26.10	-157.15	-106.31	-130.25
01/01-19-026-18W3/0	Teine	19.12	94.89	75.95	43.13	160.12	288.78	105.63
01/02-27-033-24W3/0	Baytex	50.80	-93.46	-52.60	-27.15	-130.46	-401.67	9.33
02/16-28-029-22W3/0	Crescent	-39.25	-118.46	-65.95	-93.85	851.80	34.67	-138.14
01/08-15-030-19W3/0	Baytex	-119.54	-150.13	13.45	16.46	-160.19	-46.54	86.50
01/16-25-029-22W3/0	Teine	25.75	-33.70	20.83	-7.05	-95.48	-28.05	107.23
01/09-19-029-22W3/0	Baytex	-32.86	-76.75	3.80	-22.10	49.67	-561.24	35.73
92/04-10-026-19W3/0	Crescent	133.28	4.59	89.01	115.62	-172.43	151.53	188.84
01/01-25-029-22W3/0	Teine	-76.78	-39.60	-8.85	-14.21	-158.56	2.73	123.16
01/03-17-026-18W3/0	Teine	-42.80	200.91	27.65	-23.27	-228.81	-65.79	55.79
01/07-08-031-18W3/0	Nal	61.75	-20.92	106.26	-42.02	-246.73	44.79	124.86

01/08-31-025-18W3/0	Teine	53.54	-75.61	20.87	4.86	115.36	369.32	99.54
01/12-15-030-19W3/0	Baytex	-102.27	-127.24	32.71	32.89	-202.36	119.72	99.57
02/13-01-027-20W3/0	Teine	29.57	273.14	79.44	50.55	-180.15	365.84	57.04
02/01-30-031-19W3/0	Teine	6.59	-90.43	48.20	8.95	25.92	10.14	-368.90
02/01-01-030-22W3/0	Teine	32.05	-32.79	65.44	-5.37	-188.86	-9.16	59.23
01/09-31-029-21W3/0	Baytex	93.97	28.90	97.36	20.80	-165.66	187.10	144.98
01/04-35-029-22W3/0	Teine	16.07	48.74	105.65	30.55	-110.47	9.65	142.64
01/14-16-033-24W3/0	Whitecap	33.72	-91.57	-28.13	97.92	-229.18	-31.63	-120.28
01/13-25-029-22W3/0	Teine	39.25	-31.15	43.01	2.90	-162.61	15.63	136.04
01/06-28-029-21W3/0	Baytex	26.52	-93.64	-19.24	-32.97	-146.98	-218.63	81.03
01/04-21-030-19W3/0	Teine	-140.21	-97.60	22.94	27.35	-222.61	-29.67	79.60
02/13-30-030-19W3/0	Crescent	60.84	-69.27	165.35	60.65	-242.00	93.57	22.78
02/12-16-026-19W3/0	Teine	34.27	86.43	81.69	107.44	-105.48	289.75	132.62
01/01-21-029-21W3/0	Baytex	-91.69	-87.50	10.37	-7.74	-196.79	140.37	129.59
04/05-01-026-19W3/0	Teine	-100.40	-114.35	-20.17	-13.12	-202.62	115.81	107.60
01/09-20-029-22W3/0	Crescent	20.32	-64.00	-14.19	-6.29	-206.25	17.37	61.49
04/04-28-026-19W3/0	Teine	56.35	300.17	60.16	82.23	941.35	463.94	54.51
02/12-13-033-24W3/0	Teine	90.61	-128.48	22.97	-14.46	1054.27	129.74	19.61
01/12-30-030-19W3/0	Crescent	41.51	-59.44	163.04	53.29	-210.87	-19.29	29.49
02/09-16-030-21W3/0	Baytex	29.68	121.13	78.44	29.04	-194.96	141.63	152.94
02/09-34-032-20W3/0	Teine	105.69	27.96	24.47	78.21	-82.84	-47.85	-2.88
01/09-16-033-24W3/0	Whitecap	52.31	-101.43	-21.67	-4.90	-209.82	-45.50	-145.06
04/09-12-030-22W3/0	Teine	88.48	35.44	55.53	-6.59	-182.09	-105.16	33.28
03/11-32-029-24W3/0	Whitecap	53.89	607.05	165.03	101.94	118.25	141.02	-16.26
01/09-22-034-24W3/0	Baytex	-125.86	-124.34	-178.11	-67.72	231.24	-230.38	12.36
92/16-01-030-20W3/0	Novus	-134.41	-116.23	-16.95	-45.91	10.87	-566.49	-28.93
01/05-25-029-22W3/0	Teine	19.11	-40.34	14.46	-11.37	-118.02	-14.08	50.73
01/14-05-030-21W3/0	Teine	81.50	-24.36	59.73	-17.39	-201.06	5.58	138.88
02/12-16-029-22W3/0	Baytex	-96.39	-106.48	0.32	-35.53	-157.47	-175.81	86.45
01/10-17-029-22W3/0	Teine	-120.60	-116.16	-21.54	-29.24	-165.92	4.13	105.12
01/16-05-030-21W3/0	Teine	63.72	-41.76	43.19	-38.75	-191.09	-101.25	45.85
01/12-27-033-23W3/0	Baytex	66.76	-71.50	-52.75	19.64	-223.25	129.24	44.52
01/07-33-032-20W3/0	Teine	86.93	-47.43	65.79	47.55	-215.45	-30.61	-37.71
01/01-16-030-19W3/0	Baytex	-157.38	-142.83	23.74	-9.91	242.98	17.65	81.05

01/11-21-034-24W3/0	Baytex	-92.01	-87.94	-122.82	94.52	267.34	-186.27	-8.06
01/10-14-030-19W3/0	Baytex	-99.27	-123.37	23.19	28.79	-164.40	-77.24	85.14
02/13-34-025-18W3/0	Teine	-88.75	-72.86	41.07	32.78	-196.57	404.02	109.05
02/03-02-033-26W3/0	Ish	-30.46	-11.47	-185.61	-231.35	-222.39	58.72	-28.98
02/14-29-033-23W3/0	Baytex	-80.01	-95.37	-83.56	-37.94	-189.15	-103.03	106.47
92/01-30-029-22W3/0	Crescent	-74.95	-78.97	0.47	-4.29	-218.27	116.12	-156.26
02/14-34-025-18W3/0	Teine	-12.37	-76.92	54.30	38.15	-195.60	356.76	148.67
02/10-21-029-21W3/0	Baytex	-58.55	-83.19	-8.79	-13.09	-124.36	-428.25	121.44
02/03-16-033-24W3/0	Whitecap	21.86	-82.03	-8.24	108.86	-204.45	-81.05	-67.69
91/08-21-033-23W3/0	Whitecap	54.18	-94.45	-35.07	14.82	-190.41	-32.70	60.71
01/07-06-026-18W3/0	Baytex	59.82	-51.66	-26.11	-70.57	-240.88	48.06	62.54
02/02-18-030-20W3/0	Baytex	19.39	82.94	40.68	28.25	-223.50	115.40	15.21
01/07-29-033-23W3/0	Baytex	40.83	-98.54	-28.83	-12.64	-120.06	-278.91	116.82
01/12-16-030-21W3/0	Teine	34.55	95.43	47.18	-1.62	-172.38	5.02	49.65
92/11-24-029-22W3/0	Baytex	-54.26	-36.44	-17.09	-6.55	-136.30	-141.07	120.51
01/15-21-033-24W3/0	Baytex	54.75	-92.68	-50.88	10.15	-183.70	114.89	-20.38
03/02-18-030-20W3/0	Baytex	116.08	103.99	58.69	35.81	-221.75	70.30	166.73
01/13-27-033-24W3/0	Baytex	44.27	-91.49	-82.90	-27.34	-139.32	-89.17	45.41
03/14-30-030-22W3/0	Baytex	15.08	100.32	163.12	19.69	-212.02	116.39	100.20
02/02-32-031-19W3/0	Teine	120.94	-4.74	95.54	111.88	-188.88	36.60	-77.79
01/01-22-030-19W3/0	Teine	-121.35	-97.20	19.33	52.95	-103.54	-30.90	3.77
01/03-28-029-24W3/0	Whitecap	41.14	412.92	2.55	-37.01	-208.70	-1.33	-76.35
03/08-32-025-18W3/0	Crescent	48.22	-102.03	-3.62	-7.70	-94.82	-21.51	-64.31
01/10-21-029-21W3/0	Baytex	-89.98	-93.10	-24.01	-19.03	-195.71	117.39	88.49
01/02-28-033-24W3/0	Whitecap	51.08	-121.85	-63.31	-29.79	-200.91	-69.49	-87.08
01/08-33-029-21W3/0	Teine	23.70	-63.87	48.88	-25.33	-186.13	43.83	-36.31
02/12-29-033-23W3/0	Baytex	65.97	-100.92	-68.74	-31.22	-140.89	-182.39	41.94
01/11-30-030-22W3/0	Baytex	46.40	116.21	192.90	34.46	-192.60	153.38	-48.62
03/11-17-031-19W3/0	Teine	166.21	23.29	362.00	112.34	1096.99	66.51	140.79
01/01-12-033-20W3/0	Crescent	54.59	-21.86	24.80	40.71	-166.56	-136.20	-6.27
01/09-21-034-24W3/0	Baytex	-102.57	-104.27	-197.22	-56.68	146.51	-305.73	14.38
02/08-22-030-21W3/0	Baytex	45.56	150.48	68.79	15.75	-165.85	-111.26	109.28
02/11-24-029-26W3/0	Novus	-38.83	-120.02	12.74	-46.39	-30.79	131.08	78.17
05/08-28-025-18W3/0	Crescent	63.01	-69.38	1.28	43.81	957.15	18.38	81.73

08/07-28-025-18W3/0	Crescent	66.95	-59.64	13.68	39.47	1023.71	75.43	90.95
01/04-33-029-21W3/0	Teine	16.80	-47.81	26.02	-49.35	-166.87	10.08	137.48
91/01-30-029-24W3/0	Baytex	30.98	249.16	-28.16	119.59	-95.80	-72.51	-217.46
02/08-16-030-20W3/0	Crescent	-4.08	1.93	13.77	-9.59	-231.36	82.39	-91.60
02/07-03-033-26W3/0	Ish	-31.21	-65.18	-146.91	-255.41	-218.35	55.81	-142.84
01/05-01-026-19W3/0	Teine	-49.02	-119.21	-1.83	10.60	-198.52	324.74	119.31
02/06-06-026-18W3/0	Baytex	23.30	-24.74	18.55	-4.90	-161.82	-306.30	90.93
02/16-04-033-25W3/0	Ish	30.92	-85.89	-91.14	160.50	-234.43	-40.52	-72.92
01/15-06-026-18W3/0	Baytex	-21.03	-46.17	-64.81	-94.94	-238.16	66.01	103.61
91/16-30-029-22W3/0	Crescent	-56.45	-99.66	-10.94	-12.96	-225.47	37.58	-214.08
91/06-13-030-20W3/0	Novus	34.28	-35.66	7.89	-38.54	-139.15	-557.80	16.24
02/16-18-030-24W3/0	Teine	-107.67	206.91	-21.94	106.01	-209.26	-275.51	22.87
01/03-18-029-21W3/0	Baytex	-63.21	-82.61	62.36	2.32	223.29	-418.77	133.88
92/07-24-029-22W3/0	Baytex	-139.57	-53.19	-20.88	-24.80	-208.95	12.77	109.79
03/11-17-032-26W3/0	Ish	-89.26	-64.03	-164.74	-384.84	-233.63	37.09	-238.80
01/03-26-024-14W3/0	Baytex	-89.28	-27.98	-176.03	-53.13	744.68	-63.05	37.34
03/12-32-025-18W3/0	Crescent	42.81	-84.70	-2.05	3.58	-201.50	113.03	-55.97
01/06-30-032-25W3/0	Ish	-26.69	-57.85	-112.77	-186.73	-218.67	57.62	-89.44
02/05-09-032-26W3/0	Ish	-38.88	-54.19	-160.41	-362.04	-225.93	30.75	-111.36
02/01-02-033-26W3/0	Ish	-35.21	7.14	-184.85	-243.40	-222.01	52.48	-140.87
01/04-19-026-18W3/0	Teine	68.69	85.17	72.62	19.66	127.10	259.70	-2.53
03/16-11-033-26W3/0	Ish	-17.85	-85.36	-154.38	-262.28	-214.31	21.49	-49.83
01/14-11-033-26W3/0	Ish	-7.29	-77.38	-154.08	-243.50	-199.35	50.72	-3.61
01/16-06-034-23W3/0	Baytex	27.49	-166.57	-100.34	-70.13	709.39	-552.52	12.63
91/09-03-030-20W3/0	Novus	-182.84	-143.88	-51.98	-117.09	-77.20	-649.89	-344.38
03/05-28-025-18W3/0	Crescent	5.03	-85.24	-2.85	32.92	993.87	59.77	53.30
01/07-16-026-18W3/0	Baytex	-59.30	176.88	-40.11	-165.63	-250.46	26.91	-109.88
01/07-27-025-17W3/0	Teine	12.54	-124.56	-134.53	-38.82	39.94	-61.50	69.64
02/13-28-029-21W3/0	Baytex	18.17	-105.41	0.53	-34.35	-143.12	-223.01	89.97
03/12-35-029-22W3/0	Teine	11.35	58.13	107.11	44.14	-133.96	51.47	154.59
01/12-28-029-25W3/0	Whitecap	31.15	298.61	82.98	559.35	1205.69	113.55	17.38
02/09-12-030-22W3/0	Teine	39.57	33.59	42.67	-10.94	53.61	-110.45	52.89
92/03-10-026-19W3/0	Crescent	146.94	12.86	112.34	139.99	-128.49	126.59	232.08
01/01-34-033-23W3/0	Baytex	66.32	-100.23	-55.85	-6.76	-136.87	-181.50	108.49

93/10-24-029-22W3/0	Baytex	-71.33	-50.43	-26.28	-24.28	-163.79	-101.18	104.82
04/07-28-025-18W3/0	Crescent	64.38	-68.20	21.88	59.36	946.53	-37.46	81.65
02/05-10-032-26W3/0	Ish	-87.46	-79.11	-180.22	-299.93	-245.95	12.15	-234.49
01/12-21-029-25W3/0	Whitecap	-61.73	-231.08	-65.72	449.98	1097.34	109.67	-32.51
01/12-21-029-22W3/0	Baytex	-56.85	-86.00	-36.46	-26.30	-174.74	-82.07	102.95
01/11-21-029-21W3/0	Baytex	-57.02	-92.07	-22.59	-22.53	-142.36	-295.52	109.83
01/01-20-033-23W3/0	Teine	45.41	-95.92	-35.43	-30.02	-118.96	-32.35	42.45
02/14-06-026-18W3/0	Baytex	7.74	-15.04	24.82	5.71	-142.50	-230.83	96.77
01/16-17-033-24W3/0	Crescent	44.35	-71.70	-31.03	87.31	-217.82	-5.43	1.93
01/02-21-032-26W3/0	Teine	-71.24	-58.09	-114.24	-204.98	-122.33	15.77	-174.41
02/01-16-030-21W3/0	Baytex	47.85	102.82	67.78	25.03	-214.98	182.88	177.27
02/11-26-029-25W3/0	Teine	20.79	78.45	33.11	126.91	-252.23	-57.34	27.17
03/02-17-033-24W3/0	Crescent	66.31	-72.52	-4.02	91.26	-178.38	78.39	-21.67
01/12-25-029-22W3/0	Teine	47.35	-27.09	36.43	8.99	-141.11	34.64	156.26
01/14-28-029-22W3/0	Crescent	28.05	-94.16	-11.94	-19.82	-214.38	-8.46	-223.04
01/07-05-030-21W3/0	Teine	64.30	-38.16	54.65	-10.20	-194.56	15.53	-48.84
02/15-06-033-25W3/0	Ish	-11.04	-5.48	-213.58	-275.95	-240.84	34.92	-138.72
01/16-35-029-22W3/0	Teine	23.99	10.03	75.26	10.53	-140.33	-275.38	43.60
01/08-20-034-24W3/0	Baytex	-122.14	-132.17	-183.18	42.50	235.62	-203.65	-9.27
01/02-24-029-26W3/0	Novus	-19.13	-149.14	27.57	-53.65	-174.06	108.18	104.08
01/05-30-030-19W3/0	Crescent	-141.99	-100.95	65.53	7.00	-213.40	-15.91	-3.04
02/01-32-031-19W3/0	Teine	91.69	-32.85	124.89	108.49	115.61	-21.03	-39.07
02/11-10-034-24W3/0	Baytex	-47.60	-114.46	-97.81	-32.39	-127.11	-71.98	36.60
01/14-09-033-24W3/0	Whitecap	60.44	-37.49	13.83	140.27	323.63	146.97	-47.13
02/09-19-029-22W3/0	Baytex	-53.71	-88.54	-31.17	-26.14	-177.16	-130.62	46.05
03/01-35-029-22W3/0	Teine	12.82	34.27	73.17	12.11	22.04	-42.44	114.00
02/06-18-033-25W3/0	Ish	-2.89	-93.34	-142.12	-208.57	-199.23	48.34	16.40
02/14-32-024-14W3/0	Baytex	2.81	-121.32	-67.01	-42.13	261.41	-412.15	100.73
01/15-05-034-24W3/0	Baytex	27.80	-84.31	-97.60	169.08	273.00	-200.11	-41.69
01/02-19-026-19W3/0	Baytex	8.53	68.39	22.85	-8.11	-195.46	-115.05	28.43
01/16-28-029-22W3/0	Crescent	-20.74	-110.54	-74.18	-94.28	852.89	-33.86	-84.81
01/13-19-026-18W3/0	Teine	109.27	108.89	86.54	42.46	141.11	217.71	170.66
01/01-30-029-24W3/0	Baytex	23.67	281.92	-41.61	57.66	-229.84	-31.02	-71.04
01/13-20-029-22W3/0	Crescent	2.46	-109.36	-50.68	-15.59	-237.93	96.35	-115.13

01/03-34-029-22W3/0	Crescent	-74.18	-112.74	22.41	-98.59	919.57	150.83	-142.73
02/12-21-029-21W3/0	Baytex	-43.08	-104.33	-26.78	-17.79	-217.98	115.22	104.39
93/11-24-029-22W3/0	Baytex	-71.52	-22.91	-21.43	-5.30	-171.15	-18.85	135.94
01/12-21-024-14W3/0	Baytex	-103.15	-138.18	-150.61	-85.87	-195.50	4.92	76.36
01/16-13-029-22W3/0	Teine	-111.80	-85.92	-3.71	-9.87	98.93	-71.01	64.26
03/08-30-030-19W3/0	Crescent	-49.47	-70.40	90.73	57.92	-172.48	110.10	37.36
01/08-12-033-20W3/0	Crescent	43.92	-31.78	30.89	75.98	-199.21	-1.60	29.02
03/12-20-029-22W3/0	Crescent	-37.20	-82.47	-12.25	-2.87	-219.29	109.55	30.26
02/14-19-026-19W3/0	Baytex	-11.86	46.97	-13.94	-5.79	-230.00	71.30	15.16
02/05-14-030-20W3/0	Teine	-67.26	-48.84	16.59	-17.35	764.31	103.37	64.03
02/04-09-033-25W3/0	Ish	-71.64	-18.23	-143.74	-78.94	-213.33	41.92	-2.49
03/09-18-030-21W3/0	Teine	2.91	3.92	-3.11	-16.22	-248.37	91.88	-183.38
92/08-24-029-22W3/0	Baytex	-112.55	-44.04	-11.28	-12.16	-150.63	-150.50	94.01
02/13-13-033-24W3/0	Teine	53.27	-139.19	7.34	-17.75	1022.35	179.61	-74.85
91/15-33-029-25W3/0	Whitecap	109.67	510.66	207.63	388.72	-188.46	8.50	52.88
02/02-06-031-19W3/0	Teine	77.98	87.03	140.02	70.84	-141.82	1.15	-33.49
01/06-05-030-21W3/0	Teine	79.63	-23.53	70.05	-13.20	-170.75	12.64	19.67
91/09-29-029-22W3/0	Crescent	-0.92	-89.63	-17.60	-14.65	-224.73	2.90	-230.99
01/15-31-033-23W3/0	Baytex	-19.30	-137.55	-107.53	-40.81	-196.67	14.06	59.98
01/12-21-029-21W3/0	Baytex	-4.54	-101.14	-23.90	-26.83	-137.30	-252.30	93.97
02/12-26-029-26W3/0	Novus	-71.01	-88.41	23.87	31.76	77.54	-25.11	102.54
01/08-06-026-18W3/0	Baytex	-4.25	-34.58	-30.21	-13.31	-210.91	317.19	111.48
03/15-17-026-19W3/0	Teine	44.59	7.85	37.22	56.06	-168.38	209.35	115.89
01/08-32-029-25W3/0	Whitecap	62.39	358.03	157.21	224.51	-244.66	3.28	-43.04
01/16-02-030-19W3/0	Baytex	-59.72	-237.61	-3.46	12.48	672.15	-381.17	7.42
01/14-30-029-22W3/0	Crescent	-98.18	-103.36	-19.22	-67.35	-225.51	-30.83	-229.30
91/12-21-029-24W3/0	Baytex	14.26	-35.70	-54.34	-39.89	-186.22	-89.24	-143.06
01/06-16-029-22W3/0	Baytex	-109.04	-106.08	31.13	-7.78	348.81	194.40	88.20
05/02-35-029-22W3/0	Teine	35.73	28.02	94.87	26.38	-151.50	-94.25	144.44
01/01-09-034-24W3/0	Baytex	67.59	-175.09	-59.53	9.91	736.33	-253.60	19.23
02/10-16-026-19W3/0	Teine	82.64	102.77	79.44	114.39	-190.54	359.27	149.07
02/08-30-030-19W3/0	Crescent	-56.85	-81.77	78.68	32.64	-238.02	15.88	35.22
02/03-28-026-19W3/0	Teine	24.98	251.14	21.93	50.71	1015.92	331.55	63.41
02/14-05-030-21W3/0	Teine	75.17	-27.50	53.32	-22.72	-182.02	-44.59	128.38

01/13-32-025-18W3/0	Crescent	2.22	-138.03	-13.65	12.66	-204.50	336.71	-37.31
01/16-04-034-24W3/0	Baytex	48.54	-123.37	-166.78	52.99	149.74	-268.82	21.22
01/09-34-032-20W3/0	Teine	-2.46	33.06	1.05	72.47	-49.64	-11.46	34.86
02/15-05-030-21W3/0	Teine	76.97	-30.29	56.48	-22.99	-183.49	17.32	66.66
02/04-35-029-22W3/0	Teine	36.88	22.22	75.71	8.32	-37.36	-84.92	132.02
01/05-15-030-19W3/0	Baytex	-226.99	-175.34	-22.28	-21.74	-10.24	-69.54	0.27
03/05-21-029-21W3/0	Baytex	-83.90	-76.51	-2.12	1.24	-175.58	120.34	123.91
01/13-21-030-24W3/0	Whitecap	42.81	127.82	20.45	-25.60	-183.82	-16.22	-203.69
01/05-32-029-26W3/0	Novus	-5.67	-60.24	149.64	-146.44	-206.91	62.30	-182.93
02/13-29-030-19W3/0	Crescent	27.36	-64.11	204.09	61.38	945.19	2.48	-8.23
02/03-30-029-22W3/0	Crescent	-98.21	-104.69	-31.74	-41.57	-223.54	124.25	-226.96
01/02-07-030-19W3/0	Teine	-101.95	-122.82	0.88	14.24	-212.48	-41.32	-153.62
01/04-33-025-18W3/0	Teine	15.22	-111.42	10.57	29.27	-201.51	345.95	131.24
02/01-21-029-21W3/0	Baytex	-75.84	-89.91	-9.25	-25.73	-146.91	-413.54	100.41
01/13-30-029-22W3/0	Crescent	-68.44	-98.48	-13.21	-63.75	-203.50	-57.65	-351.64
01/13-10-031-18W3/0	Crescent	79.04	-17.38	245.92	8.77	1097.49	248.57	-48.72
01/03-33-029-26W3/0	Novus	29.69	-47.39	155.19	-65.02	-195.54	80.05	-64.62
02/04-30-029-24W3/0	Baytex	30.77	251.27	12.19	88.18	-174.10	-51.93	-35.65
02/02-16-032-26W3/0	Ish	-90.04	-2.95	-187.12	-352.56	-237.83	30.92	-212.94
01/15-30-029-22W3/0	Crescent	-79.38	-112.36	-7.61	-31.57	-231.39	123.53	-264.06
02/11-06-031-19W3/0	Teine	63.76	117.98	137.11	61.59	6.24	-2.86	119.24
01/08-03-033-26W3/0	Ish	-35.46	-59.53	-144.01	-259.12	-228.19	49.61	-175.53
01/07-28-033-24W3/0	Whitecap	9.25	-128.15	-66.94	-26.86	-217.21	-85.09	-123.00
01/03-27-029-26W3/0	Novus	-5.88	18.20	74.07	-74.28	-137.03	102.73	119.45
02/14-15-034-24W3/0	Baytex	-89.70	-88.45	-94.78	-28.83	-126.41	-352.32	3.86
02/04-16-033-25W3/0	Ish	-10.16	-65.28	-93.38	-164.72	-196.32	52.09	-37.72
01/16-27-033-24W3/0	Baytex	31.48	-88.77	-96.93	-32.52	-143.32	-195.14	24.74
02/08-18-026-18W3/0	Baytex	20.54	185.38	-2.78	-1.35	-299.16	108.27	42.40
02/08-18-033-25W3/0	Ish	6.91	-87.24	-91.49	-138.71	-205.05	2.86	-94.71
02/01-25-026-20W3/0	Teine	30.86	243.96	96.00	87.33	-195.14	399.77	136.99
01/03-27-033-24W3/0	Baytex	42.45	-80.92	-69.24	-26.12	-168.24	-136.33	41.86
02/16-34-025-18W3/0	Teine	57.45	-82.97	37.17	25.03	-192.91	371.90	152.86
03/09-16-026-19W3/0	Teine	83.64	91.58	88.40	110.94	-69.90	272.44	127.65
01/12-07-030-19W3/0	Teine	-123.62	-112.27	13.82	15.15	-81.67	-56.53	100.39

02/01-28-033-23W3/0	Whitecap	62.74	-104.33	-9.41	-44.72	985.40	-12.96	-93.60
02/11-16-026-19W3/0	Teine	72.16	112.45	88.81	96.26	-123.57	300.12	129.71
01/14-26-026-19W3/0	Teine	54.30	113.22	83.86	101.05	-218.02	352.62	153.47
05/06-28-025-18W3/0	Crescent	61.16	-58.78	27.13	64.98	993.50	28.97	92.86
02/04-32-032-25W3/0	Ish	-6.50	-62.98	-138.75	-163.84	-222.34	54.67	-7.61
02/14-01-027-20W3/0	Teine	22.50	266.67	73.44	61.75	-182.44	306.96	63.17
93/07-24-029-22W3/0	Baytex	-114.23	-42.43	-6.39	-5.92	-185.30	118.19	121.24
03/12-30-030-19W3/0	Crescent	58.10	-72.33	167.24	50.13	-195.61	-10.67	8.51
01/13-29-030-19W3/0	Crescent	32.37	-64.42	210.61	61.02	942.42	8.55	-6.47
01/02-17-026-19W3/0	Teine	43.22	15.81	43.01	58.17	-164.56	98.33	127.17
01/15-32-026-19W3/0	Baytex	71.30	65.03	59.88	91.70	-239.59	76.71	85.32
01/12-31-024-14W3/0	Baytex	37.98	-128.95	-131.89	-39.93	257.65	-39.65	70.48
01/12-33-032-20W3/0	Teine	-42.05	1.44	37.03	55.83	1046.34	211.43	68.40
01/06-26-029-25W3/0	Teine	-0.64	26.65	-36.50	-50.64	-196.40	138.72	38.82
01/08-05-026-18W3/0	Teine	-20.53	83.14	-11.99	-16.23	-191.22	358.57	107.32
01/04-02-030-25W3/0	Baytex	-51.18	438.67	80.13	282.05	538.14	-168.58	-34.04
02/09-25-029-22W3/0	Teine	34.97	-32.28	35.46	-0.77	-149.13	21.66	131.06
01/15-28-029-26W3/0	Novus	20.12	32.49	120.88	-14.69	-171.31	144.97	176.33
02/13-17-026-19W3/0	Teine	5.85	-0.76	26.05	52.08	-187.61	274.08	106.76
02/01-33-029-21W3/0	Teine	18.73	-98.51	14.74	-58.15	100.89	-157.62	49.34
02/15-28-029-21W3/0	Baytex	30.98	-96.70	0.36	-23.72	-151.35	-395.19	116.79
02/04-14-030-20W3/0	Teine	-119.78	-74.68	0.08	-27.63	856.16	185.10	32.21
01/02-15-034-24W3/0	Baytex	-15.69	-151.34	-171.90	-59.31	399.97	-277.74	29.46
01/10-16-026-19W3/0	Teine	46.14	88.80	57.69	78.90	-192.16	318.27	-154.46
01/11-22-034-24W3/0	Baytex	-100.50	-102.03	-159.49	-52.10	226.95	-457.80	-2.72
02/09-30-033-23W3/0	Teine	116.23	-148.00	18.73	-16.77	1176.28	107.51	79.42
01/07-03-034-24W3/0	Baytex	64.52	-167.43	-115.86	-24.02	515.11	166.78	40.99
01/01-32-025-18W3/0	Crescent	-17.33	-116.54	-72.75	-32.20	-199.12	-9.90	-31.32
01/11-07-030-21W3/0	Teine	107.83	97.40	87.67	25.98	-136.67	-109.87	145.93
02/04-01-026-19W3/0	Teine	-101.94	-121.17	-14.32	-5.29	-208.27	286.31	80.25
02/05-28-033-24W3/0	Crescent	-1.83	-117.18	-89.57	-31.68	-215.54	-32.21	-14.35
02/13-32-025-18W3/0	Crescent	12.80	-73.54	-5.57	3.01	-197.12	87.79	-7.89
02/04-25-029-22W3/0	Teine	23.95	-39.13	22.68	5.57	-165.82	50.62	74.83
01/08-20-033-23W3/0	Teine	32.60	-116.15	-103.52	-45.83	-245.90	-46.69	57.11

03/15-11-033-26W3/0	Ish	-20.34	-91.93	-153.10	-282.20	-215.07	36.19	-90.74
02/05-28-025-18W3/0	Crescent	-7.31	-73.15	-21.30	2.51	544.81	31.86	118.00
91/03-29-029-22W3/0	Crescent	-28.90	-64.28	12.11	-4.83	-214.23	93.37	19.31
01/09-32-029-25W3/0	Whitecap	-32.99	357.17	140.44	226.98	-252.70	-16.65	-46.54
01/04-07-030-25W3/0	Whitecap	-12.52	262.42	1.21	375.06	1288.27	141.90	-4.38
01/09-32-025-18W3/0	Crescent	-11.63	-112.06	-28.73	-20.74	-188.14	4.53	-14.75
02/05-35-033-24W3/0	Whitecap	89.53	-124.24	-32.40	-21.17	998.29	132.04	31.49
03/02-36-033-24W3/0	Baytex	7.42	-105.95	-84.26	-43.42	-162.39	-123.34	-12.52
03/06-22-030-21W3/0	Baytex	20.69	148.27	61.94	11.02	-163.50	-170.43	102.40
02/07-19-029-22W3/0	Baytex	-82.55	-106.18	-8.72	9.56	-206.14	123.19	91.16
03/08-34-029-25W3/0	Whitecap	56.42	439.92	125.30	366.16	-279.08	26.72	-218.85
01/03-02-030-25W3/0	Baytex	63.47	406.17	154.71	209.05	548.28	-32.86	-30.95
01/05-34-029-24W3/0	Baytex	33.48	85.21	64.72	-21.37	-196.87	-115.38	-149.97
01/12-09-033-24W3/0	Whitecap	13.36	-69.68	41.48	45.79	948.78	96.63	-57.97
01/05-27-025-18W3/0	Teine	-99.49	-110.80	-110.53	-7.13	-203.33	334.80	111.76
02/06-17-031-19W3/0	Teine	164.32	36.29	386.94	148.41	1343.37	406.26	126.99
02/01-06-033-25W3/0	Ish	-1.49	-7.61	-198.18	-254.98	-246.55	31.32	-172.52
02/15-06-026-18W3/0	Baytex	-27.31	-47.85	-57.25	-78.92	-223.19	90.70	107.14
01/10-33-025-18W3/0	Teine	8.75	-85.20	16.51	47.37	-205.51	353.77	141.76
02/05-20-029-22W3/0	Crescent	29.83	-48.57	18.99	18.32	-203.35	9.01	75.03
02/05-21-029-22W3/0	Baytex	-1.62	-93.90	-2.69	-19.57	-240.35	107.24	99.16
01/10-29-033-23W3/0	Baytex	51.17	-108.42	-80.75	-16.62	-132.78	-266.76	65.15
02/10-30-032-25W3/0	Ish	-2.43	-63.72	-122.77	-207.58	-221.13	63.93	-130.38
02/15-11-025-18W3/0	Crescent	-42.34	-88.63	-167.18	-77.53	-190.09	76.47	-41.31
02/07-26-026-20W3/0	Baytex	25.50	72.39	-21.37	-2.03	-243.72	-114.12	3.56
04/15-35-029-22W3/0	Teine	36.47	26.83	90.27	20.79	-148.85	-80.54	140.72
02/06-29-033-23W3/0	Baytex	59.06	-100.11	-37.66	-30.18	-151.37	-242.90	111.33
02/11-29-029-21W3/0	Baytex	25.20	-54.06	34.48	-14.83	-118.08	-249.78	123.02
02/06-05-030-21W3/0	Teine	73.87	-26.02	59.54	-23.86	-197.12	-85.70	88.60
91/01-08-030-25W3/0	Whitecap	50.81	126.12	5.53	127.93	285.73	123.08	-77.96
02/06-09-032-26W3/0	Ish	-39.25	-50.36	-136.88	-256.92	-203.92	29.89	-97.17
04/05-36-029-25W3/0	Whitecap	55.98	189.42	142.10	278.57	57.95	-199.90	-34.70
03/12-16-030-20W3/0	Crescent	12.17	18.22	32.60	6.09	-197.67	18.00	-54.92
01/09-07-030-21W3/0	Teine	65.10	62.15	61.66	-3.50	-107.12	-74.08	41.64

01/01-33-026-19W3/0	Teine	23.83	159.33	6.93	57.49	821.49	328.92	21.14
01/12-05-030-24W3/0	Whitecap	42.74	627.57	156.14	-17.69	1201.46	54.27	53.42
02/14-06-030-24W3/0	Whitecap	41.79	534.99	85.74	155.48	-276.18	-100.39	-33.79
01/01-25-026-19W3/0	Teine	49.90	-151.62	47.95	29.03	-193.53	351.16	64.51
01/01-14-029-22W3/0	Baytex	-76.03	-127.72	-34.93	-43.19	854.04	218.96	-2.01
02/07-22-030-21W3/0	Baytex	78.21	135.89	67.40	14.22	-161.97	-102.15	117.36
03/10-22-033-24W3/0	Whitecap	10.27	-68.86	-13.24	-4.71	-197.36	-58.62	-129.70
01/12-05-026-18W3/0	Teine	-22.20	93.88	15.80	-33.34	-201.91	356.84	121.45
01/10-03-026-19W3/0	Teine	66.60	-164.99	-8.60	73.28	-213.45	242.84	99.34
91/08-01-030-20W3/0	Novus	-128.59	-139.38	-33.17	-93.19	-49.40	-535.49	-356.04
01/08-01-030-22W3/0	Teine	39.88	-42.86	50.04	-18.05	69.65	-220.79	93.05
01/16-19-026-18W3/0	Teine	54.95	80.44	48.99	32.97	109.55	253.12	-212.45
92/01-10-026-19W3/0	Crescent	36.18	-12.04	74.75	111.04	-180.57	32.08	160.16
02/13-30-029-22W3/0	Crescent	2.46	-130.63	-28.12	-61.24	-212.41	-60.14	-246.40
02/09-18-026-18W3/0	Baytex	-32.93	249.31	19.85	-12.63	-221.93	78.95	30.96
02/06-04-033-26W3/0	Ish	-37.67	-132.56	-206.27	-528.65	-261.83	-47.82	-183.02
01/08-18-026-18W3/0	Baytex	51.30	298.96	57.92	22.07	-178.48	-362.52	84.63
91/08-29-029-22W3/0	Crescent	-54.37	-62.22	-20.69	-25.25	-216.23	15.30	53.81
91/11-07-030-21W3/0	Teine	154.08	156.82	140.56	79.31	-104.32	119.79	216.45
02/15-36-033-24W3/0	Baytex	-45.26	-152.84	-198.89	-104.77	-112.74	-422.91	-16.26
02/09-08-033-25W3/0	Ish	18.74	-60.04	-101.98	-78.34	-180.38	-20.07	14.96
01/15-05-030-21W3/0	Teine	56.55	-34.68	37.09	-37.68	-168.07	-228.20	90.74
02/11-07-030-21W3/0	Teine	112.03	114.48	112.35	53.16	-85.22	173.75	189.99
02/12-18-026-18W3/0	Baytex	-14.27	188.67	32.19	-0.51	-253.47	145.71	127.52
01/10-27-025-17W3/0	Teine	-27.72	-143.41	-140.50	-76.06	-132.09	-85.03	44.31
01/14-33-029-25W3/0	Whitecap	2.41	297.06	72.26	153.92	-321.94	-81.87	-158.54
01/04-32-025-18W3/0	Crescent	-29.87	-110.19	-78.91	-35.93	-237.08	66.48	-86.83
03/01-32-025-18W3/0	Crescent	-44.82	-158.07	-108.51	-75.97	-243.21	-58.10	-104.25
03/15-28-029-22W3/0	Crescent	-25.92	-112.39	-68.92	-91.10	810.01	-35.74	-137.11
03/04-28-026-19W3/0	Teine	73.77	367.88	84.82	98.14	1087.78	518.61	108.28
01/01-17-033-24W3/0	Crescent	67.51	-73.96	-6.40	83.00	-185.44	87.68	3.43
01/08-05-030-21W3/0	Teine	47.56	-53.18	44.08	-38.45	-204.33	-86.55	-3.49
02/14-17-032-25W3/0	Ish	1.81	-66.71	-99.71	-145.94	-201.27	47.62	18.45
03/16-18-030-21W3/0	Teine	-17.81	-29.35	-24.17	-55.06	-132.88	-81.74	-182.30

02/05-24-026-20W3/0	Baytex	-50.66	-67.88	4.66	29.14	-220.80	118.07	106.88
01/07-30-031-19W3/0	Teine	-10.28	-94.55	-23.51	-2.21	-208.51	9.67	-350.50
02/13-25-030-22W3/0	Teine	-155.39	67.22	13.78	-76.16	-292.14	-117.84	20.23
02/15-23-026-20W3/0	Baytex	-32.27	-14.55	-38.92	-5.16	-224.77	-52.68	105.66
01/12-17-030-24W3/0	Whitecap	-39.06	172.77	-60.22	-151.36	824.22	14.93	-295.39
02/09-20-033-23W3/0	Teine	6.68	-95.90	-61.97	-37.03	-170.93	-127.64	39.21
01/03-03-030-25W3/0	Whitecap	20.47	417.77	155.44	442.82	1123.97	-59.29	-82.84
01/11-16-029-22W3/0	Baytex	-93.51	-116.07	-18.95	-53.54	-163.99	-295.12	19.68
01/15-34-029-25W3/0	Whitecap	81.89	492.28	195.04	350.21	-264.18	-37.92	34.98
92/04-29-029-22W3/0	Crescent	-55.25	-59.57	12.69	4.18	-210.89	177.31	-111.94
02/02-13-030-21W3/0	Baytex	26.49	-30.47	13.42	-65.58	707.52	19.61	51.30
02/16-22-025-18W3/0	Crescent	-89.38	-97.31	-142.04	-68.52	-200.23	68.47	-82.66
01/14-21-024-14W3/0	Teine	-120.51	-139.54	-132.09	-79.27	-29.23	-526.14	9.82
01/15-03-030-22W3/0	Teine	-2.00	-10.12	-16.92	-65.22	-196.68	-504.83	-34.81
02/09-16-029-22W3/0	Baytex	-63.24	-100.97	6.29	-8.96	-125.03	-209.02	110.71
01/14-27-029-26W3/0	Novus	-72.01	-20.82	61.08	-198.56	-262.20	65.08	82.53
01/13-18-030-19W3/0	Baytex	-78.81	-29.68	37.76	17.41	918.98	76.88	69.85
01/01-23-029-25W3/0	Teine	-29.38	-332.76	-157.89	47.37	473.19	-317.61	-65.96
02/16-28-029-21W3/0	Baytex	-44.57	-144.14	-103.70	-93.12	513.87	-588.41	-8.05
01/13-30-030-19W3/0	Crescent	67.70	-54.62	182.92	75.48	-195.31	126.43	49.05
01/10-28-029-26W3/0	Novus	33.39	40.95	127.84	6.90	-139.26	148.80	187.40
01/04-03-030-22W3/0	Teine	-9.88	-14.64	37.44	-39.92	-249.35	32.49	-68.20
91/13-28-029-22W3/0	Crescent	20.91	-90.79	-11.35	-39.99	-204.52	-68.25	-220.47
01/13-01-030-21W3/0	Crescent	42.35	-120.53	-28.46	-105.29	779.64	-30.66	-60.10
01/02-33-024-14W3/0	Baytex	6.84	-59.56	-111.38	-29.00	315.96	152.82	168.47
01/06-14-029-22W3/0	Baytex	-52.45	-82.15	44.55	9.64	283.18	-220.95	108.19
01/04-28-025-18W3/0	Crescent	-18.83	-83.47	-115.44	-20.50	-92.58	-29.30	-100.59
02/15-30-029-22W3/0	Crescent	-83.32	-102.86	-10.39	-50.18	-198.01	-19.08	-240.72
01/16-28-029-21W3/0	Baytex	-2.42	-117.82	-69.07	-37.65	694.79	-480.94	62.70
02/12-05-030-24W3/0	Whitecap	168.08	690.88	180.43	21.88	1292.20	88.91	71.84
01/13-09-033-24W3/0	Whitecap	110.93	-12.53	93.09	161.22	570.57	232.48	-16.05
02/06-09-034-24W3/0	Baytex	4.66	-98.64	-122.23	30.91	332.54	-10.39	50.75
01/08-20-030-20W3/0	Crescent	156.97	446.69	163.65	65.60	1248.35	266.52	108.77
92/16-29-029-22W3/0	Crescent	-60.09	-113.18	-29.85	-47.08	-225.40	-75.65	-327.57

02/13-31-033-23W3/0	Baytex	-14.71	-139.36	-120.04	-50.71	-168.44	-90.14	46.52
03/05-16-030-20W3/0	Crescent	18.14	8.62	19.88	14.15	-256.67	92.79	-93.52
02/05-21-029-21W3/0	Baytex	-51.42	-87.19	-7.00	-10.82	-125.62	-234.79	120.79
01/05-33-029-21W3/0	Teine	8.14	-58.60	43.96	-38.89	-104.10	-20.95	37.60
01/12-18-026-18W3/0	Baytex	-36.41	219.33	27.19	-11.86	-182.75	-295.31	43.18
01/12-29-030-19W3/0	Crescent	37.13	-62.57	197.36	79.09	938.47	-0.07	2.06
02/10-35-029-25W3/0	Whitecap	94.72	764.28	263.15	554.70	1269.48	56.03	95.36
05/02-16-030-21W3/0	Baytex	39.68	95.24	50.61	11.66	-207.54	104.32	136.72
02/16-20-029-22W3/0	Crescent	9.47	-47.73	10.43	19.82	-172.96	71.42	81.58
03/13-26-026-20W3/0	Baytex	-51.57	132.49	11.92	18.41	-219.58	59.35	86.99
01/05-27-033-23W3/0	Baytex	86.83	-64.58	19.43	63.01	-174.04	158.40	-31.46
01/08-01-033-26W3/0	Ish	-8.31	-61.55	-138.93	-249.82	-216.27	30.28	-142.85
02/01-19-026-19W3/0	Baytex	30.74	133.85	59.45	45.31	-196.42	103.65	85.57
01/05-06-026-18W3/0	Baytex	-58.73	-64.95	-97.25	-142.67	-265.92	-6.91	37.73
02/02-28-031-26W3/0	Ish	-108.13	-11.78	-213.63	-388.07	-280.08	4.87	-356.34
03/01-13-030-21W3/0	Baytex	78.93	28.89	105.74	25.74	892.81	15.08	93.25
03/09-20-029-22W3/0	Crescent	-19.78	-54.22	7.61	8.31	-157.58	-15.53	39.83
01/16-34-025-18W3/0	Teine	38.30	-26.16	66.48	50.38	-31.15	394.67	128.17
02/11-18-030-21W3/0	Teine	-37.67	-26.15	-27.02	-47.51	-290.18	-46.00	-262.18
03/08-35-026-20W3/0	Teine	66.20	361.92	127.82	103.75	-99.25	438.11	146.32
01/05-20-029-22W3/0	Crescent	50.32	-38.22	38.64	30.57	-176.04	10.44	82.11
01/13-32-032-20W3/0	Teine	3.74	-40.38	36.24	56.40	31.15	98.32	73.80
91/12-13-030-21W3/0	Novus	-102.44	-68.75	-27.08	-118.68	-433.51	-630.60	48.34
02/04-33-029-21W3/0	Teine	-21.38	-103.34	-23.56	-98.34	-153.56	-119.44	-16.24
01/16-17-026-18W3/0	Teine	-28.84	188.33	32.25	18.58	-215.34	298.52	130.58
01/13-04-033-24W3/0	Whitecap	68.51	-58.61	24.07	78.27	-173.66	2.41	-44.19
91/03-10-026-19W3/0	Crescent	135.26	10.14	92.38	123.03	-162.72	180.13	214.09
91/15-10-026-19W3/0	Crescent	120.08	5.98	73.37	121.17	-155.01	49.11	205.18
02/10-29-033-23W3/0	Baytex	89.74	-51.63	5.67	32.19	-135.74	15.35	164.59
92/06-24-029-22W3/0	Baytex	-105.50	-62.04	-24.30	-19.98	-184.10	-100.14	94.65
02/05-33-029-21W3/0	Teine	-0.12	-63.87	32.90	-50.11	-139.05	-36.63	35.66
02/04-21-024-14W3/0	Baytex	-129.19	-174.39	-244.56	-84.53	725.20	31.55	19.80
01/04-15-034-24W3/0	Baytex	-59.71	-105.47	-139.82	-36.70	109.86	-404.33	-20.39
01/04-15-030-19W3/0	Baytex	-233.82	-180.79	-26.14	-27.95	-25.80	-83.72	-7.98

01/10-16-033-24W3/0	Whitecap	26.64	-80.49	-28.02	-9.82	-79.22	-164.75	-92.96
01/05-26-029-25W3/0	Teine	-8.74	-8.13	-50.38	-79.30	-224.83	145.85	19.26
01/05-05-030-21W3/0	Teine	103.64	8.16	99.15	16.92	-108.32	8.64	91.77
92/15-10-026-19W3/0	Crescent	27.24	-0.14	47.51	96.59	-204.68	93.36	182.41
01/12-20-029-22W3/0	Crescent	-12.96	-109.08	-44.67	-17.07	-238.46	84.41	-128.59
01/08-10-032-26W3/0	Ish	-33.45	-26.88	-84.12	-147.73	-176.02	84.08	-12.69
92/02-10-026-19W3/0	Crescent	169.13	30.03	124.11	157.75	-115.61	80.23	249.59
01/07-31-029-21W3/0	Baytex	25.08	-15.74	15.25	-12.07	-123.42	-299.74	121.63
02/13-05-030-25W3/0	Whitecap	-8.51	344.98	215.81	530.88	1388.61	149.42	112.09
02/13-32-031-25W3/0	Ish	-53.77	-75.18	-89.16	-114.42	-205.65	51.90	64.34
91/01-01-030-20W3/0	Novus	-137.39	-148.44	-24.22	-95.37	-54.98	-564.12	-295.18
01/05-14-030-20W3/0	Teine	-69.30	-64.79	9.82	-16.02	780.57	176.98	50.60
02/08-20-029-22W3/0	Crescent	83.24	-3.58	104.74	75.99	508.11	249.44	165.68
02/14-26-029-22W3/0	Teine	36.17	-24.67	55.88	32.18	-160.84	156.78	152.98
01/06-15-030-24W3/0	Whitecap	45.90	271.91	26.86	-15.99	-148.85	0.39	-94.91
01/13-17-026-19W3/0	Teine	1.08	0.50	22.24	19.79	-166.63	89.55	106.61
01/03-20-031-18W3/0	Crescent	10.14	-126.67	125.01	-20.11	179.86	78.82	-76.09
05/03-24-033-24W3/0	Whitecap	37.57	-116.91	2.73	-13.91	522.88	143.81	-118.45
03/12-28-033-24W3/0	Crescent	-25.63	-155.38	-160.74	-77.16	-274.97	-131.79	-144.71
03/06-17-031-19W3/0	Teine	154.83	39.79	388.56	153.45	1343.88	443.51	134.80
03/16-35-029-22W3/0	Teine	24.58	59.46	105.10	38.64	-93.08	14.88	147.70
01/12-19-029-22W3/0	Baytex	-76.29	-119.25	-14.00	-50.29	-156.75	-274.29	59.39
02/14-04-030-25W3/0	Whitecap	-51.45	338.33	47.02	202.80	-214.22	11.15	-65.16
02/05-25-029-22W3/0	Teine	38.87	-27.15	23.14	1.42	-100.29	-8.72	132.09
03/05-36-029-25W3/0	Whitecap	49.76	193.62	144.14	288.09	90.92	-119.51	13.63
01/09-25-029-22W3/0	Teine	12.21	-51.13	15.96	-15.33	-146.12	-31.28	95.38
04/14-30-029-22W3/0	Crescent	-49.51	-99.77	-17.56	-35.27	-216.16	-17.96	-241.81
03/05-32-025-18W3/0	Crescent	10.00	-84.38	-9.08	-4.42	-189.57	122.04	-55.12
02/04-30-029-22W3/0	Crescent	-100.18	-134.00	-43.02	-72.79	-242.06	-25.41	-288.37
91/09-21-029-24W3/0	Baytex	11.99	-25.44	-44.92	-66.28	-218.24	-24.81	-233.63
02/13-06-033-25W3/0	Ish	-47.94	-30.92	-241.24	-360.25	-256.03	-22.15	-199.46
02/08-18-029-22W3/0	Baytex	-76.56	-119.01	41.31	-12.50	371.58	183.82	96.35
02/01-17-029-21W3/0	Baytex	-62.16	-89.99	-26.70	-36.49	888.86	223.53	47.36
01/02-28-034-24W3/0	Baytex	-113.00	-149.68	-187.34	10.29	266.52	-186.41	-19.88

01/14-31-033-23W3/0	Baytex	-53.72	-128.24	-130.78	-57.22	-159.46	-245.31	-1.15
01/04-01-026-19W3/0	Teine	0.52	-83.00	24.40	32.22	73.79	181.99	128.97
01/02-33-025-18W3/0	Teine	-10.47	-38.40	66.43	58.55	57.62	301.86	171.53
01/13-18-033-25W3/0	Ish	-16.13	-97.64	-127.90	-227.33	-219.49	38.58	-96.88
91/06-06-034-23W3/0	Baytex	-25.18	-140.06	-129.35	-60.27	-233.61	29.26	45.08
01/09-19-026-18W3/0	Teine	6.86	50.56	24.35	11.89	19.52	191.47	-208.39
01/01-08-030-19W3/0	Baytex	-174.09	-213.57	-55.64	-55.03	711.86	-23.56	-59.24
01/03-16-030-24W3/0	Whitecap	-9.11	147.56	-3.35	-26.15	-186.65	-17.61	-135.47
01/12-27-033-24W3/0	Baytex	49.99	-105.74	-54.71	-27.01	-136.24	-72.74	74.40
03/03-17-031-19W3/0	Teine	89.87	0.66	234.74	82.25	1169.66	-41.27	93.46
02/11-29-026-19W3/0	Baytex	111.03	285.65	94.65	117.92	-148.78	239.85	162.68
02/10-24-026-20W3/0	Baytex	-23.86	-61.58	-5.06	-1.18	-222.86	64.07	78.64
01/04-25-029-22W3/0	Teine	22.87	-20.26	20.20	3.22	-70.22	-16.36	131.27
91/01-13-030-20W3/0	Novus	-77.47	-32.36	2.46	-13.60	-159.58	-288.02	-88.79
02/16-32-025-18W3/0	Crescent	53.36	-128.42	-28.26	-22.28	-212.24	-4.66	-29.47
02/08-12-033-26W3/0	Ish	-8.05	-59.88	-148.02	-248.92	-233.32	26.69	-177.57
01/16-17-026-19W3/0	Teine	36.41	8.85	45.55	72.82	-146.36	285.11	116.93
91/14-10-026-19W3/0	Crescent	4.93	-47.20	13.34	52.74	-229.33	-19.88	133.34
01/09-30-033-23W3/0	Teine	127.24	-143.45	38.88	-15.78	979.85	199.73	87.68
01/08-16-033-24W3/0	Whitecap	78.72	-38.00	79.78	150.09	47.23	-65.23	-14.02
02/07-35-026-20W3/0	Teine	80.46	369.21	131.14	102.70	-115.62	448.58	152.42
02/11-30-030-22W3/0	Baytex	73.52	133.31	201.64	52.13	-172.53	170.78	-11.46
04/08-32-025-18W3/0	Crescent	-2.97	-104.43	-18.96	-20.06	-187.38	0.79	-19.51
91/01-30-029-22W3/0	Crescent	-73.02	-84.98	-9.07	-11.08	-192.26	18.05	-164.95
01/13-14-030-19W3/0	Baytex	-105.82	-136.32	13.09	25.01	-163.60	-56.35	77.66
01/02-14-034-24W3/0	Baytex	-101.09	-151.72	-192.21	-78.34	109.96	-409.70	7.64
01/05-29-033-23W3/0	Baytex	38.60	-95.82	-49.05	-8.52	-197.14	120.31	106.30
01/16-26-029-22W3/0	Nal	16.89	-17.43	37.41	30.13	-157.42	131.28	152.91
02/14-30-029-22W3/0	Crescent	-58.93	-95.70	-19.51	-37.09	-80.00	-75.11	-191.67
02/02-06-033-25W3/0	Ish	-0.72	3.32	-205.34	-303.70	-226.34	24.45	-128.08
01/03-17-026-19W3/0	Teine	37.86	5.23	48.71	66.66	-184.58	305.02	120.57
02/01-30-030-19W3/0	Crescent	31.69	-43.93	130.59	72.65	18.21	-29.36	45.30
91/16-19-029-24W3/0	Baytex	-40.37	2.42	-60.59	21.44	-272.48	-84.99	-309.12
02/08-01-030-22W3/0	Teine	33.66	-32.78	54.92	-10.61	-159.46	-25.92	109.40

02/02-17-026-19W3/0	Teine	32.23	11.87	53.67	68.23	-130.41	293.01	113.10
02/14-26-029-25W3/0	Teine	20.97	75.65	44.09	129.06	-253.37	-29.82	23.26
01/08-11-030-20W3/0	Crescent	43.74	-2.25	104.18	60.66	414.90	35.23	135.33
01/06-19-029-22W3/0	Baytex	-103.64	-124.44	-7.27	-25.04	-200.46	171.44	96.24
03/15-26-029-22W3/0	Nal	32.99	-8.78	55.83	39.46	-149.25	132.63	176.80
01/12-27-025-18W3/0	Teine	2.18	-72.16	20.46	47.99	-195.11	366.33	146.17
02/08-32-026-19W3/0	Baytex	72.32	120.95	42.54	82.63	-208.58	85.31	50.12
01/06-29-033-23W3/0	Baytex	63.57	-78.97	-14.84	-6.18	-148.57	-99.43	123.80
02/04-20-033-23W3/0	Teine	14.49	-146.44	-73.88	-60.96	-269.11	-67.79	-133.30
02/01-32-029-25W3/0	Whitecap	-37.15	352.00	121.17	222.36	-270.83	-21.81	-41.26
03/01-16-030-21W3/0	Baytex	68.78	114.14	32.31	18.07	-158.82	-385.93	157.91
02/13-30-025-18W3/0	Crescent	-24.27	-165.67	-254.05	-117.21	308.61	-51.99	-182.44
01/16-32-026-19W3/0	Baytex	127.04	214.85	91.51	140.85	-157.50	157.45	177.08
02/12-13-029-22W3/0	Teine	-164.03	-125.18	-32.47	-41.94	-157.57	-69.80	6.32
01/02-04-033-24W3/0	Whitecap	-0.46	-118.84	-73.31	-35.68	18.08	-339.77	-93.34
01/14-06-030-24W3/0	Whitecap	42.31	548.16	97.72	122.34	-261.35	-14.68	-24.02
01/15-05-032-25W3/0	Ish	-32.63	-68.82	-115.61	-133.13	-201.97	50.96	19.04
01/11-09-033-24W3/0	Whitecap	52.03	-41.28	67.71	112.07	568.38	-21.51	-45.99
03/01-19-026-19W3/0	Baytex	7.55	85.32	40.27	6.51	-222.22	68.59	47.53
02/01-22-029-22W3/0	Baytex	-86.80	-75.62	-30.67	-17.58	-212.55	90.13	97.60
01/13-05-030-21W3/0	Teine	73.70	4.38	67.80	-14.40	-90.46	-162.31	111.09
01/01-27-025-18W3/0	Teine	-47.57	-107.87	-98.73	-24.97	-213.88	324.89	80.24
91/16-10-026-19W3/0	Crescent	46.87	7.46	71.86	121.59	-143.69	122.41	204.45
01/01-28-029-22W3/0	Crescent	-60.53	-59.18	-19.83	-27.57	-243.60	131.26	7.23
01/09-16-029-22W3/0	Baytex	-74.41	-104.71	-7.53	-15.15	-134.85	-129.23	116.81
02/05-24-030-22W3/0	Teine	-56.74	-137.19	-29.14	-76.32	-178.15	-260.45	19.99
02/06-12-033-26W3/0	Ish	-1.63	-51.04	-134.32	-189.41	-207.67	62.24	-84.46
02/03-01-027-20W3/0	Teine	41.20	253.70	85.04	55.02	-138.58	374.69	117.15
91/02-10-026-19W3/0	Crescent	51.12	-7.91	66.54	105.93	-196.75	114.21	177.38
91/03-13-030-21W3/0	Novus	-115.93	-67.23	-35.41	-102.34	-447.09	-542.50	11.77
03/10-24-026-20W3/0	Baytex	-19.31	-62.41	-1.42	14.84	-216.74	81.84	92.92
92/12-24-029-22W3/0	Baytex	-52.27	-23.68	-5.85	10.86	-131.89	-113.19	138.07
03/12-30-032-25W3/0	Ish	9.33	-51.21	-116.08	-170.29	-208.20	51.97	-49.47
02/14-06-031-19W3/0	Teine	22.84	98.84	114.00	31.22	-185.91	-19.55	92.27

02/01-16-032-26W3/0	Ish	-84.38	8.72	-171.04	-334.94	-223.84	34.09	-183.52
02/03-03-030-25W3/0	Whitecap	93.37	498.15	222.57	552.13	1334.75	146.82	7.85
02/14-30-030-22W3/0	Baytex	49.33	116.10	165.79	35.20	-178.42	125.82	120.54
02/15-30-030-20W3/0	Baytex	128.68	113.77	157.85	81.88	-182.69	228.84	194.36
02/07-10-034-24W3/0	Baytex	0.69	-123.80	-158.14	-54.01	231.61	-318.83	25.73
02/05-32-025-18W3/0	Crescent	62.70	-88.59	18.98	30.00	-166.46	-17.48	12.30
01/12-28-033-24W3/0	Crescent	18.89	-139.29	-126.52	-50.87	12.59	-375.63	-38.74
02/09-19-026-19W3/0	Baytex	-88.14	-137.72	-84.34	-71.59	-326.93	-138.40	-72.73
01/07-34-032-20W3/0	Teine	100.00	16.03	52.74	61.15	-143.69	49.85	-92.34
02/06-32-026-19W3/0	Baytex	45.87	66.63	-1.91	46.48	-289.79	51.35	24.15
01/05-23-025-18W3/0	Teine	-157.32	-235.11	-286.58	-103.42	640.81	44.41	14.65
02/12-16-030-20W3/0	Crescent	-0.92	-15.13	0.62	-1.01	-285.44	64.82	-128.23
02/08-32-025-18W3/0	Crescent	33.97	-90.19	-4.58	-0.55	-169.45	22.91	-26.06
02/16-12-033-26W3/0	Ish	-17.31	-68.02	-158.17	-224.13	-225.94	27.29	-128.66
02/04-34-033-23W3/0	Baytex	48.33	-111.65	-93.47	-25.15	-157.12	-324.07	93.99
01/03-18-030-20W3/0	Baytex	29.72	65.85	32.70	19.71	-237.74	95.33	48.67
01/06-03-030-25W3/0	Whitecap	37.52	422.42	156.35	443.22	1255.72	93.15	-87.45
02/12-30-030-19W3/0	Crescent	87.62	-25.13	204.93	107.03	-144.36	28.56	93.12
01/16-20-029-22W3/0	Crescent	-7.72	-68.49	0.92	21.26	-204.54	125.80	13.02
01/03-27-033-23W3/0	Baytex	68.89	-105.51	2.35	-7.05	920.03	-57.34	79.85
02/12-29-029-21W3/0	Baytex	22.97	-72.31	17.65	-34.60	-5.60	-522.13	99.50
03/06-28-025-18W3/0	Crescent	17.71	-64.35	-14.09	10.56	576.23	32.39	126.56
01/03-03-033-26W3/0	Ish	-81.59	-72.01	-179.09	-327.66	-233.62	40.20	-152.72
01/02-35-029-26W3/0	Novus	63.58	46.69	177.04	122.03	-42.91	171.78	154.33
02/09-02-033-26W3/0	Ish	-10.85	-29.70	-199.83	-273.89	-237.42	24.37	-47.94
01/12-35-029-22W3/0	Teine	7.78	81.78	130.28	58.58	-103.11	74.09	200.83
02/07-31-029-21W3/0	Baytex	5.90	-3.94	12.83	-12.84	-173.23	8.06	127.61
01/13-30-025-18W3/0	Crescent	-1.35	-154.25	-240.38	-100.48	335.37	-34.39	-156.04
02/07-12-033-26W3/0	Ish	-11.39	-59.07	-144.77	-240.89	-220.89	35.18	-112.34
01/12-21-029-24W3/0	Baytex	5.68	-38.78	-66.60	-52.61	-228.92	-34.66	-225.12
01/01-30-030-19W3/0	Crescent	-13.08	-79.73	110.53	44.75	-202.55	59.51	30.20
02/13-12-033-26W3/0	Ish	-23.04	-70.36	-166.48	-286.84	-230.33	25.82	-135.00
01/15-04-033-24W3/0	Whitecap	42.07	-83.74	-17.21	15.79	83.61	-194.71	-59.56
01/05-20-033-23W3/0	Teine	-24.07	-115.51	-89.67	-62.61	-235.48	-82.69	-38.31

02/15-01-027-20W3/0	Teine	39.50	296.95	61.67	60.41	-174.76	106.99	87.81
91/10-05-033-24W3/0	Baytex	65.75	-32.98	44.51	155.89	165.21	-21.42	4.62
01/12-10-033-24W3/0	Whitecap	18.92	-130.24	-49.23	-30.83	-250.42	-50.10	-222.42
04/01-16-030-20W3/0	Crescent	-1.81	-7.57	12.56	-4.54	-265.26	81.22	-90.08
02/15-12-033-26W3/0	Ish	1.35	-35.15	-132.98	-180.39	-190.24	67.46	5.49
01/04-31-033-23W3/0	Baytex	17.09	-97.00	-53.54	-12.23	-168.70	3.03	35.53
02/04-24-030-22W3/0	Teine	-49.71	-143.16	-27.48	-77.75	-284.13	-138.86	39.24
02/14-12-033-26W3/0	Ish	-3.32	-55.21	-131.72	-209.08	-202.45	59.47	-130.23
01/15-22-026-19W3/0	Crescent	160.03	409.59	123.58	165.37	-108.53	106.47	193.94
02/06-09-030-25W3/0	Novus	-5.83	-53.67	-48.19	36.38	-341.67	39.13	-309.29
02/16-18-026-19W3/0	Baytex	-10.19	-139.77	2.88	-10.65	-218.06	-3.52	69.29
02/12-16-033-25W3/0	Ish	-5.94	-84.61	-126.34	-178.13	-209.46	1.61	-15.81
01/01-09-030-25W3/0	Novus	-79.69	-128.70	-90.77	49.20	692.25	-174.73	-84.28
02/15-09-033-24W3/0	Whitecap	35.56	-40.35	79.26	30.34	1104.94	150.49	-3.75
01/12-01-026-19W3/0	Teine	-120.19	-145.63	-41.50	-21.07	-167.19	161.36	60.63
03/06-31-029-21W3/0	Baytex	4.01	-37.26	-4.38	-38.15	-168.66	-500.06	105.86
02/06-03-030-25W3/0	Whitecap	81.22	492.08	216.59	569.33	1371.51	154.97	-31.46
02/14-19-026-18W3/0	Teine	79.97	130.93	132.15	81.51	177.73	381.43	180.43
03/10-35-029-25W3/0	Whitecap	35.98	755.17	247.22	500.86	1162.77	-61.90	70.65
01/10-35-029-25W3/0	Whitecap	177.15	885.62	331.28	666.55	1495.81	319.80	197.44
03/03-35-030-22W3/0	Baytex	29.10	75.24	153.11	34.66	-175.68	389.01	157.70
91/04-10-026-19W3/0	Crescent	146.84	9.51	110.61	122.05	-131.85	90.41	227.83
02/12-32-025-18W3/0	Crescent	48.65	-76.32	8.89	8.87	-198.97	101.64	-8.15
01/16-18-026-19W3/0	Baytex	6.84	-118.58	16.29	25.35	-192.82	114.91	88.48
01/09-27-029-25W3/0	Whitecap	66.82	187.63	133.32	395.94	-228.70	21.26	-49.92
02/07-01-033-26W3/0	Ish	6.18	-51.04	-112.18	-205.10	-200.64	55.47	-93.02
03/08-21-029-21W3/0	Baytex	-71.50	-106.64	-28.44	-34.02	-150.16	-430.66	85.77
01/06-03-033-24W3/0	Whitecap	34.31	-88.71	-23.76	18.02	-207.73	-15.82	-185.23
01/03-32-032-25W3/0	Ish	-16.39	-72.99	-132.72	-169.70	-217.00	47.81	-72.67
01/15-32-024-14W3/0	Baytex	-0.22	-135.35	-172.05	-53.10	336.49	7.99	94.28
06/08-28-033-23W3/0	Whitecap	-17.97	-186.20	-147.70	-88.59	556.38	-431.68	-115.73
06/12-30-025-18W3/0	Crescent	-109.89	-196.92	-385.43	-161.20	232.80	-73.86	-242.80
01/08-16-030-19W3/0	Baytex	-179.01	-153.99	5.57	-25.92	122.91	-1.06	53.15
02/03-16-029-22W3/0	Baytex	-27.28	-105.98	29.37	-36.45	762.60	-400.84	50.19

02/01-25-029-22W3/0	Teine	-11.24	-54.93	-23.66	-26.21	-147.97	-36.75	81.46
02/08-34-032-20W3/0	Teine	175.64	80.46	180.03	140.46	163.23	76.56	30.82
02/14-02-030-22W3/0	Crescent	-25.97	-142.00	-7.36	-109.67	793.97	128.95	-152.70
01/10-34-032-20W3/0	Teine	-58.92	-28.39	-79.96	-9.75	-235.68	-67.46	-27.96
01/16-22-031-19W3/0	Teine	125.67	63.82	321.35	138.29	1367.82	96.91	150.45
01/16-18-029-22W3/0	Baytex	0.66	-116.78	-25.15	-19.44	-186.12	-67.83	75.69
01/14-04-030-25W3/0	Whitecap	-43.14	312.52	33.27	180.95	-246.34	-15.15	-177.76
91/11-24-029-22W3/0	Baytex	-81.21	-54.05	-34.64	-20.94	-193.88	-78.94	103.63
93/15-33-029-25W3/0	Whitecap	91.37	506.44	200.78	396.98	-199.56	44.99	45.87
02/16-17-026-19W3/0	Teine	6.41	-3.13	29.61	57.45	-177.80	202.34	99.34
02/08-12-033-20W3/0	Crescent	45.52	-35.32	50.58	94.50	-146.20	122.32	34.32
02/16-36-033-24W3/0	Baytex	18.70	-117.12	-120.33	-51.83	-139.74	-218.34	19.89
02/13-16-030-21W3/0	Teine	28.85	104.82	55.76	3.68	-159.26	12.28	59.51
91/01-03-030-20W3/0	Novus	-186.98	-148.75	-40.25	-132.81	-67.87	-662.66	-305.82
02/15-17-026-19W3/0	Teine	49.11	-11.14	34.37	60.10	-155.27	244.50	110.56
01/14-17-026-19W3/0	Teine	34.98	-4.30	35.08	60.19	-178.21	270.82	112.93
01/01-30-031-19W3/0	Teine	-22.48	-123.95	-24.13	-41.52	-295.08	-56.84	-507.21
02/14-06-033-25W3/0	Ish	-39.78	-26.47	-232.27	-342.12	-256.73	-21.03	-216.34
01/09-34-032-19W3/0	Teine	-39.69	-114.62	-78.29	-27.55	-209.38	-263.90	-248.01
01/04-30-029-22W3/0	Crescent	-101.47	-121.74	-47.62	-74.26	-215.69	-101.31	-353.83
04/11-28-030-19W3/0	Crescent	70.35	-24.79	215.95	65.13	620.50	67.82	-30.25
92/13-28-029-22W3/0	Crescent	24.20	-78.26	-12.15	-18.82	-217.46	-14.55	-184.56
03/07-35-026-20W3/0	Teine	73.43	371.28	129.00	108.35	-136.77	443.55	152.51
01/14-10-026-19W3/0	Crescent	69.99	17.52	87.38	108.67	-160.07	8.10	180.36
01/16-04-033-24W3/0	Whitecap	17.63	-118.33	-57.00	-5.68	-228.87	-39.99	-216.73
03/06-04-030-25W3/0	Whitecap	-23.22	384.57	102.43	241.83	-219.20	24.63	12.42
01/04-17-026-19W3/0	Teine	33.24	6.64	65.50	75.27	-158.20	356.55	132.68
01/13-11-033-26W3/0	Ish	-15.64	-102.28	-174.78	-288.78	-234.64	35.33	-111.08
01/06-18-029-21W3/0	Baytex	-104.90	-86.42	30.44	-5.50	364.03	160.80	99.25
01/11-04-030-25W3/0	Whitecap	-38.78	295.14	36.14	180.70	-274.73	-42.27	-77.81
02/12-20-029-22W3/0	Crescent	-75.45	-79.28	-20.33	-13.98	-203.35	8.68	56.82
92/09-24-029-22W3/0	Baytex	-91.50	-50.04	-20.98	-21.84	-153.96	-409.88	102.97
92/15-26-029-25W3/0	Baytex	45.59	104.78	57.80	144.03	-222.29	85.46	-78.38
02/13-10-026-19W3/0	Crescent	32.06	-5.74	57.71	81.96	-177.87	21.08	176.10

02/13-26-026-20W3/0	Baytex	-1.60	66.05	-10.11	-9.07	-257.88	-98.92	16.02
01/05-21-029-21W3/0	Baytex	-100.10	-81.15	-3.94	2.78	-182.39	142.40	119.63
02/02-35-029-26W3/0	Novus	79.24	40.45	161.64	85.72	-156.14	127.19	133.30
01/13-13-029-22W3/0	Teine	-130.48	-112.52	-15.57	-36.21	-200.12	-12.34	40.72
02/08-34-029-25W3/0	Whitecap	78.96	500.05	202.42	366.89	-248.22	3.01	36.70
02/12-22-033-24W3/0	Whitecap	45.47	-74.79	-27.56	-12.99	-157.11	-140.85	-80.82
01/16-12-026-19W3/0	Crescent	-21.86	-85.62	-28.15	-54.18	-243.01	33.74	-179.14
01/01-32-031-19W3/0	Teine	104.16	-28.26	128.55	117.74	152.39	46.00	-36.33
01/08-27-029-25W3/0	Whitecap	29.83	281.95	85.95	505.71	1156.47	114.68	-20.06
01/04-12-033-20W3/0	Crescent	34.38	-52.76	21.18	64.26	-166.62	101.50	-1.12
02/07-10-032-26W3/0	Ish	-50.78	-47.13	-114.90	-211.65	-204.22	66.46	-137.37
01/13-28-033-24W3/0	Crescent	10.80	-129.51	-100.30	-38.08	-230.62	-48.99	-104.99
01/15-28-029-21W3/0	Baytex	23.55	-103.96	0.44	-29.13	-137.11	-277.75	98.23
01/04-32-031-19W3/0	Teine	-1.57	-66.47	-4.13	2.70	-238.99	7.94	-258.19
01/05-35-033-24W3/0	Whitecap	102.45	-129.40	-12.12	-9.95	1099.16	140.60	54.15
01/13-03-032-25W3/0	Ish	28.55	-107.45	-119.71	65.91	-233.83	52.79	-12.16
02/02-36-033-24W3/0	Baytex	16.28	-104.55	-92.60	-17.16	-206.02	116.70	44.85
02/07-06-031-19W3/0	Teine	109.69	138.16	157.90	97.25	76.91	-2.51	147.76
01/04-34-033-23W3/0	Baytex	24.37	-127.92	-122.44	-47.62	-198.22	-207.57	49.28
02/16-30-032-25W3/0	Ish	-4.60	-56.32	-126.13	-188.96	-217.53	38.68	-70.25
01/02-31-029-24W3/0	Whitecap	79.63	517.57	191.16	212.51	-119.44	42.19	9.42
01/01-14-033-26W3/0	Ish	4.46	-52.27	-117.04	-226.76	-196.21	60.28	-45.58
01/09-16-030-20W3/0	Crescent	25.20	20.28	20.69	-5.52	-149.94	-48.97	-58.24
01/10-19-029-22W3/0	Baytex	-47.08	-116.76	-38.22	-60.09	-166.34	-306.37	-20.34
04/03-24-033-24W3/0	Whitecap	35.86	-122.59	-23.17	-22.30	395.98	127.00	-137.62
01/09-07-030-19W3/0	Teine	-133.80	-130.47	17.53	-5.10	-163.27	-31.24	100.28
92/06-13-030-20W3/0	Novus	-49.10	-49.07	-17.34	-49.54	-169.56	-441.46	-67.16
04/12-01-026-19W3/0	Teine	-43.33	-141.80	-28.10	-10.44	-212.70	158.51	100.94
01/11-31-029-21W3/0	Baytex	104.91	61.71	110.01	37.64	-96.20	-77.06	220.16
02/08-16-033-24W3/0	Whitecap	46.29	-70.32	10.46	103.41	73.28	-142.95	-53.85
02/06-04-030-25W3/0	Whitecap	-87.10	279.33	42.49	167.41	-310.14	-76.72	-69.94
01/11-07-032-26W3/0	Ish	-120.22	-107.36	-196.98	-438.02	-253.32	52.36	-238.44
01/11-21-029-24W3/0	Baytex	-4.28	-57.72	-88.84	-73.83	-247.58	-42.44	-282.71
01/06-09-034-24W3/0	Baytex	-16.55	-131.97	-181.47	-15.68	103.88	-503.57	19.84

01/01-33-029-21W3/0	Teine	12.88	-96.92	8.33	-69.97	64.63	-105.85	79.50
01/05-12-033-20W3/0	Crescent	9.01	-66.79	7.29	43.78	-191.20	16.20	3.96
02/06-10-032-26W3/0	Ish	-87.50	-70.18	-169.14	-328.73	-245.21	-1.18	-236.31
02/16-25-029-22W3/0	Teine	45.60	-26.11	45.76	12.06	-128.36	14.65	150.02
03/16-28-031-26W3/0	Ish	-57.77	1.85	-166.55	-306.80	-227.27	39.75	-60.23
92/07-33-029-25W3/0	Whitecap	111.84	514.29	215.76	399.89	-174.21	46.58	18.82
01/09-27-033-24W3/0	Baytex	26.96	-72.78	-76.92	-19.93	-141.42	-192.30	16.49
92/16-30-029-22W3/0	Crescent	-46.38	-81.45	-3.21	-22.04	-168.06	-119.76	-152.14
02/11-16-029-22W3/0	Baytex	-121.41	-120.82	-29.04	-47.44	-172.03	-428.93	53.50
02/03-17-031-19W3/0	Teine	152.24	15.64	287.98	96.73	1255.29	183.41	118.07
03/14-17-031-19W3/0	Teine	191.56	53.92	407.23	153.05	1224.63	329.01	173.22
02/13-20-029-22W3/0	Crescent	-27.36	-124.39	-66.41	-30.34	-258.76	54.33	-155.96
01/02-28-029-24W3/0	Whitecap	7.58	368.19	4.39	-42.79	-161.06	-19.18	-170.40
01/08-30-029-24W3/0	Baytex	15.69	232.55	-25.68	44.55	-280.23	-9.13	-134.65
03/11-29-029-21W3/0	Baytex	30.29	-54.95	36.48	-14.13	-122.30	-241.29	126.36
02/04-03-033-26W3/0	Ish	-64.25	-49.59	-148.22	-258.84	-213.11	28.86	45.95
02/08-29-033-23W3/0	Baytex	84.13	-65.85	17.79	25.74	-145.54	-26.69	156.94
02/04-30-030-19W3/0	Crescent	-199.52	-142.89	-5.53	-30.51	-265.19	-89.73	-172.28
03/03-30-029-22W3/0	Crescent	-118.32	-100.77	-39.58	-49.51	-211.30	-25.46	-218.14
04/04-16-030-20W3/0	Crescent	24.48	29.77	30.27	24.36	-244.57	112.83	-83.96
01/02-32-031-19W3/0	Teine	174.72	21.35	136.39	130.12	-139.65	73.02	32.33
01/12-10-034-24W3/0	Baytex	-17.19	-115.12	-112.02	-39.75	-156.30	-90.04	51.55
02/04-06-033-25W3/0	Ish	-42.00	-24.91	-218.92	-319.25	-248.47	28.03	-190.13
01/04-28-033-24W3/0	Crescent	-24.17	-112.41	-112.19	-46.17	-16.40	-83.65	-61.50
01/06-08-031-18W3/0	Nal	63.70	-30.57	94.21	-3.49	-265.45	62.29	102.52
02/04-12-033-26W3/0	Ish	-19.42	-59.78	-161.13	-253.42	-213.09	35.40	-77.58
03/13-28-031-26W3/0	Ish	-60.20	4.65	-185.46	-391.69	-238.03	20.52	-214.66
01/04-04-033-24W3/0	Whitecap	-1.08	-124.32	-80.74	-13.44	-238.65	-59.33	-211.53
02/05-22-030-21W3/0	Baytex	32.38	123.38	73.70	31.67	-189.42	142.31	162.72
01/08-05-033-26W3/0	Ish	-36.06	-88.14	-160.60	-365.98	-207.79	22.13	4.94
03/09-12-030-22W3/0	Teine	39.28	29.23	40.94	-12.99	-116.07	-195.45	33.60
01/10-16-026-18W3/0	Baytex	-107.39	92.28	-86.39	-186.11	-347.85	22.14	-290.74
01/09-13-029-22W3/0	Teine	-113.73	-102.82	-17.34	-8.09	-130.33	-32.37	41.68
02/11-20-033-23W3/0	Teine	-5.99	-145.01	-100.26	-68.76	-272.53	-87.99	-132.53

03/14-19-026-19W3/0	Baytex	-27.50	13.42	-35.10	-15.40	-237.38	36.12	9.20
03/07-05-030-21W3/0	Teine	-0.80	-60.28	16.25	-49.93	-235.24	-76.79	-155.32
05/12-30-025-18W3/0	Crescent	-91.93	-174.82	-328.50	-152.69	125.91	-21.19	-234.79
02/03-13-030-21W3/0	Baytex	34.26	54.37	89.66	13.69	492.26	183.12	155.30
03/12-29-026-19W3/0	Baytex	117.25	296.75	97.41	110.25	-158.94	259.00	180.16
01/08-34-032-20W3/0	Teine	147.04	59.31	134.36	105.33	-36.28	69.31	14.28
01/10-07-033-24W3/0	Baytex	77.51	-39.13	35.64	148.37	-177.32	113.94	9.09
01/05-04-033-24W3/0	Whitecap	11.55	-112.78	-66.25	-35.51	20.30	-371.42	-77.05
02/06-01-033-26W3/0	Ish	18.90	-43.31	-83.61	-132.42	-165.61	74.46	-29.75
01/13-18-026-18W3/0	Baytex	-14.93	286.59	53.84	7.22	-154.52	-232.55	23.04
01/01-24-030-21W3/0	Baytex	11.23	62.07	68.58	20.30	-217.65	109.89	160.07
02/08-33-029-21W3/0	Teine	-10.32	-74.43	12.52	-71.86	-136.40	-72.36	18.73
02/05-03-030-22W3/0	Teine	-21.71	-39.39	9.88	-72.59	-265.19	-65.40	-35.23
02/05-12-033-20W3/0	Crescent	33.12	-49.85	31.11	69.78	-190.30	113.55	2.61
02/03-28-030-19W3/0	Crescent	29.62	-42.54	155.57	59.25	969.75	5.70	-27.96
02/14-18-030-21W3/0	Teine	2.85	-5.40	-10.15	-26.00	-265.49	-14.65	-234.27
01/02-17-033-24W3/0	Crescent	66.33	-46.91	13.38	96.86	-24.70	-13.37	9.52
02/08-21-029-21W3/0	Baytex	-109.32	-96.31	-23.31	-26.14	-203.99	100.41	82.70
92/11-34-029-24W3/0	Baytex	34.37	81.83	98.56	20.77	-180.77	151.64	-86.16
92/10-26-029-25W3/0	Baytex	73.12	92.07	56.48	108.73	-231.52	87.78	-8.07
01/12-04-033-24W3/0	Whitecap	19.28	-99.73	-46.38	-5.66	-227.35	-40.40	-136.17
01/13-28-029-21W3/0	Baytex	9.83	-108.05	-0.02	-39.43	-146.58	-225.49	89.40
01/06-25-024-14W3/0	Baytex	-106.30	-75.22	-111.94	-52.83	659.05	-316.13	43.98
02/04-26-031-23W3/0	Baytex	68.38	534.44	152.40	-0.04	618.28	-60.36	63.21
01/08-27-033-24W3/0	Baytex	43.53	-84.51	-41.29	-27.08	-120.40	-209.78	-14.88
01/13-05-030-25W3/0	Whitecap	-22.76	325.14	202.62	472.39	1323.66	132.09	72.33
04/02-16-030-21W3/0	Baytex	54.99	124.65	74.77	31.70	-173.72	117.16	171.38
01/01-31-033-23W3/0	Baytex	-80.74	-123.81	-91.75	-47.14	-149.59	-148.98	9.27
02/16-20-032-26W3/0	Ish	-52.10	30.55	-138.70	-272.39	-205.04	70.76	63.05
01/05-19-026-18W3/0	Teine	10.27	62.71	30.03	-11.05	75.41	163.18	-150.80
01/03-31-033-23W3/0	Baytex	10.73	-106.30	-72.14	-25.61	-168.51	-3.18	49.17
01/05-03-030-22W3/0	Teine	26.20	34.69	48.18	-39.58	-189.14	-161.59	46.37
01/16-31-029-25W3/0	Whitecap	-19.66	-1.39	80.04	-134.61	-252.39	-59.25	-287.64
03/01-16-030-20W3/0	Crescent	0.58	10.57	25.08	-1.97	-241.01	76.93	-68.90

04/05-32-025-18W3/0	Crescent	55.43	-116.76	-16.97	-8.52	-183.09	6.42	-38.38
04/08-28-025-18W3/0	Crescent	64.43	-61.11	12.00	49.55	988.74	17.01	84.27
01/04-21-029-21W3/0	Baytex	-30.91	-40.16	47.12	31.91	-128.96	198.33	180.89
01/11-16-026-19W3/0	Teine	81.97	129.47	96.43	103.76	-97.00	259.64	146.55
04/06-28-025-18W3/0	Crescent	91.87	-45.81	41.38	67.51	1071.71	88.76	113.62
01/15-17-033-24W3/0	Crescent	67.94	-65.17	-0.20	98.27	-185.39	21.78	5.23
03/07-31-029-21W3/0	Baytex	-8.36	-43.17	-24.89	-48.40	-202.29	-127.46	75.65
91/08-03-030-20W3/0	Novus	-187.97	-145.59	-45.06	-130.53	-79.99	-626.57	-392.07
01/04-29-029-24W3/0	Whitecap	-58.84	262.73	-155.97	-168.18	809.75	-113.69	-250.36
92/05-24-029-22W3/0	Baytex	-46.40	-23.09	9.94	12.13	-134.05	-111.91	136.14
02/07-35-029-25W3/0	Whitecap	92.45	778.57	248.33	573.60	1259.40	165.53	75.77
02/08-09-032-26W3/0	Ish	-99.74	-81.51	-206.55	-414.65	-264.70	-36.24	-267.98
91/11-34-029-24W3/0	Baytex	15.00	43.17	67.98	-10.02	-261.64	108.52	-143.30
02/07-09-030-24W3/0	Whitecap	65.74	459.75	72.00	-7.69	-178.07	17.97	-23.05
01/04-14-030-20W3/0	Teine	-99.43	-70.98	-1.46	-29.99	777.96	144.07	47.47
01/01-17-026-19W3/0	Teine	54.10	-10.19	36.40	67.35	107.81	142.72	116.32
01/13-34-025-18W3/0	Teine	47.35	-3.64	105.78	95.71	181.40	465.52	209.32
01/04-30-030-19W3/0	Crescent	-119.10	-99.50	54.60	19.44	-193.78	-36.61	-34.09
02/15-28-031-26W3/0	Ish	-56.02	7.70	-184.37	-376.45	-256.42	16.87	-218.10
02/02-11-026-19W3/0	Crescent	121.50	-17.14	18.43	110.29	860.74	-128.05	99.81
01/08-03-034-24W3/0	Baytex	63.08	-75.82	-56.23	-23.41	-122.72	-56.03	45.71
02/05-05-030-21W3/0	Teine	58.16	-47.21	43.24	-43.95	-204.55	-136.86	34.43
01/14-34-025-18W3/0	Teine	34.26	-38.01	77.52	56.88	205.21	317.94	163.51
01/16-22-025-18W3/0	Crescent	-121.34	-119.29	-205.24	-103.01	-232.66	23.68	-102.26
02/02-19-026-19W3/0	Baytex	22.89	112.41	53.61	25.03	-188.42	77.08	59.67
01/16-31-025-18W3/0	Teine	-38.37	-143.80	-20.50	-18.90	-222.03	187.97	101.58
01/03-11-030-20W3/0	Crescent	-6.11	-79.21	24.72	-11.14	881.18	147.19	-2.19
02/04-29-029-24W3/0	Whitecap	-50.77	264.23	-120.80	-178.53	755.33	22.23	-149.87
02/08-35-026-20W3/0	Teine	35.38	314.91	109.44	98.65	174.86	286.42	145.00
01/13-16-033-24W3/0	Whitecap	22.58	-83.71	-29.29	104.90	-226.97	-43.67	-115.12
01/07-28-029-21W3/0	Baytex	-12.49	-121.83	-50.64	-62.16	-186.97	-176.12	4.87
01/12-32-025-18W3/0	Crescent	3.68	-167.37	-72.23	-107.20	-251.20	-70.64	-182.63
92/08-29-029-22W3/0	Crescent	34.34	-67.03	7.07	-11.92	-163.94	-55.61	-148.65
01/13-05-033-24W3/0	Baytex	14.15	-119.87	16.43	106.59	954.76	-25.34	-91.62

01/12-29-033-23W3/0	Baytex	42.27	-116.73	-85.10	-44.88	-144.39	-328.07	44.50
01/16-30-033-23W3/0	Teine	93.98	-161.83	-28.93	-32.83	1025.79	166.82	64.06
92/10-24-029-22W3/0	Baytex	-118.36	-51.13	-29.28	-18.83	-180.92	11.92	112.06
91/01-21-033-23W3/0	Whitecap	91.81	-43.46	23.05	45.42	134.72	-89.80	59.23
01/16-15-029-22W3/0	Baytex	-93.50	-110.94	-11.31	-22.38	-154.26	-192.25	71.82
01/02-31-033-23W3/0	Baytex	-3.87	-129.91	-96.07	-35.61	-200.27	23.15	58.33
02/06-28-030-19W3/0	Crescent	50.08	-65.42	116.10	60.89	-220.32	-25.41	-89.69
01/01-21-030-19W3/0	Teine	-53.80	-71.79	39.87	50.97	-197.15	101.33	50.05
01/12-21-034-24W3/0	Baytex	-68.51	-65.75	-106.38	140.45	288.93	-261.97	8.11
03/01-20-029-22W3/0	Crescent	-33.39	-31.77	68.81	45.98	476.51	194.62	122.90
02/04-21-029-21W3/0	Baytex	-73.03	-101.14	-6.88	-25.24	-140.41	-263.29	26.44
02/08-22-026-19W3/0	Crescent	151.13	395.53	127.05	178.12	-107.20	87.29	190.59
01/09-19-030-21W3/0	Teine	-53.97	293.73	90.86	-47.47	994.36	53.86	-24.96
02/09-31-033-23W3/0	Baytex	-118.55	-139.53	-123.07	-59.42	-160.59	-418.28	-13.30
01/01-27-029-25W3/0	Whitecap	38.40	304.75	102.91	568.23	1255.56	134.77	25.83
01/08-21-033-23W3/0	Whitecap	57.55	-100.19	4.52	19.56	-173.67	-18.98	-101.76
01/08-30-030-19W3/0	Crescent	-25.22	-48.09	123.99	75.13	-152.52	166.38	64.74
01/13-21-033-24W3/0	Teine	-12.76	-101.15	-101.86	-14.81	-230.85	-0.36	9.36
01/14-20-026-18W3/0	Baytex	-50.00	-130.70	-50.45	-142.79	-288.94	-2.43	-25.71
02/10-24-030-21W3/0	Baytex	131.02	82.37	117.61	58.33	-182.54	157.15	175.95
01/04-34-029-24W3/0	Baytex	31.30	20.85	34.37	-42.22	-279.10	104.67	-182.56
01/05-21-024-14W3/0	Baytex	-116.43	-149.15	-170.29	-110.46	-207.23	41.75	56.76
02/05-01-033-26W3/0	Ish	-37.11	-70.09	-119.86	-191.50	-215.97	2.78	-139.27
02/10-22-030-21W3/0	Baytex	67.09	167.85	120.17	29.53	-137.67	-130.95	162.72
01/14-06-026-18W3/0	Baytex	-19.57	-17.67	29.39	7.93	-142.48	-234.81	108.44
01/08-21-029-21W3/0	Baytex	-108.22	-86.06	-12.70	-24.45	-169.80	-19.95	113.40
04/12-30-025-18W3/0	Crescent	-24.29	-150.16	-233.37	-108.31	243.93	-23.06	-167.82
01/13-22-033-24W3/0	Whitecap	21.35	-97.04	-39.31	-18.93	-204.29	-96.60	-157.46
91/08-16-030-20W3/0	Crescent	-7.33	-10.88	-1.88	-16.69	-285.59	60.34	-110.89
02/14-24-029-26W3/0	Novus	-46.88	-152.12	3.56	-102.57	-221.01	50.65	52.41
01/16-19-030-19W3/0	Baytex	7.71	-94.64	63.62	29.87	-200.15	120.99	103.72
03/15-35-029-22W3/0	Teine	43.75	40.17	98.83	31.80	-55.30	-40.64	149.55
01/09-18-026-18W3/0	Baytex	-30.12	255.17	29.83	0.67	-170.96	-262.00	21.74
92/09-29-029-22W3/0	Crescent	16.18	-79.32	-1.71	-25.98	-203.55	-44.97	-193.57

01/08-24-030-21W3/0	Baytex	38.26	53.73	80.67	30.86	-205.87	136.43	58.61
01/03-30-029-22W3/0	Crescent	-141.57	-114.64	-60.60	-89.66	-228.07	-82.82	-243.94
01/15-22-033-24W3/0	Whitecap	50.10	-57.70	8.81	-0.85	-199.88	-24.48	-89.85
01/15-33-029-21W3/0	Teine	-6.33	-131.94	-41.31	-120.31	-241.11	-244.31	-262.43
01/09-22-025-18W3/0	Crescent	-121.04	-119.19	-201.94	-101.32	-197.13	-17.10	-84.75
02/13-25-029-22W3/0	Teine	55.06	-23.11	60.33	21.05	-131.73	43.74	160.42
01/05-01-030-25W3/0	Baytex	58.74	469.65	139.89	253.17	863.63	-264.74	22.23
01/11-32-029-24W3/0	Whitecap	63.13	632.11	167.68	113.36	197.91	48.26	-5.26
01/08-20-029-22W3/0	Crescent	0.23	-27.94	63.48	55.69	440.70	214.28	127.65
04/03-28-026-19W3/0	Teine	9.56	209.73	17.28	28.07	867.58	308.28	34.48
01/16-15-034-24W3/0	Baytex	-150.29	-198.21	-222.88	-107.18	489.49	-505.58	-28.14
04/14-28-031-26W3/0	Ish	-33.43	21.20	-138.46	-314.16	-209.13	54.41	-52.63
02/05-18-033-25W3/0	Ish	-14.21	-98.28	-143.71	-236.16	-214.09	19.87	-3.12
01/14-34-030-19W3/0	Crescent	-43.15	-72.95	215.84	94.41	1096.28	185.84	-12.44
01/05-09-034-24W3/0	Baytex	21.85	-71.59	-86.84	120.51	337.68	-297.30	36.91
03/04-16-030-20W3/0	Crescent	9.22	24.25	35.89	20.95	-232.24	90.56	-46.90
02/09-13-029-22W3/0	Teine	-71.49	-83.91	10.94	2.44	-107.44	-6.09	75.70
03/15-24-030-21W3/0	Baytex	144.19	115.52	165.59	92.76	-142.63	230.67	217.69
03/11-22-030-21W3/0	Baytex	12.62	114.47	112.25	31.35	-227.91	212.92	146.89
02/08-25-032-26W3/0	Ish	-8.88	-53.94	-119.22	-173.90	-209.55	5.02	-101.59
02/02-01-027-20W3/0	Teine	44.09	292.00	96.70	97.83	-141.46	403.28	142.38
02/04-27-033-24W3/0	Baytex	51.43	-87.26	-59.95	-25.47	-136.31	-141.80	39.45
02/13-20-033-23W3/0	Teine	-4.04	-115.25	-98.19	-46.57	-177.34	-34.81	-15.71
03/05-30-030-19W3/0	Crescent	-150.61	-111.30	42.08	5.87	-267.37	63.40	-39.40
02/06-17-032-26W3/0	Ish	-74.59	-59.12	-158.78	-352.51	-219.85	27.52	-69.57
91/09-16-030-20W3/0	Crescent	0.35	0.97	16.31	-7.82	-258.37	80.09	-95.19
03/16-32-025-18W3/0	Crescent	42.16	-138.34	-15.50	5.63	-210.75	267.38	-44.99
02/05-30-030-19W3/0	Crescent	-122.99	-121.14	31.61	-16.81	-229.11	-52.78	-111.45
02/09-22-030-21W3/0	Baytex	70.45	170.48	127.36	30.15	-150.25	-72.80	172.31
91/12-05-033-24W3/0	Baytex	70.71	-27.72	50.79	171.96	180.62	17.99	-7.93
02/16-15-029-22W3/0	Baytex	-158.12	-138.51	-64.61	-60.05	-192.66	-212.22	51.12
02/01-28-025-18W3/0	Crescent	-30.34	-117.13	-125.91	-49.39	-187.19	-22.91	-128.97
02/12-25-029-22W3/0	Teine	42.16	-16.55	31.51	3.34	-65.36	-17.78	153.46
01/03-28-030-19W3/0	Crescent	19.30	-50.27	156.83	53.41	920.44	322.96	-34.86

01/12-20-026-19W3/0	Baytex	-64.45	-33.23	-56.68	-19.53	-235.96	-83.99	-21.89
02/09-20-029-22W3/0	Crescent	-11.25	-91.87	-29.70	-14.56	-248.05	95.40	50.22
02/04-01-027-20W3/0	Teine	21.29	235.94	71.73	36.75	-167.79	364.47	113.86
91/08-30-029-24W3/0	Baytex	25.85	245.78	4.53	49.92	-251.94	34.67	-69.94
03/16-36-033-24W3/0	Baytex	-11.11	-127.13	-123.99	-59.81	-191.78	-104.24	18.70
92/15-33-029-25W3/0	Whitecap	106.91	506.01	209.30	403.76	-206.97	47.55	52.93
91/16-03-030-20W3/0	Novus	-157.99	-142.14	-56.21	-114.68	-68.71	-644.00	-395.54
01/02-30-029-22W3/0	Crescent	-120.98	-104.15	-43.53	-54.89	-219.70	-27.78	-232.81
02/15-17-033-24W3/0	Crescent	58.62	-75.60	-12.14	74.74	-186.65	76.15	-7.09
01/08-25-029-22W3/0	Teine	40.69	-25.69	25.09	-1.19	-45.57	-3.02	126.38
01/12-04-032-25W3/0	Ish	12.92	-43.32	-104.48	-76.93	-206.12	60.76	-1.60
01/09-16-026-19W3/0	Teine	98.68	110.22	92.34	113.46	109.18	228.82	174.34
02/16-07-032-25W3/0	Ish	-26.31	-24.47	-79.39	-85.83	-185.65	79.87	23.78
02/05-19-026-18W3/0	Teine	67.48	72.76	68.02	26.19	95.43	318.59	62.81
01/10-21-029-24W3/0	Baytex	-10.60	-54.08	-78.26	-70.39	-225.86	-84.04	-254.64
01/15-17-026-18W3/0	Teine	-47.64	234.96	28.79	7.67	-224.28	362.72	64.83
01/03-27-030-19W3/0	Teine	24.17	-73.84	107.41	70.25	-203.08	132.60	88.16
04/15-28-029-22W3/0	Crescent	-30.45	-119.76	-81.68	-98.24	775.67	-46.67	-139.27
02/05-28-029-21W3/0	Baytex	40.13	-93.54	-8.68	-16.60	-156.36	-97.74	49.80
04/12-29-030-19W3/0	Crescent	25.51	-76.92	188.64	43.71	952.99	66.01	-7.69
01/13-10-026-19W3/0	Crescent	47.59	-0.46	63.66	90.40	-157.49	109.99	197.94
01/14-05-030-25W3/0	Whitecap	-59.16	287.75	181.13	424.25	1213.40	136.06	18.57
01/01-28-025-18W3/0	Crescent	-41.65	-125.83	-143.96	-57.57	-197.90	-31.34	-145.56
01/16-20-033-23W3/0	Teine	16.51	-74.21	-36.16	-10.02	-94.07	-88.34	70.57
01/12-05-026-17W3/0	Teine	27.51	-47.44	50.08	10.28	207.77	105.84	119.83
01/02-01-026-19W3/0	Teine	-112.14	-140.15	-31.99	-37.16	-234.32	-25.61	65.60
04/01-20-029-22W3/0	Crescent	51.68	-10.99	87.34	62.97	552.93	218.28	137.65
01/11-10-034-24W3/0	Baytex	-23.59	-98.25	-87.05	-29.77	-160.95	-35.14	20.07
01/14-32-029-26W3/0	Novus	5.85	-21.92	148.99	-101.69	-205.58	132.47	150.64
01/14-19-026-18W3/0	Teine	34.47	100.94	91.73	56.33	140.30	336.70	13.25

APPENDIX C: PYTHON CODE FOR THE THREE REGRESSION MODELS

1. Multiple linear regression

```
features_1 = df[['TVD','net_pay', 'surface_latitude', 'surface_longitude',
 'completion_length', 'spacing', 'proppant_completion', 'proppant_fluid','
ave_GOR']]

targets_1 = df.loc[:,df.columns == 'oil_365']


def train_model(model, X, Y, cv):
    """This function will fit the specified model and run cross validation
    Returns mean and variance in cross validation scores.
    Model: specified model must be instantiated
    X, Y: training sets to use to fit model
    cv: number of folds in cross validation"""
    model.fit(X, Y)
    scores = cross_val_score(model, X, Y, cv=cv)
    print(scores)
    return '{:0.4f} (+/- {:0.4f})'.format(scores.mean(), scores.std()*2)

def test_model(model, X, Y, cv):
    """This function will run cross validation on the test set.
    Returns mean and variance in cross validation scores.
    Model: specified model must be instantiated
    X, Y: test sets to use to fit model
    cv: number of folds in cross validation"""
    scores = cross_val_score(model, X, Y, cv=cv)
    print(scores)
    return '{:0.4f} (+/- {:0.4f})'.format(scores.mean(), scores.std()*2)


X_train, X_test, y_train, y_test = train_test_split(features_1,targets_1,
                                                    test_size=0.4,
                                                    random_state=42)

# Instantiate the model
regr = LinearRegression()
# Fit the model and generate training scores
regr_train = train_model(regr, X_train, y_train, 5)
# Generate test scores
regr_test = test_model(regr, X_test, y_test, 5)
```

```
print('Training Scores: {}'.format(regr_train))
print('Test Scores: {}'.format(regr_test))
#prediction using test set
y_pred_test=regr.predict(X_test)

#prediction using training set
y_pred_train=regr.predict(X_train)

#scores
train_set_r2 = r2_score(y_train, y_pred_train)

test_set_r2 = r2_score(y_test, y_pred_test)

#printing results
print(train_set_r2)
print(test_set_r2)
```

2. Random forest model A

```
features_1 = df[['TVD','net_pay', 'surface_latitude', 'surface_longitude',
 'completion_length', 'spacing', 'proppant_completion',
                  'proppant_fluid', 'ave_GOR']]

targets_1 = df.loc[:,df.columns == 'oil_365']


X1_train, X1_test, y1_train, y1_test = train_test_split(features_1, target
s_1, test_size=0.4, random_state = 42)


def train_model(model, X, Y, cv):
    """This function will fit the specified model and run cross validation
    Returns mean and variance in cross validation scores.
    Model: specified model must be instantiated
    X, Y: training sets to use to fit model
    cv: number of folds in cross validation"""
    model.fit(X, Y)
    scores = cross_val_score(model, X, Y, cv=cv)
    print(scores)
    return '{:0.4f} (+/- {:0.4f})'.format(scores.mean(), scores.std()*2)

def test_model(model, X, Y, cv):
    """This function will run cross validation on the test set.
    Returns mean and variance in cross validation scores.
    Model: specified model must be instantiated
```

```
    X, Y: test sets to use to fit model
    cv: number of folds in cross validation"""
    scores = cross_val_score(model, X, Y, cv=cv)
    print(scores)
    return '{:0.4f} (+/- {:0.4f})'.format(scores.mean(), scores.std()*2)


# Instantiate the model
rfr1 = RandomForestRegressor()
# Fit the model and generate training scores
rfr1_train = train_model(rfr1, X1_train, y1_train.values.ravel(), 5)
# Generate test scores
rfr1_test = test_model(rfr1, X1_test, y1_test.values.ravel(), 5)
print('Training Scores: {}'.format(rfr1_train))
print('Test Scores: {}'.format(rfr1_test))


# Randomized Search CV

# Number of trees in random forest
n_estimators = [int(x) for x in np.linspace(start = 100, stop = 3000, num
= 20)]
# Number of features to consider at every split
max_features = ['auto', 'sqrt']
# Maximum number of levels in tree
max_depth = [int(x) for x in np.linspace(3, 50, num = 8)]
# Minimum number of samples required to split a node
min_samples_split = [2, 5, 10, 15, 20, 100]

# Create the random grid
random_grid = {'n_estimators': n_estimators,
               'max_features': max_features,
               'max_depth': max_depth,
               'min_samples_split': min_samples_split}

print(random_grid)


# Random search of parameters, using 3 fold cross validation,
# search across 150 different combinations
rf_random = RandomizedSearchCV(estimator = rfr1, param_distributions = ran
dom_grid, n_iter = 150, cv = 3, verbose=2, random_state=42, n_jobs = 1)
rf_random.fit(X1_train, y1_train.values.ravel())
# Identifying best score and best parameters from the Grid Search
print(rf_random.best_score_)
best_params = rf_random.best_params_
```

```
print(best_params)


# Potential hyperparameters
param_grid = {
            "n_estimators"      : [1765,1770,1775,1780,1785,1790],
            "max_features"      : ["sqrt"],
            "min_samples_split" : [2,4,6],
            "max_depth": [14,15,16,17,18]
            }
# Instantiating grid search
grid = GridSearchCV(estimator=rfr1, param_grid=param_grid, cv=5)
# Fitting model
grid.fit(X1_train, y1_train.values.ravel())
# Identifying best score and best parameters from the Grid Search
print(grid.best_score_)
best_params = grid.best_params_
print(best_params)


# Instantiate the model
rfr1_grid = RandomForestRegressor(n_estimators=1785, max_depth=15, max_fea
tures='sqrt', min_samples_split=2,  random_state=42)
# Fit the model and generate training scores
rfr1_grid_train = train_model(rfr1_grid, X1_train, y1_train.values.ravel()
, 5)
# Generate test scores
rfr1_grid_test = test_model(rfr1_grid, X1_test, y1_test.values.ravel(), 5)
print('Training Scores: {}'.format(rfr1_grid_train))
print('Test Scores: {}'.format(rfr1_grid_test))


#Predictions
y1_pred_train = rfr1_grid.predict(X1_train)
y1_pred_test = rfr1_grid.predict(X1_test)

test_set_r2 = r2_score(y1_test, y1_pred_test)
train_set_r2 = r2_score(y1_train, y1_pred_train)

#printing results
print(test_set_r2)
print(train_set_r2)
```

3. Random forest model B

```
features_2 = df[['TVD','net_pay', 'surface_latitude', 'surface_longitude',
 'completion_length', 'proppant_completion',
                 'ave_GOR']]

targets_2 = df.loc[:,df.columns == 'oil_365']


X2_train, X2_test, y2_train, y2_test = train_test_split(features_2, target
s_2, test_size=0.4, random_state = 42)


def train_model(model, X, Y, cv):
    """This function will fit the specified model and run cross validation
    Returns mean and variance in cross validation scores.
    Model: specified model must be instantiated
    X, Y: training sets to use to fit model
    cv: number of folds in cross validation"""
    model.fit(X, Y)
    scores = cross_val_score(model, X, Y, cv=cv)
    print(scores)
    return '{:0.4f} (+/- {:0.4f})'.format(scores.mean(), scores.std()*2)

def test_model(model, X, Y, cv):
    """This function will run cross validation on the test set.
    Returns mean and variance in cross validation scores.
    Model: specified model must be instantiated
    X, Y: test sets to use to fit model
    cv: number of folds in cross validation"""
    scores = cross_val_score(model, X, Y, cv=cv)
    print(scores)
    return '{:0.4f} (+/- {:0.4f})'.format(scores.mean(), scores.std()*2)


# Instantiate the model
rfr2 = RandomForestRegressor()
# Fit the model and generate training scores
rfr2_train = train_model(rfr2, X2_train, y2_train.values.ravel(), 5)
# Generate test scores
rfr2_test = test_model(rfr2, X2_test, y2_test.values.ravel(), 5)
print('Training Scores: {}'.format(rfr2_train))
print('Test Scores: {}'.format(rfr2_test))


# Randomized Search CV

# Number of trees in random forest
```

```
n_estimators = [int(x) for x in np.linspace(start = 100, stop = 3000, num
= 20)]
# Number of features to consider at every split
max_features = ['auto', 'sqrt']
# Maximum number of levels in tree
max_depth = [int(x) for x in np.linspace(3, 50, num = 8)]
# Minimum number of samples required to split a node
min_samples_split = [2, 5, 10, 15, 20, 100]


# Create the random grid
random_grid = {'n_estimators': n_estimators,
               'max_features': max_features,
               'max_depth': max_depth,
               'min_samples_split': min_samples_split}

print(random_grid)


# Random search of parameters, using 3 fold cross validation,
# search across 150 different combinations
rf_random_2 = RandomizedSearchCV(estimator = rfr2, param_distributions = r
andom_grid, n_iter = 150, cv = 3, verbose=2, random_state=42, n_jobs = 1)
rf_random_2.fit(X2_train, y2_train.values.ravel())
# Identifying best score and best parameters from the Grid Search
print(rf_random_2.best_score_)
best_params_2 = rf_random_2.best_params_
print(best_params_2)


# Potential hyperparameters
param_grid = {
            "n_estimators"      : [395,400,405,410,415,420],
            "max_features"      : ["sqrt"],
            "min_samples_split" : [2,4,6],
            "max_depth": [41,42,43,44,45]
            }
# Instantiating grid search
grid_2 = GridSearchCV(estimator=rfr2, param_grid=param_grid, cv=5)
# Fitting model
grid_2.fit(X2_train, y2_train.values.ravel())
# Identifying best score and best parameters from the Grid Search
print(grid_2.best_score_)
best_params_2 = grid_2.best_params_
print(best_params_2)
# Instantiate the model
```

```
rfr2_grid = RandomForestRegressor(n_estimators=405, max_depth=44, max_feat
ures='sqrt', min_samples_split=2,  random_state=42)
# Fit the model and generate training scores
rfr2_grid_train = train_model(rfr2_grid, X2_train, y2_train.values.ravel()
, 5)
# Generate test scores
rfr2_grid_test = test_model(rfr2_grid, X2_test, y2_test.values.ravel(), 5)
print('Training Scores: {}'.format(rfr2_grid_train))
print('Test Scores: {}'.format(rfr2_grid_test))


y2_pred_train = rfr2_grid.predict(X2_train)
y2_pred_test = rfr2_grid.predict(X2_test)

test_set_r2_2 = r2_score(y2_test, y2_pred_test)
train_set_r2_2 = r2_score(y2_train, y2_pred_train)

#printing results
print(test_set_r2_2)
print(train_set_r2_2)
```